Scuola Internazionale Superiore di Studi Avanzati - Trieste

Gauge–Higgs Unification Theories on 5D Orbifolds

Thesis submitted for the degree of
Doctor Philosophiæ

Candidate:
Giuliano Panico

Supervisor:
Prof. Marco Serone

September 2007

SISSA - Via Beirut 2-4 - 34014 TRIESTE - ITALY

Contents

Introduction 1

1 5D Theories: the Kaluza–Klein Approach 13
- 1.1 Scalars on the Interval . . . 14
- 1.2 Gauge Fields . . . 16
- 1.3 Fermions . . . 18
- 1.4 Orbifold Compactifications . . . 20
  - 1.4.1 The $S^1/\mathbf{Z}_2$ Orbifold . . . 21
  - 1.4.2 Gauge Theories on $S^1/\mathbf{Z}_2$ . . . 24
- 1.5 The Wilson Line Interpretation . . . 25
  - 1.5.1 The non-Abelian Case . . . 26

2 The Holographic Approach 29
- 2.1 The Example of a Scalar . . . 30
- 2.2 Holography for Gauge Fields . . . 32
  - 2.2.1 An "Holographic" Gauge-Fixing . . . 33
- 2.3 The Tree-Level Effective Action . . . 35
  - 2.3.1 Scalar Fields . . . 36
  - 2.3.2 Gauge Fields . . . 39
  - 2.3.3 Fermions . . . 41
- 2.4 The One-Loop Higgs Effective Potential . . . 42
  - 2.4.1 The $SU(2) \to U(1)$ Case . . . 44
- 2.5 Holographic QCD . . . 46
  - 2.5.1 The χ**PT** Lagrangian at $\mathcal{O}(p^4)$ from Holographic QCD . . . 47
- 2.6 Holographic Anomaly . . . 50
  - 2.6.1 Anomaly in AdS/QCD . . . 55

3 5D Models with Gauge–Higgs Unification 57
- 3.1 The Gauge–Higgs Unification Mechanism . . . 57
- 3.2 A Gauge–Higgs Unification Model on $S^1/\mathbf{Z}_2$: the Gauge Sector . . . 59

3.2.1 The $U(1)'$ Subgroup and the θ_w Angle . . . 61
3.3 A Gauge–Higgs Unification Model on $S^1/\mathbf{Z}_2$: the Fermionic Sector . . . 61
3.3.1 The Fermionic Spectrum . . . 63
3.3.2 The Flavour Structure . . . 66
3.4 Gauge Bosons and Anomaly Cancellation . . . 67
3.5 One-Loop Effective Potential for the Higgs . . . 69
3.6 Quantitative Analysis . . . 71
3.6.1 Estimate of the Cut-Off . . . 73
3.7 Possible Extensions . . . 73
3.7.1 High Rank Bulk Fermions . . . 74
3.7.2 Localized Gauge Kinetic Terms . . . 74

4 A Realistic Model with Gauge–Higgs Unification **77**
4.1 The Model . . . 79
4.2 Mass Spectrum and Higgs Potential . . . 81
4.2.1 The Fermionic Sector . . . 83
4.2.2 Distribution of the Minima and Higgs Mass . . . 85
4.3 Estimate of the Cut-Off and Loop Corrections . . . 86
4.4 Phenomenological Bounds . . . 88
4.4.1 Direct Corrections: the $\widetilde{Z}b_Lb_L$ Vertex and FCNC . . . 89
4.4.2 Phenomenological Constraints . . . 91
4.5 Sensitivity, Predictivity and Fine-Tuning . . . 93
4.6 A Dark Matter Candidate . . . 95
4.7 The Lorentz Breaking as a Spontaneous Breaking . . . 97

5 Gauge–Higgs Unification at Finite Temperature **99**
5.1 The Wilson Line Dynamics at Finite Temperature . . . 101
5.1.1 Gauge Independence of the Effective Potential . . . 101
5.1.2 High Temperature Behaviour . . . 103
5.1.3 Properties of the Phase Transition . . . 105
5.2 The Electroweak Phase Transition in GHU Models . . . 108
5.2.1 The EWPT in a Simple Model . . . 109
5.2.2 The EWPT in a Realistic Model . . . 118
5.3 Estimate of Higher-Loop Corrections . . . 121

Conclusions **127**

A The Holographic Gauge-Fixing **131**

B Holography with Boundary Terms **135**
B.1 Effective Action for Scalars with Localized Mass Terms 136

C Bulk Wave Functions **139**
C.1 Gauge Fields 139
C.2 Fermions 141
C.3 Scalars 142

D Mode Decomposition **143**

E Computation of the $\widetilde{Z}\overline{b}_L b_L$ Vertex Corrections **147**

F Fermion Localization **151**

G Explicit Form of the Finite-Temperature Potential **155**
G.1 Bulk Fields Contribution 155
G.2 Boundary–Bulk Fields Contribution 157

Bibliography **157**

Introduction

The Standard Model (SM) of Electroweak (EW) and strong interactions has proved to be an extremely successful theory being able to describe almost any process of high energy Physics with a surprising degree of accuracy. Notwithstanding this success, it is now clear that the SM has to be considered as an effective model, valid up to a certain cut-off scale Λ_{SM}, rather than a truly fundamental theory. An obvious reason for this claim is the fact that the SM does not include a quantum description of gravity, which forces to consider the Planck mass as an unavoidable upper limit for its validity ($\Lambda_{SM} < M_{PL} \sim 10^{19}$ GeV).

The SM, however, presents some problems and some unsatisfactory aspects at far lower scales than the Planck mass. A first difficulty comes from cosmological observations. In the last years the evidence of the existence of a relatively large amount of non-baryonic Dark Matter (DM) has become very strong. The SM clearly lacks a stable (or almost stable) particle which could explain the DM abundance of the Universe. Another well known problem is the origin of neutrino masses. In its original formulation the SM includes massless neutrinos, but the experimental measurements, which bear evidence of neutrino oscillations, show that their mass must be non zero, although very tiny. The mechanism which could generate such small masses is yet unknown.

Though not a theoretical problem, another unsatisfactory aspect of the SM is the unexplained hierarchy of fermion masses among the three matter generations. The stability of the Yukawa couplings against radiative corrections guarantees that the fermion masses are "technically" natural. This means that no special cancellations among the parameters of the theory are needed in order to obtain the correct masses, or, in other words, no fine-tuning is associated to this hierarchy. Nevertheless, it would be nice to have a fundamental mechanism which could "naturally" explain the peculiar spectrum of fermion masses.

The above discussed issues seem to be related to one or more fundamental scales of the theory. In particular some proposed mechanism, which aim to explain the origin of neutrino masses, require the introduction of fields with high mass scales. In any case, due to the lack of a complete understanding of these problematic aspects of the SM, it is very difficult to guess the order of magnitude of the fundamental scales involved.

There are, however, two other features of the SM which seem to be more directly related to some scale of new Physics. The first of such features is the rough unification of the

running gauge couplings which become of the same order of magnitude at an energy scale $M_{GUT} \sim 10^{15}$ GeV. This behaviour could be the sign of the existence of an underlying Grand-Unified Theory (GUT) in which the EW and Strong interactions are treated on the same footing. Within this kind of scenario, the cut-off of the SM would be necessarily much lower than the gravity scale, namely $\Lambda_{SM} \sim M_{GUT}$.

Another argument seems to suggest that the cut-off of the SM can not be as high as the Planck mass or the GUT scale, but rather several orders of magnitude below, in the TeV range. A possibility of this kind would imply that some new Physics could be explored in the forthcoming collider experiments. The argument is simple and is related to one of the most obscure parts of the SM: the Higgs mechanism. Differently from fermion Yukawa's which are stable at the radiative level, the Higgs mass is quadratically divergent in perturbation theory, so that it is highly sensitive to the cut-off of the theory. For an almost arbitrary choice of the parameters of the SM, the Higgs mass, and thus the EW scale, would be unavoidably of the order of a loop factor times the cut-off of the model Λ_{SM}, which as discussed before, could be as large as M_{GUT} or M_{PL}. On the other hand, the Unitarity bound on the scattering of four gauge bosons requires a Higgs mass $m_H \lesssim$ TeV, which would be natural for a cut-off $\Lambda_{SM} \sim$ TeV. In the absence of any symmetry protecting the EW scale, a cut-off at the Planck scale would require a fine-tuning of 15 orders of magnitude in the parameters of the SM in order to have an acceptable value of the Higgs mass. This striking difference of mass scales is known as the "Big Hierarchy Problem" of the SM.

In the last few years, an accurate analysis of the EW precision data deriving from collider experiments has shown that another smaller form of hierarchy, the so called "Little Hierarchy Problem", seems to exist in the SM [1, 2]. The experimental measurements put stringent bounds on the range of acceptable Higgs masses: 115 GeV $\leq m_H \leq$ 250 GeV, where the lower bound is obtained from direct searches and the upper one is determined through a fit on the EW observables. At the same time, the experimental results also put a lower bound on Λ_{SM}. Being the SM an effective theory, it is natural to expect that it could contain non-renormalizable interactions suppressed by a power of the cut-off scale. Considering some dimension 6 operators, in the absence of suppression mechanisms for the coefficients of these operators, one can set the bound $\Lambda_{SM} \gtrsim 10$ TeV [1]. We see that, also in this case, a small clash (of one or two orders of magnitude) exists between the Higgs mass and the cut-off.

The attempt to better understand the nature of the Higgs mechanism, possibly addressing the Hierarchy problems, has been one of the guidelines for the study of the Physics beyond the SM. Of course, solving the Hierarchy problem would require the introduction of some mechanism or, better, some new symmetry which could stabilize the EW scale. Many proposals have appeared in the last decades to describe the Physics beyond the SM. Some of them try to change the nature of the Higgs. For example, the Higgs could be a

non-fundamental field related to some strongly coupled sector of the theory (such as in Technicolor models [3] or Composite-Higgs models [4]), so that the EW scale is dynamically generated by the strong sector. Another possibility, that we will treat is detail in this thesis, is given by Gauge–Higgs Unification (GHU) models in extra dimensions (ED), in which the Higgs originates from a higher dimensional gauge field and its dynamics is protected by the gauge symmetry. In the context of ED, one can also have some scenarios in which the Higgs is not present at all (Higgsless theories [5, 6]) and the breaking of the EW gauge group is obtained by a suitable choice of the boundary conditions of the fields. A class of theories inspired by the deconstruction of extra-dimensional theories, are the Little-Higgs models [7, 8] in which the Higgs is a pseudo-Goldstone boson.

At present one of the best candidate to describe the Physics beyond the SM is Supersymmetry and in particular the Minimal Supersymmetric Standard Model (MSSM). This scenario presents many nice features. First of all, it is compatible with the present experimental results. Moreover the existence of superpartners of the SM fields with opposite statistics naturally cancels the leading divergences in the Higgs mass which is now only logarithmically sensitive to the cut-off scale. Another interesting feature is the existence in the MSSM of a DM candidate which could explain the DM abundance in the Universe.

Also the MSSM, however, has some unsatisfactory aspects. Supersymmetry, which allows to stabilize the EW scale, at the same time strongly constrains the Higgs mass which at tree level has to be smaller than the Z mass: $m_H \leq m_Z$. Higgs masses in this range are not compatible with the experimental result $m_H \geq 115$ GeV, so that one has to rely on radiative corrections to get an acceptable value of m_H. As a consequence, allowed Higgs masses in the MSSM can not be much larger than the current experimental limit and, moreover, a certain amount of fine-tuning is necessarily reintroduced in the model. Finally, the hierarchy of fermion Yukawa couplings remains totally unexplained in the MSSM.

The above considerations clearly point out that it could be worth investigating alternative scenarios with respect to the standard supersymmetric one. In particular, among the previously mentioned possibilities, the class of models with extra dimensions seems the most promising. A hint of the fact that our World could actually have more than 4 space–time dimensions comes from string theory, which requires extra spatial dimensions to be consistently defined. Of course, compatibility with the experiments requires these extra dimensions either to be compactified on small spaces or to be somehow "inaccessible" for the ordinary fields of the SM. An example of the latter possibility is given by the ADD scenario [9] that predicts large sub-millimeter extra dimensions in which only gravity can propagate. This feature can be used to explain the weakness of the gravitational interactions, which are "diluted" by the extra dimensions, with respect to the EW interactions, or, in other words, it can justify the large value of M_{PL} with respect to the EW scale.

Different scenarios in which the SM fields can directly access the extra dimensions can be realized considering theories compactified on TeV-sized spaces [10]. Models of this type offer an intersting way to address the problem of the stability of the EW scale. As mentioned before, in the context of extra dimensions one can consider the GHU set-up in which the Higgs fields is identified with some of the internal components of a higher-dimensional gauge field which propagates both in the $4D$ Minkowski space–time and in the extra compact-dimensions. This mechanism was proposed several years ago [11], and received renewed interest in the last few years both in its non-supersymmetric [7, 12, 13, 14, 15] and supersymmetric [16, 17] versions.

In this scenario, the Higgs is an effective scalar from a $4D$ point of view, but its origin as a gauge field component severely constrains its dynamics preventing in many cases the appearance of divergences in the Lagrangian. This is true, in particular, in $5D$ GHU theories, in which the Higgs is identified with the fifth component of the gauge field. In this case the gauge invariance forbids the presence of a tree-level (possibly divergent) potential for the Higgs. The whole dynamics of the Higgs sector is instead determined by radiative effects, which must necessarily be finite due to the absence of possible divergent counterterms. Notice that this mechanism, which is used to generate a spontaneous Electroweak Symmetry Breaking (EWSB) at loop level, relates the EW scale to the compactification scale of the model, thus making it insensitive to the UV dynamics of the theory (*i.e.* to the cut-off scale). At the same time, the loop-factor suppression of the Higgs potential can (in part) explain the gap between the Higgs mass and the scale of new Physics, which in this context is roughly given by the compactification scale.

Noticeably, in this $5D$ GHU scenario two models have been proposed which seem to be fully compatible with the current experimental constraints. One of these [18, 19, 20, 21] is based on the Randall–Sundrum (RS) set-up [22] which considers a theory defined on a slice of AdS_5 space. A remarkable feature of this scenario is the possibility of addressing the Big Hierarchy Problem. The keypoint is that the EW scale, which is essentially determined by the near–IR–brane dynamics, is hugely red-shifted by the exponential factor of the AdS_5 metric with respect to the gravity scale, which is related to the near–UV–brane Physics. Another interesting aspect is the possibility of achieving a natural hierarchy of fermion Yukawa's by means of the exponential localization of the fermion zero-modes towards the UV or the IR brane. Finally it is worth mentioning that it has been suggested that a generalized form [23] of the original AdS/CFT correspondence [24, 25] could be valid in the RS scenario. This means that GHU models on AdS_5 can be equivalently described by a dual $4D$ model in which an elementary weakly-coupled sector of the theory is coupled with a strongly-coupled nearly conformal sector. The Higgs field arises from the strong dynamics as a composite object, and this gives the possibility of interpreting GHU models of this kind as a calculable version of the Composite-Higgs scenario mentioned before.

Another possibility, which we will thoroughly analyze in this thesis, is to construct

realistic GHU models in $5D$ considering compactifications on a flat $S^1/\mathbf{Z}_2$ orbifold [15, 26, 27]. Differently from the warped space case, in the context of flat extra dimensions the Big Hierarchy Problem can not be addressed at all. Nevertheless, the mechanism which stabilizes the EW scale can furnish a complete or, at least, a partial resolution of the Little Hierarchy Problem.

Analogously to the RS scenario, also in the flat case one can naturally obtain an exponential hierarchy of fermion masses, but, due to the absence of an exponential localization of the zero-mode wave functions, one has to rely on a different mechanism to realize suitable Yukawa couplings. To better understand this point it is useful to present firstly an alternative description of the EWSB mechanism. In the standard picture, the EWSB is spontaneously generated when the Higgs field, or, in our case the fifth component of the higher-dimensional gauge field, gets a non-trivial background. However, as pointed out in [28], the gauge invariance of the theory allows us to adopt an alternative point of view. By a (non-periodic) gauge transformation the Higgs Vacuum Expectation Value (VEV) can be set to zero at the cost of introducing "twisted" boundary conditions for the fields, or, in other words, the Higgs VEV can be effectively identified with a Wilson line phase. In this perspective, the EWSB mechanism is due to non-local effects and consequently the Higgs dynamics and in particular the Higgs effective potential are protected from divergences.

This non-locality property can be efficiently used to generate hierarchical Yukawa couplings. The main set-up [14, 15] is obtained coupling some $4D$ chiral fermion fields localized at the orbifold boundaries with pairs of massive bulk fields. The boundary fields can not couple directly with the Higgs, and they acquire mass after EWSB through the mediation of the bulk fermions. The Wilson-line nature of the Higgs VEV implies that the bulk fields can "see" the symmetry breaking only if they propagate from one boundary to the other, thus generating a suppression of the effective SM-fermions Yukawa's which are exponentially sensitive to the bulk field masses.

Although qualitatively the simplest GHU scenario on a flat orbifold is completely satisfactory, the accordance with the experiments results problematic at the quantitative level. Deriving essentially from gauge interactions, the Yukawa couplings of the fermions result smaller or at most of the same order of the gauge couplings. This is a disappointing feature, in fact it prevents the third generation Yukawa's to be large enough to give an acceptable top mass. In the minimal set-up of [15] a theoretical bound $m_t < \sqrt{2} m_W$ is found, but, actually, accessible values of the top mass are much below this limit: $m_t \lesssim 40$ GeV. Another problem related to the previous one is the too light Higgs mass, typically of order $m_H \lesssim m_W/2$. As explained before, the Higgs potential lacks a tree-level contribution, which is forbidden by the gauge symmetry, so that it is entirely generated at the radiative level. The magnitude of the various contributions to the Higgs potential is determined by the Higgs interaction couplings which are necessarily small being given by the usual EW

gauge couplings. Finally, the compactification scale, which in this case can be defined as $1/R$ where R is the radius of the S^1 covering space of the orbifold, is predicted to be too low to be compatible with the experiments, namely $1/R \lesssim 800$ GeV.

Solving the problems of the flat GHU scenario is not an easy task, naïve extensions of the basic set-up [15] typically predict too large deviations of the EW observables, hence failing to be consistent with the experiments, or have a very low cut-off, thus undermining their predictive power. Nevertheless it has been recently pointed out that all the above mentioned problems could be solved by means of two modifications of the original model [26, 27].[1]

As we discussed before, the too light value of the Higgs and top masses is due to the smallness of the Higgs couplings and in particular to the smallness of the fermion Yukawa's. Of course the allowed interactions of the Higgs are determined by the gauge invariance, whereas it is the $5D$ Lorentz symmetry which forces the bulk fields to have the same couplings with the gauge bosons and with the Higgs, which coincides with the fifth component of the gauge field. A simple, though slightly "exotic", way to enhance the Higgs couplings is to advocate a breaking of the Lorentz invariance in the extra dimension. More explicitly, we suppose that the $SO(4,1)/SO(3,1)$ symmetry is broken so that the usual $SO(3,1)$ Lorentz group is preserved. This mechanism allows at the same time to obtain a realistic top mass and to push the Higgs mass above the current experimental bounds.

Unfortunately the Lorentz breaking alone is not sufficient to solve the problem of having a too small compactification scale. To address this issue it has been proposed to introduce a $\mathbf{Z}_2$ symmetry into the model [27]. This symmetry, called "mirror symmetry", acts on a subset of the bulk fields, namely the fermions and a subgroup of the gauge fields, effectively doubling their number. Fields related by the $\mathbf{Z}_2$ symmetry satisfy twisted boundary conditions, so that in a diagonal base they give rise to couples of bulk fields with periodic and antiperiodic conditions on the covering S^1 space. The net effect of the presence of periodic and antiperiodic fields on the Higgs potential is a partial cancellation of the quadratic mass term. This cancellation helps to generate a sizable gap between the EW and the compactification scale so that the model can be fully compatible with the EW precision measurements.

An interesting by-product of the $\mathbf{Z}_2$ mirror symmetry is the presence of stable Kaluza–Klein (KK) states. In the model all the SM fields are even under the $\mathbf{Z}_2$ symmetry, so that the lightest odd particle is absolutely stable. Usually this stable state coincides with the first KK mode of an antiperiodic gauge boson related to a $U(1)$ gauge subgroup. Noticeably it has been recently shown that such state can be a realistic DM candidate whose relic abundance is consistent with the current cosmological observations [30].[2]

[1] For an alternative, possibly realistic, extension of the original set-up see also [29].

[2] Notice that this scenario is very similar to what happens in Universal Extra Dimensions [31], where

An important feature that must be adequately stressed is the fact that gauge theories in extra dimensions are non-renormalizable. This means that they are effective theories with a limited range of validity: above a certain energy scale Λ, which is the cut-off of the theory, a higher dimensional model becomes strongly coupled and enters an uncontrolled regime. The predictive power of the theory is determined by the quantity $1/(R\Lambda)$ which controls the effects of non-renormalizable operators at the compactification scale $1/R$. A necessary requirement for a sensible model is to have a large enough cut-off, so that it can be reliably used to compute physical observables. As we will see, in realistic GHU models, the cut-off is roughly given by $\Lambda \sim 5/R \sim 20$ TeV, so that these models are reasonably predictive. Moreover, in the GHU scenario, the higher dimensional gauge invariance (or, equivalently, the non-local nature of the EWSB) protects some relevant quantities (such as the Higgs potential) so that they are actually insensitive to the cut-off and can be reliably computed perturbatively.

Thus far we have considered the general features of models which aim to describe the Physics beyond the SM. In particular we focused our interest on theories with extra dimensions, showing their strengths and their weaknesses. The study of ED theories, however, especially in some complex scenarios, as, for instance, compactifications on intervals with boundary terms or localized fields, can be extremely challenging from a technical and computational point of view. As we have seen before, the possibility of constructing realistic models relies almost always on compactifications on spaces with singularities and on the presence of localized interactions. It is then clearly useful to develop some tools which could simplify the analysis of such theories and, possibly, shed some light on their inner properties.

The standard approach to the study of theories with extra dimensions is the KK decomposition, which is based on a kind of Fourier analysis of the fields along the extra dimensions. The main idea is to decompose the bulk fields on a basis of $4D$ mass eigenstates, thus rewriting an extra-dimensional field as a sum of $4D$ KK modes with different wave functions along the extra dimensions. Correspondingly, the whole theory is reinterpreted as a $4D$ effective theory containing these infinite KK towers of states. Generically, for a model with compact extra dimensions, the effective theory will contain some massless (or nearly massless) states, while the lightest KK excitations will have masses of the order of the compactification scale. Of course, at low energy, the field content of a model will be given by the massless states, while the KK modes will give corrections to the low energy observables. From this point of view, the KK approach results very useful not only to have a clear and simple understanding of the Physics of an extra dimensional theory, but also to estimate the effects of the KK modes on the low energy dynamics. In this perspective

there exists a $\mathbf{Z}_2$ symmetry, the KK-parity, which is a remnant of the group of translations along the extra dimension. As in our case, this invariance leads to stable KK states which can be potential DM candidates [32].

the compactification scale (or the KK mass scale) acts just as a cut-off for the effective low-energy theory.

In spite of its seeming simplicity, the KK approach tends to become rather involved in realistic set-ups. For example, this happens in $5D$ models compactified on an orbifold when boundary terms or localized fields are introduced at the fixed points. The origin of this difficulty is related to the fact that localized terms in the Lagrangian usually lead to complex systems of boundary equations.

There is also another, more theoretical, aspect which can not be easily understood within the KK approach. Let us consider for definiteness a gauge theory compactified on a $5D$ interval. In such theory, the boundary conditions which must necessarily be imposed on the fields at the singular points can break partially or completely the gauge invariance at the boundaries. In the low energy limit the broken part of the gauge symmetry is no more linearly realized, so that a corresponding massless gauge boson is not present. Notice that this mechanism is widely used to obtain a low energy gauge invariance which is only a subgroup of the original $5D$ gauge symmetry, and in particular it is an essential ingredient in constructing GHU models.

An interesting question which can be asked on this symmetry breaking mechanism is whether it is a soft breaking of the gauge invariance or not, or in other words if it can introduce divergences into the theory. Fortunately the answer is that the symmetry breaking is soft. A way to show this property is to realize the symmetry breaking at the boundaries through a different but equivalent mechanism. To generate a gauge symmetry breaking, we can introduce localized $4D$ scalar multiplets coupled with the gauge fields in a completely gauge-invariant way. When the scalar fields get a VEV a spontaneous breaking of the gauge symmetry happens at the boundary, moreover considering the limit in which the VEV is taken to infinity the massive scalars which arise from the localized fields are effectively decoupled from the theory (see for instance [5, 33, 34]). In this limit the boundary conditions of the bulk fields reproduce the standard conditions on an interval needed to generate the corresponding symmetry breaking. At the same time the localized scalar multiplets give rise to some $4D$ Goldstone bosons which can be either present in the low energy effective theory or eaten by the gauge field components which become massive. These considerations indicate that the symmetry breaking induced by the boundary conditions is equivalent to a spontaneous breaking and they suggest that some Goldstone fields must be present in the low energy effective description.[3]

The KK analysis of a model with gauge symmetry breaking induced by boundary conditions shows that actually in the theory there exist some $4D$ massless scalars which arise from the fifth component of the gauge field. However it is not easy to show that

[3] Another evidence of this fact is provided by the (modified) AdS/CFT correspondence in the RS scenario. In this context the gauge symmetry breaking at the IR brane corresponds in the dual $4D$ picture to a spontaneous breaking of a global symmetry, thus predicting the existence of Goldstone bosons.

these scalars are in some way related to a Goldstone field.[4]

A recently proposed alternative approach with respect to the KK decomposition in which the above discussed features can be naturally described is the so called "holographic" procedure [36, 33, 37, 38]. This approach can be used to study theories compactified on a $5D$ space with boundaries, such as an orbifold or a generic warped interval. The holographic procedure consists in separating the "boundary" degrees of freedom, namely the values of the fields at one boundary (say the UV brane for definiteness), from the "bulk" ones which are encoded in the values of the fields in the bulk and at the other boundary (the IR brane). The holographic degrees of freedom can be used to describe the theory through an effective holographic action once the bulk degrees of freedom have been integrated out. It turns out that the holographic approach is completely equivalent to the standard KK decomposition and can be used to describe the whole original $5D$ theory.

An interesting aspect of the holographic point of view is the fact that it naturally treats the gauge symmetry breaking at the IR as a spontaneous breaking. In this way the (possibly pseudo-)Goldstone bosons associated to the breaking automatically appear in the holographic effective description [38]. Remarkably the fact that the massless $4D$ scalar fields arising from a $5D$ gauge field are actually Goldstone bosons offers an alternative suggestive description of a GHU theory. In the latter, as we said before, the Higgs field is identified with above mentioned scalars so that the Higgs itself is a Goldstone boson. Of course, this property determines the form of the Higgs Lagrangian forbidding the appearance of divergences.

From a more technical point of view, the holographic procedure results simpler than the KK decomposition for many applications. In particular the choice of the UV values of the fields as effective degrees of freedom allows to treat boundary terms and localized fields (especially at the UV) in a straightforward way. This feature makes the holographic approach very useful in the study of realistic GHU models both in the flat space and in the warped space scenarios. In fact, in both cases, the light fermions (namely the ones of the first two families) are almost exactly localized near the UV brane, so that their holographic description is very simple and can be easily used to compute corrections to the SM observables.

This thesis is organized as follows. In the first chapter we present some general concepts related to theories with extra dimensions adopting the KK perspective. In particular we report the general form of the action for scalar, fermion and gauge fields on a $5D$ interval with generic warped metric. At the same time we briefly discuss the boundary conditions which are allowed in these theories. Afterwards we present the general features of orbifold compactifications including a review of Scherk–Schwarz boundary conditions and Wilson lines. In chapter 2 we give a comprehensive presentation of the holographic approach.

[4]For an example of how to handle in a KK approach these Goldstone bosons in the context of Holographic QCD see for instance [35].

In the first part of the chapter we discuss the general framework, focusing in particular on the non-trivial case of gauge fields. In the second part we present three interesting applications of the holographic procedure. We begin with the computation of the tree-level holographic action for a generic $5D$ model, showing how it can be used to compute the one-loop Higgs effective potential in GHU theories. Then we use holography to obtain the Chiral Perturbation Theory (χ**PT**) Lagrangian in Holographic QCD. As a last, more theoretical, application, we study the consequences of the introduction of a Chern–Simons (CS) term into a $5D$ gauge theory.

The last three chapters are devoted to the study of $5D$ GHU theories compactified on the orbifold $S^1/\mathbf{Z}_2$. We begin with a review of the simplest implementation of the GHU idea which gives rise to the semi-realistic model of [15]. In particular we will discuss the general framework of this model pointing out its appealing features and its shortcuts. In chapter 4 we show how the problems of the previously considered model can be solved by assuming a breaking of the Lorentz symmetry along the fifth dimension and introducing the $\mathbf{Z}_2$ mirror symmetry. Furthermore, we will present a detailed study of this theory from both a qualitative and a quantitative point of view, determining the constraints on the parameter space which arise from the EW precision measurements and giving an estimate of the amount of fine-tuning of the model. As side remarks, we briefly discuss the presence of a viable DM candidate in the theory and we suggest a possible mechanism which could give origin to a spontaneous breaking of the Lorentz invariance in a purely $5D$ context. Finally, in chapter 5, we study the properties of GHU models at finite temperature. First of all we discuss the general features of the finite-temperature Higgs effective potential at one loop, showing that an Electroweak Phase Transition (EWPT) is always present in such models at a temperature of order $1/(2\pi R)$. Then we specialize our analysis to the models presented in chapters 3 and 4, and we perform a detailed study of the phase transition using analytic and numerical techniques. As a last issue, in section 5.3, we give some evidence of the stability of the finite-temperature one-loop potential in GHU models showing that the leading higher-loop corrections are not very relevant up to temperatures well above the EWPT.

We also include at the end some, quite technical, appendices. In the first one we present a more formal derivation of the gauge-fixing procedure employed in the holographic approach of chapter 2. In the next appendix, we show how it is possible to handle boundary terms and localized fields within the holographic description and we exemplify this possibility by treating the toy model of a scalar with boundary mass terms on a warped space. In appendix C we collect some useful formulae needed to compute the holographic action for the AdS_5 and flat space cases. In appendix D we give the decomposition of the most relevant $SU(3)$ representations in terms of multiplets of the $SU(2) \times U(1)$ subgroup. This decomposition results useful in the study of the GHU models presented in chapters 3, 4 and 5. In appendix E another application of the holographic approach is given, namely

we show how one can compute the distortion of the $\widehat{Z\bar{b}_L b_L}$ vertex (see section 4.4.1) in a simplified toy model. In appendix F we analyze the localization of the fermion zero-modes in the model of chapter 4. In the last appendix the explicit form of the finite-temperature one-loop Higgs potential is reported. In particular we collect various equivalent formulae by which one express the finite-temperature contributions to the potential.

Chapter 1

5D Theories: the Kaluza–Klein Approach

The idea of constructing field theories with more than three spatial dimensions was first considered at the beginning of the twentieth century as an attempt to achieve a unified description of electromagnetism and gravity [39]. Although those original efforts proved unsuccessful, in the 1980's, the realization that string theory requires extra dimensions to be consistently defined brought new interest in the study of extra dimensional theories. At the same time the connection with string theory supplied some new tools (as, for instance, orbifold compactifications) which proved to be a valuable ingredient to construct models which could be a valid candidate to go beyond the SM.

In this chapter we will review some basic concepts related to extra-dimensional theories. As a starting point, we will present a description of such theories following the traditional KK perspective. Within this approach the $5D$ fields are expanded on a base of $4D$ mass eigenstates, and the theory is rewritten in terms of a set of KK towers of $4D$ states. Although invaluable as a tool to understand the properties of an extra-dimensional theory, the KK approach tends to become fairly cumbersome from a computational point of view. This is particularly true in the presence of localized fields, which are commonly introduced in orbifold models. A new approach to the study of extra dimensions, the holographic procedure, which results simpler than the KK perspective for many applications, will be presented in the next chapter.

In this thesis we will be interested in models with only one extra spatial dimension, thus we will assume our theory to be defined on a $5D$ segment with a generic warped metric

$$ds^2 = g_{MN}dx^M dx^N = a^2(z)\left(\eta_{\mu\nu}dx^\mu dx^\nu - dz^2\right) , \qquad (1.0.1)$$

where the fifth coordinate is defined in the interval $[z_{\rm UV}, z_{\rm IR}]$, the warp function $a(z)$ is assumed to be regular and positive and the $4D$ coordinates have been rescaled to fix

$a(z_{\rm UV}) = 1$. In our notation $4D$ indices are raised and lowered with the Minkowski metric $\eta = \text{diag}(+,-,-,-)$. Two special cases of the above metric, which are particularly interesting for model building, are the flat space limit $a(z) = 1$, and the RS scenario (i.e. AdS_5) which corresponds to $a(z) = L/z$ with $z_{\rm UV} = L$.

1.1 Scalars on the Interval

One of the simplest examples of theories in extra dimensions is given by a complex scalar field Φ in $5D$. The preliminary discussion of this case will be useful to present the KK decomposition and to introduce some important concepts related to the compactification on a segment, as for instance the issue of boundary conditions.

As a first step, it is convenient to neglect possible boundary terms localized at the extrema of the segment and consider a scalar with a purely bulk action

$$\mathcal{S}_5 = \int_{z_{\rm UV}}^{z_{\rm IR}} dz\, \mathscr{L}_5 = \int_{z_{\rm UV}}^{z_{\rm IR}} dz \sqrt{g} \left[\partial_M \Phi^\dagger \partial^M \Phi - m_\phi^2 \Phi^\dagger \Phi \right] , \tag{1.1.1}$$

where the $4D$ integral has been omitted. In order to define a consistent quantum field theory, we must also impose some conditions on the fields at the boundaries of the segment. The allowed boundary conditions can be extracted by varying the action (1.1.1)

$$\begin{aligned} \delta S[\Phi] = & \int_{z_{\rm IR}}^{z_{\rm UV}} dz \left[-a^3(z) \delta\Phi^\dagger \partial_\mu \partial^\mu \Phi + \delta\Phi^\dagger \partial_z (a^3(z) \partial_z) \Phi - a^5(z) m_\phi^2 \delta\Phi^\dagger \Phi + h.c. \right] \\ & - a^3(z_{\rm IR}) [\delta\Phi^\dagger \partial_z \Phi] \Big|_{z_{\rm IR}} + [\delta\Phi^\dagger \partial_z \Phi] \Big|_{z_{\rm UV}} + h.c. , \end{aligned} \tag{1.1.2}$$

and imposing the boundary terms to vanish, so that the tree-level bulk Equation Of Motion (EOM) correctly coincides with the Klein–Gordon equation on a warped space. The two well known possibilities are the Neumann ($\partial_z \Phi = 0$) and Dirichlet ($\Phi = 0$) boundary conditions. Generalized Neumann boundary conditions can be obtained by adding localized mass terms for the fields which are non-vanishing at the boundaries (i.e. the ones which do not satisfy Dirichlet boundary conditions):

$$S_{loc} = \int_{z_{\rm UV}}^{z_{\rm IR}} dz\, \mathscr{L}_{loc} = \int_{z_{\rm IR}}^{z_{\rm UV}} dz\, a^4(z) \left\{ \delta(z - z_{\rm IR}) b_{\rm IR} \Phi^\dagger \Phi - \delta(z - z_{\rm UV}) b_{\rm UV} \Phi^\dagger \Phi \right\} . \tag{1.1.3}$$

In this way one gets the modified boundary conditions

$$\begin{cases} \left[\partial_z \Phi - a(z) b_{\rm UV} \Phi \right] \big|_{z = z_{\rm UV}} = 0 , \\ \left[\partial_z \Phi - a(z) b_{\rm IR} \Phi \right] \big|_{z = z_{\rm IR}} = 0 . \end{cases} \tag{1.1.4}$$

In order to obtain a $4D$ effective description of our theory, we expand the $5D$ field as

$$\Phi(x,z) = \sum_n \phi_n(x) f_n(z) , \tag{1.1.5}$$

where the $\phi_n(x)$ fields represent the relevant degrees of freedom from the $4D$ point of view. The effective Lagrangian is obtained from the full $5D$ action ($\mathscr{L}_5 + \mathscr{L}_{loc}$) by simply integrating over the fifth coordinate:

$$\begin{aligned}\mathscr{L}_4(x) &= \int_{z_{\rm IR}}^{z_{\rm UV}} dz\ [\mathscr{L}_5 + \mathscr{L}_{loc}] \\ &= \sum_{n,k} \Bigg\{ \partial_\mu \phi_n^\dagger \partial^\mu \phi_k \int_{z_{\rm IR}}^{z_{\rm UV}} dz\, a^3(z) f_n^\dagger f_k + \phi_n^\dagger \phi_k \int_{z_{\rm IR}}^{z_{\rm UV}} dz \Big[- a^3(z) \partial_z f_n^\dagger \partial_z f_k - a^5(z) m_\phi^2 f_n^\dagger f_k \\ &\qquad + a^4(z) \Big(\delta(z - z_{\rm IR}) b_{\rm IR} f_n^\dagger f_k - \delta(z - z_{\rm UV}) b_{\rm UV} f_n^\dagger f_k \Big) \Big] \Bigg\} . \end{aligned} \tag{1.1.6}$$

The wave functions f_n are chosen to be the solutions of the $5D$ Klein–Gordon equation

$$m_n^2 f_n(z) + \frac{1}{a^3(z)} \partial_z (a^3(z) \partial_z f_n(z)) - a^2(z) m_\phi^2 f_n(z) = 0 , \tag{1.1.7}$$

for all values of m_n which give solutions compatible with the chosen boundary conditions. As shown before, those boundary conditions can be either Neumann or Dirichlet if no localized term is included, otherwise they assume the generalized Neumann form (see eq. (1.1.4))

$$\begin{cases} [\partial_z f_n - a(z) b_{\rm UV} f_n]|_{z=z_{\rm UV}} = 0 , \\ [\partial_z f_n - a(z) b_{\rm IR} f_n]|_{z=z_{\rm IR}} = 0 . \end{cases} \tag{1.1.8}$$

Using the bulk EOM's (eq. (1.1.7)) and the boundary conditions one can prove that the wave functions f_n are orthogonal

$$\begin{aligned}(m_n^2 - m_k^2) \int_{z_{\rm IR}}^{z_{\rm UV}} dz\, a^3(z) f_n^\dagger f_k &= \int_{z_{\rm IR}}^{z_{\rm UV}} dz \Big(- \partial_z (a^3(z) \partial_z f_n^\dagger) f_k + a^5(z) m_\phi^2 f_n^\dagger f_k \Big) \\ &\quad - \int_{z_{\rm IR}}^{z_{\rm UV}} dz \Big(- f_n^\dagger \partial_z (a^3(z) \partial_z f_k) + a^5(z) m_\phi^2 f_n^\dagger f_k \Big) \\ &= - a^3(z) \partial_z f_n^\dagger f_k \Big|_{z_{\rm UV}}^{z_{\rm IR}} + a^3(z) f_n^\dagger \partial_z f_k \Big|_{z_{\rm UV}}^{z_{\rm IR}} = 0 , \end{aligned} \tag{1.1.9}$$

where we used eq. (1.1.8) to show that the last line vanishes.[1] Choosing the normalization of the wave functions to be

$$\int_{z_{\rm IR}}^{z_{\rm UV}} dz\, a^3(z) f_n^\dagger f_k = \delta_{n,k} , \tag{1.1.10}$$

we can rewrite the effective Lagrangian (eq. (1.1.6)) in the form

$$\mathscr{L}_4(x) = \sum_n \Big[\partial_\mu \phi_n^\dagger \partial^\mu \phi_n - m_n^2 \phi_n^\dagger \phi_n \Big] . \tag{1.1.11}$$

The effective $4D$ description of our theory is thus simply given in terms of an infinite KK tower of $4D$ scalar fields with masses m_n. Notice that the $4D$ modes ϕ_n satisfy the usual Klein–Gordon equation $(\partial_\mu \partial^\mu + m_n^2)\phi_n = 0$.

[1] For simplicity we considered only the case with localized terms and generalized boundary conditions. The other cases, with the usual Neumann or Dirichlet boundary conditions, can be treated analogously.

Following the same strategy one can also handle interaction terms in the KK approach. For example, a quartic interaction of the form

$$S_5^{int} = \int_{z_{IR}}^{z_{UV}} dz\, \sqrt{g}\, \left(-\lambda_5 |\Phi|^4\right) , \tag{1.1.12}$$

gives a corresponding interaction term for the KK modes in the effective description

$$\mathscr{L}_4^{int} = -\lambda_5 \sum_{k,l,m,n} \phi_k^\dagger \phi_l^\dagger \phi_m \phi_n \int_{z_{IR}}^{z_{UV}} dz\, \sqrt{g} f_k^\dagger f_l^\dagger f_m f_n \,. \tag{1.1.13}$$

1.2 Gauge Fields

In this section we will consider a non-Abelian $5D$ gauge theory. The bulk gauge group G is taken to be a compact Lie group with generators t^A normalized such as $2\,\mathrm{Tr}[t^A\, t^B] = \delta^{AB}$. Moreover, we assume that G is broken to two subgroups H and H' respectively at the IR and at the UV boundary. This symmetry breaking is obtained by imposing suitable boundary conditions on the gauge fields, as we will discuss later. The action reads[2]

$$S = \frac{1}{2\, g_5^2} \int_{z_{IR}}^{z_{UV}} dz\, a(z) \mathrm{Tr}\left[-F_{\mu\nu} F^{\mu\nu} + 2 F_{\mu z} F_z^\mu\right] , \tag{1.2.1}$$

where the gauge field strength is $F_{MN} = F_{MN}^A t^A = \partial_M A_N - \partial_N A_M - i[A_M, A_N]$ with $A_M = A_M^A t^A$. As long as we do not introduce a gauge-fixing term, we can extract the allowed boundary conditions by varying the action in eq. (1.2.1):

$$\begin{aligned} \delta S = & \frac{2}{g_5^2} \int_{z_{UV}}^{z_{IR}} dz\, \mathrm{Tr}\left[\delta A^\mu \left(a\, D^\nu F_{\nu\mu} + D_z(a\, F_{\mu z})\right) - \delta A_z \left(a\, D^\mu F_{\mu z}\right)\right] \\ & - \frac{2}{g_5^2} \mathrm{Tr}\left[a\, F_{\mu z} \delta A^\mu\right]_{z_{IR}} + \frac{2}{g_5^2} \mathrm{Tr}\left[a\, F_{\mu z} \delta A^\mu\right]_{z_{UV}} , \end{aligned} \tag{1.2.2}$$

where we defined $D_M \equiv \partial_M - i[A_M, \cdot\,]$. To cancel the boundary variations and obtain the non-Abelian Maxwell equations in the bulk two possibilities are given. At each boundary and for each component A^A of the gauge field we can take either Dirichlet ($A_\mu^A = 0$) or Neumann ($F_{\mu z}^A = 0$) boundary conditions. The first choice induces a breaking of the transformations generated by t^A, while the symmetry is unbroken in the second case. It is now straightforward to derive the correct boundary conditions for the gauge fields: the components associated to the unbroken subgroups H and H' must satisfy Neumann conditions at the corresponding boundary, while the components related to the G/H and G/H' cosets satisfy Dirichlet conditions.

[2] In this chapter and in the next one we use a non-canonical normalization for gauge fields and fermions (see also eq. (1.3.3)). This normalization ensures that the dimensions of the fields are the same in $5D$ and in the $4D$ effective action and will be useful within the holographic approach (see footnote 4 in chapter 2).

The boundary conditions derived before and the bulk equations of motion get modified if, as usual, a gauge-fixing term is introduced into the action. Within the KK description, it is common to use a generalized form of ξ-gauge:[3]

$$\mathscr{L}_{g.f.} = -\frac{a(z)}{g_5^2 \xi} \mathrm{Tr}\left[\partial_\mu A^\mu - \xi a^{-1}(z)\partial_z(a(z)A_z)\right]^2 . \tag{1.2.3}$$

From a $4D$ point of view, $\mathscr{L}_{g.f.}$ is precisely the gauge-fixing term defining a ξ-gauge for the infinite gauge symmetry groups associated to the KK levels of the $5D$ gauge fields A_μ. Moreover, the gauge-fixing in eq. (1.2.3) permits to cancel the quadratic mixing between A_μ and A_z, thus simplifying the bulk EOM's which, at the quadratic level, take the form

$$\begin{cases} \partial_\nu \partial^\nu A_\mu^A + \left(\frac{1}{\xi} - 1\right) \partial_\mu \partial^\nu A_\nu^A - a^{-1}(z)\partial_z\left(a(z)\partial_z A_\mu^A\right) = 0 , \\ \partial_\mu \partial^\mu A_z^A - \xi \partial_z\left(a^{-1}(z)\partial_z(a(z)A_z^A)\right) = 0 . \end{cases} \tag{1.2.4}$$

The Neumann and Dirichlet boundary conditions are modified by the gauge-fixing term and become respectively

$$\begin{cases} \partial_z A_\mu = 0 \\ A_z = 0 \end{cases} , \qquad \text{and} \qquad \begin{cases} A_\mu = 0 \\ \partial_z(a(z)A_z) = 0 \end{cases} . \tag{1.2.5}$$

The Fadeev–Popov gauge-fixing procedure requires also the introduction of anticommuting ghost fields in the $5D$ theory. The ghost action corresponding to the ξ-gauge in eq. (1.2.3) is given by

$$\mathscr{L}_{gh} = -2\, a(z)\, \mathrm{Tr}\left[\omega^* \partial_\mu D^\mu \omega - \omega^* \xi a^{-1}(z)\partial_z(a(z)D_z\omega)\right] , \tag{1.2.6}$$

where the components of the ghost fields $\omega(x,z) = \omega^A t^A$ and $\omega^*(x,z) = \omega^{*A} t^A$ satisfy the same boundary conditions as the corresponding A_μ^A components.

Some commonly used gauge choices can be obtained from the gauge-fixing term in eq. (1.2.3) assigning particular values to ξ. For $\xi = 0$ one gets the Landau gauge $\partial^\mu A_\mu^A = 0$, whereas for $\xi = 1$ a $5D$ generalization of the Feynman gauge is obtained. Another useful gauge choice is the unitary gauge which is obtained in the limit $\xi \to \infty$ and corresponds to the condition $\partial_z(a(z)A_z) = 0$.

Before discussing the whole structure of the $4D$ KK spectrum, it is important to analyze the massless states of the theory which are closely related to the pattern of gauge symmetry breaking. Of course, the existence of a zero mode for a given gauge field component is determined by the boundary conditions which the latter has to satisfy. Massless modes for a given field component A^A are present in two cases, namely when Neumann or Dirichlet boundary conditions are imposed on both boundaries.

In the first case (NN boundary conditions) a massless $4D$ gauge field coming from A_μ^A is present whose wave function is flat $f_0 \propto 1$ (see eq. (1.2.4)). This is related to the fact that

[3] Other forms of gauge-fixing will be considered in section 2.2 and section 5.1.

Neumann boundary conditions do not break the gauge symmetry at the boundaries and lead to an effective theory with an explicit gauge invariance. As required by consistency, also the ghosts admit a zero mode with flat wave function.[4] On the other hand, the A_z^A component of the gauge field does not give any massless $4D$ state.

In the second case (DD boundary conditions) the reversed situation happens. The A_μ^A components and the ghosts do not admit a zero mode, while a massless $4D$ scalar coming from A_z^A is present whose wave function is $f_0 \propto a^{-1}(z)$. These scalar states play an important role in many $5D$ models, and in particular they are identified with the SM Higgs field in the GHU scenario, as we will widely discuss in the next chapters. An interesting property of the scalar zero mode is the fact that its wave function is in general not flat. In particular, in the relevant case of AdS_5 metric, the massless mode has a wave function localized towards the IR boundary ($f_0 \propto z/L$), and this feature allows to build Yukawa interactions with a natural hierarchical structure in the context of warped GHU models (see for instance [18, 19, 20]).

To study the spectrum of massive modes it is convenient to work in the unitary gauge. The condition $\partial_z(a(z)A_z) = 0$ implies that no massive scalar modes are present (only a massless scalar can be allowed depending on the boundary conditions, as discussed before). The would-be Goldstone bosons, which arise at the massive level in an arbitrary ξ-gauge and are associated to the non-linearly realized gauge symmetries, are decoupled in the unitary gauge. Similarly, no massive $4D$ ghost mode appears. The physical spectrum of massive states is thus given by a KK tower of massive $4D$ gauge fields. Of course, the detailed structure of the mass levels depends on the warping factor and on the boundary conditions. The exact mass spectrum for the flat space case will be discussed in chapter 3; for the RS case see for example [40].

1.3 Fermions

Let us now consider a $5D$ fermion field $\Psi(x, z)$. The $5D$ Clifford algebra is generated by the $5D$ gamma matrices

$$\Gamma^\mu = \gamma^\mu\,, \qquad\qquad \Gamma^z = -i\gamma_5\,, \tag{1.3.1}$$

where γ^μ are the usual $4D$ gamma matrices and $\gamma_5 = i\gamma^0\gamma^1\gamma^2\gamma^3$ is the $4D$ chirality matrix. Differently from the $4D$ case, in 5 dimensions a Weyl condition (or a Majorana condition) can not be imposed on the spinors, thus the smallest representation of the Clifford algebra is a spinor with 4 independent complex components, which corresponds to a Dirac spinor in $4D$. However, adopting a $4D$ point of view, a $5D$ spinor can be decomposed in two

[4] Notice that the flatness of the wave functions ensures the universality of the gauge couplings which is required if an unbroken gauge symmetry is present in the effective theory.

chiral components

$$\Psi = \frac{1-\gamma_5}{2}\Psi + \frac{1+\gamma_5}{2}\Psi \equiv \Psi_L + \Psi_R\,, \tag{1.3.2}$$

where, in our conventions, the L and R components satisfy $\gamma_5\Psi_{R,L} = \pm\Psi_{R,L}$.

In order to define spinors on a warped space, we have to introduce the vielbein e_M^A which is related to the $5D$ metric by $g_{MN} = e_M^A e_N^B \eta_{AB}$. Choosing the vielbein as $e_A^M = \delta_A^M/a(z)$, we can compute the spin connection ω_{MAB} whose non-vanishing components are given by $\omega_{\mu az} = (\eta_{\mu a}/a(z))\partial_z a(z)$.

The action for the bulk fermion Ψ takes the form[5]

$$S_5 = \frac{1}{g_5^2}\int_{z_{\rm UV}}^{z_{\rm IR}} dz\ \sqrt{g}\ \left[\frac{i}{2}\overline{\Psi}e_A^M\Gamma^A D_M\Psi - \frac{i}{2}(D_M\Psi)^\dagger\Gamma^0 e_A^M\Gamma^A\Psi - M\overline{\Psi}\Psi\right], \tag{1.3.3}$$

where we defined the covariant derivative $D_M = \partial_M + \frac{1}{8}\omega_{MAB}[\Gamma^A,\Gamma^B]$.

As done in the previous sections, the bulk equations of motion and the boundary conditions can be obtained from the variation of the action:

$$\begin{aligned}\delta S_5 = {} & \frac{1}{g_5^2}\int_{z_{\rm UV}}^{z_{\rm IR}} dz\ \sqrt{g}\ \left[\delta\overline{\Psi}\mathcal{D}\Psi + \overline{\mathcal{D}\Psi}\delta\Psi\right] \\ & + \frac{1}{2g_5^2}\int d^4x\ a^4(z)\left(\overline{\Psi}_L\delta\Psi_R + \overline{\delta\Psi}_R\Psi_L - \overline{\Psi}_R\delta\Psi_L - \overline{\delta\Psi}_L\Psi_R\right)\Big|_{z_{\rm UV}}^{z_{\rm IR}},\end{aligned} \tag{1.3.4}$$

where $\mathcal{D}$ is the $5D$ Dirac operator. The choice of boundary conditions for the fermions is slightly more subtle with respect to the scalar and gauge field cases. In order to set to zero the boundary terms in eq. (1.3.4) one can impose Dirichlet conditions for either Ψ_R ($\Psi_R = 0$) or Ψ_L ($\Psi_L = 0$), independently at the two boundaries. The conditions for the non-Dirichlet fields can not be arbitrarily chosen, but are determined by the bulk equations of motion. This is a consequence of the linearity of the bulk equations which mix the R and L components of the fermion field:

$$\left[\partial_z + 2\frac{\partial_z a(z)}{a(z)} \pm a(z)M\right]\Psi_{L,R} = \pm i\not{\partial}\,\Psi_{R,L}\,. \tag{1.3.5}$$

An important issue to be addressed is the existence of massless modes in the spectrum of the $4D$ effective theory. Using the KK approach we expand the L and R components of the field Ψ as

$$\Psi_{R,L} = \sum_n \psi_{R,L}^n(x) f_{R,L}^n(z)\,, \tag{1.3.6}$$

where the $4D$ degrees of freedom $\psi_{R,L}^n(x)$ satisfy the usual Dirac equation

$$i\not{\partial}\,\psi_{R,L}^n(x) = m_n\psi_{R,L}^n(x)\,. \tag{1.3.7}$$

[5]The inclusion of a mass term into the action can present some subtleties when the $5D$ segment is realized through an orbifold contruction. This point will be discussed in detail in section 1.4.1.

Solving the bulk equation (1.3.5) for the zero modes ($m_0 = 0$) is now straightforward, in fact the R and L components decouple and we get

$$\left[\partial_z + 2\frac{\partial_z a(z)}{a(z)} \pm a(z)M\right] f^0_{L,R}(z) = 0\,, \tag{1.3.8}$$

whose solutions are given by

$$f^0_{L,R}(z) = \frac{c_{L,R}}{a^2(z)} \exp\left\{\mp M \int_{z_{\rm UV}}^{z} dz'\, a(z')\right\}\,, \tag{1.3.9}$$

where $c_{L,R}$ are normalization constants. It is thus clear that a zero mode is present for a given component only if it does not vanish (has no Dirichlet conditions) at both boundaries. In this case the boundary conditions, which trivially coincide with the bulk EOM's as explained before, are obviously satisfied. Notice moreover that the wave function of the zero modes depends on the bulk mass M so that one can obtain states with different localizations by simply varying M.

It is important to stress that, although the $5D$ fermion field is a Dirac spinor and contains both R and L components, the compactification on a segment allows to obtain chiral fermions in the effective theory. This is a noticeable feature of such kind of constructions and constitutes a fundamental ingredient for the construction of realistic models in $5D$.

Finally, the massive part of the $4D$ spectrum is given by pairs of R and L spinors with the same mass which form a KK tower of Dirac fermions.

1.4 Orbifold Compactifications

A wide class of models with extra dimensions are built on spaces with a factorizable geometry $\mathcal{M}_4 \times \mathcal{C}_d$, where $\mathcal{M}_4$ is the ordinary $4D$ Minkowski space–time and $\mathcal{C}_d$ is a compact d-dimensional space. One of the simplest examples of such spaces is the cylinder $\mathcal{M}_4 \times S^1$, which is a smooth $5D$ space. However it is often useful to consider compactifications on spaces with singularities and boundaries (as we did in the preceding sections), as for example on the flat segment $\mathcal{M}_4 \times I$, where I is a 1-dimensional flat interval.

Among the non-smooth spaces a prominent role, in the context of model building, is played by orbifolds. Let us consider a smooth d-dimensional manifold $\mathcal{C}_d$ and a discrete group of isometries $\mathcal{K}$ which acts *non-freely* on it. The orbifold $\mathcal{C}_d/\mathcal{K}$ is obtained by modding out $\mathcal{C}_d$ by $\mathcal{K}$ or, in other words, by identifying points in $y \in \mathcal{C}_d$ which are connected by the $\mathcal{K}$ action: $y \sim k(y)$, with $k \in \mathcal{K}$. The fact that the $\mathcal{K}$ group acts non-freely on $\mathcal{C}_d$ means that some fixed points y_i are present for which $k(y_i) = y_i$ for some k; these points constitute the singularities of the orbifold.

Some simple examples of orbifolds are the $d = 1$ orbifold $S^1/\mathbf{Z}_2$, which has the structure of a flat 1-dimensional interval, and the $d = 2$ flat spaces $T^2/\mathbf{Z}_n$ (with $n = 2, 3, 4, 6$) which have the shape of a "pillow" with 4 ($n = 2$ case) or 3 ($n = 3, 4, 6$ cases) conical singularities.

In order to define a field theory on $\mathcal{M}_4 \times \mathcal{C}_d/\mathcal{K}$, we have to embed the $\mathcal{K}$ symmetry into the field theory built on the smooth space $\mathcal{M}_4 \times \mathcal{C}_d$. Given a field Φ on $\mathcal{M}_4 \times \mathcal{C}_d$, the action of $k \in \mathcal{K}$ on it is

$$\Phi(x, y) \to \Phi^k(x, y) = K(k)\Phi(x, k^{-1}(y)) . \tag{1.4.1}$$

The $K(k)$ elements are given by some symmetries of the theory and form a representation of the $\mathcal{K}$ group.[6] The orbifold theory is obtained imposing the theory to be invariant under the action of the group $\mathcal{K}$. In other words we must restrict the field configurations to those which are invariant under $\mathcal{K}$:

$$\Phi(x, k(y)) = K(k)\Phi(x, y) , \tag{1.4.2}$$

for any $k \in \mathcal{K}$.

1.4.1 The $S^1/\mathbf{Z}_2$ Orbifold

In this section we will analyze in detail the simplest example of orbifold $S^1/\mathbf{Z}_2$, which will be used later on to construct a realistic $5D$ model.

First of all, we briefly review how to construct a theory on the smooth manifold $\mathcal{M}_4 \times S^1$. The circle S^1 can be simply obtained from the real line $\mathbb{R}$ identifying the points connected by a translation of $2\pi R$. The fundamental domain of S^1 is thus given by the interval $[0, 2\pi R)$. To define a field theory on $\mathcal{M}_4 \times S^1$ we must require that the fields are left invariant under a translation $\tau : y \to y + 2\pi R$ up to a symmetry transformation T:

$$\Phi(x, \tau(y)) = \Phi(x, y + 2\pi R) = T\Phi(x, y) . \tag{1.4.3}$$

This particular kind of construction is known as Scherk–Schwarz compactification [41] and can be used to break part of the original symmetries of the theory.[7]

As an example of Scherk–Schwarz compactification, we consider a complex scalar Φ with a $U(1)$ symmetry. We can impose the following condition under translations

$$\Phi(x, y + 2\pi R) = e^{-2i\pi\alpha}\Phi(x, y) , \tag{1.4.4}$$

where α is an arbitrary phase. Values of α which differ by 1 are of course equivalent ($\alpha \sim \alpha + 1$), moreover using the fact that $\Phi \to \Phi^\dagger$ is a symmetry we can further identify $\alpha \sim -\alpha$, restricting α to the interval $[0, 1/2]$.

[6] The $K(k)$ elements can in principle be either global or local symmetries. However in the following we will consider only global transformations.

[7] In general, Scherk–Schwarz compactifications can be realized when the compact space $\mathcal{C}_d$ is obtained by the action of a *freely*-acting group $\mathcal{F}$ on a smooth (possibly non-compact) space $\mathcal{D}_d$, so that $\mathcal{C}_d = \mathcal{D}_d/\mathcal{F}$. The circle S^1 is an example of such spaces being given by $\mathbb{R}/t$, with t the group of translations generated by τ.

We are now able to construct the $S^1/\mathbf{Z}_2$ orbifold by modding out the circle S^1 with the $\mathbf{Z}_2$ group $\{\mathbb{1}, \zeta\}$, whose non-trivial element acts as $\zeta(y) = -y$. This transformation has two fixed points on the circle $y_1 = 0$ and $y_2 = \pi R$. The fundamental domain of the orbifold is the interval $[0, \pi R]$ and the two fixed points constitute the boundaries of the space. Now we consider a field Φ on $\mathcal{M}_4 \times S^1/\mathbf{Z}_2$ which satisfies the twisted periodicity condition in eq. (1.4.4). We must also introduce a $\mathbf{Z}_2$ symmetry transformation Z (such that $Z^2 = \mathbb{1}$) which implements the action of the ζ element on Φ (see eq. (1.4.1)):

$$\Phi(x, y) \to \Phi^{\zeta}(x, y) = Z\Phi(x, -y)\,. \tag{1.4.5}$$

To ensure consistency, we must require not only our theory to be invariant under the $\mathbf{Z}_2$ symmetry but also the boundary conditions on the fields (eq. (1.4.4)) to be unchanged under a $\mathbf{Z}_2$ transformation.

The invariance under the orbifold projection (eqs. (1.4.5) and (1.4.2)), can also be translated into boundary conditions at the extrema of the segment $[0, \pi R]$. At $y = 0$ we find

$$(\mathbb{1} - Z)\Phi(x, 0) = 0\,, \qquad (\mathbb{1} + Z)\partial_y\Phi(x, 0) = 0\,, \tag{1.4.6}$$

and diagonalizing the matrix Z as $Z = \mathrm{diag}(+1, \ldots, -1, \ldots)$, we get Neumann conditions ($\partial_y\Phi = 0$) for the components with $Z = +1$ parity and Dirichlet conditions ($\Phi = 0$) for the components with $Z = -1$.[8] Analogously at the $y = \pi R$ boundary

$$(\mathbb{1} - TZ)\Phi(x, \pi R) = 0\,, \qquad (\mathbb{1} + TZ)\partial_y\Phi(x, \pi R) = 0\,, \tag{1.4.7}$$

and, defining an effective orbifold projection $Z' \equiv TZ$ at the $y = \pi R$ fixed point, we obtain Neumann or Dirichlet boundary conditions depending on the $Z' = \pm 1$ parity.

Using eq. (1.4.2) and eq. (1.4.3), some consistency conditions can be derived for the representations of the orbifold group $\mathcal{K}$ and of the Scherk–Schwarz group t:

$$\begin{aligned} K(k)T\Phi(x, y) &= \Phi(x, k \cdot \tau(y)) \equiv K_{k\tau}\Phi(x, y) \\ TK(k)\Phi(x, y) &= \Phi(x, \tau \cdot k(y)) \equiv K_{\tau k}\Phi(x, y) \\ TK(k)T\Phi(x, y) &= \Phi(x, \tau \cdot k \cdot \tau(y)) \equiv K_{\tau k\tau}\Phi(x, y)\,. \end{aligned} \tag{1.4.8}$$

In particular the last of the above relations together with the identity $\tau \cdot \zeta \cdot \tau = \zeta$ implies the condition

$$TZT = Z\,. \tag{1.4.9}$$

[8] To derive the boundary conditions we assumed the regularity of the Φ fields. This is valid as long as no boundary localized terms are introduced into the action. If such terms are present the fields have given parity under the orbifold action but are not regular at the fixed points and satisfy mixed boundary conditions (compare the discussion in section 1.1 and in particular eq. (1.1.4)).

To explore the consequences of this condition, it is useful to consider a complex scalar field $\Phi(x, y)$ with Scherk–Schwarz $U(1)$ twist as in eq. (1.4.4). In this case we can impose two unequivalent orbifold conditions

$$\Phi(x, -y) = \pm\Phi(x, y)\,. \tag{1.4.10}$$

The consistency condition (1.4.9) implies $T^2 = 1$, and thus only two (unequivalent) values of the Scherk–Schwarz phase α can be allowed: $\alpha = 0$ which gives $T = 1$, and $\alpha = 1/2$ which gives $T = -1$. This means that we can impose only two types of periodicity conditions on the scalar field

$$\Phi(x, y + 2\pi R) = \pm\Phi(x, y)\,, \tag{1.4.11}$$

or in other words Φ can be periodic or antiperiodic on S^1.

As we saw before, a fermion field compactified on a segment generate a chiral spectrum in the $4D$ effective description. The keypoint of such feature was the fact that, although $5D$ spinors are Dirac spinors, the boundary conditions, which must be imposed when compactifying on a segment, project half of the massless modes leaving a chiral $4D$ spectrum. Of course, the same happens when compactifying a theory containing fermions on an $S^1/\mathbf{Z}_2$ orbifold. The only difference with respect to the segment case is the fact that the boundary conditions now arise from the parity operation which defines the orbifold. This also implies that the set of possible boundary conditions is more constrained than in the interval case.

Let us see in detail how the orbifold acts on fermions. Invariance under a parity transformation leads to the condition on a fermion Ψ:

$$\Psi(x, -y) = \pm\gamma_5\Psi(x, y)\,, \tag{1.4.12}$$

where the $\pm$ sign can be arbitrarily chosen. It is evident that R and L components must satisfy different (opposite) parity conditions, so that, if the $+$ sign is chosen in eq. (1.4.12), Ψ_R is even while Ψ_L is odd, and the reversed situation happens when choosing the $-$ sign.

As a consequence of the different parities of Ψ_R and Ψ_L, a simple bulk mass term of the form $m\overline{\Psi}\Psi$ (see eq. (1.3.3)) is not invariant under the orbifold projection and thus is not allowed into the action. This problem can be overcome allowing the mass parameter to be odd under parity, so that the whole mass term becomes even and can be included in the Lagrangian (see for instance [42, 17]).

In the simple case of a fermion field on a flat $S^1/\mathbf{Z}_2$ orbifold, it is easy to recognize that only one chiral zero mode is present, namely the one which corresponds to the even chiral component (see eq. (1.3.9)). The orbifold projection is thus an effective way to obtain a chiral $4D$ spectrum starting from a $5D$ theory.

1.4.2 Gauge Theories on $S^1/\mathbf{Z}_2$

An important aspect of orbifold compactifications is the possibility of using the orbifold condition to break some global or local symmetries. In general, a condition similar to the ones in eq. (1.4.2) or in eq. (1.4.3), of the form

$$\Phi(x, y'(y)) = \mathcal{T}\Phi(x, y)\,, \tag{1.4.13}$$

can restrict the symmetry related to Φ since allowed transformation $\Phi \to \Phi'$ must preserve eq. (1.4.13):

$$\Phi'(x, y'(y)) = \mathcal{T}\Phi'(x, y)\,. \tag{1.4.14}$$

In the case of global transformations $\Phi' = g\Phi$, only those g which commute with $\mathcal{T}$ are allowed, and the symmetry group is restricted to the subgroup which commutes with $\mathcal{T}$. In the case of local transformations, $\Phi' = g(x, y)\Phi$, from eq. (1.4.13) we get the condition

$$g(x, y'(y))\mathcal{T} = \mathcal{T}g(x, y)\,. \tag{1.4.15}$$

Let us now consider the $S^1/\mathbf{Z}_2$ orbifold we constructed before. In this case the condition (1.4.13) comes from the $\mathbf{Z}_2$ transformation (1.4.5). The local transformations will be given by a non-Abelian Lie group $\mathcal{G}$ with generators t^A, so that a generic transformation can be written as

$$g(x, y) = e^{i\alpha_A(x,y)t^A}\,. \tag{1.4.16}$$

Imposing eq. (1.4.13) we get

$$\alpha_A(x, -y)t^A = Z\alpha_A(x, y)t^A Z^{-1}\,, \tag{1.4.17}$$

which means that we are imposing a parity condition on the gauge parameters α_A. The unbroken gauge subgroup will be given by the transformations whose gauge parameter is even under parity. In the effective $4D$ theory, only these unbroken transformations will show up as gauge symmetries, while the transformations associated to the odd generators will be non-linearly realized.

We can now consider the gauge fields $A_M = A_M^A t^A$ associated to the gauge symmetry group $\mathcal{G}$. The orbifold action imposes the following conditions on A_M

$$A_\mu(x, -y) = ZA_\mu(x, y)Z^{-1}\,, \qquad A_y(x, -y) = -ZA_y(x, y)Z^{-1}\,, \tag{1.4.18}$$

where the relative $-$ sign between the μ and y components is due to the parity action. Diagonalizing the above conditions, one finds that the gauge field components can be either even or odd under parity according to the fact that the matrix Z commutes or anticommutes with the corresponding generators. Of course, the condition (1.4.18) matches the one in eq. (1.4.17), in the sense that even (odd) gauge fields components correspond to even (odd) gauge parameters, and eq. (1.4.18) is preserved by gauge transformations. It

is also clear that gauge field zero modes correspond to the even field components and thus to the unbroken gauge subgroup. On the contrary, scalar zero modes coming from the internal component of the gauge field are associated to the broken part of the gauge group which gives an odd A_μ but an even A_y (compare the analysis in section 1.2).

Finally the ghost fields, whose Lagrangian is given in eq. (1.2.6), satisfy the orbifold conditions

$$\omega(x,-y) = Z\omega(x,y)Z^{-1}\,, \qquad \omega^*(x,-y) = Z\omega^*(x,y)Z^{-1}\,, \tag{1.4.19}$$

which gives the same conditions as the corresponding A_μ gauge fields.

1.5 The Wilson Line Interpretation

Let us now consider again the Scherk–Schwarz compactification of a complex scalar field on S^1. An interesting property of the Scherk–Schwarz twist, is the fact that, when the $U(1)$ symmetry is local, the phase shift in eq. (1.4.4) can be reabsorbed by a *non-periodic* gauge transformation [28]

$$\Phi(x,y) \to \Phi'(x,y) = e^{i\alpha\frac{y}{R}}\Phi(x,y)\,. \tag{1.5.1}$$

This transformation, however, also changes the A_y component of the gauge field which gets a VEV

$$A_y \to A'_y = A_y + \frac{\alpha}{R}\,. \tag{1.5.2}$$

In other words two equivalent descriptions of the model can be used: it can be viewed as a compactification with a twist associated to the $2\pi R$ translation and no background for A_y, or a compactification with usual periodicity conditions and a non-trivial VEV for the A_y field. Notice that the A_y background, which corresponds to a flat field strength $F = 0$, is not a gauge-invariant quantity. To construct a gauge invariant operator we must consider the Wilson loop[9]

$$\mathcal{W} = \exp\left\{ i\int_0^{2\pi R} A_y dy \right\}\,. \tag{1.5.3}$$

In the case of the $S^1/\mathbf{Z}_2$ orbifold compactification, we can again perform a non-periodic gauge transformation (as in eqs. (1.5.1) and (1.5.2)) obtaining a theory without a Scherk–Schwarz twist but with modified orbifold boundary conditions for A_y. In fact, using the orbifold condition $A_y(-y) = -A_y(y)$, we get from eq. (1.5.2)

$$A'_y(x,-y) = -A'_y(x,y) + \frac{2\alpha}{R}\,. \tag{1.5.4}$$

[9]Notice that $\mathcal{W}$ is invariant only under periodic gauge transformations. A fully covariant quantity will be defined in section 1.5.1 (eq. (1.5.15)).

The action of the orbifold ζ transformation on A'_y is then the composition of a parity operation and of a non-periodic gauge transformation with parameter $\frac{2\alpha}{R}y$. Correspondingly the ζ action on the Φ field is modified:

$$\Phi'(x,y) \to \Phi'^{\zeta}(x,y) = \pm e^{2i\frac{\alpha y}{R}}\Phi'(x,-y)\,. \tag{1.5.5}$$

This transformation rule is compatible with the periodicity condition only for $\alpha = 0$ or $\alpha = 1/2$, and in this way we recover the conditions on α we already encountered in the previous section.

As we discussed before, the Scherk–Schwarz twist can be interpreted as a Wilson line connecting the two fixed points (see eq. (1.5.3)), however in this case the Wilson line can take only discrete values:

$$\mathcal{W} = \exp\left\{i\int_0^{2\pi R} A_y\, dy\right\} = \pm 1\,. \tag{1.5.6}$$

1.5.1 The non-Abelian Case

As we have shown, in the case of a $U(1)$ gauge theory compactified on S^1, a continuous Wilson loop is present. An important feature is the fact that the Wilson loop value, or equivalently the phase α, being related to the VEV of A_y, is not a free parameter of the theory, but rather a dynamical quantity whose value is determined by the dynamics of the theory itself.

From a phenomenological point of view the existence of such degrees of freedom is very appealing. Being associated to the A_y component of the gauge field, they appear as scalar fields in the $4D$ effective description, but at the same time their interactions are severely constrained by the higher-dimensional gauge invariance. Moreover, deriving essentially from a Wilson line phase, these scalars have an intrinsic *non-local* nature which protects them from divergences. In particular they do not have a tree-level mass term and their effective potential is finite at all orders. It is thus clear that all these properties make them a possible candidate to give the Higgs field in extra-dimensional models (this is the gauge–Higgs unification scenario which we will thoroughly discuss in chapter 3).

On the other hand, when an orbifold condition is imposed in the $U(1)$ case, α can not take arbitrary values and a discrete Wilson line appears. Different values of α now define different theories and are no more determined dynamically. Continuous Wilson lines, however, can be present in orbifold compactifications when a non-Abelian gauge invariance is included as we will discuss in the following.

Let us consider a complex scalar field Φ in the fundamental representation of a non-Abelian gauge group $\mathcal{G}$. As a first step we will consider a compactification on S^1. The orbifold condition in eq. (1.4.3) can straightforwardly be generalized to the non-Abelian case

$$\Phi(x, y + 2\pi R) = e^{2i\pi\beta}T\Phi(x,y)\,, \tag{1.5.7}$$

where T is a global transformation and we also included a phase factor $e^{2i\pi\beta}$ which is compatible with the symmetries of the action. The corresponding condition on the gauge fields is

$$A_M(x, y + 2\pi R) = T A_M(x, y) T^\dagger . \tag{1.5.8}$$

Under a gauge transformation $g(x, y)$ the T matrix changes as

$$T' = g(x, y + 2\pi R) T g^\dagger(x, y) . \tag{1.5.9}$$

In order to ensure T' to be independent of the coordinates, $g(x, y)$ must satisfy the condition

$$g^\dagger(x, y + 2\pi R)\partial_M g(x, y + 2\pi R) T = T g^\dagger(x, y)\partial_M g(x, y) . \tag{1.5.10}$$

As discussed in section 1.4.2, the periodicity condition breaks part of the symmetry of the theory. In particular the unbroken (global or local) symmetries are those which leave the boundary conditions unchanged (see eq. (1.4.17)).

As we did in the Abelian case, we can remove the T matrix from the periodicity condition performing a non-periodic gauge transformation. If we rewrite T as $T = \exp\{i\alpha_A t^A\}$, we can set T to the identity through the gauge transformation

$$g(x, y) = e^{-i\alpha_A t^A \frac{y}{2\pi R}} , \tag{1.5.11}$$

which of course satisfies eq. (1.5.10). At the same time the A_y gauge field component gets a constant shift

$$A'_y = g(x, y) A_y g^\dagger(x, y) - \frac{\alpha_A t^A}{2\pi R} . \tag{1.5.12}$$

In analogy to the Abelian case (see eq. (1.5.3)), we can also define a gauge covariant quantity which is the Wilson loop

$$\mathcal{W}(x) = P \exp\left\{ i \int_0^{2\pi R} A_y(x, y) dy \right\} . \tag{1.5.13}$$

Notice that this quantity transforms covariantly only under periodic gauge transformations (as the Abelian Wilson loop in eq. (1.5.3)):

$$\mathcal{W}'(x) = g(x, 0)\mathcal{W}(x) g^\dagger(x, 2\pi R) . \tag{1.5.14}$$

Instead, a fully covariant quantity is given by

$$\widetilde{\mathcal{W}}(x) = \mathcal{W}(x)\, T , \tag{1.5.15}$$

which transforms as

$$\widetilde{\mathcal{W}}'(x) = g(x, 0)\widetilde{\mathcal{W}}(x) g^\dagger(x, 0) . \tag{1.5.16}$$

Going in the gauge in which $\langle A_y \rangle = 0$, it is easy to show that the eigenvalues of the Wilson loop $\widetilde{\mathcal{W}}$ are independent of the coordinates. These eigenvalues, commonly called

non-integrable phase factors, are gauge invariant quantities (see eq. (1.5.16)) and constitute the non-Abelian analogue of the Abelian α phase.

Let us now discuss what happens in the $S^1/\mathbf{Z}_2$ orbifold case. The orbifold action on scalars is given by eq. (1.4.5), while the condition on gauge fields is in eq. (1.4.18). The consistency condition in eq. (1.4.9) in the non-Abelian case becomes

$$e^{4i\pi\beta}TZT = Z\,. \tag{1.5.17}$$

This condition imposes some constraints on the allowed boundary conditions or equivalently on the values of the non-integrable phases. Two interesting cases are given by the choices $\beta = 0$ and $\beta = 1/2$ which correspond to periodic and antiperiodic conditions for the scalar when $T = \mathbb{1}$. As discussed in section 1.4.2, we can diagonalize the Z matrix defining even t^a ($Zt^aZ = t^a$) and odd $t^{\widehat{a}}$ ($Zt^{\widehat{a}}Z = -t^{\widehat{a}}$) gauge generators under parity. Rewriting the matrix T as $T = \exp\left\{i\alpha_a t^a + i\alpha_{\widehat{b}} t^{\widehat{b}}\right\}$, we get

$$ZTZ = \exp\left\{i\alpha_a t^a - i\alpha_{\widehat{b}} t^{\widehat{b}}\right\} \tag{1.5.18}$$

and the condition (1.5.17) (recall that $Z^2 = \mathbb{1}$) is clearly satisfied by setting $\alpha_a = 0$.

This means that in an orbifold compactification with a non-Abelian gauge group there are still continuous non-integrable phases which are associated to the gauge components which are odd under parity or, in other words, to the part of the gauge invariance which is broken by the orbifold construction. This feature is not surprising, in fact, as we saw before (sect. 1.4.2), scalar zero modes (associated to A_y) are present only for the gauge components which are odd under parity and these zero modes are exactly related to the continuous non-integrable phases.

Chapter 2

The Holographic Approach

In the preceding chapter we studied extra-dimensional theories adopting the KK point of view. As we widely discussed, this standard approach consists in expanding the fields on a basis of mass eigenstates and rewriting the theory in terms of infinite $4D$ KK towers. The low-energy effective theory is simply obtained by integrating out the massive KK states and retaining only the zero modes.

A useful alternative to this approach is the so called "holographic" procedure [36, 33, 37, 38]. It is based on a different, and somewhat "peculiar", choice of degrees of freedom, namely one separates the value $\widehat{\Phi}(x) = \Phi(x, z_{\rm UV})$ of the $5D$ fields at one boundary from the "bulk" degrees of freedom contained in $\Phi(x, z)$ for $z \neq z_{\rm UV}$. By integrating out the latter, one gets an effective holographic Lagrangian for the boundary field $\widehat{\Phi}(x)$ which is not a mass eigenstate but rather a linear combination of all the KK modes. As long as $\widehat{\Phi}(x)$ has a non-vanishing overlap with the zero-mode, however, it can safely be used to describe the lightest state and the holographic Lagrangian is a perfectly valid effective description of the original theory. For any physical process, the holographic theory will give exactly the same results as the standard KK effective theory for the zero-modes.

The peculiar choice of degrees of freedom of the holographic approach clearly owes its origin to the AdS/CFT correspondence [24, 25], which has been conjectured to be applicable also in RS-like models (see [43] for a review). When a dual AdS/CFT interpretation is possible, holography is necessary [25] to compute correlators of the dual $4D$ theory, because the boundary values of $5D$ fields are sources for the $4D$ operators. However, it is important to stress that the holographic procedure we will describe is just a technical tool which can be applied to any $5D$ theory even if no $4D$ dual exists as it is the case, for instance, when the space is flat.

Though completely equivalent to the standard KK decomposition, the holographic approach offers an elegant and compact description of a $5D$ theory, and moreover it proves much simpler for certain applications. An example is the calculation of "universal" corrections induced by KK exchange [33, 44] (see also [27, 19] for the application to more realistic

models). Another interesting application is the determination of three-point functions and in particular of the $Z\bar{b}b$ vertex [20] (see also [27] and appendix E).

In this chapter we will describe in detail the holographic procedure beginning with the simple case of a $5D$ scalar and arriving to the more complex and interesting cases of fermion and gauge fields [38]. Particular attention will be devoted to the treatment of the scalar degrees of freedom which may arise, depending on the boundary conditions, from the fifth gauge-field component. As a matter of fact, these scalars play an important role in many interesting models, and a holographic effective theory in which they are included can then have very useful applications.

In the (flat or warped) models of GHU, for instance, the scalars which come from an extended EW gauge group in $5D$ are interpreted as the Higgs field (see section 3.1) and its dynamics could be described by the holographic effective theory which we discuss. Moreover, when an AdS/CFT interpretation is possible, the scalars correspond to (possibly pseudo-)Goldstone bosons of a spontaneously broken global symmetry of the dual $4D$ theory [18]. This is the reason why GHU models in warped space also describe a Composite Higgs. The simplest version of AdS/QCD (discussed in detail in [35]) is also based on this observation, the mesons arise from the fifth component of $SU(3)_L \times SU(3)_R$ gauge fields when the bulk group is broken at the IR to its vector subgroup. In this case, the holographic effective Lagrangian is interpreted as the one of $\chi\mathbf{PT}$.

In this chapter we will also present some applications of the holographic procedure [38]. First of all we will derive the tree-level effective action for a generic $5D$ gauge theory, and we will use this result to compute the one-loop Higgs effective potential in GHU models. As a second example, we will apply the holographic approach to a simple model of AdS/QCD, deriving the $\chi\mathbf{PT}$ Lagrangian at tree-level. From a more theoretical point of view, we will study the consequences of introducing a CS term into the $5D$ Lagrangian, showing that it makes a gauged Wess–Zumino–Witten term to appear in the holographic Goldstone-bosons action.

2.1 The Example of a Scalar

To introduce the concepts of the holographic approach avoiding any technical complication we start with the simple case of a scalar field on a flat space.[1] Our starting point is the standard $5D$ action

$$S[\Phi] = \frac{1}{2}\int_{z_{UV}}^{z_{IR}} dz \left[\partial_\mu \Phi \partial^\mu \Phi - (\partial_z \Phi)^2 - m_\phi^2 \Phi^2\right], \tag{2.1.1}$$

[1] By restricting to flat space, we will avoid the complication due to the localized mass-terms which are commonly introduced in warped compactifications in order to obtain a zero-mode (compare section 1.1). The general treatment of the scalars can be found in the appendix B.

where we omitted the d^4x integral and ∂_z is the derivative along the extra coordinate. The theory is defined by the partition function

$$\mathcal{Z} = \int \mathcal{D}\Phi(x,z)_{b.c.}\, e^{iS[\Phi]}\,, \tag{2.1.2}$$

where the "*b.c.*" subscript means that suitable boundary conditions are imposed on the field configurations one integrates over. The allowed boundary conditions are extracted by varying the action as shown in section 1.1. Two possible boundary conditions can be imposed, namely Neumann ($\partial_z\Phi = 0$) or Dirichlet ($\Phi = 0$) conditions on each brane.

To discuss the holographic approach, we must first of all make a distinction between the two boundaries and treat them in a different way. We will consider a field which is, for the moment, unconstrained at the UV and satisfies a given boundary condition at the IR. We introduce a $4D$ scalar "source" field $\phi(x)$ and an "holographic" path integral, in which the allowed $5D$ field configurations are only those which reduce to $\phi(x)$ at the UV brane. The holographic partition function and the corresponding holographic action are defined as

$$Z\left[\phi(x)\right] \equiv e^{iS_h[\phi(x)]} = \int \mathcal{D}\Phi(x,z)_{\widehat{\Phi}(x)=\phi(x)}\, e^{iS[\Phi]}\,, \tag{2.1.3}$$

where $\widehat{\Phi}(x) \equiv \Phi(x, z_{\rm UV})$ and the IR boundary conditions are understood. It is very easy to make contact with the standard definition (2.1.2) of the partition function which also includes boundary conditions at the UV. Depending on whether Φ is Dirichlet or Neumann we have, respectively

$$\mathcal{Z} = Z\left[\phi(x) = 0\right], \quad \text{or} \quad \mathcal{Z} = \int \mathcal{D}\phi(x)\, Z\left[\phi(x)\right]. \tag{2.1.4}$$

In words, this is just the usual statement that in the Dirichlet case ϕ is a non-dynamical source to be put to zero at the end of the calculation, while Neumann boundary conditions are obtained by making the source dynamical. While the first (Dirichlet) case of eq. (2.1.4) is trivial, one should be careful with the second one. Integrating eq. (2.1.3) in $\mathcal{D}\phi$ as done in eq. (2.1.4) is the same as integrating over the $5D$ field Φ without any boundary condition at the UV. Its variation $\delta\Phi$ is then also unconstrained and hence, to cancel the action variation (see eq. (1.1.2) with $a(z) = 1$), the Neumann boundary condition $[\partial_z\Phi]_{z_{\rm UV}} = 0$ arises as an equation of motion. Notice that, even though the equivalence (2.1.4) has been written in a fully quantum form, we have only proved it at tree-level having shown that the classical equations of motion (including the boundary conditions) are the same.[2]

[2] In section 2.4 we will use holography to compute the 1-loop Higgs effective potential and the result matches the one obtained with the standard KK approach. This success, however, does not rely on the validity of the equivalence at one-loop order because the effective potential is completely determined by the tree-level spectrum.

2.2 Holography for Gauge Fields

Let us now consider a $5D$ gauge theory with gauge group G broken to $H \subset G$ at the IR. As in section 1.2, we take G to be a compact Lie group and call $t^A = \{t^a, t^{\widehat{a}}\}$ its generators normalized as $2\,\mathrm{Tr}[t^A\, t^B] = \delta^{AB}$. The t^a's are the generators of the subgroup H while the $t^{\widehat{a}}$'s generate the right coset G/H, in the sense that any element $g \in G$ can be uniquely decomposed as:

$$g = e^{i\alpha^A t^A} = e^{i\gamma_R^{\widehat{a}} t^{\widehat{a}}} \circ e^{ih_R^a t^a} \equiv \gamma_R[g] \circ h_R[g]\,, \tag{2.2.1}$$

where $h_R[g] \in H$. The gauge action (eq. (1.2.1)), its variation (eq. (1.2.2)) and the determination of the allowed boundary conditions have been discussed in section 1.2. Recalling that field components related to the unbroken gauge subgroup satisfy Neumann boundary conditions, whereas the other components satisfy Dirichlet conditions, at the IR we have[3]

$$(F)^a_{\mu\, z}\,(x, z_{\text{IR}}) = 0\,, \qquad (A)^{\widehat{a}}_{\mu}\,(x, z_{\text{IR}}) = 0\,, \tag{2.2.2}$$

while the UV boundary conditions need not to be specified, at the moment.

Analogously to eq. (2.1.3), the holographic action is defined as

$$Z\,[B_\mu] \equiv e^{iS_h[B_\mu]} = \int \mathcal{D}A_\mu(x,z)_{\widehat{A}_\mu = B_\mu} \mathcal{D}A_z(x,z) \exp\left[iS\,[A]\right], \tag{2.2.3}$$

where $\widehat{A}_\mu = A_\mu(x, z_{\text{UV}})$ and we introduced $4D$ vector sources B^A_μ for each generator of G.[4] As for the scalar, any boundary condition at the UV can be implemented once we have the holographic action (2.2.3). If a given component A^A_μ is Dirichlet we simply have to put the corresponding source B^A_μ to zero, if it is Neumann we have to make it dynamical. If $\left[\delta A^A_\mu\right]_{z_{\text{UV}}} \neq 0$, indeed, the Neumann condition $\left[F^A_{\mu z}\right]_{z_{\text{UV}}} = 0$ arises as an equation of motion in order to cancel the action variation (1.2.2). To recover a standard $5D$ theory with G broken to $H' \subset G$ at the UV, then, we just have to make dynamical the sources associated to H' and put the others to zero.

By construction, the action is invariant under local $5D$ transformations $g(x,z) \in G$ which act on the gauge fields as

$$A_M \to A^{(g)}_M \equiv g\,[A_M + i\,\partial_M]\,g^\dagger\,. \tag{2.2.4}$$

The IR boundary conditions (2.2.2), however, are only H-invariant and hence the allowed transformations must reduce to H at the IR, *i.e.* $g(x, z_{\text{IR}}) = h \in H$. The action and the measure (including the UV constraint $\widehat{A} = B$) in eq. (2.2.3) are invariant under the

[3] At this point we consider a gauge theory without gauge fixing. An appropriate gauge choice will be used in section 2.2.1, where we will also discuss how the boundary conditions in eq. (2.2.2) get modified.

[4] Thanks to the non-canonical normalization of the bulk fields (see footnote 2 in chapter 1), we can obtain sources with the usual dimensions of the $4D$ fields by simply identifying them with the UV values of the bulk fields.

"bulk" local group $\mathcal{G}_B$, which we define as the set of allowed transformations which reduce to the identity at the UV brane, $\mathcal{G}_B \equiv \{g(x,z) \in G : g(x,z_{\rm IR}) \in H\,, g(x,z_{\rm UV}) = \mathbb{1}\}$. Due to the $\mathcal{G}_B$ invariance, the integrand in eq. (2.2.3) has flat directions and the path integral is ill-defined. This requires a gauge-fixing of the local $\mathcal{G}_B$ group which we will discuss in the next subsection.

It is important to remark that the holographic action defined by eq. (2.2.3) is gauge invariant under the full $4D$ local group G in the sense that

$$Z\left[B_\mu^{(\widehat{g})}\right] = Z\left[B_\mu\right]\,, \tag{2.2.5}$$

where $\widehat{g}(x)$ is a generic $4D$ local G transformation. This is easily shown by performing a $5D$ gauge transformation $g(x,z)$ which reduces to $\widehat{g}(x)$ at the UV, $g(x,z_{\rm UV}) = \widehat{g}(x)$, and of course belongs to H, $g(x,z_{\rm IR}) = h(x)$, at the IR.[5] When an AdS/CFT interpretation is possible (as for $a(z) = L/z$ in eq. (1.0.1)), the $5D$ model would be dual to a $4D$ strongly coupled theory with global G invariance and the holographic partition function (2.2.3) would be interpreted as the partition function of the $4D$ theory in the presence of sources B_μ^A for the global currents J_μ^A. Of course, the gauge invariance (2.2.5) is necessary for this interpretation to be possible.

2.2.1 An "Holographic" Gauge-Fixing

To fix the $\mathcal{G}_B$ gauge invariance of eq. (2.2.3) we will go to the axial gauge, in which the fifth component A_z of the gauge field is put to zero. It is clear that any consistent gauge-fixing would lead to the same physical results and one could even not fix the gauge at all as done for instance in [35]. Our choice, however, appears particularly convenient because the scalar degrees of freedom are directly parametrized by a $4D$ Goldstone boson matrix Σ (see eq. (2.2.12)) and the G invariance of the holographic theory is explicit. Moreover, in the axial gauge there are no ghosts and this is useful in view of a possible AdS/CFT interpretation.

Starting from a generic gauge field configuration a unique local transformation $\overline{g}$ exists which puts A_z to zero, *i.e.* $A_z^{(\overline{g})} = 0$, and reduces to the identity on the UV brane. This is the Wilson Line

$$\overline{g}(x,z) \;=\; \mathcal{W}\left(z_{\rm UV}, z\,; A\right) \;\equiv\; \mathrm{P}\left\{\exp\left[-i\int_{z_{\rm UV}}^{z} dz'\, A_z^A(x,z')\, t^A\right]\right\}\,, \tag{2.2.6}$$

on a straight path going from the UV brane to a generic point z. In general, $\overline{g}$ does not belong to the symmetry group $\mathcal{G}_B$ since it does not reduce to H at the IR and therefore

[5] If seen as a map to G/H, $h(x)$ is just the identity. After rotating to the Euclidean, the problem of finding the $5D$ transformation g which permits to prove eq. (2.2.5) is exactly the same of finding a homotopy which deforms into the identity the generic $S^4 \to G/H$ map $\widehat{g}(x)$. We will assume that $\pi_4(G/H)$ is trivial, so that g always exists.

it cannot be used to reach the axial gauge. This was to be expected, of course, given that the theory has to contain physical scalars. In order for $\overline{g}$ to be useful we have to formally restore the full G invariance of eq. (2.2.3) at the IR. To this end we introduce a $4D$ field

$$\Sigma(x) \,=\, \exp\left[i\,\sigma_{\widehat{a}}(x)t^{\widehat{a}}\right]\,, \tag{2.2.7}$$

and change the boundary conditions (2.2.2) by rotating them with $\Sigma^{-1} \in G$:

$$\left(F^{(\Sigma^{-1})}\right)^{a}_{\mu\, z}(x, z_{\rm IR}) = 0\,, \qquad \left(A^{(\Sigma^{-1})}\right)^{\widehat{a}}_{\mu}(x, z_{\rm IR}) = 0\,. \tag{2.2.8}$$

Under IR gauge transformations we take Σ to transform as a Goldstone field

$$\Sigma(x) \,\to\, \Sigma^{(g)}(x) \,=\, \gamma_R\left[g(x, z_{\rm IR}) \circ \Sigma(x)\right]\,, \tag{2.2.9}$$

where $\gamma_R[\cdot]$ is the projector from G to the right G/H coset defined by eq. (2.2.1). It is easily checked that the boundary conditions (2.2.8), given the transformation rule (2.2.9) for the Goldstone-boson field, are now invariant under generic transformations $g(x, z_{\rm IR}) \in G$.

It should be noted that no extra dynamics has been introduced in the theory when we added the Goldstone field Σ. We apparently added $dim(G/H)$ new real $4D$ (axion-like) scalars $\sigma_{\widehat{a}}$, but we simultaneously enlarged the IR gauge group by adding $dim(G/H)$ symmetry transformations. We could put Σ to $\mathbb{1}$ fixing in this way the G/H invariance at the IR and recover the original theory with no Σ field, boundary conditions as in eq. (2.2.2) and restricted gauge invariance. It is worth remarking that a $4D$ Goldstone field localized at the IR would naturally appear if, as usually assumed (see for instance [5, 33, 34]), the symmetry-breaking boundary conditions originate from some localized Higgs multiplet whose massive fluctuations have been decoupled by taking the VEV to infinity. The present discussion could be more directly applied to that case, in which the theory one starts with is fully G-invariant. Our gauge-fixing procedure is however self-consistent even without this interpretation, a more formal derivation can be found in appendix A.

Instead of fixing the gauge group, up to now we have enlarged it. But now that $\overline{g}$ in eq. (2.2.6) belongs to the symmetry group we can easily go through a Fadeev-Popov procedure to fix the gauge. We write

$$1 \,=\, \int \mathcal{D}g(x,z)_{\widehat{g}=\mathbb{1}}\,\delta\left[A_z^{(g)}\right]\,\mathrm{Det}\left\{D_z\left[A^{(g)}\right]\right\}\,, \tag{2.2.10}$$

where the Haar measure of G is understood in the group integral. To prove the above identity one performs the change of variable $g \to g \circ \overline{g}$, so that in the new variable the delta function condition is simply $g = \mathbb{1}$ and the integral only receives contributions from the $g \sim \mathbb{1}$ region. For $g \sim \mathbb{1}$, $dg \sim \Pi_A\, d\alpha_A$ and the identity is immediately demonstrated. The determinant in eq. (2.2.10) could be associated to a ghost action. However, since $A_z^{(g)}$

is the only component of $A^{(g)}$ which enters in $D_z[A^{(g)}]$ and it is fixed to zero by the delta function, the determinant is just a constant which we can drop. As customary, in the axial gauge there are no ghosts.

We now multiply our partition function by "1" written as in eq. (2.2.10) and with very standard manipulations we arrive to

$$Z^{g.f.}[B_\mu] = \int\int \mathcal{D}\Sigma(x)\,\mathcal{D}A_\mu(x,z)_{\widehat{A}_\mu=B_\mu} \exp\left[iS\left[A_\mu, A_z=0\right]\right] . \qquad (2.2.11)$$

For simplicity, in the above equation we did not write the IR boundary conditions on the A_μ integral. Those are given by eq. (2.2.8) and depend on Σ. Note that the action $S\left[A_\mu, A_z=0\right]$ is still invariant under G transformations which are constant along the extra coordinate. If we change variable $A_\mu \to A_\mu^{(\Sigma)}$ in the second functional integral, then, we can further simplify eq. (2.2.11) by moving the dependence on Σ from the IR to the UV brane. We finally get

$$\begin{aligned} Z^{g.f.}[B_\mu] &\equiv \int \mathcal{D}\Sigma(x)\, \exp\left[iS_h\left[B_\mu, \Sigma\right]\right] \\ &= \int\int \mathcal{D}\Sigma(x)\,\mathcal{D}A_\mu(x,z)_{\widehat{A}_\mu=B_\mu^{(\Sigma^{-1})}} \exp\left[iS\left[A_\mu, A_z=0\right]\right] , \end{aligned} \qquad (2.2.12)$$

where the IR boundary conditions are now given by eq. (2.2.2) in which, since $A_z = 0$, we can take $F_{\mu z} = -\partial_z A_\mu$. In eq. (2.2.12) we also defined the holographic action $S_h\left[B_\mu, \Sigma\right]$. When a dual AdS/CFT interpretation is possible this is the effective action for the Goldstone bosons in the presence of sources for the currents.

From our procedure the gauge invariance of eq. (2.2.12) should be automatic. We can immediately check that $S_h\left[B_\mu^{(g)}, \Sigma^{(g)}\right] = S_h\left[B_\mu, \Sigma\right]$. Indeed, due to eq. (2.2.9) $\Sigma^{(g)} = g \circ \Sigma \circ h$ so that

$$\left(B^{(g)}\right)^{((\Sigma^{(g)})^{-1})} = B^{((\Sigma^{(g)})^{-1}\circ g)} = B^{(h^{-1}\circ\Sigma^{-1})} = \left(B^{(\Sigma^{-1})}\right)^{(h^{-1})} . \qquad (2.2.13)$$

Under a generic element of G, the boundary value $\widehat{A}_\mu = B_\mu^{(\Sigma^{-1})}$ of the $5D$ field only rotates with an H transformation. The latter can be removed by a change of variable since both the action and the IR boundary conditions are H invariant. This demonstrates the gauge invariance of S_h and, as a by-product, the gauge invariance of $Z^{g.f.}[B_\mu]$.

2.3 The Tree-Level Effective Action

In the previous section we have shown how to separate the bulk degrees of freedom from the boundary ones, thus rewriting the partition function of a $5D$ theory in terms of $4D$ holographic fields. In this section we will perform a second step: integrating out the bulk degrees of freedom in order to compute the tree-level effective holographic action for a generic $5D$ theory.

As we did in the previous section, first of all we will discuss the case of a scalar field on a flat space. This simple example will be useful to present the main properties of the holographic action, and in particular to show how to extract the $4D$ spectrum of a theory from the holographic description. Afterwards, we will consider the interesting cases of gauge fields and fermions.

2.3.1 Scalar Fields

We consider a $5D$ scalar field whose holographic action $S_h[\phi]$ is defined by eq. (2.1.3). To obtain the effective action we must integrate out the bulk degrees of freedom, namely we must perform the $\mathcal{D}\Phi$ integration in eq. (2.1.3) with the UV conditions $\widehat{\Phi}(x) = \phi(x)$. The integration can be done semi-classically by expanding the Φ field around its classical background $\overline{\Phi}$ which is given by the solution of the bulk equations of motion

$$\partial_\mu \partial^\mu \overline{\Phi} - \partial_z^2 \overline{\Phi} + m_\phi^2 \overline{\Phi} = 0\,, \tag{2.3.1}$$

which satisfies the usual IR boundary conditions and the "holographic" condition $\widehat{\overline{\Phi}}(x) = \phi(x)$ at the UV. The semi-classical expression for the holographic action S_h is thus

$$e^{iS_h[\phi(x)]} = e^{iS[\overline{\Phi}]} \int \mathcal{D}\Phi'(x,z)_{\widehat{\Phi}'(x)=0} \exp\left\{ \frac{i}{2} \int \Phi' \left. \frac{\delta^2 S}{\delta \Phi^2} \right|_{\Phi=\overline{\Phi}} \Phi' + \dots \right\}, \tag{2.3.2}$$

where the path integral is performed over the field $\Phi' \equiv \Phi - \overline{\Phi}$.

In this chapter we will consider only the tree-level effective action, which is obtained by substituting the solution $\overline{\Phi}$ of the equations of motion into the action $S[\Phi]$ and neglecting the corrections coming from the path integral in eq. (2.3.2). Inserting $\overline{\Phi}$ into eq. (2.1.1) and integrating by parts the $(\partial_z \Phi)^2$ term, the bulk term clearly vanishes due to the equations of motion and we are left only with a boundary contribution. The whole tree-level holographic Lagrangian is given by

$$\mathscr{L}_h[\phi] = \frac{1}{2}\, \overline{\Phi} \partial_z \overline{\Phi} \big|_{z_{\rm UV}}\,. \tag{2.3.3}$$

The explicit form of the effective Lagrangian depends on the IR boundary conditions of the field Φ. As shown before, two possibilities are there: the Neumann and the Dirichlet cases. To find the solutions of the equations of motion it is convenient to use a mixed momentum–space representation, namely we perform a Fourier transform along the $4D$ coordinates and express $\overline{\Phi}$ and the Lagrangian in terms of the $4D$ momentum p and of the usual coordinate along the extra dimension z. In the Neumann case the solution of the equations of motion $\overline{\Phi}$ satisfy $\partial_z \overline{\Phi}|_{z_{\rm IR}} = 0$ and is given by

$$\overline{\Phi}(p,z) = \frac{\cos[\omega(z_{\rm IR} - z)]}{\cos[\omega(z_{\rm IR} - z_{\rm UV})]} \phi(p)\,, \tag{2.3.4}$$

where $\omega^2 \equiv p^2 - m_\phi^2$. Substituting this solution into eq. (2.3.3) we find the holographic Lagrangian[6]

$$\mathscr{L}_h[\phi] = \frac{1}{2}\phi(-p)\,\omega\tan[\omega(z_{\rm IR} - z_{\rm UV})]\,\phi(p)\,. \tag{2.3.5}$$

On the other hand, in the Dirichlet case $\overline{\Phi}$ satisfy $\overline{\Phi}|_{z_{\rm IR}} = 0$ and is given by

$$\overline{\Phi}(p,z) = \frac{\sin[\omega(z_{\rm IR} - z)]}{\sin[\omega(z_{\rm IR} - z_{\rm UV})]}\phi(p)\,. \tag{2.3.6}$$

Plugging this solution into eq. (2.3.3) we find

$$\mathscr{L}_h[\phi] = -\frac{1}{2}\phi(-p)\,\omega\cot[\omega(z_{\rm IR} - z_{\rm UV})]\,\phi(p)\,. \tag{2.3.7}$$

An interesting feature of the holographic effective Lagrangian (eqs. (2.3.5) and (2.3.7)) is the fact that it contains an infinite series of higher-order operators (as can be seen by an expansion in p^2) which are induced by the integration of the bulk degrees of freedom.

As we discussed in section 2.1, the dynamical properties of the source ϕ are determined by the UV boundary conditions of the $5D$ field Φ. If Φ has Neumann boundary conditions, the source ϕ has to be treated as a dynamical $4D$ field. This is, of course, the most interesting situation. In fact the source ϕ has a non-trivial overlap with all the KK modes of the $5D$ field Φ, or, in other words, the field ϕ is a linear combination of all the KK states. This also means that the holographic action completely describes the original $5D$ theory at tree level. In particular the spectrum of the theory is simply given by the zeroes of the quadratic term of the Lagrangian in eq. (2.3.5) or eq. (2.3.7) (*i.e.* the zeroes of the inverse propagator of ϕ). When Neumann IR conditions are imposed, we obtain a tower of states with masses $m_n^2 = \pi^2 n^2/\left(z_{\rm IR} - z_{\rm UV}\right)^2 + m_\phi^2$, with $n = 0, 1, \ldots$; whereas in the Dirichlet case we get $m_n^2 = \pi^2\left(n + 1/2\right)^2/\left(z_{\rm IR} - z_{\rm UV}\right)^2 + m_\phi^2$. Is is clear that these spectra coincide with the usual ones for a scalar on a segment. Notice that in the Neumann–Neumann case a zero mode is correctly present in the spectrum.

The case in which Φ has Dirichlet boundary conditions at the UV is in some sense trivial. In this case the source ϕ has no overlap with the KK modes (which obviously vanish at the UV) and the original theory is obtained setting to zero the holographic field thus getting a trivially vanishing effective action. This can be simply understood recalling that in the holographic procedure we integrate out the bulk degrees of freedom and in this case everything is in the bulk because the field Φ is zero at the UV. Nevertheless also in this case we can extract the spectrum of the theory using the holographic procedure. For this purpose, we interpret ϕ as a *static* source coupled with the bulk degrees of freedom and the expressions in eqs. (2.3.5) and (2.3.7) as effective Lagrangians for this source. In this

[6]Notice in eq. (2.3.5) the holographic field ϕ has dimension $[\phi] = 3/2$ and not 1 as a usual $4D$ scalar. To obtain the standard normalization one usually introduce a factor $1/g^2$ in front of the $5D$ action, where g is a constant with dimension $[g] = -1/2$.

case, the spectrum will be no longer given by the zeroes of the quadratic term, but rather by its poles. This is a consequence of having integrated out all the dynamical degrees of freedom (remember that ϕ is now non-dynamical), which means that the KK modes show up as singularities in the effective action.[7] With Neumann IR conditions (eq. (2.3.5)), we obtain a spectrum $m_n^2 = \pi^2 (n + 1/2)^2 / (z_{\rm IR} - z_{\rm UV})^2 + m_\phi^2$, with $n = 0, 1, \ldots$; while in the Dirichlet case (eq. (2.3.7)) $m_n^2 = \pi^2 (n + 1)^2 / (z_{\rm IR} - z_{\rm UV})^2 + m_\phi^2$. Again this spectrum coincides with the usual one.

Interactions

An interesting issue is how to treat interactions within the holographic procedure. As we briefly discussed in section 1.1, in the KK approach an interaction term in $5D$ simply translates into a corresponding interaction among the KK modes in the effective theory. When the heavy states are integrated out to obtain the low energy action for the zero modes, a series of higher order effective interactions arises for the light states.

A similar situation occurs in the holographic approach. In this case it is the integration of the bulk degrees of freedom which generates higher order interaction terms for the holographic fields. It is thus clear that interactions must be treated with a perturbative approach [36], expanding in a series with respect to the coupling constants.

As an example we will introduce a cubic interaction $-\frac{1}{3}\lambda\Phi^3$ into the $5D$ scalar action in eq. (2.1.1). To obtain the full tree-level holographic action we should solve the complete classical bulk equation of motion

$$\partial_\mu \partial^\mu \overline{\Phi} - \partial_z^2 \overline{\Phi} + m_\phi^2 \overline{\Phi} + \lambda \overline{\Phi}^2 = 0 \,, \tag{2.3.8}$$

with $\overline{\Phi}|_{z_{\rm UV}} = \phi$ and usual IR boundary conditions. The presence of a quadratic term in $\overline{\Phi}$ forces us to use a series expansion in λ:

$$\overline{\Phi} = \overline{\Phi}_0 + \lambda \overline{\Phi}_1 + \ldots \,, \tag{2.3.9}$$

where $\overline{\Phi}_i$ are of $\mathcal{O}(\lambda^0)$. At the IR boundary $\overline{\Phi}_i$ satisfy the same condition as Φ, whereas at the UV we have $\overline{\Phi}_0|_{z_{\rm UV}} = \phi$ and hence for $i \geq 1$ we get $\overline{\Phi}_i|_{z_{\rm UV}} = 0$.

[7] To clarify this point it is useful to consider a theory compactified on AdS_5 and its dual $4D$ description (see [37]). In this case, the bulk degrees of freedom correspond to a strongly-coupled nearly conformal sector of the $4D$ theory and the non-dynamical source ϕ corresponds to a classical source coupled to this sector. When the conformal sector is integrated out, we get an effective description in terms of the source. In this description the inverse propagator of ϕ gives the two point function of the CFT operators coupled to the source, and thus its poles correspond to the mass spectrum of the strongly-coupled sector. Notice that when the source ϕ is dynamical (*i.e.* Φ has Neumann boundary conditions at the UV) the situation is much different. In this case the spectrum is given by the eigenstates of system given by the strong sector *and* the field ϕ (and not of the strong sector alone as in the previous case), and the mass levels correspond to the zeroes of the quadratic term in the holographic action.

The $\mathcal{O}(\lambda^0)$ term of the holographic action is of course obtained from eq. (2.3.3). The $\mathcal{O}(\lambda)$ terms S_h^1 are given by

$$S_h^1[\phi] = \lambda \int_{z_{\rm UV}}^{z_{\rm IR}} dz \left[\partial_\mu \overline{\Phi}_1 \partial^\mu \overline{\Phi}_0 - \partial_z \overline{\Phi}_1 \partial_z \overline{\Phi}_0 + m_\phi^2 \overline{\Phi}_1 \overline{\Phi}_0 - \frac{1}{3} \overline{\Phi}_0^3 \right] . \tag{2.3.10}$$

Integrating by parts we get

$$S_h^1[\phi] = \lambda \int_{z_{\rm UV}}^{z_{\rm IR}} dz \left[-\overline{\Phi}_1 (\partial_\mu \partial^\mu \overline{\Phi}_0 - \partial_z \partial_z \overline{\Phi}_0 + m_\phi^2 \overline{\Phi}_0) - \frac{1}{3} \overline{\Phi}_0^3 \right] - \lambda \int d^4x \, \overline{\Phi}_1 \partial_z \overline{\Phi}_0 \Big|_{z_{\rm UV}}^{z_{\rm IR}} . \tag{2.3.11}$$

In eq. (2.3.11) the first term in the square brackets vanishes because $\overline{\Phi}_0$ satisfies the bulk equation of motion at $\mathcal{O}(\lambda^0)$. At the same time the boundary term gives a zero contribution as can be easily shown using the UV and IR boundary conditions of $\overline{\Phi}_i$. Thus, at $\mathcal{O}(\lambda)$, we obtain the simple interaction term

$$S_h^1[\phi] = -\frac{1}{3} \lambda \int_{z_{\rm UV}}^{z_{\rm IR}} dz \, \overline{\Phi}_0^3 . \tag{2.3.12}$$

Interactions due to the exchange of bulk degrees of freedom appear only at higher order in λ. It is interesting to notice that in order to compute the holographic action at first order in the coupling constants we only need the solution of the equation of motion $\overline{\Phi}_0$ of the non-interacting theory.

2.3.2 Gauge Fields

Let us now consider the gauge fields. In this case we will concentrate on the quadratic part of the holographic action. This restriction will simplify the discussion, but at the same time will allow us to obtain some interesting results, such as the computation of the 1-loop effective potential (see section 2.4).

With a bulk group G broken to H at the IR and to H' at the UV the $4D$ dynamical degrees of freedom are the gauge fields B'_μ associated to H' and the Goldstone bosons Σ which parametrize the G/H coset. The action $S_h[B', \Sigma]$ is defined in eq. (2.2.12), one simply has to put to zero the sources associated to G/H'. To compute the quadratic part of S_h at tree-level one has to solve the linearized classical EOM's and then put the solutions back into the quadratic $5D$ action.[8] For what concerns the boundary conditions, one has to impose eq. (2.2.2) at the IR and the holographic condition $\widehat{A} = B^{(\Sigma^{-1})}$ at the UV. It is convenient to separate the longitudinal and transverse components of the gauge fields and to go to the $4D$ momentum space. We parametrize the solutions as

$$\begin{cases} A_t^{\mu,A}(p,z) = \widehat{A}_t^{\mu,A}(p) f_t^A(p^2,z) , \\ A_l^{\mu,A}(p,z) = \widehat{A}_l^{\mu,A}(p) f_l^A(p^2,z) , \end{cases} \tag{2.3.13}$$

[8] As discussed in the previous section, to obtain the full effective action one should solve the complete bulk equations of motion using a suitable perturbative expansion.

where $\widehat{A}$ indicates as usual the value of the $5D$ field at the UV, so that $f^A_{t,l}(z_{\rm UV}) = 1$. The bulk EOM's are easily extracted by varying the Yang–Mills action in the axial gauge. This is done in appendix C.1 and the result is

$$\begin{cases} p^2 f^A_t + \dfrac{1}{a(z)}\partial_z(a(z)\partial_z) f^A_t = 0\,, \\ \dfrac{1}{a(z)}\partial_z(a(z)\partial_z) f^A_l = 0\,. \end{cases} \tag{2.3.14}$$

According to eq. (2.2.2), the components associated to H (*i.e.* $f^a_{t,l}$) are Neumann at the IR while the $f^{\widehat{a}}_{t,l}$'s are Dirichlet. Given the UV condition $f^A_{t,l}(z_{\rm UV}) = 1$ the solutions are completely determined, even though analytic expressions can only be obtained in very special cases.[9] Notice that $f^A_l(p^2, z) = f^A_t(p^2 = 0, z)$ and that the form of each f^A only depends on whether the corresponding generators belong to H or to G/H. We can then write

$$\begin{aligned} f^a_t(p^2, z) &= F^+(p^2, z)\,, \qquad f^{\widehat{a}}_t(p^2, z) = F^-(p^2, z)\,, \\ f^a_l(p^2, z) &= F^+(0, z)\,, \qquad f^{\widehat{a}}_l(p^2, z) = F^-(0, z)\,, \end{aligned} \tag{2.3.15}$$

where $F^{+(-)}$ is the solution with Neumann (Dirichlet) IR boundary conditions. The explicit form of $F^{+(-)}$ in the cases of flat and AdS_5 space are reported in appendix C.1.

It is straightforward to substitute the solutions back into the quadratic bulk action, in this way one gets

$$S_h = -\frac{1}{2g_5^2}\int d^4x \sum_A \widehat{A}^A_\mu \left(\Pi^A_l P^{\mu\nu}_l + \Pi^A_t P^{\mu\nu}_t\right)\widehat{A}^A_\nu\,, \tag{2.3.16}$$

where $\Pi^A_{t,l}(p^2) = \partial_z f^A_{t,l}(p^2, z_{\rm UV})$ and $P_{t,l}$ are the transverse and longitudinal projectors. The holographic fields B_μ and Σ only enter the above equation through $\widehat{A}$. Remember that

$$\widehat{A}_\mu = B'^{(\Sigma^{-1})}_\mu = \Sigma^\dagger \left(B'_\mu + i\,\partial_\mu\right)\Sigma\,, \tag{2.3.17}$$

where the only components of B' are those associated to the UV group H'. A particular but interesting case is when, as it happens for orbifold compactifications, a matrix $\mathcal{P}$ exists which commutes with all generators of H and anticommutes with the others.[10] In this case eq. (2.3.16) can be rewritten as

$$\begin{aligned} S_h = -\frac{1}{2g_5^2}\int d^4x\ {\rm Tr}\Big[& B'^{(\Sigma^{-1})}_\mu \left(\Pi^0_l P^{\mu\nu}_l + \Pi^0_t P^{\mu\nu}_t\right) B'^{(\Sigma^{-1})}_\nu \\ & + \mathcal{P} B'^{(\Sigma^{-1})}_\mu \left(\Pi^1_l P^{\mu\nu}_l + \Pi^1_t P^{\mu\nu}_t\right) \mathcal{P} B'^{(\Sigma^{-1})}_\nu \Big]\,, \end{aligned} \tag{2.3.18}$$

where $\Pi^{0,1}_t(p^2) = \partial_z F^+(p^2, z_{\rm UV}) \pm \partial_z F^-(p^2, z_{\rm UV})$ and $\Pi^{0,1}_l = \Pi^{0,1}_t(0)$.

[9] Of course, the EOM for the longitudinal part is easily integrated.

[10] In orbifold compactifications the matrix $\mathcal{P}$ is simply given by the matrix Z introduced in section 1.4.

2.3.3 Fermions

We now add massive bulk fermions Ψ^I in some representation of the group G, their bulk action is in eq. (1.3.3). The holographic procedure for the fermions presents some subtleties [37] which we will briefly discuss here. First of all, due to the fact that the bulk EOM's are of first order, the left- and right-handed components can not be simultaneously used as effective degrees of freedom. Instead, for each component Ψ^I one must choose either $\widehat{\Psi}^I_L$ or $\widehat{\Psi}^I_R$ as the holographic field. It is simpler to take the same chirality for all the components, we will use the left-handed part and then the G multiplet $\chi_L = \widehat{\Psi}_L$ will be our holographic degree of freedom.

To obtain the holographic action we have to integrate out the bulk imposing the UV conditions $\Psi_L(z = z_{\rm UV}) = \chi_L$. This condition forces the Φ_L fluctuations we integrate over to vanish at the UV boundary $\delta\Psi_L(z = z_{\rm UV}) = 0$. On the other hand the right-handed components Ψ_R must be integrated out completely, thus their UV variation $\delta\Psi_R$ is unconstrained. Considering the variation of the $5D$ action given in eq. (1.3.4), it is clear that an arbitrary variation of Ψ_R at the UV is not compatible with the condition $\Psi_L(z = z_{\rm UV}) = \chi_L$. In other words, in order to cancel the boundary terms in the variation of the action an arbitrary variation of Ψ_R would require a Dirichlet condition for Ψ_L ($\Psi_L(z = z_{\rm UV}) = 0$) which is incompatible with the holographic condition. To solve this problem, one must add to the action a localized mass-term, whose sign depends on the chirality of the holographic field. In our case we always have the same sign

$$S_m = \frac{1}{2g_5^2}\int_{UV} d^4x \sum_I \left(\overline{\Psi}^I_L \Psi^I_R + h.c.\right) , \tag{2.3.19}$$

and the boundary term is G invariant.

To recover the original UV boundary conditions, as usual, the Dirichlet sources must be put to zero while the Neumann ones must be made dynamical. It is correct to proceed in this way, the only problem is that the holographic theory would not contain any dynamical field associated to the components $\Psi^{i'}$ of the multiplet whose left-handed component is Dirichlet at the UV. The right-handed part of such fields might give rise to zero-modes whose dynamics could not be described in the holographic theory. As discussed in [37], the solution consists in keeping $\widehat{\Psi}^{i'}_L$ dynamical and introducing right-handed Lagrange multipliers $\mu^{i'}_R$ to dynamically impose the Dirichlet boundary condition. One adds to the action the term

$$S_{L.m.} = -\frac{1}{g_5^2}\int d^4x \sum_{i'} \left(\overline{\chi}^{i'}_L \mu^{i'}_R + h.c.\right) . \tag{2.3.20}$$

The Lagrange multipliers $\mu^{i'}_R$ will describe the massless or light states associated to $\Psi^{i'}_R$. Notice that, if the action contains extra operators localized at the UV, the inclusion of the Lagrange multipliers is necessary. Such terms are considered in appendix B, where we will

show how the holographic procedure allows to treat them in a simple and straightforward way.

Having chosen the same chirality for all the sources, the full Lagrangian for Ψ (including the boundary term (2.3.19)) is gauge invariant and the manipulations of section 2.2 can easily be repeated. The fermion contribution to the gauge-fixed partition function (2.2.12) can be schematically written as

$$Z_f^{g.f.}[\chi_L, \Sigma] \equiv \exp iS_h[\chi_L, \Sigma] = \int \mathcal{D}\Psi(x,z)_{\widehat{\Psi}_L=\Sigma_f^{-1}\chi_L} \exp\left[iS_f[\Psi; A_\mu, A_z=0]\right], \quad (2.3.21)$$

where Σ_f represents the Goldston-boson matrix in the appropriate G representation and S_f is the full fermionic action which includes bulk and boundary terms (1.3.3, 2.3.19) and possibly (2.3.20). As before, we concentrate on the quadratic part of the holographic action. The solutions of the EOM's (eq. (1.3.5)) can be parametrized as

$$\Psi_L^I(p,z) = \widehat{\Psi}_L^I(p) f_L^I(p,z), \qquad \Psi_R^I(p,z) = \frac{\not{p}}{p}\widehat{\Psi}_L^I(p) f_R^I(p,z), \quad (2.3.22)$$

with $f_L^I(p, z_{\text{UV}}) = 1$ and suitable boundary conditions on the IR boundary. As for the gauge field, the $f_{L,R}^I(p,z)$ functions have only two forms $f_{L,R}^I(p,z) = f_{L,R}^{\pm}(p,z)$ depending on whether Ψ_L^I satisfies N or D conditions at the IR boundary.[11] Substituting into the action we find that the bulk contribution (eq. (1.3.3)) vanishes, and we get only a contribution from the boundary terms in eq. (2.3.19) (and possibly from (2.3.20)):

$$S_h = \frac{1}{g_5^2}\int d^4x \sum_I (\overline{\chi}_L \Sigma_f)^I \, \Pi_f^I(-\partial^2)\, i\not{\partial}\left(\Sigma_f^\dagger \chi_L\right)^I + S_{L.m.} \quad (2.3.23)$$

where $\Pi_f^I(p^2) = f_R^I(p, z_{\text{UV}})/p$. As for the gauge part, if the IR boundary conditions are determined by the projection matrix $\mathcal{P}_f$ (*i.e.* $\Psi_{L,R}(z_{\text{IR}}) = \pm\mathcal{P}_f\Psi_{L,R}(z_{\text{IR}})$), the above equation can be written in the simpler form

$$S_h = \frac{1}{2g_5^2}\int d^4x\, \overline{\chi}_L \Sigma_f \left(\Pi_f^0(-\partial^2) + \Pi_f^1(-\partial^2)\mathcal{P}_f\right) i\not{\partial}\left(\Sigma_f^\dagger \chi_L\right) + S_{L.m.}, \quad (2.3.24)$$

where $\Pi_f^{0,1}(p^2) = \left(f_R^+(p, z_{\text{UV}}) \pm f_R^-(p, z_{\text{UV}})\right)/p$.

2.4 The One-Loop Higgs Effective Potential

The general formalism presented in the previous sections could be applied to several models of New Physics. For example, in the Higgsless models of EWSB one would consider a SM bulk gauge group $G = SU(2) \times U(1)_Y$ broken to $U(1)_{EM}$ at the IR and completely unbroken at the UV. In the holographic effective theory one would find the SM gauge bosons and the Goldstones which arise from the IR breaking. The latter are eaten by

[11] The explicit form of such functions for the AdS_5 and flat space cases can be found in appendix C.2.

the gauge fields becoming massive and the EWSB is obtained without introducing any physical scalar in the spectrum. The models of GHU (or of Composite Higgs) are more interesting from the holographic point of view, since they lead to physical $4D$ scalars whose dynamics can be studied with the holographic formalism. As we will discuss in detail in chapter 3, in this case one has an "extended" EW bulk gauge group ($G = SU(3)$ in [15, 27], $G = SO(5)$ in [19, 20, 21]) broken at the IR in such a way that a complex Higgs doublet of scalars arises (respectively, $H = SU(2) \times U(1)$ and $H = SO(4)$) as a Goldstone boson. The surviving UV gauge group H' is the SM $SU(2) \times U(1)_Y$ and the EWSB comes from the Higgs taking a VEV. Since the UV boundary conditions break part of the bulk group, the Higgs is really a pseudo-Goldstone boson and these models are similar to the old Composite-Higgs scenario.

Since the EWSB occurs radiatively in this scenario, it is important to compute the one-loop Higgs potential. This is quite a difficult task with the standard KK approach (see for instance [45]) and the holographic procedure [19, 38], as we will show below, is much simpler. In this section we will mostly keep the discussion general but we will later specify to a toy $SU(2) \to U(1)$ example in order to show how our final formulae can be applied to a concrete model.

At one loop, the effective potential is just the vacuum energy in the presence of a constant background (which we denote by $\overline{\Sigma}$) for the Goldstone fields. In principle, we should integrate at one-loop level the bulk degrees of freedom in eqs. (2.2.12, 2.3.21), and later integrate the holographic fields. The Goldstones, however, only appear in the UV boundary conditions and thus they are directly coupled only with the holographic fields and not with the bulk degrees of freedom.[12] As a consequence, to compute the effective potential at one loop, we only need to consider loops with boundary fields, so that integrating out the bulk will not give any contributions to the potential. Moreover, at one-loop level the only part of the holographic action which we need is the quadratic tree-level one we already computed in the previous section.

As shown in section 2.2, the holographic effective action is gauge invariant. Once the non-dynamical sources are put to zero, the H' invariance still survives and then a gauge-fixing is needed in order to compute the gauge field contribution to the effective potential. The Landau gauge $\partial_\mu B'^\mu = 0$ is a particularly useful choice since no quadratic mixing can appear between the scalar fluctuations and ${B'}_\mu$. The quadratic action for ${B'}_\mu$ with a VEV for Σ is (see eq. (2.3.16))

$$S_h = -\frac{1}{2g_5^2} \int d^4x \sum_A \left[\overline{\Sigma}^\dagger {B'}_\mu \overline{\Sigma}\right]^A \Pi_t^A P_t^{\mu\nu} \left[\overline{\Sigma}^\dagger {B'}_\nu \overline{\Sigma}\right]^A , \tag{2.4.1}$$

[12] Notice that this is true only if we choose holographic degrees of freedom with the same chirality within each multiplet, as we did here. If this prescription is not used, the Goldstone bosons can not be disentangled from the bulk and one gets also a bulk contribution to the one-loop effective potential.

it can schematically be rewritten as

$$S_h = -\frac{1}{g_5^2}\int d^4x\; P_t^{\mu\nu}\sum_{a',b'} B'^{a'}_{\mu}\,\Pi_g^{a',b'}(p^2,\overline{\Sigma})\,B'^{b'}_{\nu}\,, \tag{2.4.2}$$

where a' and b' run over the generators of H'. Remembering that the ghosts do not contribute in the Landau gauge and that a transverse vector in $4D$ has 3 real components, the gauge contribution to the Higgs potential reads

$$V_g(\overline{\Sigma}) = \frac{3}{2}\int \frac{d^4p_E}{(2\pi)^4}\log\left[\mathrm{Det}\left(\Pi_g(-p_E^2,\overline{\Sigma})\right)\right]\,, \tag{2.4.3}$$

where we rotated the momenta to the Euclidean. It is easy to check that the Goldstone bosons fluctuations do not contribute to the potential, eq. (2.4.3) then contains the full $5D$ gauge contribution. Notice that the integrals involved in the effective potential are divergent, but they can always be made finite by subtracting the vacuum energy, *i.e.* the potential at $\overline{\Sigma}=0$. This is because the two solutions to the quadratic equations ($F^{\pm}$ in the case of the gauge field) become the same in the large Euclidean momentum limit. The inverse propagators Π_t^A then become all equal so that the dependence on $\overline{\Sigma}$ drops from eq. (2.4.1). The divergent part of the potential is therefore always independent of $\overline{\Sigma}$.

To compute the contribution of the fermions it is useful, as a first step, to integrate out the Lagrange multipliers in the holographic action, *i.e.* to put to zero the sources associated to Dirichlet fields.[13] In this way one obtains the quadratic action in χ_L from eq. (2.3.23):

$$S_h = \frac{1}{g_5^2}\int d^4x\;\sum_{i',j'}\overline{\chi}_L^{i'}\Pi_f^{i',j'}(\overline{\Sigma})\chi_L^{j'}\,, \tag{2.4.4}$$

where i' and j' run over the left-handed fermion components with Neumann boundary conditions at the UV. The effective potential follows trivially:

$$V_f(\overline{\Sigma}) = -2\int \frac{d^4p_E}{(2\pi)^4}\log\left[\mathrm{Det}\left(\Pi_f(\overline{\Sigma})\right)\right]\,. \tag{2.4.5}$$

2.4.1 The $SU(2)\to U(1)$ Case

The above formulas permit to derive the effective potential for a generic gauge group G broken to arbitrary subgroups at the UV and IR boundaries. Applying them to a concrete model is extremely simple once the group-theoretical aspects have been worked out. To show this let us discuss explicitly the simple case of an $SU(2)$ bulk gauge theory broken to $U(1)$ (the same $U(1)$ subgroup) at both branes. This leads to a residual $U(1)$ invariance and to a charged physical Higgs scalar. We choose $\sigma^3/2$ to be the unbroken

[13] The same result would be obtained if including all the left-handed fermions and the Lagrange multipliers.

$SU(2)$ generator, where σ^i are Pauli matrices. This pattern of symmetry breaking can be obtained by the projection matrix $\mathcal{P} = \sigma^3$. The Goldstone boson matrix is

$$\Sigma = \exp\left[is_1\frac{\sigma^1}{2} + is_2\frac{\sigma^2}{2}\right] = \cos\left(\frac{s}{2}\right)\mathbb{1} + i\frac{s_i}{s}\sin\left(\frac{s}{2}\right)\sigma^i\,, \tag{2.4.6}$$

where $s_i(x)$ $(i = 1, 2)$ are the Goldstone boson fields and $s \equiv \sqrt{s_1^2 + s_2^2}$. Using the unbroken $U(1)$ we align the Goldstone boson VEV along the σ^2 direction, thus we get

$$\overline{\Sigma}\mathcal{P}\overline{\Sigma}^\dagger = \begin{pmatrix} \cos s & -\sin s \\ -\sin s & -\cos s \end{pmatrix}. \tag{2.4.7}$$

At the UV, the only unbroken generator is σ_3 so that $B' = B'^3\sigma^3/2$. From eq. (2.3.18),

$$S_h = -\frac{1}{4g_5^2}\int d^4x\, P_t^{\mu\nu}\, B'^3_\mu\left(\Pi_t^0 + \cos 2s\;\Pi_t^1\right)B'^3_\nu\,, \tag{2.4.8}$$

and the gauge contribution to the effective potential can be easily found to be

$$V_g(s) = \frac{3}{2}\int\frac{d^4p_E}{(2\pi)^4}\log\left[\Pi_t^0 + \cos 2s\;\Pi_t^1\right]. \tag{2.4.9}$$

Let us now take a bulk fermion Ψ in the fundamental representation of $SU(2)$, with boundary conditions generated by the projection matrix $\mathcal{P}_f = \mathcal{P}$, *i.e.* $\Psi_{L,R} = \pm\mathcal{P}\Psi_{L,R}$ at both boundaries. Once we integrate out the Lagrange multiplier, the holographic action at the quadratic level becomes (see eq. (2.3.24))

$$S_h = \frac{1}{2g_5^2}\int d^4x\;\overline{\chi}_L^1(\Pi_f^0 + \cos s\,\Pi_f^1)i\not{p}\,\chi_L^1\,, \tag{2.4.10}$$

and the fermion contribution to the effective potential is

$$V_f(s) = -2\int\frac{d^4p_E}{(2\pi)^4}\log\left[\Pi_f^0 + \cos s\;\Pi_f^1\right]. \tag{2.4.11}$$

The explicit expressions for $\Pi_{t,s,f}^{0,1}$ are reported in appendix C for the AdS and flat space cases, the result matches those obtained by a KK computation in [15, 45].

Notice that the results obtained for the gauge group $SU(2)$ can be used to derive the effective potential in more interesting and complex models. When a single Higgs doublet is present, its VEV can be aligned along one of the broken generators and the system can be split in many $SU(2)$-like subsystems each with a different charge q with respect to the Higgs VEV. In this case the effective potential can be computed summing the corresponding $SU(2)$ contributions with s replaced by qs. Consider for instance $SU(3)$ broken to $SU(2)\times U(1)$ at both boundaries. In this case an $SU(2)$ doublet of Goldstone bosons arises. The gauge fields in the unbroken subgroup can be split into four $SU(2)$-like

subsets with charges $q_1 = 1$, $q_2 = q_3 = 1/2$ and $q_4 = 0$. The gauge contribution to the effective potential is

$$V_g^{SU(3)}(s) = V_g(s) + 2V_g(s/2)\,. \tag{2.4.12}$$

Analogously we can treat fermion fields. For a bulk fermion in the fundamental representation of $SU(3)$ we find a field with charge $q = 1/2$ which gives a contribution

$$V_{f,fund}^{SU(3)}(s) = V_f(s/2)\,, \tag{2.4.13}$$

while a bulk fermion in the symmetric representation gives a field with charge $q = 1$ and a field with charge $q = 1/2$ and in this case

$$V_{f,sym}^{SU(3)}(s) = V_f(s) + V_f(s/2)\,. \tag{2.4.14}$$

These expressions for the effective potential coincide in the flat space case with the ones found in [15].

2.5 Holographic QCD

Holographic QCD is a phenomenological attempt, inspired by AdS/CFT, of describing low energy (large N_c) strongly coupled QCD by means of a $5D$ weakly coupled model on the warped interval. One considers [46, 47] an $SU(3)_L \times SU(3)_R$ bulk gauge group which accounts for the global chiral symmetry of QCD and breaks it to its vector subgroup through the background profile of a bulk scalar field. An interesting limit is when the profile is exactly localized at the IR, in which case the breaking is equivalent to the one obtained by boundary conditions. Taking the limit does not significantly affect the degree of accordance of the model with real-world QCD, a detailed analysis of this case has been performed in [35]. In this section we discuss this simplified limit of AdS/QCD and then consider a $5D$ theory with chiral gauge group $G = \Gamma_L \times \Gamma_R$, with Γ any compact Lie group. More explicitly, each element g of G is the direct product of two elements (g_L and g_R) of Γ, *i.e.* $g = g_L \times g_R$. For applications to QCD one takes $\Gamma = SU(2)$ or $SU(3)$ and interprets the holographic partition function in eq. (2.2.3) as the QCD partition function in the presence of sources for the chiral group currents. The IR boundary conditions are chosen to break G to its vector subgroup $\Gamma_V \sim \Gamma$ whose elements are couples $g = g_V \times g_V$ of equal elements $g_V \in \Gamma$ acting on the two chiral subspaces. The results of section 2.2 could be directly applied to this case, but this would lead us to a non-standard parametrization of the Goldstone degrees of freedom. It is easier to restart from the beginning and adapt the discussion of section 2.2 to the case of a chiral gauge group [38].

We have two $5D$ gauge fields A_L and A_R, the first transforming under g_L and the second under g_R. The IR boundary conditions are

$$A_{L,\mu} = A_{R,\mu}\,, \qquad F_{L,\mu z} = -F_{R,\mu z}\,. \tag{2.5.1}$$

By looking at eq. (1.2.2) we see that eq. (2.5.1) ensures the cancellation of the boundary variations of the gauge action. Moreover, eq. (2.5.1) is covariant under the vector subgroup only, so that it restricts the allowed $5D$ local transformations to those which are vector-like at the IR. As in sect. 2.2.1, we want to enlarge the $5D$ group and allow any transformation at the IR. This is easily done by defining, as customary in QCD, a matrix

$$U(x) \,=\, \exp\left[i\,\sigma_a(x) t^a\right] \,\in \Gamma\,, \tag{2.5.2}$$

which transforms under G as:

$$U \,\longrightarrow\, U^{(g)} \,=\, g_R \circ U \circ g_L^{-1}\,. \tag{2.5.3}$$

The new boundary conditions

$$\left(A_L^{(U)}\right)_\mu \,=\, A_{R,\mu}\,, \qquad \left(F_L^{(U)}\right)_{\mu z} \,=\, -F_{R,\mu z}\,, \tag{2.5.4}$$

are now covariant under the full chiral group. Note that U plays exactly the same role as Σ in sect. 2.2.1, using one or the other is just a reparametrization of the Goldstone degrees of freedom.

One can now go through the same manipulations of sect. 2.2.1 and get

$$\begin{aligned} Z^{g.f.}\left[l_\mu,\, r_\mu\right] &\equiv \int \mathcal{D}U(x)\, \exp\left[iS_{\chi\mathbf{PT}}\left[l_\mu,\, r_\mu,\, U\right]\right] \\ &= \iint \mathcal{D}U(x)\, \mathcal{D}A_{L,\mu}(x,z)_{\widehat{A}_{L,\mu}=l_\mu^{(U)}}\, \mathcal{D}A_{R,\mu}(x,z)_{\widehat{A}_{R,\mu}=r_\mu}\, \exp\left[iS\left[A_\mu,\, A_z=0\right]\right]\,, \end{aligned} \tag{2.5.5}$$

where the IR conditions are simply given by eq. (2.5.1). One can easily check that the expression in eq. (2.5.5) is gauge invariant under the full chiral group. The holographic action $S_{\chi\mathbf{PT}}\left[l_\mu, r_\mu, U\right]$ depends on the Goldstone matrix U and on the chiral sources l_μ, r_μ. In AdS/QCD this is interpreted as the action of chiral perturbation theory.

2.5.1 The χPT Lagrangian at $\mathcal{O}(p^4)$ from Holographic QCD

At tree level, the $\chi\mathbf{PT}$ effective action is

$$\begin{aligned} S_{\chi\mathbf{PT}} \,=\, \frac{1}{g_5^2}\int d^4x \int_{z_{\mathrm{UV}}}^{z_{\mathrm{IR}}} dz\, a(z)\, \mathrm{Tr}\Big[&-\frac{1}{2}F_{L,\mu\nu}F_L^{\mu\nu} - \frac{1}{2}F_{R,\mu\nu}F_R^{\mu\nu} \\ &+\partial_z A_{L,\mu}\partial_z A_L^\mu + \partial_z A_{R,\mu}\partial_z A_R^\mu\Big]\,, \end{aligned} \tag{2.5.6}$$

where $A_{L,R}$ satisfy the bulk EOM's with the IR boundary conditions given in eq. (2.5.1) and UV boundary conditions

$$\begin{cases} \widehat{A}_{L,\mu} = U\left(l_\mu + i\partial_\mu\right)U^\dagger\,, \\ \widehat{A}_{R,\mu} = r_\mu\,. \end{cases} \tag{2.5.7}$$

It is useful to define the vector and axial combinations of the gauge fields

$$\mathcal{V}_\mu \equiv \frac{1}{2}(A_{L,\mu} + A_{R,\mu})\,, \qquad \mathcal{A}_\mu \equiv \frac{1}{2}(A_{L,\mu} - A_{R,\mu})\,, \tag{2.5.8}$$

which satisfy simple boundary conditions at the IR

$$\begin{cases} \partial_z \mathcal{V}_\mu(x, z_{\rm IR}) = 0\,, \\ \mathcal{A}_\mu(x, z_{\rm IR}) = 0\,. \end{cases} \tag{2.5.9}$$

Of course, computing $S_{\chi\mathbf{PT}}$ from eq. (2.5.6) would require to solve the full bulk EOM's which include all the interactions, and this can only be done order by order in a given perturbative expansion (see section 2.3.1). As customary in $\chi\mathbf{PT}$, we expand in powers of the momentum and treat the external sources l_μ and r_μ as terms of $\mathcal{O}(p)$. Given that U is of $\mathcal{O}(p^0)$, eq. (2.5.7) implies that the boundary value of the fields ($\widehat{A}_{L,R}$, $\widehat{\mathcal{V}}$ and $\widehat{\mathcal{A}}$) are also of $\mathcal{O}(p)$. Our present goal is to determine the holographic effective action up to $\mathcal{O}(p^4)$, which was first obtained in [47] (for the simplified model we are considering see [35]) after a long KK calculation. In the mixed momentum–space representation we can expand the solutions of the full EOM's as

$$\begin{cases} \mathcal{V}_\mu(p,z) = f_V^0(z)\,\widehat{\mathcal{V}}_\mu(p) + \mathcal{V}_\mu^{(3)}(p,z,\widehat{\mathcal{V}},\widehat{\mathcal{A}})\,, \\ \mathcal{A}_\mu(p,z) = f_A^0(z)\,\widehat{\mathcal{A}}_\mu(p) + \mathcal{A}_\mu^{(3)}(p,z,\widehat{\mathcal{V}},\widehat{\mathcal{A}})\,, \end{cases} \tag{2.5.10}$$

where $\mathcal{V}_\mu^{(3)}$ and $\mathcal{A}_\mu^{(3)}$, whose explicit form we will not need, represent $\mathcal{O}(p^3)$ contributions to the solutions. The latter terms are trilinear combinations of the momentum p_μ and of the boundary fields $\widehat{\mathcal{V}}_\mu(p)$ and $\widehat{\mathcal{A}}_\mu(p)$. It is important to remark that the tensorial structure of the solutions implies that no $\mathcal{O}(p^2)$ terms appear in eq. (2.5.10) and that the next correction will be of $\mathcal{O}(p^5)$. The first term of each expansion is a solution of the linearized bulk EOM's (eq. (2.3.14)) at zero momentum. At the UV, $f_{V,A}^0(z_{\rm UV}) = 1$ and they are, respectively, Neumann or Dirichlet at the IR boundary. The higher-order terms, on the contrary, vanish at the UV while their IR boundary conditions are the same as the corresponding zero-order terms.

Substituting the solutions of the EOM's into the effective action, we see that the terms in the first line of eq. (2.5.6) only contribute at $\mathcal{O}(p^4)$, and just the leading order of the series in eq. (2.5.10) needs to be plugged in. On the other hand, the terms in the second row of eq. (2.5.6) will give a $\mathcal{O}(p^2)$ term when substituting the leading ($\mathcal{O}(p)$) terms of eq. (2.5.10) while an $\mathcal{O}(p^4)$ term could arise when taking one $\mathcal{O}(p)$ and one $\mathcal{O}(p^3)$ term. The latter contribution, however, vanishes. This is easily verified by integrating by parts ∂_z and remembering that the $\mathcal{O}(p^3)$ terms vanish at the UV boundary while the ones of $\mathcal{O}(p)$ verify the linearized EOM's at zero momentum. Thus, the effective action at $\mathcal{O}(p^4)$

can be written as

$$S_h = -\frac{2}{g_5^2}\int_{UV} d^4x\ \mathrm{Tr}\left[\mathcal{V}_\mu \partial_z \mathcal{V}^\mu + \mathcal{A}_\mu \partial_z \mathcal{A}^\mu\right] \\ -\frac{1}{2g_5^2}\int d^4x \int_{z_{\rm UV}}^{z_{\rm IR}} dz\ a(z)\mathrm{Tr}\left[F_{L,\mu\nu}F_L^{\mu\nu} + F_{R,\mu\nu}F_R^{\mu\nu}\right]\,, \tag{2.5.11}$$

where the fields are now simply the solutions of the linearized bulk EOM's at zero momentum. Notice that in this expression the first line gives $\mathcal{O}(p^2)$ terms, while $\mathcal{O}(p^4)$ operators come from the second one.

The linearized bulk EOM's (2.3.14) at zero momentum can be analytically solved

$$\begin{cases} f_V^0(z) = 1\,, \\ f_A^0(z) = \left(\int_z^{z_{\rm IR}} \frac{dz'}{a(z')}\right)\left(\int_{z_{\rm UV}}^{z_{\rm IR}} \frac{dz'}{a(z')}\right)^{-1}\,, \end{cases} \tag{2.5.12}$$

and it follows from eq. (2.5.7) that

$$\widehat{\mathcal{A}}_\mu = \frac{i}{2}U(D_\mu U)^\dagger = -\frac{i}{2}(D_\mu U)U^\dagger \equiv u_\mu\,, \tag{2.5.13}$$

where we defined $D_\mu U = \partial_\mu U + iUl_\mu - ir_\mu U$. The kinetic term for the Goldstone bosons, *i.e.* the $\mathcal{O}(p^2)$ action, is immediately obtained from the first line of eq. (2.5.11).[14] It is

$$S_h^{(2)} = \frac{f_\pi^2}{2}\int d^4x\ \mathrm{Tr}\left[(D_\mu U)(D^\mu U)^\dagger\right]\,, \tag{2.5.14}$$

where the Goldstone-boson decay constant f_π is given by

$$f_\pi = \frac{1}{g_5}\left(\int_{z_{\rm UV}}^{z_{\rm IR}} \frac{dz}{a(z)}\right)^{-1/2}\,. \tag{2.5.15}$$

Using the boundary conditions in eq. (2.5.7), the definitions of $\mathcal{V}$ and $\mathcal{A}$ in eq. (2.5.8) and the solutions of the bulk EOM's in eq. (2.5.12), one gets

$$F_{L,\mu\nu} + F_{R,\mu\nu} = f_{+\mu\nu} + i\frac{1 - f_A^0(z)^2}{2}[u_\mu, u_\nu]\,, \tag{2.5.16}$$

$$F_{L,\mu\nu} - F_{R,\mu\nu} = f_A^0(z)\ f_{-\mu\nu}\,, \tag{2.5.17}$$

where we defined

$$f_{\pm\mu\nu} \equiv U\, l_{\mu\nu}\, U^\dagger \pm r_{\mu\nu}\,, \tag{2.5.18}$$

with $l_{\mu\nu}$ and $r_{\mu\nu}$ the field strengths obtained from l_μ and r_μ. Substituting these expressions in the second line of eq. (2.5.11), we find the $\mathcal{O}(p^4)$ terms of the effective action

$$S_h^{(4)} = -\frac{1}{4g_5^2}\int d^4x \int_{z_{\rm UV}}^{z_{\rm IR}} dz\ a(z)\,\mathrm{Tr}\Big\{ -\frac{(1 - f_A^0(z)^2)^2}{2}u_\mu u_\nu\,[u^\mu, u^\nu] \\ +2i(1 - f_A^0(z)^2)f_{+\mu\nu}u^\mu u^\nu + f_{+\mu\nu}f_+^{\mu\nu} + f_A^0(z)^2 f_{-\mu\nu}f_-^{\mu\nu}\Big\}\,. \tag{2.5.19}$$

[14] Notice that $\partial_z f_V^0(z_{\rm IR}) = 0$, and thus the term containing $\mathcal{V}_\mu$ in the first line of eq. (2.5.11) vanishes.

In the $\Gamma = SU(3)$ case it is trivial to express the above action in the standard form of chiral perturbation theory [48]. From eq. (2.5.19) we find the values of the coefficients

$$\begin{cases} L_1 = \dfrac{1}{16 g_5^2} \displaystyle\int_{z_{UV}}^{z_{IR}} dz\; a(z)(1 - f_A^{0\,2})^2 \\ L_{10} = -\dfrac{1}{2 g_5^2} \displaystyle\int_{z_{UV}}^{z_{IR}} dz\; a(z)(1 - f_A^{0\,2}) \\ H_1 = -\dfrac{1}{4 g_5^2} \displaystyle\int_{z_{UV}}^{z_{IR}} dz\; a(z)(1 + f_A^{0\,2}) \end{cases} , \qquad \begin{cases} L_2 = 2L_1 \\ L_3 = -6L_1 \\ L_9 = -L_{10} \end{cases} , \tag{2.5.20}$$

which are in agreement with those derived in [35].[15]

2.6 Holographic Anomaly

It is interesting to study, using the holographic perspective which we described in this chapter, the consequences of adding a CS term to the $5D$ gauge action. In this section we will work out the holographic Goldstone-bosons Lagrangian and find that, as expected [49], the CS makes a gauged Wess–Zumino–Witten (WZW) term [50, 51, 52] appear. We will initially consider a quite general case, but we will later specify to AdS/QCD, where a CS term is needed in order to mimic the Adler–Bardeen chiral anomaly. Notice that, from a purely $5D$ point of view, the CS is usually introduced [53] in order to cancel localized gauge anomalies [54]. Our approach, however, is different. We will simply add the CS to the action and study its consequences on the holographic theory. For simplicity, we will not consider bulk fermions at all, so that there is clearly no localized anomaly to be canceled. In the presence of a bulk fermion content which gives rise to localized anomalies the analysis of this section should be generalized taking also into account the anomalous variation of the fermionic measure, and not only the one of the CS term as we will do here.

Let us consider, as in sect. 2.2, a pure gauge theory with bulk group G broken to H at the IR and add to the gauge action the term

$$S_{CS} = -i\,c \int \omega_5(A) = -i\,c \int \mathrm{Tr}\left[A(dA)^2 + \frac{3}{2}A^3(dA) + \frac{3}{5}A^5\right] , \tag{2.6.1}$$

where c is a real coefficient and we introduced a matrix-form notation defining $A = -iA_M^A T^A\, dx^M$.[16] We want to explore the consequences of including S_{CS} in the definition (2.2.3) of the holographic partition function. First of all we observe that, under a generic infinitesimal gauge transformation

$$\delta_\alpha S_{CS} = -i\,c \int d\omega_4^1(\alpha, A) = i\,c \int \omega_4^1(\alpha(z_{UV}), A(z_{UV})) - i\,c \int \omega_4^1(\alpha(z_{IR}), A(z_{IR})) , \tag{2.6.2}$$

[15] The factor of 2 difference with the result of [35] is due to the normalization of the $SU(3)$ generators.

[16] In this section we use many definitions and results of [52].

so that the gauge invariance of the action has been spoiled. In eq. (2.2.3), however, the bulk gauge group $\mathcal{G}_B$ is gauged, meaning that it is used to remove unphysical degrees of freedom and make the theory consistent. For this reason, no anomalous variations of the action under $\mathcal{G}_B$ can be allowed. Remembering that $\mathcal{G}_B$ elements reduce to the identity at the UV and to the H subgroup at the IR, and using the IR boundary conditions (2.2.2) for the gauge fields, this translates into the condition

$$\mathrm{Tr}(T^a\{T^b, T^c\}) = 0\,, \tag{2.6.3}$$

on the H generators which define the CS. The T^a's, therefore, must provide an anomaly-free representation (whose existence we are going to assume in the following) of the H subgroup. Eq. (2.6.3) ensures the $\mathcal{G}_B$ invariance of the action as it makes the IR term in eq. (2.6.2) vanish. The UV term in the variation (2.6.2) is, on the contrary, perfectly allowed for what concerns the definition of the holographic partition function. It simply changes eq. (2.2.5) into

$$Z\left[B_\mu^{(\widehat{g})}\right] = \exp\left[-c\int \omega_4^1(\widehat{\alpha}, B)\right] Z\left[B_\mu\right]\,, \tag{2.6.4}$$

where $\widehat{g} = \exp[i\widehat{\alpha}]$ is an infinitesimal gauge transformation. If some of the sources have to be made dynamical, of course, one should also worry about the cancellation of the UV anomaly in eq. (2.6.4). This could be done, for instance, by adding localized fermions in a suitable representation.

When an AdS/CFT interpretation is possible, $Z[B]$ is the partition function of a G-invariant $4D$ theory in the presence of sources for the currents and eq. (2.6.4) corresponds to a $4D$ anomaly. The global group G is spontaneously broken to H and eq. (2.6.3) states that the unbroken group is anomaly free. This is very much the same as in QCD, where the global symmetry $SU(3)_L \times SU(3)_R$ is spoiled by the chiral anomaly while the unbroken vector subgroup is anomaly free. Eq. (2.6.4), however, is not enough to mimic the standard QCD Adler–Bardeen anomaly, since the latter preserves the vector invariance. More generally, in a $4D$ theory with anomalous global symmetry group G which is spontaneously broken to an anomaly free H, one adopts a regulator in which the H invariance is preserved in all correlators so that the anomaly $G_{\widehat{\alpha}}(B)$ vanishes, for a generic gauge field configuration, whenever $\widehat{\alpha} \in Lie(H)$. The anomaly $\int \omega_4^1(\widehat{\alpha}, B)$ which appears in eq. (2.6.4), on the contrary, only vanishes (due to eq. (2.6.3)) when the sources also are restricted to H, *i.e.* when B, $\widehat{\alpha} \in Lie(H)$. In the language of Ref. [52], eq. (2.6.4) is the "canonical" anomaly while what would be needed is the "shifted" anomaly. The two forms of the anomaly correspond to different choices of the regulator and one can convert one into the other by adding suitable local counterterms to the action. Following [52], we consider a "shifted" CS term

$$\widetilde{S}_{CS} = -i\,c\int \widetilde{\omega}_5(A_h, A) = -i\,c\int \left[\omega_5(A) + dB_4(A_h, A)\right] = S_{CS} + i\,c\int_{UV} B_4(B_h, B)\,, \tag{2.6.5}$$

where A_h, B_h are the restrictions of A, B to $Lie(H)$ and B_4 is defined by [52]

$$B_4(A_h, A) = \frac{1}{2}\mathrm{Tr}\left[(A_h A - A A_h)(F + F'_h) + A A_h^3 - A_h A^3 + \frac{1}{2} A_h A A_h A\right] , \qquad (2.6.6)$$

with $F'_h = dA_h + A_h^2$ and $F = dA + A^2$. In eq. (2.6.5) we used the fact that, due to the boundary conditions, $A(z_{\mathrm{IR}}) = A(z_{\mathrm{IR}})_h$ and $B_4(A_h, A_h) = 0$. If $\widetilde{S}_{CS}$, and not S_{CS}, is added to the gauge action, the anomalous variation of the holographic partition function becomes

$$Z\left[B_\mu^{(\widehat{g})}\right] = \exp\left[-c\, G_{\widehat{\alpha}}(B)\right] Z\left[B_\mu\right] , \qquad (2.6.7)$$

where $G_{\widehat{\alpha}} = -\int \delta_{\widehat{\alpha}} \widetilde{\omega}_5$ is the shifted anomaly as defined in [52]. It vanishes, for any $B \in Lie(G)$, when $\widehat{\alpha} \in Lie(H)$.

Having identified the correct term to be added to the $5D$ action, let us now see how it affects the holographic effective action. It is well known that the anomalous variation (2.6.7) of the partition function *requires* the presence of the gauged WZW term in the effective action of the Goldstone bosons. The latter term, indeed, is not gauge-invariant and it is precisely designed to reproduce the anomaly (2.6.7). Showing that it arises, as we will do in the following, is then just a check of internal consistency. It is worth remarking that, from the purely $5D$ point of view, one could also use the canonical CS (2.6.2), the manipulations which follow would not change significantly. Of course, having failed to reproduce the anomaly (2.6.7), one would not obtain the correct gauged WZW. From the point of view of holographic QCD, on the contrary, the shifted CS is the only correct choice.

In order to fix the $\mathcal{G}_B$ gauge invariance of the holographic partition function we cannot simply follow sect. 2.2. The CS, indeed, spoils the invariance of the gauge action under generic G transformations, so that G is broken to H not only by the IR boundary conditions (2.2.2). The trick which we used in eq. (2.2.8) to restore the full bulk G invariance, therefore, is not useful in the present case. We will need a more formal, but completely equivalent, gauge-fixing procedure, which is discussed in appendix A. The final result is

$$Z^{g.f.}\left[B_\mu\right] = \int \mathcal{D}\Sigma \int \mathcal{D}A_\mu(x,z)_{\widehat{A}_\mu = B_\mu^{(\Sigma^{-1})}} \exp\left[iS\left[A^{(\Lambda)}\right]\right] , \qquad (2.6.8)$$

where $A_M = \{A_\mu, 0\}$ and Λ is any $5D$ transformation which interpolates from Σ at the UV, $\Lambda(z_{\mathrm{UV}}) = \Sigma$, to the identity at the IR, $\Lambda(z_{\mathrm{IR}}) = \mathbb{1}$. When rotated to the Euclidean, Λ is an extension of Σ from the 4-sphere S^4 of space–time to a $5D$ disk D_5, with boundary S^4, obtained by shrinking the IR brane to a point.

The CS term $\widetilde{S}_{CS}$ gives the only non-trivial contribution to $S\left[A^{(\Lambda)}\right]$. When the latter is absent the action is invariant and eq. (2.6.8) reduces to eq. (2.2.12). We define

$$S_{wzw} = i\, c \int \left[\widetilde{\omega}_5(A_h, A) - \widetilde{\omega}_5((A^{(\Lambda)})_h, A^{(\Lambda)})\right] , \qquad (2.6.9)$$

and rewrite

$$S\left[A^{(\Lambda)}\right] = S_{wzw} - ic\int \widetilde{\omega}_5(A_h, A) + S_g\left[A\right], \tag{2.6.10}$$

where S_g is the standard gauge action. We added the term $\widetilde{S}_{CS} = ic\int\widetilde{\omega}_5(A_h, A)$ to the definition of S_{wzw} in order to make it vanish when $\Sigma = \mathbb{1}$. It should be noted that, thanks to eq. (2.2.13), $\widetilde{S}_{CS}$ does not contribute to the anomalous variation of the gauge-fixed partition function (2.6.8) since $\widetilde{\omega}_5(A_h, A)$ is H invariant. One could check that, on the contrary, S_{wzw} varies and that its variation reproduces the anomaly in eq. (2.6.7).

It is convenient to rewrite S_{wzw} in a more explicit form, this will also allow us to check that it coincides with the result of [52]. Using manipulations which are similar to those explained before to eq. (116) of [52], and noticing that $A^{(g)}$ as defined in that paper (eq. 109) corresponds to $A^{(g^{-1})}$ in our conventions, we get

$$\begin{aligned}\widetilde{\omega}_5(A_h, A) - \widetilde{\omega}_5((A^{(\Lambda)})_h, A^{(\Lambda)}) &= \omega_5(\Lambda^{-1}d\Lambda) - dB_4((A^{(\Lambda)})_h, A^{(\Lambda)}) \\ &\quad + dB_4((A)_h, A) + dB_4(-d\Lambda\Lambda^{-1}, A^{(\Lambda)}).\end{aligned} \tag{2.6.11}$$

To obtain the WZW action of eq. (2.6.9) we must integrate eq. (2.6.11) over the $5D$ space. Since $A(x, z_{\text{IR}}) \in Lie(H)$ and $\Lambda(z_{\text{IR}}) = \mathbb{1}$, no IR contribution comes from integrating the exact forms in the r.h.s. of eq. (2.6.11). Using the UV holographic condition $\widehat{A} = B^{(\Sigma^{-1})}$ and remembering that $\Lambda(z_{\text{UV}}) = \Sigma$, we get

$$\begin{aligned}S_{wzw} = \; & ic\int_5 \omega_5(\Lambda^{-1}d\Lambda) + ic\int B_4((B)_h, B) \\ & -ic\int\left[B_4\left((B^{\Sigma^{-1}})_h, B^{\Sigma^{-1}}\right) + B_4(-d\Sigma\Sigma^{-1}, B)\right],\end{aligned} \tag{2.6.12}$$

where $\int_5$ represents the $5D$ space–time integral. The above formula coincides with the result of [52] (eqs. (115, 116)), given that $\Lambda(z)$ is an extension of the Goldstone boson matrix Σ to the disk D_5 obtained by shrinking the IR boundary to a point. This disk has however the opposite orientation than the one considered in [52], this explains the seeming sign difference.

Notice that $\omega_5(\Lambda^{-1}d\Lambda)$ is proportional to the Maurer–Cartan 5-form (see eq. (2.6.1)), so that its integral only depends on the boundary value of Λ, *i.e.* on the holographic field Σ.[17] We can then rewrite the gauge-fixed holographic action as

$$\begin{aligned}e^{iS_h[B_\mu,\Sigma]} &= \exp\left[iS_{wzw}\left[B_\mu, \Sigma\right]\right] \\ &\times \int \mathcal{D}A_\mu(x,z)_{\widehat{A}_\mu = B_\mu^{(\Sigma^{-1})}} \exp\left[iS_g[A_\mu, A_z = 0] - i\widetilde{S}_{CS}[A_\mu, A_z = 0]\right],\end{aligned} \tag{2.6.13}$$

[17] If $\pi_5(G)$ is non-trivial, the integral can also depend on the topology of Λ, in the sense that two topologically unequivalent extensions of Σ give different results. The difference is however quantized, so that it does not affect the path integral if c, as we will show below, is also quantized.

where we used the fact that the WZW term depends only on the holographic fields and factorized it out of the functional integral. As discussed above, the $\widetilde{S}_{CS}[A]$ term is invariant under H transformations, so that the functional integral term of eq. (2.6.13) is perfectly G-invariant. The above equation shows that, in the presence of the CS term, the holographic action splits in two parts. The first is simply S_{wzw} and its gauge variation reproduces the anomaly in eq. (2.6.7), while the second one is gauge-invariant.

In the above discussion we assumed (see footnote 17) that, if $\pi_5(G)$ is non trivial, the coefficient c of the CS term is quantized. We will now prove that this assumption is necessary to ensure the consistency of our $5D$ model. As we already discussed, the bulk local $\mathcal{G}_B$ invariance of the $5D$ action is gauged. Therefore, as we already did to derive eq. (2.6.3), we must require $\exp[i\widetilde{S}_{CS}]$ to be invariant under any $\mathcal{G}_B$ transformation. In particular, let us consider a generic $\mathcal{G}_B$ element g which reduces to the identity at the IR brane also. After rotating to the Euclidean, such transformations are maps from S^5 (obtained by shrinking both boundaries to a point) to the group G. Let us now start from the trivial $5D$ field configuration $A = 0$ and vary the CS term in eq. (2.6.5) with g, the variation is just the integral of the CS form ω_5 on the pure gauge configuration $A = 0^{(g)}$. As we already mentioned, $\omega_5(gdg^{-1}) = -\omega_5(g^{-1}dg)$ is proportional to the Maurer–Cartan 5-form and thus its integral on S^5 is quantized and depends on the $\pi_5(G)$ homotopy class to which the map g belongs. Summarizing, the $\mathcal{G}_B$ invariance requires, for any $g \in G$

$$\frac{i\,c}{2\pi}\int_{S^5}\omega_5(g^{-1}dg) \in \mathbb{Z}\,. \tag{2.6.14}$$

If $\pi_5(G) = 0$, the above equation gives no restriction on c since $\int_{S^5}\omega_5(g^{-1}dg) = 0$. If, on the contrary, $\pi_5(G)$ is non-trivial, $\int_{S^5}\omega_5(g^{-1}dg) = i\,\gamma\,n$ with n integer and eq. (2.6.14) imposes c to be quantized:

$$c = \frac{2\pi\,m}{\gamma}\,, \tag{2.6.15}$$

where m is an integer.

In the framework of $4D$ effective action, the quantization condition of the WZW term [51, 55] seems weaker than what we find here. It depends indeed on the homotopy of G/H, and not of G. It might occur, a priori, that a non-trivial map $g \in G$ (for which $\int\omega_5 \neq 0$) becomes homotopically trivial if it seen as an element of G/H. Due to eq. (2.6.14), the existence of the map g would imply quantization from the $5D$ point of view, while no restriction would appear in the standard $4D$ framework. As discussed in [55], however, this can not happen if, as in our case (2.6.3), the generators which define the CS form provide an anomaly-free embedding of H. In this case, G maps for which $\int\omega_5 \neq 0$ are topologically non-trivial in G/H also and then the $5D$ quantization condition coincides with the standard $4D$ one. In the next section we will provide an explicit example of this fact, we will apply the $5D$ condition (2.6.14) to the case of QCD and show that the result coincides with the well-known $4D$ one.

2.6.1 Anomaly in *AdS/QCD*

It is useful to apply the results of the previous section to the concrete case of *AdS/QCD*. We consider, as in sect. 2.5, a gauge group $G = \Gamma_L \times \Gamma_R$ broken to its diagonal subgroup $H = \Gamma_V$. To apply the formalism previously outlined, we must choose a representation of G such that the H embedding is anomaly-free (2.6.3). The generators are

$$T_a^L = \begin{pmatrix} t_a & 0 \\ 0 & 0 \end{pmatrix}, \qquad T_a^R = \begin{pmatrix} 0 & 0 \\ 0 & -(t_a)^T \end{pmatrix}, \tag{2.6.16}$$

where t_a denote the generators of Γ normalized to $2\mathrm{Tr}[t_a, t_b] = \delta_{ab}$. The vector combinations

$$T_a = \begin{pmatrix} t_a & 0 \\ 0 & -(t_a)^T \end{pmatrix}, \tag{2.6.17}$$

are the generators of the unbroken subgroup Γ_V. The gauge field is $A = A_L^a T_a^L + A_R^a T_a^R$ and to rewrite our results with the common notation we also define $A_{L,R} = A_{L,R}^a t^a$.

The CS form is

$$\omega_5(A) = \omega_5(A_L) - \omega_5(A_R), \tag{2.6.18}$$

where ω_5 is given in eq. (2.6.1), it is manifest that $\omega_5(A)$ vanishes for $A \in Lie(\Gamma_V)$, hence Γ_V is anomaly free. The 4-form B_4 (eq. (2.6.6)) which enters in the definition of the shifted CS (eq. (2.6.5)) is now

$$B_4 = \frac{1}{2}\mathrm{Tr}\left[(\mathcal{V}A - A\mathcal{V})(F + F_V) + A\mathcal{V}^3 - \mathcal{V}A^3 + \frac{1}{2}\mathcal{V}A\mathcal{V}A\right], \tag{2.6.19}$$

where $\mathcal{V} = 1/2(A_L^a + A_R^a)T^a$ denotes the vectorial part of the gauge field, $F \equiv dA + A^2$ is the field strength of the gauge field and $F_V \equiv d\mathcal{V} + \mathcal{V}^2$. The above equation can be rewritten as

$$B_4 = \frac{1}{2}\mathrm{Tr}\left[(F_R A_R + A_R F_R)A_L + A_L A_R^3 + \frac{1}{4}(A_R A_L)^2 - (L \leftrightarrow R)\right], \tag{2.6.20}$$

and coincides with the Adler–Bardeen counterterm [56].

The general gauge-fixing procedure of the previous section could be directly applied to the present case. This would lead, however, to a non-standard parametrization of the Goldstone degrees of freedom. Analogously to what we did in sect. 2.5, we need to adapt the previous discussion to the case of *AdS/QCD*. As discussed in appendix A, the final result is the same as eq. (2.6.8) in which Λ is now given by

$$\Lambda(x, z) = \begin{pmatrix} \widetilde{U}^{-1} & 0 \\ 0 & \mathbb{1} \end{pmatrix}, \tag{2.6.21}$$

where $\widetilde{U}$ is an extension on the disk of the Goldstone boson matrix $U(x)$, *i.e.* $\widetilde{U}(x, z_{\mathrm{UV}}) = U(x)$, $\widetilde{U}(x, z_{\mathrm{IR}}) = \mathbb{1}$.

With Λ given in eq. (2.6.21), all the other formulas of the previous section can be directly applied. The $\chi\mathbf{PT}$ action (compare with eq. (2.5.5)) is

$$\exp\left[i\widetilde{S}_{\chi\mathbf{PT}}[l_\mu, r_\mu, U]\right] = \exp[iS_{wzw}[l_\mu, r_\mu, U]] \times \int \mathcal{D}A_{L,\mu}(x,z)_{\widehat{A}_{L,\mu}=l_\mu^{(U)}} \mathcal{D}A_{R,\mu}(x,z)_{\widehat{A}_{R,\mu}=r_\mu} \exp[i\widetilde{S}[A_\mu, A_z = 0]]\,, \qquad (2.6.22)$$

where $\widetilde{S} \equiv S_g + \widetilde{S}_{CS}$. The explicit form of the WZW term can be read from eq. (2.6.12), it can be checked that it coincides with the $4D$ result reported in [50, 57]. When the sources are set to zero, eq. (2.6.12) simplifies and we are left with the usual ungauged WZW term

$$S_{wzw}[0,0,U] = i\,c \int_5 \omega_5[(\widetilde{U}d\widetilde{U}^{-1})^5] = \frac{i\,c}{10}\int_5 \mathrm{Tr}\left[(\widetilde{U}d\widetilde{U}^{-1})^5\right]\,. \qquad (2.6.23)$$

As discussed before, when $\pi_5(G)$ is non-trivial the coefficient of the Chern–Simons term is quantized. In particular, in the $G = SU(N)_L \times SU(N)_R$ case with $N \geq 3$, $\pi_5(G) = \mathbb{Z}^2$. The quantization condition can be easily obtained from eq. (2.6.14), g represents in this case the more general map from S^5 to $SU(N)_L \times SU(N)_R$ and ω_5 is given by eq. (2.6.18), notice that its "$L-R$" form is due to the requirement of having an anomaly-free $SU(N)_V$. It is well known that, for a generic $SU(N)$ element such as g_L or g_R, one has

$$\int_{S^5} \omega_5(g^{-1}dg) = \int_{S^5} \frac{1}{10}\mathrm{Tr}\left[(g^{-1}\,dg)^5\right] = 48\pi^3 n\,i\,, \qquad (2.6.24)$$

with n integer. The quantization condition then becomes $c = m/(24\pi^2)$ and substituting in eq. (2.6.23) one obtain the usual quantized form of the WZW term

$$S_{wzw}[0,0,U] = \frac{i\,m}{240\pi^2}\int_5 \mathrm{Tr}\left[(\widetilde{U}d\widetilde{U}^{-1})^5\right]\,. \qquad (2.6.25)$$

Notice that we obtained the standard quantization condition from purely $5D$ consistency requirements.

Chapter 3

5D Models with Gauge–Higgs Unification

In this chapter we will discuss the possibility of constructing models of EWSB in the context of extra-dimensional theories. One particularly interesting scenario is based on the gauge–Higgs unification mechanism, which relies on the possibility of identifying the Higgs multiplet with the internal components of a higher-dimensional gauge field.

As a first issue, we will briefly review the gauge–Higgs unification mechanism in a $U(1)$ toy model compactified on S^1. This simple example will give us the possibility of presenting the main virtues of the GHU models without entering into the subtleties of non-Abelian gauge groups and orbifold compactifications.

After this introduction, we will concentrate on a (semi-)realistic model compactified on $S^1/\mathbf{Z}_2$ with an extended gauge group $SU(3) \times U(1)$ [15]. Although this model reproduces all the qualitative features of the SM, it presents some problems at the quantitative level. In particular the predicted top and Higgs masses are much below their experimental limits. A possible way to solve these problems and get a fully realistic model will be the subject of the next chapter.

3.1 The Gauge–Higgs Unification Mechanism

As we said, in the GHU scenario the Higgs field is identified with the internal components of a higher-dimensional gauge field. As one could easily guess, this peculiar origin of the Higgs field has deep and interesting consequences on its properties. First of all the higher-dimensional gauge invariance heavily constrains the form of the Higgs effective Lagrangian. In particular a tree-level mass term for the Higgs is forbidden, and this means that the Higgs can acquire a mass only at loop level and moreover this mass is finite and stable against radiative corrections. This feature is clearly related to the non-local nature of the Higgs field. In fact, as discussed in section 1.5, the A_y component, which is identified with

the Higgs, is closely related to the Wilson loop $\mathcal{W}$ (eq. (1.5.3)) which wraps around S^1. In particular the Higgs VEV can be seen as a Wilson loop phase or equivalently as a Scherk–Schwarz twist in the periodicity conditions of the fields on the circle (see eq. (1.4.4)). The non-local nature of the Higgs VEV, guarantees not only the stability of the Higgs mass but also the finiteness of the whole Higgs effective potential at any loop order [58]. Clearly, this is another remarkable property of the GHU scenario which allows to stabilize the EW scale relating it to the compactification scale of the model rather than to the cut-off of the theory.

When we compactify our theory on an orbifold and not on a smooth manifold, some subtleties arise due to the presence of boundaries. In fact at the fixed points of the $S^1/\mathbf{Z}_2$ orbifold the gauge symmetry is broken and localized mass terms could be generated which would destabilize the Higgs potential and the EW scale. Fortunately, also in this case a remnant of the non-Abelian bulk gauge symmetry (the shift symmetry), as we will better discuss in section 3.5, forbids the appearance of dangerous localized terms, thus preserving the finiteness properties of the GHU scenario. A useful insight on the orbifold scenario can also be obtained adopting the holographic prospective of the previous chapter. The holographic effective description clearly shows that the gauge symmetry breaking at the boundaries is actually a spontaneous breaking. As a by-product of this breaking some (pseudo-)Goldstone bosons are present which are identified with the Higgs field in the GHU scenario. From this point of view, the dynamics of the Higgs is constrained by its Goldstone nature, and the EW scale still continues to be stabilized.

Let us now concentrate on a simple toy model. We will consider a $U(1)$ gauge theory compactified on S^1, coupled with a fermion Ψ with bulk mass mass m [12]. In this case the Higgs field is identified with the zero mode of A_y. Of course, at tree level the Higgs can not have a mass term, but it acquires mass at the radiative level through diagrams containing fermion loops. At 1-loop level we can compute the Higgs mass by simply summing over the diagrams with two external Higgs fields and a loop given by fermion KK modes. Allowing the Higgs field to get a VEV, or equivalently imposing a Scherk–Schwarz periodicity condition for the fermions (see eq. (1.4.4)), we find

$$m_H^2 = 4\frac{g_5^2}{2\pi R}\int \frac{d^4p}{(2\pi)^4}\sum_n \frac{p^2 - p_{y,n}^2 + m^2}{\left(p^2 + p_{y,n}^2 + m^2\right)^2}\,, \tag{3.1.1}$$

where we defined $p_{y,n} = (n+\alpha)/R$ and the $4D$ momentum has been rotated into the Euclidean. Notice that every single piece in the sum is quadratically divergent, so that, if we truncate the sum up to a certain KK level, we obtain an infinite result. This feature is however not surprising, in fact a truncation of the KK tower spoils the higher-dimensional gauge invariance which forbids the presence of a mass term for the Higgs and protects it from divergences. Instead, the correct way to regularize eq. (3.1.1) is to perform the sum over the whole KK tower and then integrate over the $4D$ momentum [58]. Computing the

sum we get

$$\sum_n \frac{p^2 - p_{y,n}^2 + m^2}{\left(p^2 + p_{y,n}^2 + m^2\right)^2} = 2\pi^2 R^2 \frac{\cosh(2\rho\pi R)\cos(2\pi\alpha) - 1}{[\cosh(2\rho\pi R) - \cos(2\pi\alpha)]^2}\,, \tag{3.1.2}$$

where $\rho^2 \equiv p^2 + m^2$. This expression vanishes as $1/\cosh(2p\pi R)$ for large momentum, and substituting it into eq. (3.1.1), we obtain a finite value of the radiative mass term for any α. Moreover we obtain that the mass term is related to the $5D$ gauge coupling and to the compactification radius and scales as $m_H^2 \sim g_5^2/R^3$.

With an analogous computation one can also show that, not only the mass term, but the whole Higgs effective potential is finite.[1]

3.2 A Gauge–Higgs Unification Model on $S^1/\mathbf{Z}_2$: the Gauge Sector

Undoubtedly, the GHU mechanism we described in the previous section presents some features which are very appealing from a phenomenological point of view. Nevertheless in order to implement this idea in a realistic scenario one must add some other ingredients. First of all the the SM structure requires the presence of chiral fermions and this can not be obtained on a smooth space like S^1. An easy way to address this problem is to compactify our theory on an orbifold. We already showed in chapter 1 that orbifold compactifications can generate a chiral spectrum by projecting out fermion zero modes of only one chirality. In this chapter we will use a different approach and we will obtain a chiral $4D$ spectrum by simply introducing chiral fermions localized at the orbifold fixed points.

A second issue is the necessity to reproduce the SM model $SU(2) \times U(1)_Y$ EW gauge group and to get at the same time a Higgs doublet in the correct representation. This structure can be obtained choosing a $5D$ theory with an extended gauge group. The basic idea is to construct a theory with a bulk gauge group G which has the SM group as a subgroup and to use the orbifold projection to break G down to $SU(2) \times U(1)_Y$. At the same time we can try to identify the Higgs doublet with the massless scalars coming from A_y, which are associated to the broken gauge generators.

In this chapter we will present a possible realization of these ideas which has been proposed in [15]. The model is based on a $5D$ gauge theory with bulk gauge group $G = SU(3)_s \times SU(3)_w \times U(1)'$ compactified on $S^1/\mathbf{Z}_2$. The $SU(3)_s$ gauge group, which is identified with the QCD gauge group, is supposed to be left unbroken by the orbifold action. From the effective action point of view it will give some massless gauge fields (the gluons) and a KK tower of massive gauge fields whose mass levels are $m_n = n/R$ with $n \geq 1$. The presence of the $SU(3)_s$ subgroup does not affect the EW properties of the gauge sector and we will neglect it in the following analysis.

[1] To be more precise, the Higgs effective potential contains a divergent part which is independent of the Higgs VEV. This divergent part corresponds to vacuum–to–vacuum 1-loop diagrams. Once this divergent piece has been regularized, a finite Higgs potential is obtained.

Let us now focus on the $SU(3)_w \times U(1)'$ subgroup which gives origin to the SM $SU(2) \times U(1)_Y$ group and to the Higgs doublet. The choice of this $5D$ gauge symmetry is in some sense not the minimal one. In fact the SM gauge group can be embedded simply in an $SU(3)$ group and at the same time the orbifold breaking gives a scalar doublet which could be identified with the Higgs. This construction, however, has a great shortcoming, namely it fixes the weak mixing angle θ_w at a value which is incompatible with the experimental results. The extra $U(1)'$ factor is a possible solution to this problem.

In order to better explain the weak mixing angle problem and its solution, it is convenient to start describing a theory with only an $SU(3)_w$ gauge group. The $\mathbf{Z}_2$ orbifold projection is embedded in the gauge group through the matrix (see section 1.4.2 and in particular eq. (1.4.18))

$$Z = e^{2\pi i \sqrt{3} t^8} = \begin{pmatrix} -1 & 0 & 0 \\ 0 & -1 & 0 \\ 0 & 0 & 1 \end{pmatrix} , \tag{3.2.1}$$

where t^A are the usual $SU(3)$ generators normalized as $2\,\mathrm{Tr}[t^A t^B] = \delta^{AB}$. The orbifold action breaks the $SU(3)_w$ group to $SU(2) \times U(1)$, where the $U(1)$ subgroup is the one generated by t^8. The massless $4D$ degrees of freedom are given by the gauge fields arising from A_μ in the adjoint representation $(\mathbf{3}_0 \oplus \mathbf{1}_0)$ of $SU(2) \times U(1)$, and a complex scalar doublet arising from A_y in the $\mathbf{2}_{1/2}$ representation. The $4D$ gauge coupling associated to the $SU(2)$ subgroup is related to the $5D$ one by $g = g_5/\sqrt{2\pi R}$. Of course, given the fact that both the $SU(2)$ and the $U(1)$ $4D$ gauge subgroups come from the same $SU(3)$ group, their coupling constants are not independent but rather they are related by $g_{U(1)}/g = \tan\theta_w = \sqrt{3}$. The value of the weak mixing angle predicted by this simple model is not compatible with the experimental value $\sin^2\theta_w \simeq 0.23$.

In this model an additional spontaneous symmetry breaking $SU(2) \times U(1) \to U(1)_e$ is induced when A_y (or in other words the Higgs field) gets a VEV. Using the unbroken $SU(2)$ symmetry we can align the VEV along the t^7 generator:[2]

$$\langle A_y \rangle = \frac{2\alpha}{g_5 R} t^7 . \tag{3.2.2}$$

Notice that the parameter α is a Wilson line phase (see section 1.5) whose associated Wilson line is

$$\mathcal{W} = e^{4\pi i \alpha t^7} . \tag{3.2.3}$$

As a consequence, the EWSB in this model is equivalent to a Wilson-line symmetry breaking. Due to the fact that α is a Wilson-line phase, values of α which differ by an integer

[2]To use a simpler notation, in this chapter and in chapters 4 and 5 we adopt the standard form of the $5D$ action in which the bulk fieds are canonically normalized. In this case the field strength and the covariant derivative are given by $F_{MN} = \partial_M A_N - \partial_N A_M - ig_5[A_M, A_N]$ and $D_M = \partial_M - ig_5[A_M, \cdot]$. The normalization used in the previous chapters can be easily obtained by rescaling the bulk fields with the $5D$ gauge couplings (compare footnote 2 in chapter 1).

are equivalent ($\alpha \sim \alpha + 1$).

3.2.1 The $U(1)'$ Subgroup and the θ_w Angle

As already anticipated, a possible way to solve the problem of having a reasonable value of the weak mixing angle θ_w is the introduction of an extra $U(1)'$ subgroup into the gauge group G.[3] This extra factor is not affected by the orbifold projection (*i.e.* it is left unbroken). The hypercharge generator Y is taken to be the linear combination $Y = \frac{1}{\sqrt{3}} t^8 + t'$ of the $U(1)$ and $U(1)'$ generators, so that the charge of a field under $U(1)_Y$ is given by the sum of the $U(1)$ and $U(1)'$ charges. The gauge field A_Y associated to the hypercharge and its orthonormal combination A_X are

$$A_Y = \frac{g' A^8 + \sqrt{3} g A'}{\sqrt{3g^2 + g'^2}}, \qquad A_X = \frac{\sqrt{3} g A^8 - g' A'}{\sqrt{3g^2 + g'^2}}. \tag{3.2.4}$$

The $U(1)_Y$ coupling g_Y is related to the $SU(3)_w$ coupling g and to the $U(1)'$ charge $g = g'_5/\sqrt{2\pi R}$ as

$$g_Y = \frac{\sqrt{3} g g'}{\sqrt{3g^2 + g'^2}}. \tag{3.2.5}$$

By suitably choosing g' we can adjust the weak mixing angle to the correct value, according to the relation

$$\sin^2 \theta_W = \frac{{g_Y}^2}{g^2 + {g_Y}^2} = \frac{3}{4 + 3g^2/g'^2}. \tag{3.2.6}$$

As we will better discuss in section 3.4, the $U(1)_X$ subgroup is anomalous and the corresponding field acquires a large localized mass term. As a consequence its zero mode decouples from the effective theory leaving only a tower of massive KK excitations. The $U(1)_X$ subgroup is thus broken and the low-energy $4D$ gauge group is the usual SM one $SU(2) \times U(1)_Y$.

The presence of the extra $U(1)'$ factor does not change the EWSB mechanism. As in the previously discussed $SU(3)_w$ case, when A_y gets a VEV, which can be written as in eq. (3.2.2), a spontaneous breaking occurs: $SU(2) \times U(1)_Y \to U(1)_{EM}$.

3.3 A Gauge–Higgs Unification Model on S^1/Z_2: the Fermionic Sector

Let us now discuss how to introduce matter fields in the above described scenario. One possibility is to include massive $5D$ bulk fermions and massless localized chiral fermions with a mixing between them, so that the matter fields are identified with the lowest KK

[3] Another possible solution to this problem consists in adjusting θ_w by introducing different localized kinetic terms for $SU(2)$ and $U(1)$ gauge bosons at the orbifold fixed points [15] (see section 3.7.2). This approach, however, generates a distortion of the field wave functions and, consequently, too large corrections to the EW observables.

Bulk Fields		Boundary Fields ($y = 0$)	
		Doublets	Singlets
Ψ^b: $(\mathbf{3},\mathbf{3})_0$ Ψ^t: $(\mathbf{3},\overline{\mathbf{6}})_0$	*coupled to*	Q_L: $(\mathbf{3},\mathbf{2})_{1/6,0}$	b_R: $(\mathbf{3},\mathbf{1})_{-1/3,0}$ t_R: $(\mathbf{3},\mathbf{1})_{2/3,0}$
Ψ^l: $(\mathbf{1},\mathbf{3})_{-2/3}$ Ψ^ν: $(\mathbf{1},\overline{\mathbf{6}})_{-2/3}$	*coupled to*	L_L: $(\mathbf{1},\mathbf{2})_{1/6,-2/3}$	l_R: $(\mathbf{1},\mathbf{1})_{-1/3,-2/3}$ ν_R: $(\mathbf{1},\mathbf{1})_{2/3,-2/3}$

Table 3.1: Fermion content of the model for a quark and lepton generation. For bulk fields we reported the $SU(3)_s \times SU(3)_w$ representation and the $U(1)'$ charge. For localized fields the $SU(3)_s \times SU(2)$ representation and the $U(1)$ and $U(1)'$ charges are given.

mass eigenstates. As we will show, in this set-up Yukawa couplings are exponentially sensitive to the bulk mass terms, and the observed hierarchy of fermion masses can be naturally explained.

In the quark sector, for every generation we introduce a couple of periodic bulk fermions $(\Psi^t, \widetilde{\Psi}^t)$ with opposite $\mathbf{Z}_2$ parities, in the representation $(\mathbf{3},\overline{\mathbf{6}})$ of $SU(3)_c \times SU(3)_w$, and $(\Psi^b, \widetilde{\Psi}^b)$ in the $(\mathbf{3},\mathbf{3})$. At the orbifold fixed point $y = 0$, we have a left-handed doublet $Q_L = (t_L, b_L)^T$ and two right-handed fermion singlets t_R and t_L of $SU(2) \times U(1)$, all these fields are in the fundamental representation of $SU(3)_s$.[4] The parity assignments for the bulk fermions allow for a bulk mass term which mixes Ψ and $\widetilde{\Psi}$, as well as boundary couplings $e_{1,2}$, with mass dimension 1/2, which mix the bulk fermions with the localized fields Q_L, t_R and b_R. The matter Lagrangian can be splitted into a bulk and a boundary part:

$$\mathscr{L} = \mathscr{L}_\Psi + \delta(y)\mathscr{L}_0 \,. \tag{3.3.1}$$

The bulk piece for each quark family[5] is given by

$$\mathscr{L}_\Psi = \sum_{a=t,b} \left\{ \overline{\Psi}^a i \not{D}_5 \Psi^a + \overline{\widetilde{\Psi}}^a i \not{D}_5 \widetilde{\Psi}^a - M_a \left(\overline{\Psi}^a \widetilde{\Psi}^a + \overline{\widetilde{\Psi}}^a \Psi^a \right) \right\} , \tag{3.3.2}$$

[4] In the original model of [15] and in a subsequent development [26], the $(\Psi^t, \widetilde{\Psi}^t)$ doublet was in the $(\overline{\mathbf{3}},\mathbf{6})$ representation and $(\Psi^\nu, \widetilde{\Psi}^\nu)$ (see below) was in the $(\mathbf{1},\mathbf{6})$. The present set-up is however completely equivalent to the original proposal. Moreover, in [15, 26] localized fermions were introduced at both the orbifold fixed points. This possibility proves less appealing from a phenomenological point of view, in fact in this set-up it is more difficult to construct a model compatible with the experimental constraints.

[5] For simplicity we consider here a Lagrangian without mixing among different fermion families. Given the fact that the EWSB is nearly entirely due to the third generation of quarks (see sections 3.5 and 3.6), this simplifying assumption has no relevant effect on the main properties of the model. The problem of embedding a non-trivial flavour structure in this set-up will be briefly discussed at the end of this section.

while the boundary part is

$$\mathscr{L}_0 = \overline{Q}_L i\not{D}_4 Q_L + \bar{t}_R i\not{D}_4 t_R + \bar{b}_R i\not{D}_4 b_R + \left(e_1^b\,\overline{Q}_L\psi^b + e_1^t\,\overline{Q}_L\psi^t + e_2^b\,\bar{b}_R\chi^b + e_2^t\,\bar{t}_R\chi^t + \text{h.c.}\right), \tag{3.3.3}$$

where $\psi^{t,b}$ and $\chi^{t,b}$ are the doublet and singlet $SU(2)$ components of the bulk fermions $\Psi^{t,b}$ (see appendix D for the decomposition of the bulk fields).

The leptonic sector is built in an analogous manner. For each generation we introduce a couple of bulk fermions with opposite orbifold parities $(\Psi^l, \widetilde{\Psi}^l)$ in the representation $(\mathbf{1},\mathbf{3})$, and a couple $(\Psi^\nu, \widetilde{\Psi}^\nu)$ in the $(\mathbf{1},\overline{\mathbf{6}})$. At $y = 0$ we add a left-handed doublet L_L and two right-handed singlets l_R and ν_R, which are all singlets of $SU(3)_s$. As in the quark case, bulk masses are introduced between Ψ and $\widetilde{\Psi}$ and bulk and localized fields are coupled through boundary terms. Due to the fact that the EWSB is mostly determined by the third quark generation, in the following we will neglect the leptonic sector. The fermion content of the model is summarized in table 3.1.

For future use, we introduce the parameters $\lambda^a = \pi R M_a$ and $\varepsilon_i^a = \sqrt{\pi R/2}\,e_i^a$. We also define the dimensionless Euclidean momentum variables $x = \pi R p$ and $x^a = \pi R\sqrt{p^2 + M_a^2}$.

3.3.1 The Fermionic Spectrum

Having defined the matter content of the model, we want now to study the $4D$ fermionic spectrum and in particular the masses of the light states (the SM fields) after EWSB. Before deriving the effective action of the theory, it is useful to report the decomposition of the bulk fields with respect to the unbroken subgroup $SU(2) \times U(1)$ of the $SU(3)_w$ gauge group. The fundamental representation decomposes as $\mathbf{3} = \mathbf{2}^-_{1/6} \oplus \mathbf{1}^+_{-1/3}$, while for the antisymmetric one finds $\overline{\mathbf{6}} = \overline{\mathbf{3}}^+_{-1/3} \oplus \mathbf{2}^-_{1/6} \oplus \mathbf{1}^+_{2/3}$, where we also reported the relative parities of the various components. The $\psi^{t,b}$ fields are thus given by the $\mathbf{2}^-_{1/6}$ components of the $\Psi^{t,b}$ fields, while $\chi^{t,b}$ correspond to the singlets $\mathbf{1}^+_{2/3}$ and $\mathbf{1}^+_{-1/3}$. The fact that the doublets and the singlets have opposite parities is necessary to ensure the existence of couplings between boundary and bulk fields. Notice, moreover, that the coupling given in eq. (3.3.3) are the only ones allowed by the parity assignments.

To study the low energy properties of the theory it is useful to adopt the holographic description presented in the previous chapter. The effective action for the bulk fields becomes simpler when written in terms of L-handed sources $(\Psi_L^t, \widetilde{\Psi}_L^t)$ and $(\Psi_L^b, \widetilde{\Psi}_L^b)$. To avoid cumbersome formulae, here we will report the holographic actions for the bulk fields in the absence of couplings with the localized fermions. The holographic Lagrangian for

the $(\Psi^t, \widetilde{\Psi}^t)$ system in the Euclidean momentum space is given by[6]

$$\begin{aligned}\mathscr{L}_t = &-x^t \tanh(x^t) \left(\overline{\phi}_1^t \frac{\not{p}}{p^2} \phi_1^t + \frac{\overline{\chi}^t + \overline{\phi}_2^t}{\sqrt{2}} \frac{\not{p}}{p^2} \frac{\chi^t + \phi_2^t}{\sqrt{2}} \right) \\ &+x^t \frac{\cos(2\pi\alpha) - \cosh(2x^t)}{\sinh(2x^t)} \left(\overline{\phi}_3^t \frac{\not{p}}{p^2} \phi_3^t + \overline{\widetilde{\psi}}_2^t \frac{\not{p}}{p^2} \widetilde{\psi}_2^t \right) \\ &+x^t \frac{\cos(4\pi\alpha) - \cosh(2x^t)}{\sinh(2x^t)} \left(\overline{\widetilde{\psi}}_1^t \frac{\not{p}}{p^2} \widetilde{\psi}_1^t + \frac{\overline{\chi}^t - \overline{\phi}_2^t}{\sqrt{2}} \frac{\not{p}}{p^2} \frac{\chi^t - \phi_2^t}{\sqrt{2}} \right) , \end{aligned} \tag{3.3.4}$$

where we expressed the result in terms of the $SU(2)$ components of the bulk fields (see appendix D for the notation and the details of the decomposition). From eq. (3.3.4) one can easily extract the spectrum of the bulk fields,[7] which is given by a tower with charge $q = 2$ with respect to the Higgs and masses $m_n^2 = \left(\frac{n+2\alpha}{R}\right)^2 + M_t^2$, a tower with charge $q = 1$ and masses $m_n^2 = \left(\frac{n+\alpha}{R}\right)^2 + M_t^2$, and a tower which is not coupled with the Higgs $m_n^2 = \left(\frac{n}{R}\right)^2 + M_t^2$.

The holographic description of $(\Psi^b, \widetilde{\Psi}^b)$ is

$$\mathscr{L}_b = -x^b \tanh(x^b) \overline{\widetilde{\psi}}_1^b \frac{\not{p}}{p^2} \widetilde{\psi}_1^b + x^b \frac{\cos(2\pi\alpha) - \cosh(2x^b)}{\sinh(2x^b)} \left(\overline{\chi} \frac{\not{p}}{p^2} \chi + \overline{\widetilde{\psi}}_2^b \frac{\not{p}}{p^2} \widetilde{\psi}_2^b \right) . \tag{3.3.5}$$

In this case the $4D$ spectrum is given by a tower with charge $q = 1$ with respect to the Higgs and masses $m_n^2 = \left(\frac{n+\alpha}{R}\right)^2 + M_b^2$ and a tower not coupled with the Higgs with $m_n^2 = \left(\frac{n}{R}\right)^2 + M_b^2$.

The low energy Lagrangian for the localized fields can be obtained by integrating out the holographic degrees of freedom which describe the bulk fields, and retaining the localized fields as effective degrees of freedom. After a straightforward computation one finds

$$\begin{aligned}\mathscr{L}_{loc}^t = \overline{t} \Bigg\{ \not{p} \Bigg[1 + \frac{{\varepsilon_1^b}^2}{x^b} P_L f_0(x^b, 0) + \frac{{\varepsilon_2^t}^2}{2x^t} P_R f_0(x^t, 0) + \left(\frac{{\varepsilon_1^t}^2}{x^t} P_L + \frac{{\varepsilon_2^t}^2}{2x^t} P_R \right) f_0(x^t, 2\alpha) \Bigg] \\ + \frac{i}{\pi R} \frac{\varepsilon_1^t \varepsilon_2^t}{\sqrt{2}} f_1(x^t, 2\alpha) \Bigg\} t , \end{aligned} \tag{3.3.6}$$

$$\mathscr{L}_{loc}^b = \overline{b} \left\{ \not{p} \left[1 + \left(\frac{{\varepsilon_1^b}^2}{x^b} P_L + \frac{{\varepsilon_2^b}^2}{x^b} P_R \right) f_0(x^b, \alpha) + \frac{{\varepsilon_1^t}^2}{x^t} P_L f_0(x^t, \alpha) \right] + \frac{i}{\pi R} \varepsilon_1^b \varepsilon_2^b f_1(x^t, 2\alpha) \right\} b , \tag{3.3.7}$$

[6] For simplicity we omit the $\widehat{\ }$ symbol and use the same notation for the bulk fields and their UV values.

[7] As explained in the previous chapter in this case the spectrum is given by the zeroes of the two point functions. Notice that to extract the spectrum from eqs. (3.3.4) and (3.3.5) we must rotate the momentum back to the Minkowskian.

where $t = t_L + t_R$ and $b = b_L + b_R$, $P_{L,R}$ are the L and R projectors, and the functions $f_{0,1}$ are defined as

$$f_0(x,\alpha) = \mathrm{Re}\left[\coth(x + i\pi\alpha)\right] = \frac{\sinh(2x)}{\cosh(2x) - \cos(2\pi\alpha)}\,, \tag{3.3.8}$$

$$f_1(x,\alpha) = \mathrm{Im}\left[\coth(x + i\pi\alpha)\right] = -\frac{\sin(2\pi\alpha)}{\cosh(2x) - \cos(2\pi\alpha)}\,. \tag{3.3.9}$$

When the localized fields are taken into account, the spectrum of the theory, which we obtained before in the absence of boundary couplings, is distorted and some light modes appear which correspond to the SM matter fields. The exact distorted spectrum can be extracted from eqs. (3.3.6) and (3.3.7) determining the zeroes of the quadratic Lagrangian. When the physical mass induced for the light states is much smaller than the masses of the bulk fields, to a very good approximation the SM-quark spectrum can be computed neglecting the momentum dependence induced by higher derivative operators in eqs. (3.3.6) and (3.3.7). In this way one finds

$$m_a = \left|\frac{m_0^a}{\sqrt{Z_1^a Z_2^a}}\right|\,, \qquad a = t, b\,, \tag{3.3.10}$$

where

$$m_0^t = \frac{\varepsilon_1^t \varepsilon_2^t}{\sqrt{2\pi R}} f_1(\lambda^t, 2\alpha)\,, \tag{3.3.11}$$

$$m_0^b = \frac{\varepsilon_1^b \varepsilon_2^b}{\pi R} f_1(\lambda^b, \alpha)\,, \tag{3.3.12}$$

$$Z_i^t = 1 + \delta_{i1}\frac{\varepsilon_1^{b\,2}}{\lambda^b} f_0(\lambda^b, 0) + \delta_{i2}\frac{\varepsilon_2^{t\,2}}{2\lambda^t} f_0(\lambda^t, 0) + \frac{\varepsilon_i^{t\,2}}{2^{\delta_{i2}}\lambda^t} f_0(\lambda^t, 2\alpha)\,, \tag{3.3.13}$$

$$Z_i^b = 1 + \frac{\varepsilon_i^{b\,2}}{\lambda^b} f_0(\lambda^b, \alpha)\delta_{i1}\frac{\varepsilon_1^{t\,2}}{\lambda^t} f_0(\lambda^t, \alpha)\,. \tag{3.3.14}$$

An interesting property of the masses of the light states is their exponential suppression in the bulk masses $m_a \sim \exp(-2\pi R M_a)$. This behaviour can be easily derived from eqs. (3.3.10)–(3.3.14) taking into account the exponential suppression of $f_1(x,\alpha)$ for large values of x ($f_1(x,\alpha) \sim \exp(-2x)$, see eq. (3.3.9)). From a physical point of view, this suppression can be understood recalling that the EWSB in this model is generated by a Wilson line and thus is due to non-local effects. In this context, Yukawa couplings for the boundary fields can be generated only through non-local operators involving Wilson lines that connect the two boundaries and wind around the internal space. The resulting masses of the light states are thus exponentially sensitive to the bulk masses M_a. Another way to understand this property is to consider the tree-level diagrams which generate a mass term for the boundary fields in the low-energy Lagrangian (eqs. (3.3.6) and (3.3.7)). Clearly the localized fields do not couple directly with the Higgs, thus they can acquire

a mass only through their mixing with the bulk fields. Moreover, the bulk fields can "feel" the symmetry breaking only if they wrap around the orbifold, thus they provide an exponential suppression in the mass diagrams in which they appear as internal lines. Notice that, given the fact that the boundary fields are all localized at the same boundary, the bulk fields in the mass diagrams must propagate from one boundary to the other twice, so that the suppression factor is not $\exp(-\pi R M_a)$ but rather $\exp(-2\pi R M_a)$.[8]

It is useful to study the mass equation for the top quark (eq. (3.3.10)) in the limit of large bulk–to–boundary couplings ($\varepsilon^t \gg 1$). For simplicity we also take $\varepsilon^b = 0$, and we get

$$m_t \simeq \sqrt{2}\frac{\sin(4\pi\alpha)}{4\pi R}\frac{2\lambda^t}{\sinh(2\lambda^t)}\,. \tag{3.3.15}$$

The top mass decreases monotonically with λ^t, and using the mass formula for the W boson ($m_W = \alpha/R$, see section 3.4), we obtain

$$m_t \lesssim \sqrt{2} m_W\,. \tag{3.3.16}$$

This constraint is clearly not compatible with the experimental value of the top mass, and constitute a major problem of this model. Various ways to solve this problem have been proposed. One possibility is given by the introduction of bulk fermions in higher-rank representations of the $SU(3)_w$ gauge group which couple to the localized fields.[9] In this way one can get a larger group-theoretical factor multiplying eq. (3.3.15). In this approach, however, a large number of bulk fermions is present in the model and this necessarily leads to a very low cut-off. Another possibility to solve the problem of getting a larger top mass is given by the introduction of Lorentz-breaking terms into the Lagrangian [26, 27]. This scenario seems more appealing from a phenomenological point of view and will be considered in detail in the next chapter.

3.3.2 The Flavour Structure

To conclude the description of the fermionic sector of the theory, we will briefly discuss, along the lines of [15], how to embed a more general flavour structure into the model. In the set-up we described before, three fermion generation (which we now denote by $I = 1, 2, 3$) were already present, but the whole construction was chosen to be flavour blind, so that no mixing appears among different generations. This was simply obtained by assuming the bulk mass matrix $(M_a)_{IJ}$ and the boundary couplings $(\varepsilon_i^a)_{IJ}$ to be diagonal in the flavour indices. Of course, a non-trivial flavour structure is obtained when $(M_a)_{IJ}$ and $(\varepsilon_i^a)_{IJ}$ are allowed to be arbitrary matrices. However, due to the possibility of redefining

[8] When left- and right-handed fields are localized at different fixed points the exponential suppression, as expected, is $\exp(-\pi R M_a)$ [15, 26].

[9] A possible implementation of this idea can be found in [29].

the bulk and the localized fields, we can always diagonalize either the bulk mass matrix or the boundary couplings (but not both of them at the same time).

The computation of the masses of the SM matter fields is similar to the one described before. As we said, we can assume the boundary couplings to be flavour-diagonal, at the price of having a non-diagonal bulk mass matrix. The latter can be written as $M_a = E_a^\dagger M_a^D F_a$, where E_a and F_a are unitary matrices and M_a^D is diagonal. The mass matrix for the bulk fields can thus be diagonalized by the redefinition $\Psi'_a = E_a \Psi^a$ and $\widetilde{\Psi}'_a = F_a \widetilde{\Psi}^a$. With this redefinition, the coupling of the boundary fields with the Ψ'_a bulk fields become non-diagonal and involve the E_a matrices. The couplings of the right-handed boundary fields a_R, which are mixed only with the corresponding bulk fermion Ψ^a, can be diagonalized by the redefinition $a'_R = U_a a_R$. On the other hand, the left-handed boundary fields couple with two different bulk fields, so that their couplings can not be diagonalized.

The contribution coming from Ψ'_b to the wave function Z_1^a of the left-handed field a_L is now given by $\widetilde{Z}_1^a(\Psi'_b) = U_b^\dagger Z_1^a(\Psi'_b) U_b$, where $Z_1^a(\Psi'_b)$ is the contribution of a bulk field with flavour-diagonal mixing. The total wave function $\widetilde{Z}_1^a = \sum_b \widetilde{Z}_1^a(\Psi'_b)$ is now non-diagonal. The wave-function corrections for the right-handed fields a_R are instead unchanged and diagonal: $\widetilde{Z}_2^a = Z_2^a$. The induced mass matrix $\widetilde{m}_0^a$ for the localized fermions is given by $\widetilde{m}_0^a = m_0^a U_a$. We can now diagonalize the wave functions $\widetilde{Z}_1^a$ for the left-handed fields by a unitary transformation $a'_a = V_a^\dagger a_L$ which gives $\widetilde{Z}_1^a = V_a \mathcal{Z}_1^a V_a^\dagger$ with $\mathcal{Z}_1^a$ diagonal. In the new basis the mass matrix is $\widetilde{m}_0^a = m_0^a U_a V_a$, so that the physical masses are obtained diagonalizing the matrix

$$(m_a)_{IJ} = \frac{(m_0^a)_{II}(V_a U_a)_{IJ}}{\sqrt{(Z_2^a)_{II}(\mathcal{Z}_1^a)_{JJ}}}, \tag{3.3.17}$$

where no sum is meant on the I and J indices.

In principle, the analysis of the EWSB in this model should take into account the possibility of having a non-trivial flavour structure. Nevertheless, as we will discuss in detail in sect. 3.5 and sect. 3.6, the part of the Higgs effective potential due to the fermions is totally dominated by the contributions of bulk fields with small bulk masses. Due to the exponential suppression of the SM fermion masses with the bulk mass parameters, the bulk fields with small masses are usually the ones coupled with the third quark generation and in particular to the top. Moreover, the experimental results indicate that the third quark generation has small mixing with the light ones, so that it can be safely treated separately. Consequently, as the EWSB mechanism is concerned, it is a reasonably good approximation to neglect the non-trivial flavour structure as we will do in the following.

3.4 Gauge Bosons and Anomaly Cancellation

Before analyzing the effective action and the $4D$ spectrum of the gauge sector of the model, it is necessary to discuss the issue of anomalies. As we anticipated in section 3.2.1,

anomalies are crucial in the model to obtain a realistic value of the weak mixing angle θ_w. Since the bulk fermions are strictly vector-like, the only anomalies that can arise come from the localized fermions. Given the fact that all the boundary fermions are localized at the same fixed point, all anomalies that do not involve the extra $U(1)_X$ gauge subgroup vanish. This is a direct consequence of the usual cancellation of anomalies arising from the SM spectrum of fermions (notice that the localized fields reproduce exactly the SM matter fields).

On the other hand, the $U(1)_X$ subgroup is anomalous and its anomalies can be canceled by means of a $4D$ version of the Green–Schwarz mechanism [59]. One introduces a neutral $4D$ axion at $y = 0$, transforming non-homogeneously under the $U(1)_X$ subgroup, with non-invariant $4D$ Wess–Zumino couplings compensating for the one-loop anomaly. In this way the anomalies are canceled and the axion is eaten by the gauge field A_X. In a suitable gauge, the net effect of the anomaly on the gauge bosons is the appearance of localized quadratic terms in A_X, with a mass term M_X whose natural size is the cut-off scale of the model. For $M_X \gg 1/R$, the localized mass term simply results in an effective change (from Neumann to Dirichlet) of the boundary conditions of A_X at the $y = 0$ fixed point.

Let us now analyze the effective description of the gauge sector and in particular the spectrum of the light states. As we did for the fermionic sector, we again use the holographic approach to describe the theory at low energy. In this case the holographic effective Lagrangian after EWSB is given by

$$\begin{aligned}\mathscr{L}_g = -\frac{p}{2}P_t^{\mu\nu}\Bigg\{ & \frac{\cos(2\pi\alpha)-\cosh(2p\pi R)}{\sinh(2p\pi R)}\left(A^1_\mu A^1_\nu + A^2_\mu A^2_\nu\right) \\ & + \frac{-4g_5^2\sinh^2(p\pi R) - g_{Y5}^2\sin^2(2\pi\alpha)}{2g_5^2\sinh(2p\pi R)} A^Y_\mu A^Y_\nu + \frac{3-4\cosh(2p\pi R)+\cos(4\pi\alpha)}{4\sinh(2p\pi R)} A^3_\mu A^3_\nu \\ & + \frac{g_{Y5}}{g_5}\frac{\sin^2(2\pi\alpha)}{2\sinh(2p\pi R)}\left(A^Y_\mu A^3_\nu + A^3_\mu A^Y_\nu\right)\Bigg\}, \end{aligned} \tag{3.4.1}$$

where we set to zero the non-dynamical sources corresponding to the gauge fields which are odd at the $y = 0$ boundary, namely $A_\mu^{4,5,6,7}$ and A_X, moreover we did not include the Higgs fluctuations. The mass spectrum can be easily deduced from the holographic Lagrangian.[10] The KK towers are the following:

$$\begin{aligned} & m_n^{(1)} = \frac{n+\alpha}{R}, \quad m_n^{(2)} = \frac{n+m_Z(\alpha)}{R}, && n \in [-\infty, \infty], \\ & m_n^{(3)} = \frac{n}{R}, \quad m_n^{(4)} = \frac{n+1}{R}, \quad m_n^{(5)} = \frac{n+1/2}{R}, && n \in [0, \infty]. \end{aligned}$$

The SM gauge bosons W, Z and γ are associated to the $n = 0$ modes of $m_n^{(1)}$, $m_n^{(2)}$ and $m_n^{(3)}$, so that the W mass equals

$$m_W = \frac{\alpha}{R}. \tag{3.4.2}$$

[10] Notice that to get the whole spectrum one has to take into account also the bulk degrees of freedom which have been integrated out to obtain eq. (3.4.1).

The Z mass $m_Z(\alpha)$ is defined by the mass equation

$$\sin^2(\pi m_Z R) = \frac{1}{4\cos^2\theta_W}\sin^2(2\pi\alpha)\,. \tag{3.4.3}$$

By expanding the sines in eq. (3.4.3) one recovers at leading order the SM relation $m_Z = m_W/\cos\theta_W$, as expected. Corrections due to the localized mass terms for A_X are however present, so that $\rho_{SM} \neq 1$.

3.5 One-Loop Effective Potential for the Higgs

As we discussed before the Higgs doublet in this model is identified with the internal components $A_y^{4,5,6,7}$ of the bulk gauge subgroup $SU(3)_w$. The EWSB is spontaneously generated when A_y acquires a VEV and this breaking is equivalent to a Wilson-line symmetry breaking. As we saw in section 3.1, the bulk gauge invariance forbids the appearance of any local Higgs potential in the bulk. This property is enough to ensure the finiteness of the Higgs potential at any loop order for a theory compactified on the circle. On the other hand, when we consider an orbifold compactification, localized divergent terms could in principle be present at the boundaries. Actually, this does not happen, in fact a Higgs potential localized at the fixed points is forbidden by a non-linearly realized gauge symmetry which is left unbroken by the orbifold boundary conditions [60].

To show how this symmetry arises, we take a theory with a compact bulk gauge group G broken to the subgroup H at the boundaries of the orbifold. In the bulk, a gauge transformation with parameters ξ^A has the form

$$\delta A_M^A = \partial_M \xi^A + i f^{ABC}\xi^B A_M^C\,. \tag{3.5.1}$$

Using the property of the structure constants $f^{\hat{a}bc} = f^{\hat{a}\hat{b}\hat{c}} = 0$, where we denoted by t^a and $t^{\hat{a}}$ respectively the generators of H and G/H, a gauge transformation along an element of G/H can be written as

$$\begin{aligned}
\delta_{G/H} A_\mu^a &= i f^{a\hat{b}\hat{c}}\xi^{\hat{b}} A_\mu^{\hat{c}}\,,\\
\delta_{G/H} A_\mu^{\hat{a}} &= \partial_\mu \xi^{\hat{a}} + i f^{\hat{a}\hat{b}c}\xi^{\hat{b}} A_\mu^c\,,\\
\delta_{G/H} A_y^a &= i f^{a\hat{b}\hat{c}}\xi^{\hat{b}} A_y^{\hat{c}}\,,\\
\delta_{G/H} A_y^{\hat{a}} &= \partial_y \xi^{\hat{a}} + i f^{\hat{a}\hat{b}c}\xi^{\hat{b}} A_y^c\,.
\end{aligned} \tag{3.5.2}$$

At the boundaries, the non-zero fields are A_μ^a and $A_y^{\hat{a}}$, and the gauge parameters $\xi^{\hat{a}}$ vanish (but *not* their derivative along the fifth dimension). Computing eq. (3.5.2) at the fixed points, we obtain a gauge transformation which acts on the even field components as

$$\begin{aligned}
\delta_{G/H} A_\mu^a &= 0\,,\\
\delta_{G/H} A_y^{\hat{a}} &= \partial_y \xi^{\hat{a}}\,.
\end{aligned} \tag{3.5.3}$$

The presence of this unbroken gauge transformation implies that the theory is invariant under the shift symmetry

$$A_y^{\widehat{a}} \to A_y^{\widehat{a}} + \partial_y \xi^{\widehat{a}}\,, \tag{3.5.4}$$

which acts on the fields at the boundaries. In the GHU scenario we are considering, $A_y^{\widehat{a}}$ is identified with the Higgs field ($\widehat{a} = 4, 5, 6, 7$) and this symmetry ensures that its potential is still finite in a model compactified on $S^1/\mathbf{Z}_2$.

The one-loop Higgs potential can be easily derived from the holographic description of the model (eqs. (3.3.4), (3.3.5), (3.3.6), (3.3.7), and (3.4.1)) as explained in section 2.4. The gauge contribution is given by

$$V_g(\alpha) = 2\,V_A(\alpha) + V_A[m_Z(\alpha)]\,, \tag{3.5.5}$$

where $V_A(\alpha)$ represent the contribution of a gauge field with charge $q = 1$ with respect to the Higgs:

$$\begin{aligned} V_A(\alpha) &= \frac{3}{16\pi^6 R^4}\int_0^\infty dx\; x^3 \ln\left[f_0(x,\alpha)\right] \\ &= -\frac{9}{64\pi^6 R^4}\sum_{n=1}^{\infty}\frac{1}{n^5}\cos(2k\pi\alpha)\,. \end{aligned} \tag{3.5.6}$$

The one-loop contribution to the Higgs effective potential coming from the fermionic sector can be split into a bulk and a boundary term. The bulk term can be obtained from the holographic Lagrangian in eqs. (3.3.5) and (3.3.6) and is given by

$$V_f^{bulk}(\alpha) = V_{\Psi^t}(\alpha) + V_{\Psi^t}(2\alpha) + V_{\Psi^b}(\alpha)\,, \tag{3.5.7}$$

where V_{Ψ^a} is given by the contribution of a bulk fermion pair with charge $q = 1$ with respect to the Higgs:

$$\begin{aligned} V_\Psi(\alpha) &= \frac{-1}{2\pi^6 R^4}\int_0^\infty dx\; x^3 \ln\left[f_0(x^a,\alpha)\right] \\ &= \frac{3}{8\pi^6 R^4}\sum_{n=1}^{\infty}\frac{1+2n\lambda+\frac{4}{3}n^2\lambda^2}{n^5}e^{-2n\lambda}\cos(2\pi n\alpha)\,. \end{aligned} \tag{3.5.8}$$

An interesting property of $V_\Psi(\alpha)$ is the fact that it is exponentially suppressed in the bulk mass parameter λ. This means that the fermionic contribution to the Higgs potential is dominated by bulk fermions with small mass parameters. As we showed in section 3.3, also the SM fermion masses are exponentially sensitive to the bulk masses, so that the light generations are coupled to heavy bulk fermions, and the third generation (and in particular the top quark) is coupled to bulk fields with small λ. Thus, as expected, the most relevant fermionic contribution to the potential is induced by the bulk fermions which give mass to the top quark, namely the $(\Psi^t, \widetilde{\Psi}^t)$ couple. For this reason, in the numerical

analysis we can safely neglect the corrections due to the light quark generations and to the leptons.

The boundary contribution coming from the t and the b fields can be extracted from eqs. (3.3.7) and (3.4.1). In this case one finds:

$$V_t(\alpha) = \frac{-1}{4\pi^6 R^4}\int_0^\infty dx\, x^3 \ln\left[\prod_{i=1}^{2}\left[1+\delta_{i1}\frac{\varepsilon_1^{b\,2}}{x^b}f_0(x^b,0)+\delta_{i2}\frac{\varepsilon_2^{t\,2}}{2x^t}f_0(x^t,0)\right.\right.$$
$$\left.\left.+\frac{\varepsilon_i^{t\,2}}{2^{\delta_{i2}}x^t}f_0(x^t,2\alpha)\right]+\prod_{i=1}^{2}\left[\frac{\varepsilon_i^{t\,2}}{2^{\delta_{i2}}x}f_1(x^t,2\alpha)\right]\right], \qquad (3.5.9)$$

$$V_b(\alpha) = \frac{-1}{4\pi^6 R^4}\int_0^\infty dx\, x^3 \ln\left[\prod_{i=1}^{2}\left[1+\frac{\varepsilon_i^{b\,2}}{x^b}f_0(x^b,\alpha)+\delta_{i1}\frac{\varepsilon_1^{t\,2}}{x^t}f_0(x^t,\alpha)\right]\right.$$
$$\left.+\prod_{i=1}^{2}\left[\frac{\varepsilon_i^{b\,2}}{x}f_1(x^b,\alpha)\right]\right]. \qquad (3.5.10)$$

From the effective potential we can determine the Higgs mass, which reads

$$m_H^2(\alpha_{min}) = \left(\frac{g_4 R}{2}\right)^2 \frac{\partial^2 V}{\partial\alpha^2}\bigg|_{\alpha=\alpha_{min}}, \qquad (3.5.11)$$

where α_{min} is the position of the minimum of the potential.

3.6 Quantitative Analysis

As we showed in the previous sections, the model presented in this chapter has all the qualitative features to represent a possible extension of the SM. Moreover it has the advantage of including a mechanism which stabilizes the EW scale and explaining the hierarchy of fermion masses by the non-local origin of the Yukawa couplings. Unfortunately, at the quantitative level, this model fails to be compatible with the experimental constraints. In particular the values of the Higgs and top masses as well as the compactification scale $1/R$ are too small.

The crucial parameter that sets the scale of the model is α, whose value is determined minimizing the full effective potential $V(\alpha)$. The effective potential is invariant under the shift $\alpha \to \alpha + 1$ and under the transformation $\alpha \to -\alpha$. Thus unequivalent vacua of the theory correspond to the values of α in the interval $[0, 1/2]$. The $\alpha = 0$ and the $\alpha = 1/2$ points are always stationary points of the potential and they correspond to an enhancement of the unbroken symmetry. In particular for $\alpha = 0$ we do not have a spontaneous breaking of the $SU(2) \times U(1)_Y$ symmetry (the Higgs has a vanishing VEV). On the other hand, when $\alpha = 1/2$ the $SU(2) \times U(1)_Y$ group is broken to a $U(1) \times U(1)$ subgroup and not simply to the usual $U(1)_{EM}$ electromagnetic group. This can be easily seen noticing that the Z mass in eq. (3.4.3) vanishes for $\alpha = 1/2$, thus giving rise to an extra $U(1)$ unbroken

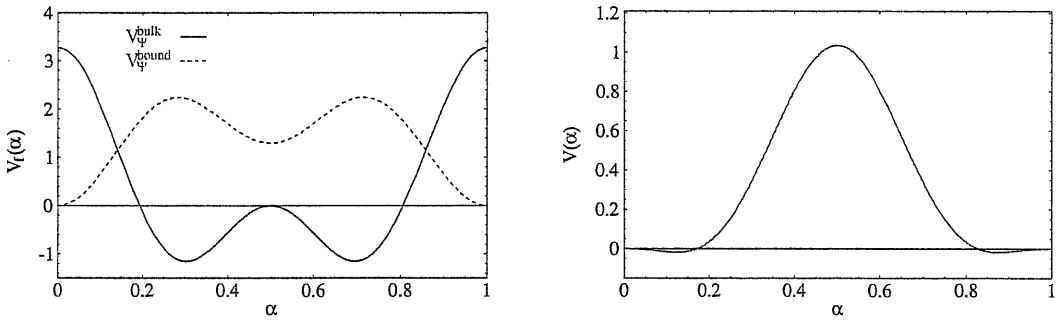

Figure 3.1: Contribution of bulk and boundary fermions to the Higgs effective potential (left) and total effective potential (right) for $\lambda^t = 1.92$, $\lambda^b = 2.8$, $\varepsilon^t_{1,2} = 6.1$, and $\varepsilon^b_{1,2} = 3.3$. The minimum of the potential is at $\alpha_{min} = 0.12$, the Higgs mass is $m_H = 9.7$ GeV, the top and bottom masses are $m_t = 10.3$ GeV and $m_b = 1.1$ GeV.

subgroup (the W mass in eq. (3.4.2) is however non zero, so that the $SU(2)$ subgroup is broken). Instead, for a generic value of α the usual EWSB occurs.

Obtaining a potential with a non trivial minimum is not automatic. In a model with only bulk gauge fields, the minimum of the potential is always at $\alpha = 0$, thus hindering any symmetry breaking. A negative contribution to the Higgs mass is instead given by (periodic) bulk fermions. When the fermion contribution dominates (namely for small values of the bulk masses λ^a) a non trivial minimum appears at $\alpha \sim 0.3$ (see the left plot of figure 3.1). When the bulk masses increase, the gauge contribution becomes more relevant and the minimum moves to lower values of α. However, one can not obtain arbitrarily small values of α. In fact when the fermionic and the gauge contribution are nearly compensating, the $\alpha = 0$ stationary point becomes a local minimum and a barrier appears between the symmetry breaking and the symmetry preserving phase. A further increase of the bulk masses causes the minimum to jump to the symmetric point $\alpha = 0$, and this usually happens for $\alpha \sim 0.1 - 0.2$ (see figure 3.1).[11]

From the lower bound $\alpha \gtrsim 0.1$, using the W mass formula in eq. (3.4.2), we derive an upper bound on the compactification scale of the model $1/R \lesssim 800$ GeV. This value is in conflict with the experimental bounds for models with localized interactions that do not conserve the KK momentum, which requires roughly $1/R \sim few$ TeV [61]. The Higgs mass computed using eq. (3.5.11) is also too small, at most $m_H \sim 30$ GeV, which is a value much below the current experimental bound $m_H > 115$ GeV. Finally, as we discussed in section 3.3, the top mass is necessarily too low in this set-up. We derived the theoretical bound $m_t \lesssim \sqrt{2} m_W \sim 110$ GeV, however, accessible values in the model are much lower. In fact as can be seen from eq. (3.3.15), for the typical values of the bulk mass $\lambda^t \sim 1.5$ needed to obtain $\alpha \sim 0.1$, the actual value of the top mass is $m_t \lesssim 30$ GeV.

[11] The exact position of the minimum at which the jump occurs depends on the boundary couplings. It is however not possible to obtain values of α smaller than $\alpha \sim 0.1$.

3.6.1 Estimate of the Cut-Off

The model described here, as any $5D$ theory, is non-renormalizable and hence has a definite energy range of validity, out of which the theory enters in a strong coupling uncontrolled regime. It is fundamental to have an estimate of the maximum energy Λ which we can probe using the effective $5D$ Lagrangian. Clearly, we have to check that Λ is significantly above the compactification scale $1/R$, otherwise the model has no perturbative range of applicability.

A reliable estimate of the cut-off can be obtained defining Λ as the energy scale at which the one-loop vacuum polarization corrections for the various gauge-fields propagators is of order of the tree-level terms. This can be taken as a signal of the beginning of a strong coupling regime. The relevant gauge fields are those of $SU(3)_s$ and $SU(3)_w$, the Abelian ones associated to $U(1)'$ typically receive smaller corrections. The one-loop vacuum polarizations can be estimated using a Pauli–Villars regularization in a non-compact $5D$ space. For simplicity one can neglect the effects of the compactification which should give small finite corrections. Given our definition of the cut-off, a different Λ is associated to every gauge subgroup, and in particular the most relevant ones are Λ_s related to $SU(3)_s$ and Λ_w corresponding to $SU(3)_w$. Of course, the "true" cut-off of the model will coincide with the smallest of all possible Λ's. A reasonable approximation is to assume that the gauge contribution is nearly of the same order as that of the fermions associated to the first two generations, so that the two contributions cancel. In this case one finds:

$$\begin{aligned} (\Lambda_s R)\frac{\alpha_s}{12}\frac{1}{2}(24+12) \sim 1 \quad &\Rightarrow \quad \Lambda_s \sim \frac{6}{R}, \\ (\Lambda_w R)\frac{\alpha_w}{12}\frac{1}{2}(60+12) \sim 1 \quad &\Rightarrow \quad \Lambda_w \sim \frac{10}{R}, \end{aligned} \tag{3.6.1}$$

where the multiplicity of the bulk fermions for the symmetric and fundamental representation has been taken into account.[12] The cut-off of the theory can thus be estimated to be $\Lambda \sim 6/R$, which means that the model has an acceptable range of perturbativity, and is reasonably predictive.

3.7 Possible Extensions

As we saw before, the model we described in this chapter, although qualitatively realistic, suffers some critical problems from a quantitative point of view. In particular the Higgs and the top masses are incompatible with the experimental values and the compactification

[12] Notice that the estimates in eq. (3.6.1), which were derived in [27], differ significantly from those reported in [15, 26]. In fact the fermion multiplicities were not taken into account in [15, 26] where the cut-off was estimated using the naïve dimensional analysis. In addition, the Pauli–Villars regularization gives rise to a 5D loop factor in the vacuum polarization diagram which is $24\pi^2$ and not $24\pi^3$ as naïvely expected.

scale is too small with respect to the current bounds. A fully realistic way to modify this model in order to make it compatible with the experimental measurements will be presented in the next chapter. Nevertheless, it is interesting to discuss here two earlier attempts to solve some of the problems of the model considering an extension of the original set-up. The first possibility we will consider is the introduction of bulk fermions in a higher rank representation of the $SU(3)_w$ group. A second scenario is obtained including large localized gauge kinetic terms into the Lagrangian.

By analyzing these two attempts we will see that solving the problems of GHU models in $5D$ is not a simple task, so that some naïve (and even some more complex) constructions are not sufficient to obtain a satisfactory scenario. Moreover these extended models show some interesting features at finite temperature as we will see in chapter 5.

3.7.1 High Rank Bulk Fermions

A possible way to lower the position of the minimum of the Higgs potential is to consider $5D$ massive bulk fermions in large $SU(3)_w$ representations. For example one can take a completely symmetric representation of large rank r, whose dimension is given by $d(r) = (r+1)(r+2)/2$. This representation contains component whose charge q with respect to the Higgs takes all the values ranging from 0 to r. The multiplicity of charged states with $q \neq 0$ is $N_q = 1 + [(r-q)/2]$, where $[\ldots]$ denotes the integer part. If $r \gg 1$ and the bulk mass is not too large, one can easily find minima with $\alpha \sim 1/r$, and, more importantly, the second derivative of the potential V'' at the minimum grows very quickly with r (see for example the zero temperature potential in figure 5.12 (a)). This allows to obtain a reasonable Higgs mass $m_H \sim 110$ GeV for $r \sim 8$. Moreover these fermions, if included in the correct $SU(3)_s$ representation, can also couple with the third quark generation giving an enhancement of the top mass.

A major problem of this set-up is the fact that the cut-off of the model rapidly decreases as we include a larger number fermions in the bulk. In order to limit the number of bulk fields we can introduce high rank fermions which are singlets of $SU(3)_s$ instead of considering fermions in the fundamental representation. However, with this choice the high rank fields can not couple with the quarks and the enhancement of the top mass can not be obtained. By a rough estimate of the cut-off, one gets that these extended models are on the edge of perturbativity for $r \sim 8$.

3.7.2 Localized Gauge Kinetic Terms

In the orbifold scenario we considered, no symmetry forbids the occurrence of localized kinetic terms for the gauge fields [62] (see also [63]). For simplicity we will consider $SU(3)_w$-invariant localized kinetic terms for the $4D$ components of the gauge fields, moreover we

will not introduce localized terms for the $U(1)'$ subgroup.[13] The Lagrangian for the $SU(3)_w$ gauge fields is then given by

$$\mathscr{L}_g = -\frac{1}{2}\,\mathrm{Tr}\,F_{MN}F^{MN} - \big(l_1\delta(y) + l_2\delta(y-\pi R)\big)\,\mathrm{Tr}\,F_{\mu\nu}F^{\mu\nu}\,, \tag{3.7.1}$$

where $l_{1,2}$ are dimension -1 couplings. It is convenient to define the dimensionless parameters $c_i = l_i/(\pi R)$. Of course, the presence of localized terms will distort the KK spectrum and the wave functions of the A_μ fields (the spectrum and the form of the wave functions can be found in [15]). Before the EWSB, the $SU(3)_w$ subgroup is unbroken, and this means that the corresponding gauge components admit zero modes whose wave functions are flat as required to preserve the universality of gauge couplings. On the other hand, after EWSB, the wave functions of the massive SM gauge bosons are no longer flat in the extra dimension, so that the concept of $4D$ effective gauge coupling constant is no more universal. To be more precise, the strength of the coupling of the SM gauge bosons with a given mode will depend on the shape of the wave function of the latter.

The localized kinetic terms modify the gauge contribution to the Higgs potential. The boundary contribution to the potential is reported in ref. [15], eq. (46). For $c_i \gg 1$, the boundary contribution tend to exactly cancel the α dependence of the bulk contribution, resulting in a suppression of the total gauge contribution to the Higgs potential. The effective potential is thus dominated by the fermion contribution and the position of its minimum is at $\alpha \sim 0.3$. Notice, moreover, that the localized kinetic terms do not break the shift symmetry in eq. (3.5.4), and thus the finiteness of the effective potential is not spoiled.

The analysis of the model for generic values of c_i is quite involved, and we therefore will only consider the special case in which $c_1 \gg 1$ and $c_2 \ll 1$, which present a substantial simplification. In this limit we obtain an effective gauge coupling constant for the fields localized at $y = 0$:

$$g_4 = \frac{g_5}{\sqrt{c_1}\sqrt{2\pi R}}\,. \tag{3.7.2}$$

The W mass is now equal to

$$m_W \simeq \frac{\sin(\pi\alpha)}{\pi\sqrt{c_1}R}\,, \tag{3.7.3}$$

and the expression for the Higgs mass is modified as

$$m_H \simeq \frac{g_4 R}{2}\sqrt{c_1}\sqrt{V''(\alpha)}\,. \tag{3.7.4}$$

Clearly, the corrections due to a sizable value of c_1 result in an improvement of the model. The W mass is lowered with respect to the compactification scale $1/R$ by a factor $\sqrt{c_1}$ and thus the experimental constraints on R can be satisfied with a larger value of α. At

[13] Localized terms involving A_y are allowed, but their presence considerably complicates the analysis.

the same time the Higgs mass is enhanced and can be made compatible with the current bounds. Finally also the top mass becomes larger, but obtaining a realistic value would however require $c_1 \gg 10$ in the model described here.

On the other hand, the distortions of the wave functions give large deviations from the SM predictions resulting hardly compatible with the experiments. Moreover the introduction of large localized kinetic terms also affects the cut-off of the model which scales roughly as $\Lambda_w \to \Lambda_w/c$. From the results in eq. (3.6.1), one finds that, in order to ensure perturbativity, the localized couplings can be at most $c \sim 5$.

Chapter 4

A Realistic Model with Gauge–Higgs Unification

As we saw in the last chapter, GHU models in $5D$ present some nice features from a phenomenological point of view at the qualitative level. Although not completely solving the hierarchy problem in the Higgs sector, the higher dimensional gauge invariance and the non-local nature of the EWSB, provide an interesting way to stabilize the electroweak scale by relating it to the compactification scale of the model. Moreover, the exponential sensitivity of the light-fields masses to the mass parameters of the bulk fermions seems a reasonable mechanism to explain the huge mass difference among the three fermion generation of the SM.

Unfortunately the simplest implementations of the GHU idea on a flat $S^1/\mathbf{Z}_2$ orbifold fail at the quantitative level, resulting incompatible with the experimental results. The origin of this failure is clearly related to the stringent constraints imposed on the theory by the higher dimensional gauge symmetry together with the $5D$ Lorentz invariance. Roughly speaking, the Higgs mass is generally too light because the Higgs effective potential is radiatively induced, giving rise to a small effective SM-like quartic coupling. At the same time, the top has a small mass because the Yukawa couplings, which are effective couplings in these theories, are engineered in such a way that they are always smaller than the electroweak gauge couplings, essentially due to the 5D Lorentz symmetry. Finally, the scale of new physics is too low, because in minimal models there is no way to generate a sizable gap between the EW scale and $1/R$.

It has recently been pointed out that it is possible to get rid of all the above problems by increasing the Yukawa (gauge) couplings of the Higgs field with the fermions, by assuming a Lorentz symmetry breaking in the fifth direction [26, 27]. More precisely, one advocates a breaking of the $SO(4,1)/SO(3,1)$ symmetry (so that the usual $SO(3,1)$ Lorentz symmetry is unbroken), which is the one that forces the fields to couple in the same way to the gauge bosons and to the Higgs. In this way, the Yukawa couplings are not constrained

anymore to be smaller than the electroweak gauge couplings and we have the possibility to get Yukawa's of order one, as needed for the top quark. Stronger Yukawa couplings lead also to a larger effective Higgs quartic coupling, resulting in Higgs masses above the current experimental bound $m_H > 115$ GeV. Furthermore, again due to the larger Yukawa couplings, the Higgs effective potential is totally dominated by the fermion contribution. The latter effect, together with a proper choice of the spectrum of 5D fermion fields, can lead to a substantial gap between the EW and compactification scales. In non-universal models of extra dimensions of this sort, where the SM fermions have sizable tree-level couplings with KK gauge fields, the EW precision tests generically imply quite severe bounds on the compactification scale. At the price of some fine-tuning on the microscopic parameters of the theory, however, one can push $1/R$ in the multi-TeV regime, hoping to get in this way a potentially realistic model.

Another fundamental ingredient to get a realistic model is an exact discrete $\mathbf{Z}_2$ symmetry, called "mirror symmetry" [27]. It essentially consists in doubling a subset of bulk fields ϕ, namely all the fermions and some of the gauge fields, in pairs ϕ_1 and ϕ_2 and requiring a symmetry under the interchange $\phi_1 \leftrightarrow \phi_2$. Periodic and antiperiodic fields arise as suitable linear combinations of ϕ_1 and ϕ_2 and the symmetry constrains the couplings of the Higgs with periodic and antiperiodic fermions with the same quantum numbers to be equal. When this is not the case, as in [26], the contributions to the Higgs mass-term of the bulk fields must be finely canceled in order to get a hierarchy between the compactification and EW scale. This adjustment was shown in [26] to be the main source of fine-tuning. Thanks to the mirror symmetry, on the contrary, a natural partial cancellation occurs in the potential. As we will discuss, with this set-up a difference of an order of magnitude between the compactification and EW scale, with $1/R \sim 1$ TeV, is completely natural. Such a scale is still too low to pass the EW precision tests, but the required amount of fine-tuning is significantly lowered.

A remarkable feature of this set-up is the fact that all SM states are even under the mirror symmetry, so that the lightest odd particle is absolutely stable. In a large fraction of the parameter space of the model, such a state is the first KK mode of an antiperiodic gauge field. The mirror symmetry represents then an interesting way to get stable non-SM particles in non-universal extra dimensional theories, where KK parity is not a suitable symmetry. Interestingly, the DM candidate obtained in these kind of models seems to lead to realistic relic densities and to be compatible with the cosmological observations [30].

In this chapter we will analyze a realistic scenario based on the ideas discussed before, namely the breaking of the Lorentz symmetry and the mirror symmetry. In particular we will present the model proposed in [27] and we will show that it is indeed compatible with the experimental results. Furthermore, the constraints coming from the EW precision tests will be discussed together with an estimate of the fine-tuning of the model. Finally, from a more theoretical point of view, we will show a possible mechanism which could

generate the breaking of the Lorentz symmetry in a natural way in the context of $5D$ orbifold theories.

4.1 The Model

The model is mainly based on the one presented in the last chapter. A new ingredient is the introduction of the $\mathbf{Z}_2$ mirror symmetry. The gauge group is taken to be $G = SU(3)_w \times G_1 \times G_2$, where $G_i = U(1)_i \times SU(3)_{i,s}$, $i = 1, 2$, with the requirement that the Lagrangian is invariant under the $\mathbf{Z}_2$ symmetry $1 \leftrightarrow 2$. The periodicity and parities of the fields on the $S^1/\mathbf{Z}_2$ space coincide with the ones discussed in section 3.2 for the electroweak $SU(3)_w$ sector, whereas for the Abelian $U(1)_i$ and non-Abelian coloured $SU(3)_{i,s}$ fields we now have (omitting for simplicity vector and gauge group indices):

$$A_1(y \pm 2\pi R) = A_2(y)\,, \qquad A_1(-y) = \eta A_2(y)\,, \tag{4.1.1}$$

where $\eta_\mu = 1$, $\eta_5 = -1$, denoting by Greek indices the $4D$ directions. The unbroken gauge group at $y = 0$ is $SU(2) \times U(1) \times G_+$, whereas at $y = \pi R$ we have $SU(2) \times U(1) \times G_1 \times G_2$, where G_+ is the diagonal subgroup of G_1 and G_2. The $\mathbf{Z}_2$ mirror symmetry also survives the compactification and remains as an exact symmetry of our construction. It is clear from eq. (4.1.1) that the linear combinations $A_\pm = (A_1 \pm A_2)/\sqrt{2}$ are respectively periodic and antiperiodic on S^1.[1] Under the mirror symmetry, $A_\pm \to \pm A_\pm$, so that we can assign a multiplicative charge $+1$ to A_+ and -1 to A_-. The massless $4D$ fields are the gauge bosons in the adjoint of $SU(2) \times U(1) \subset SU(3)_w$, the $U(1)_+$ and gluon gauge fields A_+ and a charged scalar doublet Higgs field, arising from the internal components of the odd $SU(3)_w$ $5D$ gauge fields, namely $A_w^{4,5,6,7}$. The $SU(3)_{+,s}$ and $SU(2)$ gauge groups are identified respectively with the SM $SU(3)_{QCD}$ and $SU(2)_L$ ones, while the hypercharge $U(1)_Y$ is the diagonal subgroup of $U(1)$ and $U(1)_+$. The extra $U(1)_X$ gauge symmetry which survives the orbifold projection is anomalous and its corresponding gauge boson gets a mass of the order of the cut-off scale Λ of the model.[2] Of course, as in the original model, a Higgs VEV, *i.e.* a VEV for the extra-dimensional components of the $SU(3)_w$ gauge fields, induces the additional breaking to $U(1)_{EM}$.

The presence of the mirror symmetry also requires some changes in the fermionic sector of the model (compare section 3.3). We introduce a certain number of couples of bulk fermions $(\Psi, \widetilde{\Psi})$, with identical quantum numbers and opposite orbifold parities. There are couples $(\Psi_1, \widetilde{\Psi}_1)$ which are charged under G_1 and neutral under G_2 and, by mirror symmetry, the same number of couples $(\Psi_2, \widetilde{\Psi}_2)$ charged under G_2 and neutral under G_1. No bulk field is simultaneously charged under both G_1 and G_2. In total, we introduce

[1] Notice that the antiperiodic gauge fields A_- are not connections of a gauge group. In fact G_- is not a gauge group but rather a symmetric quotient $(G_1 \times G_2)/G_+$.

[2] See sections 3.2 and 3.4 for a detailed discussion.

one pair of couples $(\Psi^t_{1,2}, \widetilde{\Psi}^t_{1,2})$ in the antifundamental $(\overline{\mathbf{3}})$ representation of $SU(3)_w$ and one pair of couples $(\Psi^b_{1,2}, \widetilde{\Psi}^b_{1,2})$ in the symmetric $(\mathbf{6})$ representation of $SU(3)_w$.Both pairs have $U(1)_{1,2}$ charge $+1/3$ and are in the fundamental representation of $SU(3)_{1,2,s}$. The boundary conditions of these fermions follow from eqs. (4.1.1) and the twist matrix in eq. (3.2.1). In particular, the combinations $\Psi_\pm = (\Psi_1 \pm \Psi_2)/\sqrt{2}$ are respectively periodic and antiperiodic on S^1.

Finally, we introduce massless chiral fermions, with charge $+1$ with respect to the mirror symmetry, localized at $y = 0$. As explained in the previous chapter, as far as electroweak symmetry breaking is concerned, we can focus on the top and bottom quark only, neglecting all the other SM matter fields. The mirror symmetry and the boundary conditions (4.1.1) imply that the localized fields can couple only to A_+. Hence, we have an $SU(2)$ doublet Q_L and two singlets t_R and b_R, all in the fundamental representation of $SU(3)_{+,s}$ and with charge $+1/3$ with respect to the $U(1)_+$ gauge field A_+.

As we anticipated, another ingredient to obtain a realistic model is the assumption of a breaking of the $SO(4,1)/SO(3,1)$ symmetry. In the following we will break this symmetry explicitly at tree-level, a possible mechanism which could induce the Lorentz symmetry breaking as a spontaneous breaking will be discussed in section 4.7. The most general $5D$ Lorentz-breaking effective Lagrangian density, gauge invariant and mirror symmetric, up to dimension $d < 6$ operators, is the following

$$\mathscr{L} = \mathscr{L}_g + \mathscr{L}_\Psi + \delta(y)\mathscr{L}_0 + \delta(y - \pi R)\widehat{\mathscr{L}}_\pi\,, \tag{4.1.2}$$

with

$$\begin{aligned}\mathscr{L}_g = \sum_{i=1,2}\Big[&-\frac{1}{2}\mathrm{Tr}\, G_{i\mu\nu}G^{i\mu\nu} - \rho_s^2 \mathrm{Tr}\, G_{i\mu 5}G^{i\mu 5} - \frac{1}{4}F_{i\mu\nu}F^{i\mu\nu} - \frac{\rho^2}{2}F_{i\mu 5}F^{i\mu 5}\Big] \\ &-\frac{1}{2}\mathrm{Tr}\, F_{\mu\nu}F^{\mu\nu} - \rho_w^2 \mathrm{Tr}\, F_{\mu 5}F^{\mu 5}\,, \end{aligned}\tag{4.1.3}$$

$$\begin{aligned}\mathscr{L}_\Psi = \sum_{i=1,2}\sum_{a=t,b}\Big\{ &\overline{\Psi}^a_i\big[i\not{D}_4(A_i) + k_a D_5(A_i)\gamma_5\big]\Psi^a_i + \overline{\widetilde{\Psi}}^a_i\big[i\not{D}_4(A_i) + \widetilde{k}_a D_5(A_i)\gamma_5\big]\widetilde{\Psi}^a_i \\ &-M_a(\overline{\widetilde{\Psi}}^a_i\Psi^a_i + \overline{\Psi}^a_i\widetilde{\Psi}^a_i)\Big\}\,, \end{aligned}\tag{4.1.4}$$

$$\begin{aligned}\mathscr{L}_0 = &\,\overline{Q}_L i\not{D}_4(A_+)Q_L + \bar{t}_R i\not{D}_4(A_+)t_R + \bar{b}_R i\not{D}_4(A_+)b_R \\ &+ \big(e_1^t\overline{Q}_L\Psi^t_+ + e_1^b\overline{Q}_L\Psi^b_+ + e_2^t\bar{t}_R\Psi^t_+ + e_2^b\bar{b}_R\Psi^b_+ + \mathrm{h.c.}\big) + \widehat{\mathscr{L}}_0\,. \end{aligned}\tag{4.1.5}$$

In eq. (4.1.3), we have denoted by $G_i = DA_{i,s}$ the gluon field strengths for $SU(3)_{i,s}$ and for simplicity we have not written the ghost Lagrangian and the gauge-fixing terms. For the same reason, in eqs. (4.1.4) and (4.1.5) we have only schematically written the dependencies of the covariant derivatives on the gauge fields and in eq. (4.1.5) we have not distinguished the doublet and singlet components of the bulk fermions, denoting all of

them simply as Ψ^t_+ and Ψ^b_+. Notice that Ψ_+ is the only bulk fermion that can have a mass-term mixing with the localized fields, since mixing with Ψ_- and $\widetilde{\Psi}_-$ is forbidden by the mirror symmetry and the relevant components of $\widetilde{\Psi}_+$ vanish at $y = 0$ due to the boundary conditions. Extra brane operators, such as for instance localized kinetic terms, are included in $\widehat{\mathscr{L}}_0$ and $\widehat{\mathscr{L}}_\pi$. Additional Lorentz violating bulk operators like $\overline{\Psi}\gamma^5\widetilde{\Psi}$, $\overline{\Psi}\partial_y\Psi$ or $\overline{\Psi}i\not{D}_4\gamma^5\Psi$ can be forbidden by requiring invariance under the inversion of all spatial (including the compact one) coordinates, under which any fermion transforms as $\Psi \to \gamma^0\Psi$. This $\mathbf{Z}_2$ symmetry is a remnant of the broken $SO(4,1)/SO(3,1)$ Lorentz generators. Notice that our choice of $U(1)$ charges allows mixing of the top quark with a bulk fermion in the $\overline{\mathbf{3}}$ while the bottom couples with a $\mathbf{6}$ of $SU(3)_w$. In the model presented in the previous chapter, the choice of taking bulk fermions neutral under the $U(1)$ led to the opposite situation. As we will see, this greatly reduces the deviation from the SM of the $Z\bar{b}_L b_L$ coupling (see [26]), which becomes negligible.

Strictly speaking, the Lagrangian (4.1.2) is not the most general one, since we are neglecting all bulk terms which are odd under the $y \to -y$ parity transformation and can be introduced if multiplied by odd couplings. If not introduced, such couplings are not generated and thus can consistently be ignored.

A detailed study of the model using the general Lagrangian (4.1.2) is a too complicated task. For this reason, we take $k_a = \widetilde{k}_a$ which considerably simplifies the analysis[3] and set $\rho_w = 1$. The latter choice can always be performed without loss of generality by rescaling the compact coordinate, and hence the radius of compactification as well as the other parameters of the theory.[4] Moreover, we neglect all the localized operators which are encoded in $\widehat{\mathscr{L}}_0$ and $\widehat{\mathscr{L}}_\pi$. The latter simplification requires a better justification that we postpone to the section 4.3.

4.2 Mass Spectrum and Higgs Potential

In this section we will describe the mass spectrum of the model. Of course, the introduction of the $\mathbf{Z}_2$ symmetry and of the Lorentz-breaking parameters determines deep changes in the spectrum with respect to the one reported in section 3.3 and section 3.4.

In particular the Lorentz violating factor ρ^2 distorts the spectrum of the KK gauge bosons, so that the analytic formulae for the $SU(3)_w \times U(1)_+$ gauge bosons are slightly involved.[5] The only unperturbed tower is the one associated to the W boson, whose

[3] It should be emphasized that there is no fine-tuning associated to $k/\widetilde{k}$ and thus this choice represents only a technical simplification [27].

[4] Strictly speaking, in a UV completion where the theory is coupled to gravity and the Lorentz violation is, for instance, due to a flux background (see section 4.7 and ref. [26]), ρ_w cannot be rescaled away by redefining the radius of compactification, since the latter becomes dynamical and ρ_w essentially corresponds to a new coupling in the theory. In our context, however, R is simply a free parameter.

[5] In the case in which $\rho = 1$ the mass spectrum clearly coincides with the one reported in section 3.4.

masses are $m_n = m_W + n/R$, where the W mass is given by the usual formula

$$m_W = \frac{\alpha}{R}. \tag{4.2.1}$$

The mass spectra of the KK towers associated to the $U(1)_-$ gauge field A_- and to the $\pm$ gluons are trivial and given by $m_n = (n+1/2)\rho/R$ for $U(1)_-$, $m_n = n\rho_s/R$ for $SU(3)_{+,s}$ and $m_n = (n+1/2)\rho_s/R$ for $SU(3)_{-,s}$.

As we did in the previous chapter, we can adopt the holographic point of view to describe the gauge sector of the model and to compute the Higgs effective potential. The only gauge fields which contribute to the Higgs potential are A_w, associated to $SU(3)_w$, and A_+, associated to $U(1)_+$. The relevant part of the holographic effective action is given by (compare eq. (3.4.1))

$$\begin{aligned}\mathscr{L}_g = -\frac{p}{2}P_t^{\mu\nu}\Bigg\{ & \frac{\cos(2\pi\alpha)-\cosh(2p\pi R)}{\sinh(2p\pi R)}\left(A^1_\mu A^1_\nu + A^2_\mu A^2_\nu\right) \\ & + \frac{1}{12g_5^2}\left[\frac{1-4\cosh(2p\pi R)+3\cos(4\pi\alpha)}{\sinh(2p\pi R)}\, g_{Y5}^2 + 4\rho(3g_5^2 - g_{Y5}^2)\tan\left(\frac{p\pi R}{\rho}\right)\right] A^Y_\mu A^Y_\nu \\ & + \frac{3-4\cosh(2p\pi R)+\cos(4\pi\alpha)}{4\sinh(2p\pi R)} A^3_\mu A^3_\nu + \frac{g_{Y5}}{g_5}\frac{\sin^2(2\pi\alpha)}{2\sinh(2p\pi R)}\left(A^Y_\mu A^3_\nu + A^3_\mu A^Y_\nu\right)\Bigg\}.\end{aligned} \tag{4.2.2}$$

From the effective holographic Lagrangian we can simply derive the gauge contribution to the Higgs effective potential:

$$\begin{aligned}V_g(\alpha) = \frac{3}{2}\int\frac{d^4q}{(2\pi)^4}\log\Big[& 4{g'_5}^2\sinh(\pi qR)\cosh(\pi qR/\rho)\big(\cos(4\pi\alpha)-\cosh(2\pi qR)\big) \\ & + 3{g_5}^2\rho\sinh(\pi qR/\rho)\cosh(\pi qR)\big(3+\cos(4\pi\alpha)-4\cosh(2\pi qR)\big)\Big] \\ & + \frac{3}{2}\int\frac{d^4q}{(2\pi)^4}\log\Big[\big(\cos(2\pi\alpha)-\cosh(2\pi qR)\big)^2\Big] + \text{“}\alpha\text{-ind. terms”}.\end{aligned} \tag{4.2.3}$$

Notice that the above integrals are divergent but they can be made finite by adding suitable α-independent terms which we have not written for simplicity. As explained in section 2.3.1, the spectrum of the KK states can be easily extracted from the effective action in eq. (4.2.2) or from the expression of effective potential in eq. (4.2.3). In particular the KK masses are given by the zeroes of the functions in the square brackets in eq. (4.2.3) (when the $4D$ momentum is rotated back to the Minkowskian). The zeroes of the last line correspond to the unperturbed aforementioned W tower, while the expression in the first two lines provides the mass equation for the neutral gauge boson sector. Notice that for $\rho \neq 1$ the Z boson tower can not be separated from the ones associated to the photon and to A_X; all of them arise from the zeroes of the first term in eq. (4.2.3). The solution at $q = 0$ corresponds to the physical massless photon while the first non-trivial one determines the Z boson mass.

4.2.1 The Fermionic Sector

Let us now consider the fermionic sector of the model. In the bulk couples of periodic and antiperiodic fields related by the mirror symmetry are present. First of all we will discuss the spectrum of the bulk fields neglecting the boundary couplings which mix the periodic fermions with the localized fields. Using the holographic description as in the last chapter (see eqs. (3.3.4) and (3.3.5)), one can straightforwardly obtain the $4D$ spectrum of the KK modes. For the Ψ^t fields the KK towers are given by

$$\begin{aligned} \left(m_n^{(1)}\right)^2 &= k_t^2 \frac{\left(n+\frac{\eta}{2}\right)^2}{R^2} + M_t^2\,, & n &\in [0,+\infty]\,, \\ \left(m_n^{(2)}\right)^2 &= k_t^2 \frac{\left(n+\frac{\eta}{2}+\alpha\right)^2}{R^2} + M_t^2\,, & n &\in [-\infty,+\infty]\,, \end{aligned} \tag{4.2.4}$$

where $\eta = 0$ for periodic fermions and $\eta = 1$ for antiperiodic fermions. Analogously, for the Ψ^b fields one finds:

$$\begin{aligned} &\left(m_n^{(1)}\right)^2 = k_b^2 \frac{\left(n+\frac{\eta}{2}+\alpha\right)^2}{R^2} + M_b^2\,, \quad \left(m_n^{(2)}\right)^2 = k_b^2 \frac{\left(n+\frac{\eta}{2}+2\alpha\right)^2}{R^2} + M_b^2\,, \qquad n \in [-\infty,+\infty]\,, \\ &\left(m_n^{(3)}\right)^2 = \left(m_n^{(4)}\right)^2 = k_b^2 \frac{\left(n+\frac{\eta}{2}\right)^2}{R^2} + M_b^2\,, \qquad n \in [0,+\infty]\,. \end{aligned} \tag{4.2.5}$$

The bulk fermion contribution to the Higgs effective potential is now given by

$$V_f^{bulk}(\alpha) = V_{\Psi_+^t}(\alpha) + V_{\Psi_+^b}(2\alpha) + V_{\Psi_+^b}(\alpha) + V_{\Psi_-^t}(\alpha) + V_{\Psi_-^b}(2\alpha) + V_{\Psi_-^b}(\alpha)\,, \tag{4.2.6}$$

where the expression for the contribution for a pair of (periodic or antiperiodic) modes with charge q is

$$V_\Psi(q\alpha) = \frac{3k^4}{8\pi^6 R^4} \sum_{n=1}^{\infty} n^{-5} \left(1 + 2n\frac{\lambda}{k} + \frac{4}{3}n^2\frac{\lambda^2}{k^2}\right) e^{-2n\frac{\lambda}{k}} \cos\left[2\pi n q\left(\alpha + \frac{\eta}{2q}\right)\right]. \tag{4.2.7}$$

Comparing eq. (4.2.7) with the fermion contribution to the potential in the Lorentz preserving case (eq. (3.5.8)), it is easily seen that a Lorentz-breaking paremater $k > 1$ determines a great enhancement of the potential. The potential gets larger by a factor k^4 and moreover the exponential suppression with respect to the bulk mass λ gets milder.

Notice that the presence of periodic and antiperiodic fermions is necessary to obtain small values of α_{min}. Indeed, as one can see from eq. (4.2.7), they permit a cancellation of the cosine terms with odd n in the sum. This generates a partial cancellation of the leading induced Higgs mass term, lowering the position of the minimum of the potential. The $\mathbf{Z}_2$ mirror symmetry plays an essential role in this mechanism. In fact it ensures that periodic and antiperiodic fermions have exactly the same mass and Lorentz breaking parameters. If the antiperiodic bulk fermions are simply introduced into the theory without the mirror

symmetry, as in [26], a certain degree of tuning among the parameters for periodic and antiperiodic fields is required to obtain an acceptable cancellation of the Higgs mass term.

Of course, to compute the full fermionic contribution to the Higgs effective potential and the exact spectrum of the periodic fields we must include also the contribution of the boundary fermions. The corrections due to the localized fields can be obtained computing the holographic action as described in section 3.3. We find that the contributions to the effective potential are given by

$$V_t(\alpha) = \frac{-1}{4\pi^6 R^4}\int_0^\infty dx\, x^3 \ln\left[\prod_{i=1}^{2}\left[1+\frac{\varepsilon_i^{t\,2}}{k_t x^t} f_0\left(\frac{x^t}{k_t},\alpha\right)+\delta_{i1}\frac{\varepsilon_1^{b\,2}}{k_b x^b} f_0\left(\frac{x^b}{k_b},\alpha\right)\right]\right.$$
$$\left.+\prod_{i=1}^{2}\left[\frac{\varepsilon_i^{t\,2}}{k_t x} f_1\left(\frac{x^t}{k_t},\alpha\right)\right]\right], \tag{4.2.8}$$

$$V_b(\alpha) = \frac{-1}{4\pi^6 R^4}\int_0^\infty dx\, x^3 \ln\left[\prod_{i=1}^{2}\left[1+\delta_{i1}\frac{\varepsilon_1^{t\,2}}{k_t x^t} f_0\left(\frac{x^t}{k_t},0\right)+\delta_{i2}\frac{\varepsilon_2^{b\,2}}{2k_b x^b} f_0\left(\frac{x^b}{k_b},0\right)\right.\right.$$
$$\left.\left.+\frac{\varepsilon_i^{b\,2}}{2^{\delta_{i2}} k_b x^b} f_0\left(\frac{x^b}{k_b},2\alpha\right)\right]+\prod_{i=1}^{2}\left[\frac{\varepsilon_i^{b\,2}}{2^{\delta_{i2}} k_b x} f_1\left(\frac{x^b}{k_b},2\alpha\right)\right]\right]. \tag{4.2.9}$$

The exact spectrum can be extracted form the potential, and is simply given by the zeroes of the arguments of the logarithms (with the $4D$ momentum rotated back to the Minkowskian) in eqs. (4.2.8) and (4.2.9).

It is important to study in detail the masses of the SM fermions. A very good approximation of the top and bottom quark masses is obtained neglecting the momentum dependence in the mass equation. In this way we get

$$m_a = \left|\frac{m_0^a}{\sqrt{Z_1^a Z_2^a}}\right|, \quad a = t, b \tag{4.2.10}$$

where

$$\begin{aligned}
m_0^t &= \frac{\varepsilon_1^t \varepsilon_2^t}{k_t \pi R} f_1\left(\frac{\lambda^t}{k_t},\alpha\right), \\
m_0^b &= \frac{\varepsilon_1^b \varepsilon_2^b}{\sqrt{2} k_b \pi R} f_1\left(\frac{\lambda^b}{k_b},2\alpha\right), \\
Z_i^t &= 1+\frac{\varepsilon_i^{t\,2}}{k_t \lambda^t} f_0\left(\frac{\lambda^t}{k_t},\alpha\right)+\delta_{i1}\frac{\varepsilon_1^{b\,2}}{k_b \lambda^b} f_0\left(\frac{\lambda^b}{k_b},\alpha\right). \\
Z_i^b &= 1+\delta_{i1}\frac{\varepsilon_1^{t\,2}}{k_t \lambda^t} f_0\left(\frac{\lambda^t}{k_t},0\right)+\delta_{i2}\frac{\varepsilon_2^{b\,2}}{2k_b \lambda^b} f_0\left(\frac{\lambda^b}{k_b},0\right)+\frac{\varepsilon_i^{b\,2}}{2^{\delta_{i2}} k_b \lambda^b} f_0\left(\frac{\lambda^b}{k_b},2\alpha\right).
\end{aligned} \tag{4.2.11}$$

Now for small α the top mass is given by

$$m_t \simeq k_t m_W \frac{2\lambda_t/k_t}{\sinh(2\lambda_t/k_t)}. \tag{4.2.12}$$

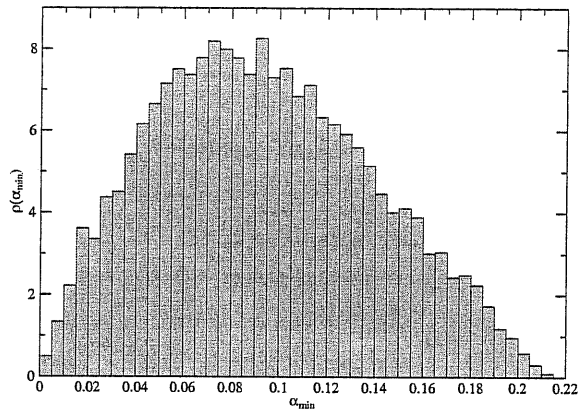

Figure 4.1: Distribution of α_{min} for uniformly distributed input parameters in the ranges $0.5 < \rho < 2$, $0.25 < \lambda_{t,b} < 1.25$, $2 < k_t < 3$, $0.75 < k_b < 1.5$, $0.75 < \varepsilon_t^{1,2} < 2.5$, $0.1 < \varepsilon_b^{1,2} < 0.45$.

With respect to the original model without Lorentz breaking (eq. (3.3.15)), we see that the top mass is enhanced by a factor k_t, so that $k_t \sim 2 - 3$ is needed to get the top mass in the correct range.[6]

For a large range of the microscopic parameters, the bulk–boundary fermion system also gives the lightest new particles of our model. Such states are colored fermions with a mass of order M_b, and, in particular, before EWSB, they are given by an $SU(2)$ triplet with hypercharge $Y = 2/3$, a doublet with $Y = -1/6$ and a singlet with $Y = -1/3$. For the typical values of the parameters needed to get a realistic model, the mass of these states is of order $1.5 - 2$ TeV.

4.2.2 Distribution of the Minima and Higgs Mass

As discussed before, the presence of bulk antiperiodic fermions, whose coupling with the Higgs are the same as for periodic fermions due to the mirror symmetry, allows for a natural partial cancellation of the leading Higgs mass terms in the potential, lowering the position of its global minimum α_{min}. This can be seen from the histogram in fig. 4.1, which shows the distribution $\rho(\alpha_{min})$ for random (uniformly distributed) values of the input parameters, chosen in the ranges which give the correct order of magnitude for the top and bottom masses. We are neglecting the points with unbroken EW symmetry ($\alpha_{min} = 0$), which are about half of the total. An important feature of the distribution in fig. 4.1 is the fact that a lower bound on the possible values of α_{min} is not present in this case, differently from what happens in the model of [15] presented in the last chapter in

[6]Notice that the top mass in eq. (4.2.12) for k_t=1 is a factor $\sqrt{2}$ smaller than the one in eq. (3.3.15). This is due to the different choice of the representations of the bulk fields with respect to the model presented in chapter 3.

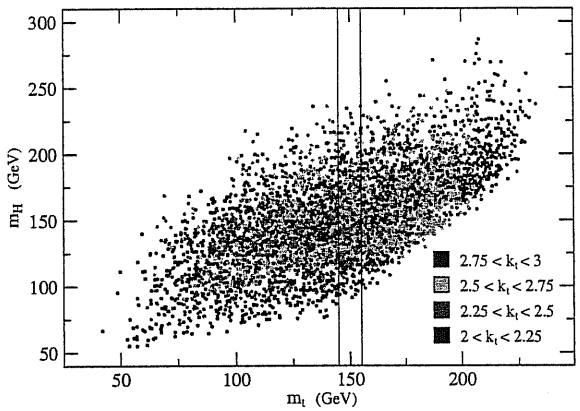

Figure 4.2: Higgs and top masses for points with $\alpha_{min} < 0.05$. Different colors label different values of k_t. The region among the two vertical black lines corresponds to the physical top mass.

which $\alpha_{min} \gtrsim 0.1$. The possibility of getting arbitrary small values of α_{min} is obviously extremely important. In fact it allows to get a sizable gap between the W mass and the compactification scale $1/R$, moreover small values of α_{min} is important to lower the corrections to the SM observables.

Another important quantity is the Higgs mass, which can be computed from the effective potential by eq. (3.5.11). The full Higgs effective potential is dominated by the fermion contribution and the enhancement due to the Lorentz breaking parameters also help in getting a reasonable Higgs mass. In fig. 4.2 the Higgs mass is plotted versus the top one and different colors label different ranges of the input parameter k_t. We see how realistic values of m_t can be obtained already for $k_t = 2$. The two vertical black lines in fig. 4.2 identify the region of physical top mass. This is taken to be around 150 GeV, which is the value one gets by running the physical top mass using the SM RGE equations up to the scale $1/R$. From fig. 4.2 we see that the Higgs mass, for acceptable top masses, lies in the $[100, 200]$ GeV range.

4.3 Estimate of the Cut-Off and Loop Corrections

Let us now discuss the cut-off of the model. As in the last chapter, we define Λ as the energy scale at which the one-loop vacuum polarization corrections for propagators is of order of the tree-level terms. The relevant gauge fields are those of $SU(3)_{i,s}$ and $SU(3)_w$, the Abelian ones associated to $U(1)_{1,2}$ typically giving smaller corrections for any reasonable choice of ρ^2. Due to the Lorentz violation, however, the transverse (A_μ) and longitudinal (A_y) gauge bosons couple differently between themselves and with matter, so that they should be treated separately. We denote by $\Lambda_s^{(\mu)}$, $\Lambda_s^{(y)}$, $\Lambda_w^{(\mu)}$ and $\Lambda_w^{(y)}$ the resulting cut-offs (due to the mirror symmetry, the cut-offs associated to the two $SU(3)_s$ gauge groups

coincide). Again we assume that the gauge contribution is approximately of the same order as that of the fermions associated to the first two generations. In this case, by taking $k_t \simeq 2 \div 3$, $k_b \simeq 1$, which are the typical phenomenological values, we get

$$\begin{aligned}
(\Lambda_s^{(\mu)} R)\frac{\alpha_s}{6}\frac{1}{2}\left(\frac{12}{k_t}+\frac{24}{k_b}\right) \sim 1 \quad &\Rightarrow \quad \Lambda_s^{(\mu)} \sim \frac{6}{R}\,, \\
(\Lambda_s^{(y)} R)\frac{\alpha_s}{6}\frac{1}{2}\Big(12k_t+24k_b\Big) \sim \rho_s^2 \quad &\Rightarrow \quad \Lambda_s^{(y)} \sim \frac{3\rho_s^2}{R}\,, \\
(\Lambda_w^{(\mu)} R)\frac{\alpha_w}{6}\frac{1}{2}\left(\frac{12}{k_t}+\frac{60}{k_b}\right) \sim 1 \quad &\Rightarrow \quad \Lambda_w^{(\mu)} \sim \frac{5}{R}\,, \\
(\Lambda_w^{(y)} R)\frac{\alpha_w}{6}\frac{1}{2}\Big(12k_t+60k_b\Big) \sim 1 \quad &\Rightarrow \quad \Lambda_w^{(y)} \sim \frac{4}{R}\,.
\end{aligned} \tag{4.3.1}$$

As can be seen from eq. (4.3.1), $\Lambda^{(\mu)}$ and $\Lambda^{(y)}$ (both for the strong and weak coupling case) scale respectively as k and $1/k$ in the Lorentz violating parameters. This is easily understood by noting that the loop factor scales as $1/k$ [26]. Thus $\Lambda^{(\mu)} \sim 1/\alpha \times k \sim k$ and $\Lambda^{(y)} \sim 1/(\alpha\, k^2) \times k \sim 1/k$. Due to the group factor of the $SU(3)_w$ symmetric representation, the electroweak and strong interactions give comparable values for the cut-off. Independently of the strong interactions,[7] the cut-off in the model is quite low: $\Lambda \sim 4/R$. The doubling of the fields due to the mirror symmetry has the strongest impact, since it decreases the electroweak cut-off estimate by a factor of 2. As far as the Lorentz violation is concerned, we see that eq. (4.3.1) gives, for $k_t = k_b = \rho_s = 1$, $\Lambda_s^{(y)} \sim 3/R$. In the absence of Lorentz breaking, therefore, the final cut-off would have been as low as $3/R$. Even though eq. (4.3.1) only provides an order–of–magnitude estimate, we can use it to place upper bounds on the allowed values of the Lorentz violating parameters k_t and k_b. To ensure $\Lambda \gtrsim 4/R$, we impose $k_t \lesssim 3$ and $k_b \lesssim 1.2$.

Once we have an estimate for the value of the cut-off in the theory, we can also give an estimate of the natural size of the coefficients of the operators appearing in the Lagrangian (4.1.2). In particular, since we have neglected them, it is important to see the effect of the localized operators appearing in $\widehat{\mathscr{L}}_{0,\pi}$ when their coefficients are set to their natural value. At one-loop level, several localized kinetic operators are generated at the fixed points. In the fermion sector, which appears to be the most relevant since it almost completely determines the Higgs potential, for simplicity we consider operators of the form[8]

$$\widehat{\mathscr{L}}_{0,\pi} = \sum_i a^i_{0,\pi}\, \overline{\psi}^i\, i\, \partial\!\!\!/_4\, \psi^i\,, \tag{4.3.2}$$

[7] Since ρ_s^2 is essentially a free parameter in our considerations, we could anyhow increase $\Lambda_s^{(y)}$ by taking ρ_s^2 significantly larger than unity.

[8] Among all possible localized operators, those with derivatives along the internal dimension require special care and are more complicated to handle [64]. It has been pointed out in [65] that their effect can however be eliminated by suitable field redefinitions (see also [66]).

where ψ^i indicates here the components of the bulk fields which are non-vanishing at the $y = 0$ or $y = \pi R$ boundaries. Such operators are logarithmically divergent at one-loop level and thus not very sensitive to the cut-off scale; anyhow, computing their coefficients $a^i_{0,\pi}$ using a PV regularization and setting $\Lambda \sim 4/R$, they turn out to be of order $10^{-3}R$. By including these terms in the full Lagrangian, it can be verified that the shape of the effective potential, the Higgs and the fermion masses receive very small (of order per-mille) corrections [27]. Localized operators can however sizeably affect the position of the minimum of the effective potential when it is tuned to assume small values. We will came back on this in section 4.5.

Finally, let us comment on the predictability of the Higgs mass at higher loops. Although finite at one-loop level, the Higgs mass will of course develop divergences at higher orders, which require the introduction of various counterterms (see [67] for a two-loop computation of the Higgs mass term). The crucial point of identifying the Higgs with a Wilson line phase is the impossibility of having a local mass counterterm at any order in perturbation theory. This is true both in the Lorentz invariant and in the Lorentz breaking case. For this reason, the Higgs mass is computable. In the Lorentz invariant case, it weakly depends on the remaining counterterms needed to cancel divergences loop by loop. In the Lorentz breaking case, the Higgs mass still weakly depends on higher-loop counterterms, with the exception of ρ_w^2, which is an arbitrary parameter directly entering in the Higgs mass formula. However, as we have already pointed out, ρ_w always enters in any physical observable together with R, so that it can be rescaled by redefining the radius of compactification. Thanks to this property, the Higgs mass remains computable also in a Lorentz non-invariant scenario.

4.4 Phenomenological Bounds

A full and systematic analysis of all the new physical effects predicted by the model is a quite complicated task, mainly because it greatly depends on the the flavour structure of the model. For simplicity, we will focus in the following on flavour and CP conserving new physics effects, and we will only give an order–of–magnitude estimate of the bounds arising from Flavour Changing Neutral Currents (FCNC). Due to the strong constraints on FCNC and CP violation in the SM, this is a drastic but reasonable simplification, since flavour does not play an important role in the mechanism of EWSB. The only exception to this flavour universality is given by the third quark family, that has to be treated separately.

The analysis of flavour and CP conserving new physics effects requires in general the introduction of 18 dimension 6 operators in the SM to fit the data (see *e.g.* [68]). It has recently been pointed out in [69] that, out of these 18 operators, only 10 are sensibly constrained. In a given basis (see [69] for details), 7 of these operators are parametrized by the universal parameters $\widehat{S}$, $\widehat{T}$, $\widehat{U}$, V, X, W and Y introduced in [44] extending the

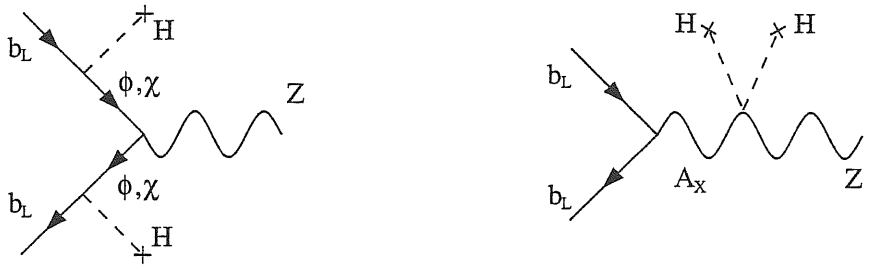

Figure 4.3: The tree-level corrections to the $\widehat{Z}\overline{b}_L b_L$ vertex and to the b_L propagator. The first distortion of the $\widehat{Z}\overline{b}_L b_L$ coupling is generated through the Higgs-mediated mixing of b_L with the component (ϕ) of the $SU(2)$ triplet which has $T_3 = -1$, and with the singlet χ ($T_3 = 0$), both coming from Ψ_b. The second correction is due to mixing of the KK tower of A_X with the Z boson.

usual S, T, U basis [70]. The remaining 3 operators are parametrized by the distortion δg_b (or the ϵ_b parameter [71]) of the $\widehat{Z}\,\overline{b}_L b_L$ coupling and other two parameters which describe the deviation of the up and down quark couplings to the $\widehat{Z}$ holographic boson.

4.4.1 Direct Corrections: the $\widehat{Z}\overline{b}_L b_L$ Vertex and FCNC

Being all light fermions almost completely localized at $y = 0$ (see fig. F.2 in appendix F for a quantitative idea of this effect), their couplings with the SM gauge fields are universal and not significantly distorted. Thus the two parameters describing the deviations of the up and down quark couplings to $\widehat{Z}$ are totally negligible. On the contrary, as in other models based on extra dimensions [72, 19], the bottom quark coupling is typically distorted by new physics (the top even more, but its coupling to the $\widehat{Z}$ is at the moment practically unconstrained). Moreover, in many cases the corrections to δg_b turn out to give strong constraints on the models. For example in a previous version [26] of the model presented in this chapter, in which the top and bottom quark were coupled with bulk fermions respectively in the symmetric and in the fundamental representation of $SU(3)_w$ (as in the model described in chapter 3), the $\widehat{Z}\overline{b}_L b_L$ corrections were the source of the tightest bounds on the parameter space. As we will now see in some detail, the simple idea of reversing the mixing of the localized bottom and top quark with respect to [26] strongly reduces δg_b.

To be more precise, the distortion of the $\widehat{Z}\,\overline{b}_L b_L$ coupling is due to two effects. One of those is the mass-term mixing of the b_L with the KK tower of the $SU(2)_w$ triplet and singlet fermions coming from the bulk field in the rep. **6** of $SU(3)_w$. The second distortion is a consequence of the delocalization of b_L, which then also couples to gauge bosons components orthogonal to $\widehat{Z}$. Both effects are proportional to the mixing parameters $\varepsilon_1^{t,b}$. The tree-level diagrams which contribute to the corrections of the $\widehat{Z}\,\overline{b}_L b_L$ coupling are shown in figure 4.3. Interestingly enough, at leading order in $\alpha = m_W R$, the former distortion exactly vanishes in the (very good) approximation of neglecting the bottom

mass. This can be understood by noting that the b_L mixes with the component of an $SU(2)_w$ triplet which has $T_3 = -1$ and with a singlet ($T_3 = 0$). The mixing with the triplet state leads to an increase (in magnitude) of g_b, whereas the singlet makes it decrease. The two effects turn out to exactly compensate each other. The distortion due to the delocalization of b_L is instead non-vanishing. An explicit computation along the lines of the one reported in appendix E gives, at leading order in α:

$$\delta g_b = g_b - g_b^{SM} = \frac{g_b^{SM} \pi^2 \alpha^2}{4 Z_1^b \cos^2\theta_W} \sum_{i=t,b} \frac{{\varepsilon_1^i}^2}{\lambda_i^2} F\left(\frac{\lambda_i}{k_i}\right) , \tag{4.4.1}$$

where $F(x)$ is defined in eq. (E.0.10) and Z_1^b is the wave-function normalization factor needed to canonically normalize the b_L field, defined in the eq. (4.2.11). From a KK point of view, the distortion is caused by the KK tower of the A_X gauge field, which mixes to the lowest mass eigenstate of the Z boson and couples to b_L in the bulk. Since $F(x)$ is a positive function, $\delta g_b < 0$. In the typical range of parameters of phenomenological interest, $-\delta g_b \lesssim 2\alpha^2$ and it comfortably lies inside the experimentally allowed region (at 1 σ form the central value) if $\alpha \lesssim 3 \times 10^{-2}$. As we will now discuss, stronger bounds on α arise from universal corrections and the non-universal corrections to $\widehat{Z\bar{b}_L b_L}$ can be neglected in the global fit.

Now we will briefly consider the issue of the FCNC which are typically generated at tree-level when integrating out the massive KK modes. For simplicity, consider here the case in which the bulk–to–boundary couplings ε_i are diagonal in flavour space and the non-trivial flavour structure, as described in section 3.3.2, is totally encoded in non-trivial bulk mass matrices, which can now involve not only the bulk mass terms M_i but also the Lorentz violating factors k_i. The FCNC are induced by tree-level couplings which arise from diagrams such as the one on the left of fig. 4.3, in which the non-standard fermions switches at some point to the KK mode of a different family.

The strongest bounds on the couplings of FCNC are the ones involving d and s quarks, $\lesssim 10^{-5}$. In particular, one should worry that, in presence of a generic flavour mixing, a light quark (d or s) can first switch to a state of the heavy KK tower of the corresponding bulk fermions which then switches to the much lighter states of the KK towers of the third quark generation. The latter emits a Z boson and then switches to another heavy KK tower and thus eventually to another light quark (s or d), resulting in a FCNC. By a rough estimate [26], one has

$$g_{FCNC} \sim \frac{\varepsilon_1^c \varepsilon_1^u}{\lambda^c \lambda^u} \left(\frac{m_W}{M_1}\right)^2 , \tag{4.4.2}$$

where M_1 is the mass of the lightest non-SM fermion, which is typically of order M_b (see section 4.2). Considering that for the c and the u quarks one can take $\lambda^c \lambda^u \gtrsim 10$ and, at the same time, one can naturally take $\epsilon_1^{u,c} \sim 0.1$, it is reasonable to expect that g_{FCNC} can be made smaller than 10^{-5} or 10^{-6}.

FCNC are also induced by the exchange of the massive KK modes of the Z gauge boson and gluons [61], due to the non-universality of their couplings to different families. This effect, which is present even in the absence of EWSB, comes from the fact that quarks of different families have different wave functions. The fact that different generations have the same distribution of localized fields in the model we discussed, can however strongly suppress this effect. Flavour non-universality in the KK couplings, indeed, arises in this case only from diagrams in which the brane quark q is changed to a bulk KK fermion, which emits a KK gauge boson, and then back to the brane. The effective coupling of this diagram can be estimated as [26]

$$\frac{\delta g_{KK}}{g_{KK}} \sim \frac{\varepsilon^{q2}}{\lambda^{q2}} \,. \tag{4.4.3}$$

For the light families, if ε^q is moderately small ($\lesssim 10^{-1}$), we expect the coupling (4.4.3) to be naturally of order of $10^{-3} - 10^{-4}$, since $\lambda^{q2} \gtrsim 10$. In this way, the resulting FCNC — due to their stronger couplings, gluons give the dominant contribution — is of the same order of magnitude of that estimated for the Z and thus within the current limits.

4.4.2 Phenomenological Constraints

Having shown that the distortions of the Z boson couplings with the quarks do not impose any relevant constraint on the model, and the FCNC are under control, we are then left with the 7 universal parameters $\widehat{S}$, $\widehat{T}$, $\widehat{U}$, V, X, W and Y.

Before discussing the constraints which arise from the fit on the EW precision measurements, it is useful to review briefly the definition of the universal parameters [44, 69]. These parameters can be used to describe the corrections due to new Physics in the class of "universal" theories in which the deviations from the SM reside in the self-energies of the vector bosons. The category of universal models is quite broad and in particular it includes the possibility of having new heavy vector states as long as they are coupled to the light SM fermions through the usual $SU(2) \times U(1)_Y$ currents. The gauge interactions of the light fermions are thus of the form

$$\mathscr{L}_{int} = \overline{\psi} \gamma^\mu \left(g\, t^a \widehat{A}^a_\mu + g'\, Y \widehat{A}^Y_\mu \right) \psi \,, \tag{4.4.4}$$

where $\widehat{A}^a_\mu$ and $\widehat{A}^Y_\mu$ are a combination of the light and the heavy gauge bosons corresponding to the $SU(2) \times U(1)_Y$ gauge group. Notice that in the model we are considering in this chapter the light SM fermions are nearly exactly localized at the UV boundary (see appendix F) so that the $\widehat{A}^a_\mu$ and $\widehat{A}^Y_\mu$ fields coincide with the holographic electoweak bosons which we presented in chapter 2.

The universal parameters are defined starting from the inverse propagators $\Pi_{i,j}$ of the holographic gauge bosons and considering an expansion in the momentum p^2 up to $\mathcal{O}(p^4)$. This expansion contains 12 parameters, however three of them can be reabsorbed in the

definitions of the SM parameters g, g' and v, and two others are determined requiring the photon to be massless and to couple with $Q = t^3 + Y$. The remaining 7 parameters are

$$\begin{cases} \widehat{S} = \dfrac{g}{g'}\Pi'_{3Y}(0) \\ \widehat{T} = \dfrac{\Pi_{33}(0) - \Pi_{W^+W^-}(0)}{m_W^2} \\ \widehat{U} = -(\Pi'_{33}(0) - \Pi'_{W^+W^-}(0)) \end{cases}, \qquad \begin{cases} V = \frac{1}{2}m_W^2(\Pi''_{33}(0) - \Pi''_{W^+W^-}(0)) \\ X = \frac{1}{2}m_W^2\Pi''_{3Y}(0) \\ Y = \frac{1}{2}m_W^2\Pi''_{YY}(0) \\ W = \frac{1}{2}m_W^2\Pi''_{33}(0) \end{cases}. \tag{4.4.5}$$

The corrections to the universal parameters are induced by the dimension 6 operators

$$\begin{aligned} \mathcal{O}_{3Y} &= (H^\dagger \tau^a H) F^a_{\mu\nu} B^{\mu\nu}, & \mathcal{O}_H &= \left|H^\dagger D_\mu H\right|^2, \\ \mathcal{O}_{YY} &= (D_\rho B_{\mu\nu})^2/2, & \mathcal{O}_{33} &= (D_\rho F^a_{\mu\nu})^2/2, \end{aligned} \tag{4.4.6}$$

which affect respectively Π'_{3Y}, $\Pi_{33} - \Pi_{W^+W^-}$, Π''_{YY} and Π''_{33} (in our notation τ^a are the Pauli matrices).

Let us now discuss the constraints on the model presented in this chapter. From the holographic Lagrangian in eq. (4.2.2), one easily finds, at tree-level and at leading order in α,

$$\begin{cases} \widehat{S} = \dfrac{2}{3}\alpha^2\pi^2 \\ \widehat{T} = \alpha^2\pi^2 \\ \widehat{U} = -\dfrac{2}{3}\alpha^4\pi^4 \\ V = \dfrac{14}{45}\alpha^6\pi^6 \end{cases}, \qquad \begin{cases} X = \dfrac{14}{45}\tan(\theta_w)\alpha^4\pi^4 \\ Y = \dfrac{\rho^2\sin^2(\theta_w) + 1 + 2\cos(2\theta_w)}{9\rho^2\cos^2(\theta_w)}\alpha^2\pi^2 \\ W = \dfrac{1}{3}\alpha^2\pi^2 \end{cases}. \tag{4.4.7}$$

Since α has to roughly be of order 10^{-2}, we see from eq. (4.4.7) that the 3 parameters $\widehat{U}$, V and X are totally negligible. This is actually expected for any universal theory [44]. Notice that the universal parameters essentially depend only on α, the other parameter entering is ρ, which affects only Y.

In fig. 4.4, we report the constraints on the Higgs mass and the compactification scale due to all electroweak flavour and CP conserving observables, obtained by a χ^2 fit using the values in eq. (4.4.7) [27].[9] To better visualize the results, the value of the ρ parameter has been fixed to the Lorentz-symmetric value ($\rho = 1$), hence a χ^2 fit with 2 d.o.f. has been used. The fit essentially does not depend on ρ, as can be checked determining ρ by a minimization of the χ^2 function, which gives a plot which is almost indistinguishable from that reported in fig. 4.4. Due to their controversial interpretation (see *e.g.* [73]), the NuTeV data have been excluded from the fit (nevertheless, the inclusion of such experiment leaves the results essentially unchanged). From fig. 4.4 one can extract a lower bound on

[9] See table 2 of [44] for a detailed list of the observables included in the fit.

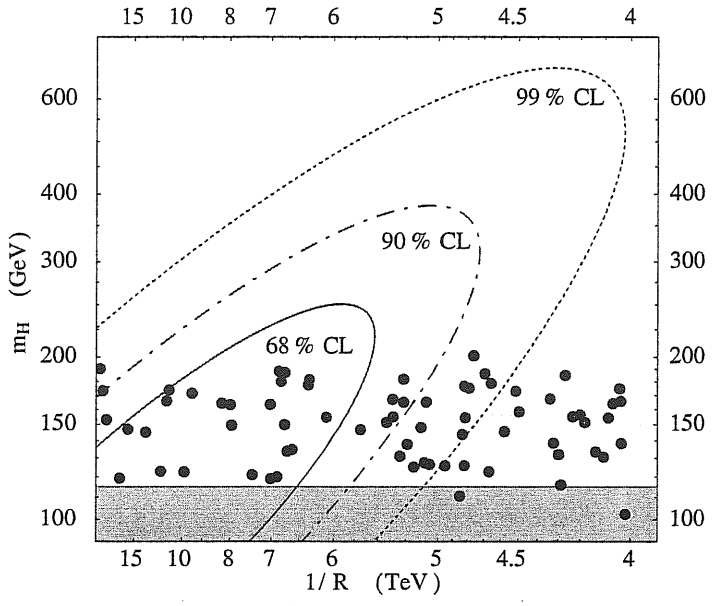

Figure 4.4: Constraints coming from a χ^2 fit on the EW precision tests. The contours represent the allowed regions in the $(1/R, m_H)$ plane at 68 %, 90 % and 99 % confidence level (2 d.o.f.). The shaded band shows the experimentally excluded values for the Higgs mass ($m_H < 115$ GeV). The blue dots represent the predictions of our model for different values of the microscopic parameters (only points with the correct top and bottom masses are plotted).

the compactification scale $1/R \gtrsim 4 - 5$ TeV (which corresponds to $\alpha \lesssim 0.016 - 0.02$) and an upper bound on the Higgs mass which varies from $m_H \lesssim 600$ GeV at $1/R \sim 4$ TeV to $m_H \lesssim 250$ GeV for $1/R \gtrsim 10$ TeV. Notice that the values for $\widehat{S}$, W and Y (for $\rho = 1$) found in eq. (4.4.7) are exactly those expected in a generic $5D$ theory with gauge bosons and Higgs in the bulk, as reported in eq. (20) of [44]. On the contrary, the $\widehat{T}$ parameter in eq. (4.4.7) is much bigger and is essentially due to the anomalous gauge field A_X. A heavy Higgs is allowed in the model because of this relatively high value of the $\widehat{T}$ parameter, which compensates the effects of a high Higgs mass.

Analyzing the models obtained by a random scan of the microscopic parameters, it can be shown that the bound on the compactification scale can be easily fulfilled if a certain fine-tuning on the parameters is allowed. On the other hand, the bounds on the Higgs mass does not require any tuning.

4.5 Sensitivity, Predictivity and Fine-Tuning

As expected, the constraints arising from the electroweak observables require a quite stringent bound, $1/R \gtrsim 4.5$ TeV, on the size of the compactification scale. Differently from

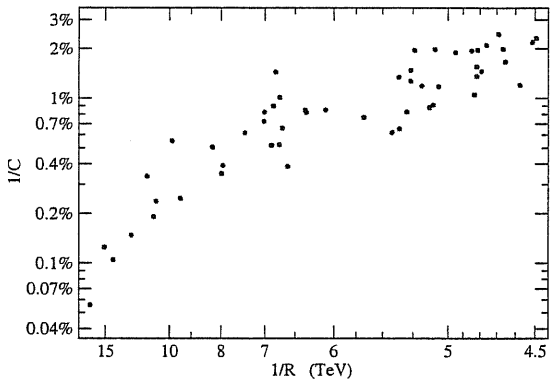

Figure 4.5: Inverse sensitivity for those points which pass the χ^2 test.

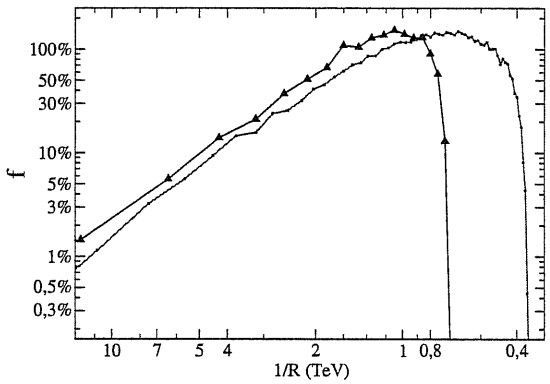

Figure 4.6: Bayesian measure of the fine-tuning at fixed (black) and not fixed (red) top mass.

scenarios of GHU in flat space considered in the previous chapter, the present model can satisfy such a bound (see fig. 4.4) for suitable choices of the microscopic input parameters. It is clear, however, that a certain cancellation (fine-tuning) must be at work in the Higgs potential to make its minimum $\alpha = m_W R$ as low as 0.018.

The fine-tuning is commonly related [74] to the sensitivity of an observable (α, in our case) with respect to variations of the microscopic input parameters.[10] Following [27], we define

$$C \equiv \text{Max}\left\{\left|\frac{\partial \log \alpha}{\partial \log I}\right|\right\}, \tag{4.5.1}$$

as the maximum of the logarithmic derivatives of α with respect to the various input parameters I. The fine-tuning, defined as $f = 1/C$, is plotted in fig. 4.5 for the points which pass the χ^2 test. For $1/R \sim 4.5$ TeV, the fine-tuning of our model is 1 %.

According to a more refined definition [75], the fine-tuning should be intended as an estimate of how unlike is a given value for an observable. This definition is not directly related to the sensitivity, even though it reduces to $f = 1/C$ in many common cases. In this framework, the fine-tuning is computed from the probability distribution $\rho(\alpha)$ of the output observable for "reasonable" distributions of the input microscopic parameters. One defines [27]

$$f = \frac{\alpha\rho(\alpha)}{\langle\alpha\rho(\alpha)\rangle}, \tag{4.5.2}$$

where[11] $\langle\alpha\rho(\alpha)\rangle = \int d\alpha\, \alpha\, [\rho(\alpha)]^2$. The choice of the range of variation of the input parameters[12] is the strongest ambiguity of the procedure, and must reflect physically well

[10] In the particular case at hand, the sensitivity of α is related to the cancellation of the Higgs mass term in the effective potential. As a consequence, one expects the amount of tuning to scale roughly as α^2, as confirmed numerically.

[11] This definition of $\langle\alpha\rho\rangle$ is not precisely the one given in [75]. The difference however disappears when, as in case at hand, the input variables are uniformly distributed.

[12] The results are almost independent of the detailed form of the probability distribution of the input.

motivated assumptions. The distribution shown in fig. 4.1, which we will use, has been obtained with quite generic ranges, which however reflect our prejudice on the physical size of the top and bottom quark masses. Even though this does not make an important difference (see fig. 4.6), we can make our assumption more precise by further restricting to points in which the top (not the b, due to the lack of statistic) has the correct mass. The straightforward application of eq. (4.5.2) gives rise to the fine-tuning plot of fig. 4.6. At $1/R = 4.5$ TeV this prescription gives a fine-tuning of 10 %. One could also relax the assumption of having EWSB. Since the fraction of points without EWSB is about one half of the total, one could argue, very roughly, that the resulting fine-tuning will increase of a factor two and be of order 5 %. This result strongly depends on the assumption we did on the fermion mass spectrum. In practice, what we observe is a certain correlation among the requirements of having a massive top and a high compactification scale, in the sense that points with massive top (and light b) also prefer to have small minima.

Independently on how one defines the fine-tuning, however, the high value of C at small α represents a problem by itself. The high sensitivity, indeed, makes α unstable against quantum corrections or deformations of the Lagrangian with the inclusion of new (small) operators. The effects on the observables of localized kinetic terms for bulk fermions, as described in section 4.3, which lead to very small corrections to all other observables considered in this paper, can completely destabilize the compactification scale at small α. A similar effect is found when including in the effective potential the very small contributions which come from the light fermion families. For $\alpha \sim 0.02$ the corrections which come in both cases are of order 50 %, so that the compactification radius is effectively not predicted in terms of the microscopic parameters of the model.

4.6 A Dark Matter Candidate

As we anticipated, the presence of the $\mathbf{Z}_2$ mirror symmetry has interesting consequences from a cosmological point of view. Given the fact that all the SM particles are even under the symmetry, the lightest $\mathbf{Z}_2$ odd KK particle (LKP) in the model is absolutely stable and can possibly give a viable dark matter candidate. In section 4.1 we showed that the $\mathbf{Z}_2$ odd states are given by the KK towers of the antiperiodic fields. The lightest of such states, in a large part of the parameter space, is given by the first KK mode ($A_-^{(1)}$) of the antiperiodic field A_- associated to the $U(1)_{1,2}$ gauge subgroups. The mass of this state, which clearly is the DM candidate of the model, is $\rho/(2R)$. The electroweak bounds discussed in section 4.4 require $A_-^{(1)}$ to be heavier than about 2 TeV.[13]

$A_-^{(1)}$ has very small couplings with the SM states and is technically a Weakly Interacting

This is because the ranges which are considered are not so wide. Uniform distributions have been used to derive the results which follow.

[13] Following [30], we will assume $\rho \simeq 1$.

Massive Particle (WIMP), however it is considerably more massive than usual WIMP DM candidates. Due to its large mass, $A_-^{(1)}$ has a small pair annihilation rate and this would lead to a too early departure from thermal equilibrium and to an overproduction of DM by one order of magnitude or more [30]. On the other hand, the model predicts many other extra $\mathbf{Z}_2$-odd fields of mass comparable with the DM one, and in particular the next–to–lightest KK particle (NLKP) is often a strongly interacting state. If the mass splitting between LKP and NLKP is small enough, coannihilation effects can take place delaying the decoupling and lowering the LKP relic density.

In the following we will present the results obtained in [30], where is shown that the coannihilation effects can actually lead to realistic relic abundances. Two different scenarios have been analyzed: the first one is given by the model described in this chapter, while the second is a variant of the latter in which the $\mathbf{Z}_2$ mirror symmetry is assumed to act only on the $U(1)$ gauge subgroup and not on the colour group $SU(3)_s$, so that the whole gauge group is $G = SU(3)_s \times SU(3)_w \times U(1)_1 \times U(1)_2$.

Let us start with the second case, which is slightly simpler. In this set-up the NLKP is a $\mathbf{Z}_2$ odd fermion $b_-^{(1)}$ arising from the KK tower associated to the bottom quark. Of course a necessary condition to have coannihilations between the LKP and $b_-^{(1)}$ is a small mass difference between the two states: $\left(m_{b_-^{(1)}} - m_{A_-^{(1)}}\right)/m_{A_-^{(1)}} \leq 0.1$. Even if this condition is fulfilled, in general, coannihilation effects are too small to get a realistic relic density. However in some regions of the parameter space, the $b_-^{(1)}$ pair annihilation rate can be greatly enhanced by resonance effects. In particular the s-channel annihilation diagram, with the first KK mode ($g_+^{(1)}$) of the periodic gluon tower, becomes resonant for splittings $\left|2m_{b_-^{(1)}} - m_{g_+^{(1)}}\right|$ below the $g_+^{(1)}$ decay width. In [30] it has been shown that this effects can actually lead to an acceptable relic density. Of course, the requirement of having a small mass splitting results in a fine-tuning on the model which has been estimated to be in the range $3\,\% - 10\,\%$ depending on the region of the parameter space one considers.

In the case in which the $SU(3)_s$ gauge subgroup is doubled by the $\mathbf{Z}_2$ symmetry, there are two particles which can coannihilate with the DM candidate $A_-^{(1)}$, namely the $b_-^{(1)}$ state, as in the previous set-up, and the first KK mode ($g_1^{(1)}$) of the antiperiodic gluon field. Coannihilations lead to an acceptable reduction of the relic density in two different cases. The first case is analogous to the one described for the previous set-up, namely when $A_-^{(1)}$ and $b_-^{(1)}$ are nearly degenerate in mass and the s-channel annihilation diagram for $b_-^{(1)}$ is in resonance. The second case is when $A_-^{(1)}$ coannihilates only with $g_-^{(1)}$, which is possible for a mass splitting $\left(m_{g_-^{(1)}} - m_{A_-^{(1)}}\right)/m_{A_-^{(1)}} \leq 0.06$. In this case the annihilation rate for $g_-^{(1)}$ is large enough to generate an acceptable suppression of the LKP relic density. Also in this set-up the amount of fine-tuning required to obtain a realistic amount of DM is in the range $3\,\% - 10\,\%$.

In both models considered before, an upper bound on the LKP particle is found, namely

$m_{A_-^{(1)}} \lesssim 5$ TeV. Putting together the results obtained in the DM analysis with the study of the fine-tuning deriving from the EW precision tests, one finds that the "preferred" value of the LKP mass is in the range $2.5 - 3$ TeV.

Unfortunately, the phenomenology of DM searches within the models considered here seems less appealing than in other possible scenarios. In particular the interactions of the LKP with ordinary matter are very suppressed, thus hindering the possibility of a direct detection. Moreover the zero-temperature annihilation rate is particularly small, making it hard to see annihilation signals in dark matter halos.

4.7 The Lorentz Breaking as a Spontaneous Breaking

In this chapter we have essentially shown how it is possible to get a realistic model with gauge-Higgs unification at the price of explicitly breaking the $SO(4,1)/SO(3,1)$ Lorentz generators. In light of this breaking, one could wonder whether it is correct to consider this model as a "canonical" $5D$ theory or not. Indeed, contrary to the usual "spontaneous" breaking of the $SO(4,1)/SO(3,1)$ Lorentz symmetry induced by the compactification, which implies that at short distances $\Delta x \ll R$ the model is effectively a $5D$ Lorentz-invariant theory (in the bulk), the explicit breaking we advocate implies that at arbitrarily short scales the $SO(4,1)$ symmetry is not recovered. This is clearly a theoretical issue, which is mainly related to the possible existence and form of an underlying UV completion of the model. Moreover, the concept of gauge-Higgs unification itself relies on the existence of a $5D$ interpretation. It is clear that we can always consider the model as an IR effective description of a $4D$ moose theory for which the "accidental" $SO(4,1)$ Lorentz symmetry is not recovered in the fermionic sector [7]. From this point of view, the model would resemble more a moose-based little Higgs model rather than a gauge-Higgs unification model. We would like to point out, however, that the $SO(4,1)$ Lorentz breaking can have a simple origin in the context of a purely $5D$ theory.

A particularly elegant and interesting explanation is the following. Consider an axion-like field Φ, which for simplicity we take to be dimensionless, invariant under the shift $\Phi \to \Phi + 2\pi$. In light of this shift symmetry, one can take twisted periodicity conditions for Φ, which read

$$\Phi(y + 2\pi R) = \Phi(y) + 2\pi\,. \tag{4.7.1}$$

Scherk–Schwarz reductions of the form (4.7.1) are not new, appearing in Supergravity as a way to obtain gauged SUGRA or theories with fluxes (see *e.g.* [76]). Consistency of eq. (4.7.1) with the $\mathbf{Z}_2$ orbifold action $y \to -y$ requires that Φ should be $\mathbf{Z}_2$ odd. This is welcome, implying that all the excitations of Φ are massive. Due to the twisted condition (4.7.1), the VEV of Φ is non-trivial. The background configuration Φ_0 which satisfies the

field equations of motion and eq. (4.7.1) is

$$\Phi_0(y) = \frac{y}{R}\,, \tag{4.7.2}$$

which clearly induces a spontaneous breaking of the $SO(4,1)/SO(3,1)$ Lorentz symmetry. The Lorentz violating factors k_i introduced in eq. (4.1.2) are then reinterpreted as due to couplings involving Φ and bulk fields. It turns out that if one also imposes a $\mathbf{Z}_2$ global symmetry under which $\Phi \to -\Phi$, the lowest dimensional operators which couple Φ and bulk fields read

$$\frac{\gamma_1}{f_\Phi^2}\partial_M\Phi\,\partial_N\Phi\,\overline{\Psi}\gamma^M D^N\Psi\,, \qquad \frac{\gamma_2}{f_\Phi^2}\partial_M\Phi\,\partial_N\Phi\,F^{PM}F_P{}^N\,, \tag{4.7.3}$$

where $\gamma_{1,2}$ are dimensionless couplings and f_Φ is the "Φ decay constant". When $\langle\Phi\rangle = \Phi_0$, the operator (4.7.3) precisely induces the Lorentz violating terms which appear in the Lagrangian. Since one must consider values of k_i which are not close to 1, the effective coupling constant of the operators in eq. (4.7.3) is strong (of order 1) and thus insertions of these operators have to be resummed. This is what have been effectively done in our previous analyses.[14] Notice that eq. (4.7.2) can also be interpreted as a non-vanishing flux for the 1-form field-strength $H_1 = d\Phi \sim dy$ or else for a non-vanishing flux for the Hodge dual 4-form field-strength $H_4 \sim dx^0 \wedge dx^1 \wedge dx^2 \wedge dx^3$.

The above picture, which however is not necessary for the model we have presented, shows that the Lorentz violating factors k_j can have a natural origin in a 5D framework. Finally, notice, that the factors k_i effectively imply that different fermions "see" a different radius of compactification. Their effect is then quite similar to recent ideas in the context of Higgsless models in 5D warped models, in which it has been advocated that different fields could propagate in internal spaces with different sizes [77].

[14] Of course, operators similar to the ones in eq. (4.7.3) involving more Φ's should be taken into account. However, if one assumes that $\gamma_{1,2}$ are large so that one can take $Rf_\Phi \ll 1$, these are naturally suppressed.

Chapter 5

Gauge–Higgs Unification at Finite Temperature

As we have thoroughly shown in the last chapters, models with extra dimensions constitute a concrete and reasonable proposal to explain the physics beyond the SM. Among many different scenarios, the GHU idea, implemented either in a flat or in a warped space context, seems to be one of the most appealing possibilities. We already presented in detail the advantages of GHU theories showing that, by a careful modification of the basic GHU set-up, fully realistic models can be actually constructed on a flat $S^1/\mathbf{Z}_2$ orbifold.

Many of the characteristic properties of GHU models are closely related to the identification of the Higgs VEV with a non-local Wilson line phase. This property protects the Higgs potential from divergences thus stabilizing the EW scale, and, at the same time, gives Yukawa coplings which are exponentially sensitive to the parameters of the model, so that a natural hierarchy of fermion masses can be obtained. Being the Higgs potential entirely radiatively generated, the mechanism which induces the EWSB in a GHU set-up deeply differs from the SM one. In particular the existence of an EWSB is related to the presence of (periodic) bulk fermions which give a negative mass contribution to the Higgs.

In the light of the success of the GHU scenario and of its peculiar properties, it is worth investigating, along the lines of [78], the finite-temperature behaviour of these kind of theories. In particular it is interesting to understand whether a phase transition happens at a temperature of the order of the EW scale and what are the properties of such a transition. Besides a purely theoretical interest, this type of analysis is also important from a cosmological point of view. One of the main motivations to study the detailed nature of the EWPT in the SM has been the realization that, under certain assumptions (namely a sufficiently strong CP violation and first order phase transition), it could satisfy the necessary requirements for baryogenesis [79]. Given the actual bounds on the value of the Higgs mass and amount of CP violation in the SM, it has definitively established that the SM phase transition is unable to give a successful baryogenesis.

In simple higher dimensional scenarios in which the Higgs is realized as a $5D$ scalar field, things are even worse. In fact in this case the EWPT can not be of first order [80], thus hindering any possibility to achieve baryogenesis. On the contrary, the properties of the finite-temperature effective potential in GHU models deeply differ from what one usually expects either in $4D$ or in higher-dimensional theories. At high temperatures, it is known that the leading boson and fermion contributions to the Higgs mass are proportional in $4D$ to T^2 [81], while in extra dimensional theories with n compact toroidal dimensions they are proportional to $(LT)^n T^2$ [80], where L is the length of the extra circles, taken all equal, for simplicity. In GHU models in $5D$ the order parameter is given by the VEV of the Wilson line phase and its non-local nature is responsible for a radically different behaviour at high temperatures: the fermion contribution is exponentially suppressed with the temperature, whereas the boson contribution has a leading term proportional to T/L (in the $5D$ case $L = 2\pi R$), plus terms exponentially suppressed with T. The mass of the Wilson line phase at zero temperature is radiatively induced and proportional to $1/L^2$; when the latter is negative, a symmetry breaking is generated, but then at temperatures of order $T \sim 1/L$ a phase transition occurs and the symmetry is restored. This will always happen, due to the presence of the bosonic contribution of the 5D gauge fields.[1]

In this chapter we will study analytically the finite-temperature behaviour of the Higgs potential in a general framework. For simplicity we will not include the Lorentz breaking parameters in our analysis, nor the possibility of having a $\mathbf{Z}_2$ mirror symmetry. However many of the results presented in this chapter can be easily generalized to include such modifications as we will briefly discuss in section 5.2.2, where we will present the finite-temperature properties of the model described in chapter 4.

The first part of this chapter will be devoted to the study of the main features of one-loop effective potential for Wilson line phases at finite temperature, namely their structure, their gauge independence and their high-temperature behaviour. Then we will present the results of a numerical analysis of the first order EWPT which appears in the models described in chapters 3 and 4. Finally, we give support to the idea that the phase transition can safely be studied in perturbation theory in Wilson line based models, by computing the leading IR divergent higher-order contributions to the Wilson line effective potential in a simple 5D model compactified on S^1. This analysis will show that the leading corrections are safely small up to temperature of order $T \sim 1/L$ and start to be relevant well above the phase-transition temperature.

[1]The restoration at high temperatures of a symmetry broken at zero temperature is not a universal feature. It has recently been observed, for instance, that in little Higgs theories the electroweak gauge symmetry remains broken even at high temperatures, at least up to the maximum temperature which can be studied in the effective theory [82]. In non-Abelian theories, it can also happen that the Higgs and the confining phases are connected without the appearance of any phase transition. This is what lattice simulations predict for the SM (see section 5.2).

5.1 The Wilson Line Dynamics at Finite Temperature

The form of the one-loop effective potential at $T = 0$ for Wilson line phases on S^1 or $S^1/\mathbf{Z}_2$ orbifold models has already been discussed in chapter 3. The non-local nature of Wilson lines imply that their potential is completely UV finite, modulo irrelevant constant vacuum energy terms.

The effective potential at finite temperature, in the imaginary time formalism, is obtained from that at zero temperature by simply compactifying the Euclidean time direction on a circle of radius $1/(2\pi T)$, where T is the temperature. Fields satisfying Bose/Fermi statistic must be taken to satisfy periodic/antiperiodic boundary conditions along the Euclidean time direction.[2] The bosonic and fermionic contributions to the one-loop Wilson line effective potential at finite temperature are then easily evaluated. For each bosonic and fermionic degree of freedom with charge q and bulk mass term M, one has

$$V(T, q\alpha) = \frac{(-)^{2\widetilde{\eta}} T}{2} \sum_{k,m=-\infty}^{+\infty} \int \frac{d^3p}{(2\pi)^3} \log \left\{ p^2 + \left[2\pi(m + \widetilde{\eta})T \right]^2 + M_k^2(q\alpha) \right\}, \qquad (5.1.1)$$

where $M_k^2(q\alpha) = M^2 + (k + q\alpha)^2/R^2$ are the masses of the states at KK level k, including a possible bulk mass term M, m are the Matsubara frequencies and $\widetilde{\eta} = 0$ or $1/2$ for bosons and fermions, respectively. It is important to recall that eq. (5.1.1) is valid not only for compactifications on S^1 but also on orbifolds, such as $S^1/\mathbf{Z}_2$. In the latter case, the effect of the parity projection in the diagonal basis for the fields amounts simply to reducing the number of physical degrees of freedom with a given charge q with respect to the Wilson line phase. We collect in appendix G several equivalent ways in which one can compute the effective potential (5.1.1). Notice that eq. (5.1.1) is valid also for gauge fields A_M; in this case one has to take into account a multiplicity factor equal to 3, the number of transverse polarization of a 5D gauge field. Moreover, the gauge contribution is gauge independent. We will discuss in more detail this important aspect in next subsection.

5.1.1 Gauge Independence of the Effective Potential

The effective potential $V(H_0)$ in standard spontaneously broken gauge theories, such as the SM, where H_0 is the VEV of the Higgs field, is generally gauge-dependent [81]. This is easily seen at one-loop level, where the effective potential is obtained by evaluating a trace. In this case one can see, working for instance in an R_ξ-gauge, that the contributions of the would-be Goldstone bosons, ghosts and longitudinal gauge bosons, outside the minimum for the Higgs field, do not cancel anymore and leave a non-trivial ξ-dependent, and thus gauge dependent, term.

[2] For a comprehensive review of finite-temperature field theory and for the reference to the original literature see *e.g.* [83].

In gauge-Higgs unification models, where the Higgs field is identified with the KK zero mode of the gauge field A_5, such problem does not occur, at least at one-loop level. This is expected since at tree level A_5 is a modulus, namely any constant value of this field satisfies the equations of motion. In order to show more explicitly the gauge independence of the one-loop effective potential, we define in the following a class of gauge-fixing Lagrangians $\mathscr{L}_\xi$ that are a sort of generalization of the 4D t'Hooft background gauges[3]:

$$\mathscr{L}_\xi = -\frac{1}{\xi}\mathrm{Tr}\left(\bar{D}_\mu A^\mu + \xi \bar{D}_5 A^5\right)^2, \tag{5.1.2}$$

where $\mu = 0,1,2,3$ runs over the $4D$ directions and $\bar{D}_M = \partial_M - ig_5[\bar{A}_M, \cdot\,]$ is the covariant derivative in terms of the classical field configuration $\bar{A}_M = \delta_{M5}\alpha/(g_5 R)\hat{t}$, $\hat{t}$ being the direction in group space where the VEV is aligned. For $\xi = 1$, the gauge-fixing term (5.1.2) reduces to the usual 5D background field gauge commonly used in the literature to derive the one-loop effective potential of Wilson line phases [28]; for $\xi = 0$, we instead get the 4D Landau gauge $\partial_\mu A^\mu = 0$, whereas for $\xi \to \infty$, eq. (5.1.2) gives $\bar{D}_5 A^5 = 0$; the latter condition is precisely the unitary gauge in which all the would-be Goldstone bosons associated to the non-linearly realized gauge symmetries are decoupled, as we will see more explicitly in the following. From a 4D point of view, eq. (5.1.2) is precisely the gauge-fixing term defining an R_ξ-gauge for the infinite gauge symmetry groups associated to all KK levels of the 5D gauge fields $A_\mu(x,y)$. The full 5D Lagrangian for the gauge fields is then

$$\mathscr{L} = -\frac{1}{2}\mathrm{Tr}\left(F_{MN}F^{MN}\right) + \mathscr{L}_\xi + \mathscr{L}_{gh}, \tag{5.1.3}$$

where $\mathscr{L}_{gh}$ is the ghost Lagrangian associated to the gauge-fixing (5.1.2):

$$\mathscr{L}_{gh} = -\mathrm{Tr}\left[\omega^*(\bar{D}_\mu D^\mu + \xi \bar{D}_5 D^5)\omega\right]. \tag{5.1.4}$$

It is not difficult to derive the quadratic Lagrangian, in momentum space, for the gauge, scalar and ghost fields A_μ, A_5 and ω. As discussed before, the only non-trivial task is to derive the linear combination of fields that couples diagonally with A_5, in which base the effect of the background is simply to shift the KK level of the mode. For definiteness (and because this will be the case we analyze mostly), we consider an $SU(3)$ gauge theory on the orbifold $S^1/\mathbf{Z}_2$, where $SU(3)$ is broken by the orbifold parity to $SU(2)\times U(1)$ and thus to $U(1)$ by the Wilson line phase α. The quadratic Lagrangian of this model reads, in momentum space,

$$\begin{aligned}\mathscr{L}_{quad.} = &\sum_{i=1,2}\sum_{n=-\infty}^{+\infty}\left[A^{(i)\dagger}_{\mu,n}\Delta^{(i)}_{\mu\nu,n}A^{(i)}_{\nu,n} + A^{(i)\dagger}_{5,n}\Delta^{(i)}_{55,n}A^{(i)}_{5,n} + \omega^{(i)\dagger}_n\Delta^{(i)}_{55,n}\omega^{(i)}_n\right]\\ &+\sum_{i=3,4}\sum_{n=0}^{+\infty}\left[A^{(i)}_{\mu,n}\Delta^{(0)}_{\mu\nu,n}A^{(i)}_{\nu,n} + A^{(i)}_{5,n}\Delta^{(0)}_{55,n}A^{(i)}_{5,n} + \omega^{(i)*}_n\Delta^{(0)}_{55,n}\omega^{(i)}_n\right].\end{aligned} \tag{5.1.5}$$

[3] Compare the gauge fixing chosen in section 1.2. The gauge-fixing Lagrangian in eq. (5.1.2) is similar to the one in eq. (1.2.3), apart from the gauge background which is not included in eq. (1.2.3).

In eq. (5.1.5), the fields $(A_\mu^{(1,2)}, A_5^{(1,2)}, \omega^{(1,2)})$ represent the linear combination of fields that couples diagonally to the Higgs field, with charge $q = 1, 2$. The fields $(A_\mu^{(3,4)}, A_5^{(3,4)}, \omega^{(3,4)})$, instead, do not couple to A_5. The explicit form of these linear combinations of fields, in terms of the usual $SU(3)$ Gell–Mann field decompositions, can be found in appendix D. Notice that due to the different $\mathbf{Z}_2$ parities of A_μ and A_5, we have $A_{5,0}^{(3)} = A_{\mu,0}^{(4)} = \omega_0^{(4)} = 0$. The inverse propagators are

$$\begin{aligned} \Delta_{\mu\nu,n}^{(q)} &= \eta_{\mu\nu}\left[p^2 + \frac{(n+q\alpha)^2}{R^2}\right] + \frac{1-\xi}{\xi} p_\mu p_\nu\,, \qquad q = 0, 1, 2, \\ \Delta_{55,n}^{(q)} &= p^2 + \xi\frac{(n+q\alpha)^2}{R^2}\,, \qquad q = 0, 1, 2, \end{aligned} \tag{5.1.6}$$

where $p^2 = p_\mu p^\mu$. It is clear from eq. (5.1.6) that when $\xi \to \infty$, all scalar fields $A_{5,n}$ decouple from the theory, with the only exception of $A_{5,0}^{(4)}$, namely the Higgs field. It is now easy to establish the independence on the parameter ξ of the one-loop effective potential. Indeed, for each KK-mode level n and charge q, the gauge, scalar and ghost contributions give a total factor

$$\frac{\Delta_{55,n}^{(q)}}{\left[\Delta_{55,n}^{(q)} \det \Delta_{\mu\nu,n}^{(q)}\right]^{1/2}} = \sqrt{\xi}\left(p^2 + \frac{(n+q\alpha)^2}{R^2}\right)^{-\frac{3}{2}}, \tag{5.1.7}$$

where the determinant in eq. (5.1.7) is meant to be taken only on the 4×4 polarization matrix of the gauge fields. Aside from the irrelevant $\sqrt{\xi}$ factor, which is reabsorbed in the functional measure, all the non-trivial ξ-dependence in eqs. (5.1.6) cancels out in eq. (5.1.7), leaving an effective contribution of three scalar degrees of freedom with twist q. As stated before, this equals the total contribution of a 5D gauge field A_M with the same twist.

The gauge independence of the potential is trivially extended at finite temperature. Indeed, in the imaginary time formalism, eq. (5.1.7) still holds, the only modification being given by the Matsubara frequency modes, that are all integer-valued for gauge, scalar and ghost fields.

5.1.2 High Temperature Behaviour

The one-loop effective potential for Wilson line phases at finite temperature has been computed in ref. [84] (see also ref. [85]), where it has been shown that at temperatures of order $T \sim 1/L$ the symmetry is restored. Its high temperature behaviour is peculiar, as can be seen by studying the bosonic and fermionic contribution to the Higgs thermal mass at $\alpha = 0$:

$$m_H^2(T, \alpha = 0) = \left(\frac{g_4 R}{2}\right)^2 \left.\frac{\partial^2 V}{\partial \alpha^2}\right|_{\alpha=0}. \tag{5.1.8}$$

For $T \gg 1/L$, the mass (5.1.8) can easily be extracted from eq. (G.1.3), using the known asymptotic behaviour of Bessel functions for large values of their argument. For massless bosonic and fermionic bulk fields ($M = 0$ in eq. (G.1.3)) with twist q, one finds respectively[4]

$$m_H^2(T,0) = \frac{g_4^2}{16\pi^2}\left(\frac{2}{3}\pi^2 q^2 n_B\right)\frac{T}{L}\left\{1 + O\left[(LT)^{\frac{3}{2}}e^{-2\pi LT}\right]\right\}, \tag{5.1.9}$$

$$m_H^2(T,0) = -\frac{g_4^2}{16\pi^2}\left(2\sqrt{2}\pi^2 q^2 n_F\right)\frac{T}{L}(LT)^{\frac{3}{2}}e^{-\pi LT}\left[1 + O\left(\frac{1}{LT}\right)\right], \tag{5.1.10}$$

where n_B and n_F denote the effective number of bosonic and fermionic degrees of freedom of the field. The exponential terms appearing in eqs. (5.1.9), (5.1.10) and the linear temperature dependence of the boson contribution are a characteristic feature of the non-local nature of the Higgs potential. They are different from the typical contributions expected for models in extra dimensions where one gets a thermal mass of order LT^3 [80], or for the 4D Standard Model, in which the Higgs thermal mass, at high temperatures, goes like T^2.

The leading high temperature dependence of the one-loop thermal mass can be understood by studying the UV behaviour of the one-loop mass correction at zero temperature. Since this is in general quadratically divergent, power counting implies that its leading finite temperature contribution will be of order T^2. This counting can also be used in models in extra dimensions. Since at a given T, the effective number of KK modes contributing to the thermal ensemble is roughly given by LT, one would generally get a leading high temperature contribution to the thermal mass of order $(LT)T^2 = LT^3$, in agreement with ref. [80]. For Wilson line potentials, however, the analysis is different, since they are finite at zero temperature, with a one-loop mass saturated by the compactification scale $1/L^2$, times $g_4^2/(16\pi^2)$, a $4D$ loop factor. The non-local nature of the potential is such that all Matsubara mode contributions, but the zero mode one, are exponentially suppressed at high temperatures. The only relevant contribution arises then from bosons, which admit a zero Matsubara mode. Consequently, the thermal mass has a linear dependence on T, reproducing the leading term in eq. (5.1.9). Since the effective number of KK modes contributing in the thermal ensemble is still LT, eq. (5.1.9) can alternatively be understood as the sum of the one-loop, zero temperature, mass corrections of the (LT) KK modes: $(LT)/L^2 = T/L$. The naïve power counting argument, applied instead to a truncated sum of KK modes, would predict the wrong LT^3 dependence. In fact, a naïve truncation of the KK sum would spoil the shift symmetry $\alpha \to \alpha + 1$ of the Wilson line phase, resulting also in a fake divergent zero temperature effective potential, as discussed in section 3.1.

[4]Recall that theories in extra dimensions are non-renormalizable and thus are effective theories valid up to an UV cut-off scale $\Lambda \gg 1/R$. For this reason, one cannot consider temperatures larger than (or of the same order of) Λ, because at these scales the theory becomes strongly coupled.

The high-T contribution to the Higgs thermal mass of massive bulk fields, with mass M, is further exponentially suppressed. In particular, for $M \gg 1/L$, the linear dependence on T appearing in the first term in eq. (5.1.9) is suppressed by a factor e^{-ML}. The same is true for the whole effective potential, as is clear from eq. (G.1.3). The effective potential is thus exponentially insensitive to UV physics and completely determined by the light 5D degrees of freedom.

Given the high T behaviour of the bosonic and fermionic contributions to the Higgs mass in eqs. (5.1.9) and (5.1.10), we can establish on quite general grounds that if a gauge symmetry breaking occurs at $T = 0$, namely $M^2(T = 0, \alpha = 0) < 0$, it will be restored at a sufficiently high temperature when $M^2(T, \alpha = 0) \geq 0$. Since Wilson line effective potentials are gauge invariant, $V(-\alpha) = V(\alpha)$, and thus $\alpha = 0$ is always an extremum of the potential. Consequently, at sufficiently high T, $\alpha = 0$ turns to a minimum of the potential, at least locally.

5.1.3 Properties of the Phase Transition

An analytical study of the nature of the phase transition occurring in Wilson line based models is not totally straightforward, due to the non-local nature of the order parameter. The essential features of the transition, however, can quantitatively be studied by properly approximating the exact one-loop formulae for the potential appearing in appendix G.

As we will show, the phase transition is typically of first order and is related to the presence of a cubic term in the bosonic contribution of the effective potential. This is very similar to what happens, for instance, in the SM, where a cubic term in the Higgs field appearing in the effective potential at finite temperature is responsible for the generation of a first-order phase transition, for sufficiently low values of the Higgs mass. The cubic term in the Wilson line phase α appears from a high temperature expansion of the bosonic contribution in, say, eq. (G.1.3). For massless fields with $M = 0$, charge q_B and for $LT > 1$, we can safely drop all Matsubara modes but the zero mode in the sum over m appearing in eq. (G.1.3). For each degree of freedom, the resulting potential is

$$V_B(T, \alpha) \simeq -\frac{T}{\pi^2 L^3} \sum_{\widetilde{k}=1}^{\infty} \frac{\cos(2\pi \widetilde{k} q_B \alpha)}{\widetilde{k}^4} \,. \tag{5.1.11}$$

Interestingly enough, the potential (5.1.11) admits a very simple polynomial expression in α, which can be found by carefully Taylor expanding it in powers of α. Since a naïve expansion in α would lead to the appearance of an infinite number of ill-defined sums, a regularization has to be taken to give a meaning to the resulting expression. We will use in the following the ζ-function regularization, according to which $\zeta(-2n) = \sum_{k=1}^{\infty} k^{2n} = 0$ for all positive integers n. As a consequence, in the expansion of the cosine function in eq. (5.1.11), all terms but the first three, constant, quadratic and quartic in α, vanish. All

the odd derivatives in the expansion vanish since $\zeta(-2n+1)$ is finite for $n > 0$, but care has to be taken for the third derivative. The latter in fact does not vanish, due to the relation

$$\lim_{x\to 0^+} \sum_{n=1}^{\infty} \frac{\sin(nx)}{n} = \frac{\pi}{2}. \tag{5.1.12}$$

This is at the origin of the α^3 term in the expansion of the potential (5.1.11). It only arises for massless 5D bosonic fields, since for massive fields the sum over n is absolutely convergent, resulting in a trivially vanishing third derivative of the potential.

Putting all terms together and recalling that $\zeta(0) = -1/2$, one gets

$$V_P(T,\alpha) = -\frac{\pi^2 T}{3L^3}\left[\frac{1}{30} - (q_B\alpha)^2 + 2(q_B\alpha)^3 - (q_B\alpha)^4\right]. \tag{5.1.13}$$

The expressions (5.1.11) and (5.1.13) are identical for $0 \leq \alpha \leq 1/q_B$. Since $V_P(T, q_B\alpha = 0) = V_P(T, q_B\alpha = 1)$, by periodically extending V_P to all values of α, one gets a complete identity between the two expressions. Indeed, it is straightforward to check that the Fourier series of the polynomial (5.1.13) agrees with eq. (5.1.11). Notice that the α^3 term is a non-analytic term, since it corresponds to a $(H^\dagger H)^{3/2}$ operator, when written in a manifestly gauge-invariant form.

Let us now study how the phase transition schematically occurs in a model with one massless $5D$ gauge boson and one massless fermion, with charges respectively q_B and q_F with respect to the Higgs. We take $q_F > q_B$, because in this case the analysis is further simplified, as we will see. There is no need to specify, in this simple set-up, which is the underlying theory which gives rise to these fields and to the Wilson line. As a consequence, the analysis is general and it can be applied for any gauge group and compact space (S^1 or $S^1/\mathbf{Z}_2$).

At zero temperature, the effective potential is given by the first row in eq. (G.1.5) with $M = 0$. By summing the fermionic and bosonic contributions, we get

$$V(0,\alpha) = \frac{3}{4\pi^2 L^4} \sum_{\tilde{k}=1}^{\infty} \frac{\left[8\cos(2\pi\tilde{k}q_F\alpha) - 3\cos(2\pi\tilde{k}q_B\alpha)\right]}{\tilde{k}^5}. \tag{5.1.14}$$

The potential is unstable at $\alpha = 0$ and develops a minimum at $\alpha \simeq 1/(2q_F)$, where the "Higgs mass" is approximately given by

$$m_H^2 \simeq \frac{g_4^2}{16\pi^2}\frac{1}{L^2} 24 q_F^2 \zeta(3), \tag{5.1.15}$$

where, as rough approximation, we have neglected the bosonic contribution in eq. (5.1.15). At finite temperature, as we have already discussed, the fermion contribution is less and less relevant, resulting in a phase transition for $T \sim 1/L$. The transition is more efficiently studied by starting from temperatures slightly above the critical one, when $TL > 1$.

In this regime, it is a good approximation to use the high-temperature expansion for the potential. The bosonic contribution has been already computed and gives rise to the polynomial potential (5.1.13) multiplied by a multiplicity factor of 3. The fermionic contribution, unfortunately, does not admit a simple finite polynomial expansion which accurately approximates the exact one-loop result, like the bosonic case. As such, a rough approximation will be used to put it in a simple polynomial form. By expanding the modified Bessel functions and retaining only the modes $m = 0, -1$ and $\tilde{k} = 1$ in eq. (G.1.3), we roughly get

$$V_F(T, \alpha) \simeq \frac{4\sqrt{2}}{L^4}(LT)^{5/2} e^{-\pi LT} \cos(2\pi q_F \alpha) \,. \tag{5.1.16}$$

No α^3 term arises from the fermion contribution. If we expand the cosine in eq. (5.1.16) and retain only terms up to α^4 we see that the effective potential for $LT > 1$, resulting by summing V_B and V_F, has the schematic form[5]

$$\frac{L^4}{\pi^2} V(T, q\alpha) \simeq a(x)\, \alpha^2 - b(x)\, \alpha^3 + c(x)\, \alpha^4 \,, \tag{5.1.17}$$

where $x = LT$ and

$$\begin{aligned} a(x) &= q_B^2 x - 8 q_F^2 \sqrt{2} x^{5/2} e^{-\pi x} \,, \\ b(x) &= 2 x q_B^3 \,, \\ c(x) &= q_B^4 x + \frac{8}{3} q_F^4 \sqrt{2} \pi^2 x^{5/2} e^{-\pi x} \,. \end{aligned} \tag{5.1.18}$$

eq. (5.1.17) is valid for $0 \leq \alpha \leq 1/(2q_F)$, which is the relevant range in α for the study of the phase transition. The analysis of the latter for potentials like eq. (5.1.17) is standard (see *e.g.* ref. [86]). For $x >> 1$, the potential admits only a minimum at $\alpha = 0$. As the temperature decreases, an inflection point appears at $T = T_1$, below which a non-trivial minimum and maximum appear. The critical temperature T_C is defined as the temperature when $V(T_C, q\alpha_{min}(T_C)) = 0$, namely when the non-trivial minimum is as deep as the minimum at zero. This is given by the largest root of the equation $b^2(x_C) - 4a(x_C)c(x_C) = 0$ which, for $q_F > q_B$, is nearly equivalent to the vanishing of the term $a(x)$ in eq. (5.1.17). The critical temperature has only a logarithmic dependence on the charges q_B and q_F and is of order $1/L$, as mentioned. At $T = T_C$, we get

$$\alpha_{min}(x_C) = \frac{b(x_C)}{2c(x_C)} \simeq \frac{6 q_B}{\pi^2 q_F^2} \,. \tag{5.1.19}$$

Below the critical temperature T_C, $\alpha_{min}(T)$ becomes the new global minimum of the potential. The value $|H(T_C)|/T_C = 2\alpha_{min}(T_C)/(g_4 R T_C)$ is one of the relevant parameters

[5] As we said, this is generally a rough approximation but it is enough for our analytical estimates. All our results in the following section are instead based on numerical analysis which take into account the exact form of the one-loop boson and fermion contribution to the potential, as reported in appendix G.

to study, if one wants to get baryogenesis at the electroweak phase transition (see *e.g.* ref. [83]). One necessary (but not sufficient) requirement is that $|H(T_C)|/T_C > 1$, otherwise sphalerons at $T < T_C$ would wash out any previously generated baryon asymmetry [79].[6] It is also a good parameter to measure the strength of the first-order phase transition. Since the Higgs mass (5.1.15) is proportional to q_F, whereas $\alpha_{min}(x_C) \sim q_B/q_F^2$ and $T_C \sim 1/L$, we conclude that

$$\frac{|H(T_C)|}{T_C} \sim \frac{q_B}{q_F^2}\,. \tag{5.1.20}$$

The strength of the first-order phase transition is inversely proportional to q_F^2 and hence to the value of the Higgs mass.

In presence of several massless bosonic and fermionic fields, with charges $q_{B,i}$ and $q_{F,i}$, the potential can still be put in the form (5.1.17), provided that one substitutes in eqs. (5.1.18) $q_B^k \to \sum_i n_{B,i} q_{B,i}^k$ and $q_F^k \to \sum_i n_{F,i} q_{F,i}^k$, where $n_{B(F),i}$ are the multiplicities of the bosons and fermions with charges $q_{B(F),i}$ ($k = 2, 3, 4$).

For more generic field configurations, such as massive bulk fermions, localized fields or localized gauge kinetic terms, the analytical study of the phase transition is more involved and one has to rely on numerical methods to safely establish its nature. However, since the coefficient $b(x)$ multiplying the α^3 term in eq. (5.1.17) will still be non-vanishing (unless the model has no massless bosons coupled to the Wilson line phase), we expect that the phase transition will be of first order. We show in next section that this is what generally happens for the model described in chapter 3, by numerically studying the one-loop Higgs potential in a more complicated setting. We will also see that the analytical studies performed in this subsection are still approximately valid.

5.2 The Electroweak Phase Transition in GHU Models

In this section, we want to establish the nature of the electroweak phase transition in the models with gauge-Higgs unification based on 5D orbifolds, which we presented in the previous chapters. We will mainly focus on the simple model of chapter 3 and its generalizations, which turn out to have some interesting features as the EWPT is concerned. Lately we will also analyze the realistic model presented in chapter 4.

Before summarizing the results, it might be useful to review the nature of the EWPT in the SM [87]. The properties of the transition are known to essentially depend on the value of the Higgs quartic coupling λ, or equivalently on the Higgs mass m_H. For $m_H < m_W$, the transition is always of the first order, with a strength that is inversely proportional to the Higgs mass [88, 89]. In this regime, the SM phase transition can reliably be computed in perturbation theory, although the resummation of an infinite class of certain IR divergent

[6] The bound $|H(T_C)|/T_C > 1$ is derived by an analysis of sphaleron dynamics in the SM. This analysis has not been repeated for Wilson lines in $5D$ and thus deviations from the bound $H(T_C)/T_C > 1$ could be present.

higher loop diagrams (so called "daisy" or "ring" diagrams) has to be performed. Also in the SM case, the presence of a first-order phase transition can be traced back to the presence of a term in the potential which is cubic in the Higgs field. Since the effective potential is generally a gauge-dependent quantity, care has to be taken in the gauge-fixing procedure [90] or a gauge-invariant formalism has to be advocated [91]. Around the critical temperature, perturbation theory is less and less reliable as m_H approaches m_W. For $m_H \gtrsim m_W$, perturbation theory breaks down and one has to consider non-perturbative methods, such as lattice computations. The latter seem to indicate that in this regime of Higgs masses, the SM does not actually have a phase transition but rather a crossover, since the Higgs and the confining phase are continuously connected [92]. As already anticipated, these features have important consequences form a cosmological point of view. In fact the absence of a first order phase transition implies that the condition $|H(T_C)|/T_C > 1$ can not be fulfilled, thus forbidding the possibility of achieving a successful baryogenesis at the EWPT.

5.2.1 The EWPT in a Simple Model

We report below the results obtained in [78] by analyzing the properties of the electroweak phase transition in the simple model presented in chapter 3 and its generalizations. The results, including all the figures, have been obtained by a numerical computation using the exact one-loop effective potentials. To avoid technical complications, a slightly simplified model has been considered. Namely the extra $U(1)'$ factor needed to get the correct weak mixing angle has been neglected. This change, however, mildly affects the properties of the phase transition and all the other results obtained.

As discussed in chapter 3, the simplest implementation of the model predicts a very low Higgs mass $m_H \lesssim 40$ GeV. For Higgs masses of this order, the EWPT in the SM can be reliably studied in perturbation theory. It is thus reasonable to compare the results in GHU models with those obtained in the SM at one-loop level, for the same values of the Higgs and top mass. On the other hand, in the extended versions of the model, the Higgs mass can be considerably larger ($m_H \gtrsim m_W$). In this case a comparison with the SM can not be given due to the fact that perturbation theory in the SM breaks down. On the contrary in GHU models perturbativity seems to be present even at large Higgs masses, as we will better discuss in section 5.3.

Only Bulk Fields

First of all we consider a minimal set-up, in which we consider gauge fields and a couple of bulk fields, with opposite $\mathbf{Z}_2$ parities, in the representation $(\mathbf{3}, \overline{\mathbf{6}})$ of $SU(3)_s \times SU(3)_w$. No boundary fermions are introduced.

In this theory, a first order phase transition appears for $\lambda \leq 2.1$, where $\lambda = ML/2$ is

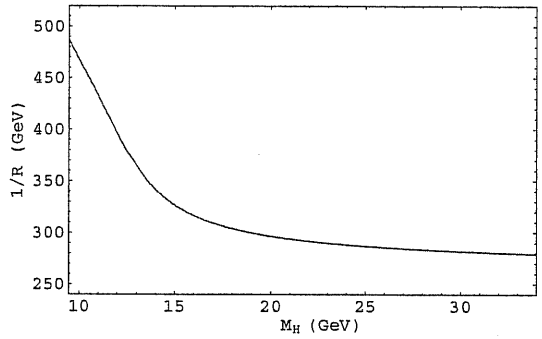

Figure 5.1: Compactification radius as function of the Higgs mass (only bulk fields).

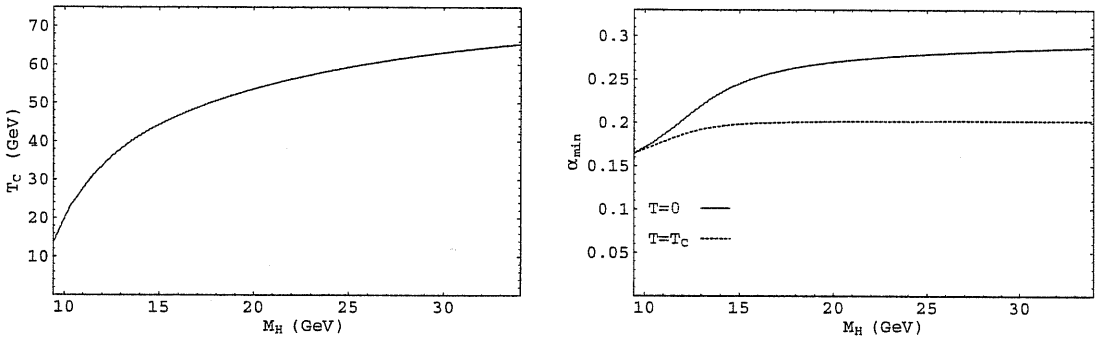

(a) (b)

Figure 5.2: (a) Critical temperature and (b) position of the minimum at $T = 0$ and at $T = T_C$, as function of the Higgs mass (only bulk fields).

the properly rescaled bulk fermion mass, while outside this range no symmetry breaking occurs. The critical temperature of the transition is $T_C \sim 1/L$. We report in figures 5.1 and 5.2 how the compactification radius, the critical temperature and the minimum of the potential (at $T = 0$ and at $T = T_C$) depend on the Higgs mass, whose value depends on λ. In figure 5.3 (a), we plot $|H(T_C)|/T_C$ as function of m_H. The phase transition is strongly first order, as expected for such low values of m_H. In figure 5.3 (b), we plot the latent heat as function of m_H (normalized in units of the critical temperature), whose expression is given by

$$\Delta Q = T\frac{\partial}{\partial T}V(T,\alpha_{min})\Big|_{T=T_C} - T\frac{\partial}{\partial T}V(T,\alpha=0)\Big|_{T=T_C} . \qquad (5.2.1)$$

For simplicity, we normalize the effective potential so that $V(T,\alpha=0)=0$, in which case the second term in eq. (5.2.1) vanishes. Finally, in figure 5.4 we show the shape of the effective potential, for $m_H = 25\,\mathrm{GeV}$, at various temperatures.

For high values of m_H (which correspond to low values of the bulk fermion mass λ), the

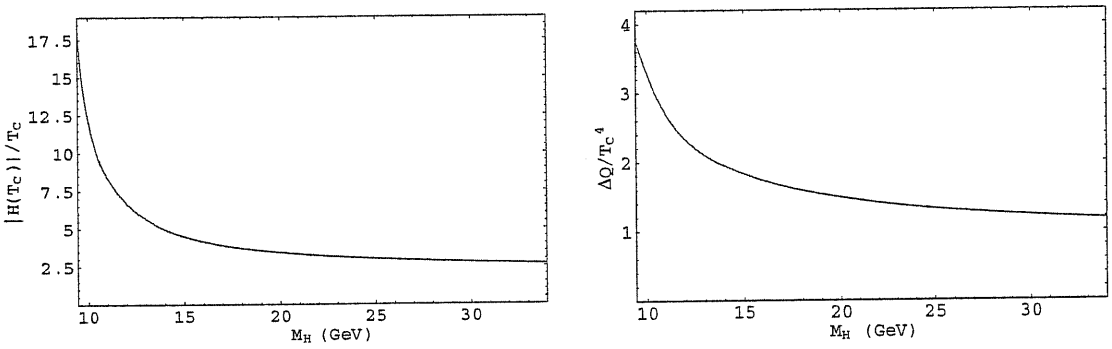

(a) (b)

Figure 5.3: (a) Phase transition strength and (b) latent heat as function of the Higgs mass (only bulk fields).

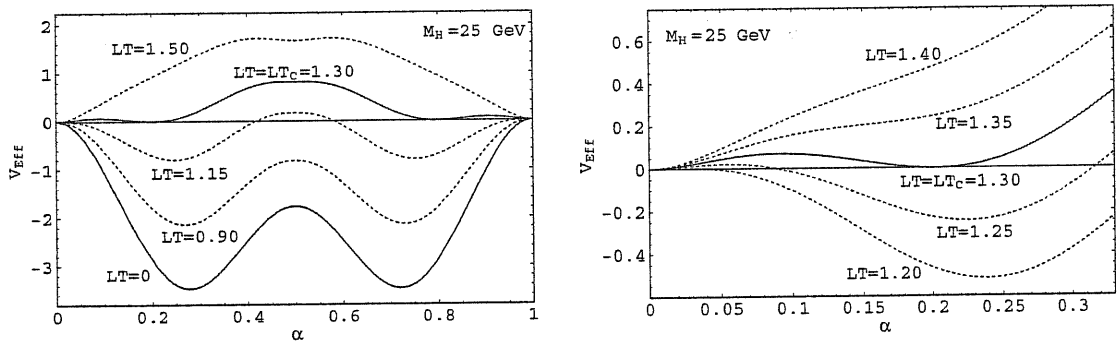

(a) (b)

Figure 5.4: (a) Effective potential (for $m_H = 25\,\text{GeV}$) at various temperatures. (b) Detail near the phase transition (only bulk fields).

behaviour of $\alpha_{min}(T_C)$ and $|H(T_C)|/T_C$ in figures 5.2 (b) and 5.3 (a) can be understood by applying the considerations of section 5.1.3. Around the critical temperature the potential (5.1.17) has only a mild dependence on λ, at least for $\lambda \lesssim 1.5$, since as first approximation it implies only the shift $\pi LT \to \sqrt{4\lambda^2 + (\pi LT)^2}$ in eq. (5.1.16). Hence, although the Higgs mass at $T = 0$ is sensibly dependent on λ, α_{min} and $|H(T_C)|/T_C$, as computed in eqs. (5.1.19) and (5.1.20), are essentially independent of m_H for low values of λ (high values of m_H).

For larger values of λ, both T_C and m_H starts to exponentially depend on λ, resulting in a linear dependence of T_C on m_H. On the contrary, $\alpha_{min}(T_C)$ remains still constant. These behaviours are roughly reproduced by the left part of figures 5.2 (b) and 5.3 (a).

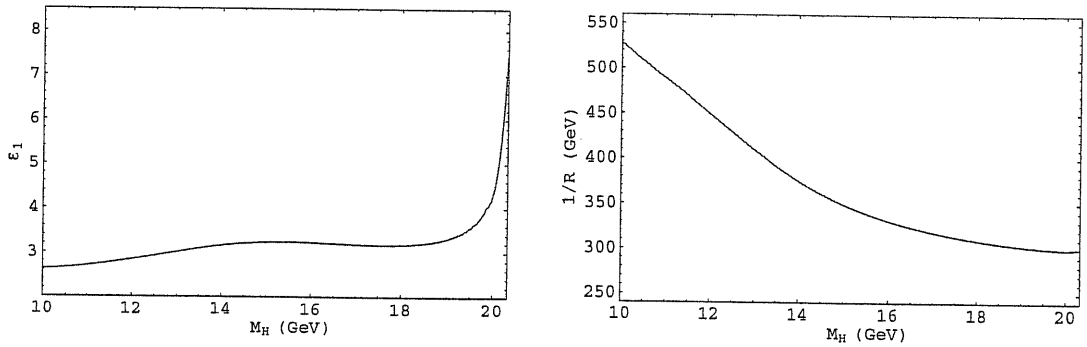

(a) (b)

Figure 5.5: (a) Values of the ε_1 coupling and (b) compactification radius as function of the Higgs mass (inclusion of boundary fermions).

Inclusion of Boundary Fermions

We now add the boundary fermions, namely a doublet Q_L localized at the $y = 0$ fixed point and the singlet t_R localized at $y = \pi R$.[7] Notice that the localization of the fields differs from the one used in the model described in chapter 3 in which the boundary fields were all introduced at the same boundary. Considering localized fields on both boundaries introduce some technical complications in the theory (mainly related to the issue of anomaly cancellation), and moreover seems less appealing from a phenomenological point of view [26]. Nevertheless, as we will see in the following, when considered in the semi-realistic set-up of chapter 3, the possibility of introducing left-handed and right-handed boundary fields at different fixed points, together with the inclusion of localized gauge kinetic terms for the gauge fields can give reasonable Higgs and top masses for acceptable values of c_i (see section 3.7.2 and ref. [15]).

The relevant formulae for the effective potential in presence of boundary fields are given in appendix G, eqs. (G.2.1). Since the potential does not significantly depend on the bulk–to–boundary couplings ε_i, the crucial dependence being given by the bulk fermion mass λ, we have set $\varepsilon_2 = \varepsilon_1$ and fixed the overall scale by the requirement of having a top mass $m_t = 45$ GeV. The effective potential is studied for $0.85 \leq \lambda \leq 1.85$. Again, the electroweak phase transition is of first order, with a critical temperature of order $1/L$ (see figs. 5.5–5.8).

For comparison, in figs. 5.6 (a) and 5.7, we plotted the critical temperature, $|H(T_C)|/T_C$ and the latent heat as function of the Higgs mass for both the 5D model and the SM, with $m_t = 45$ GeV. For the SM case, we plot both the naïve one-loop ($SM_{Unres.}$) and one-loop improved (SM_{Daisy}) results, the latter obtained by resumming the leading daisy diagrams

[7] The mixing of the boundary fields with the bulk fermions is given in eq. (G.0.1).

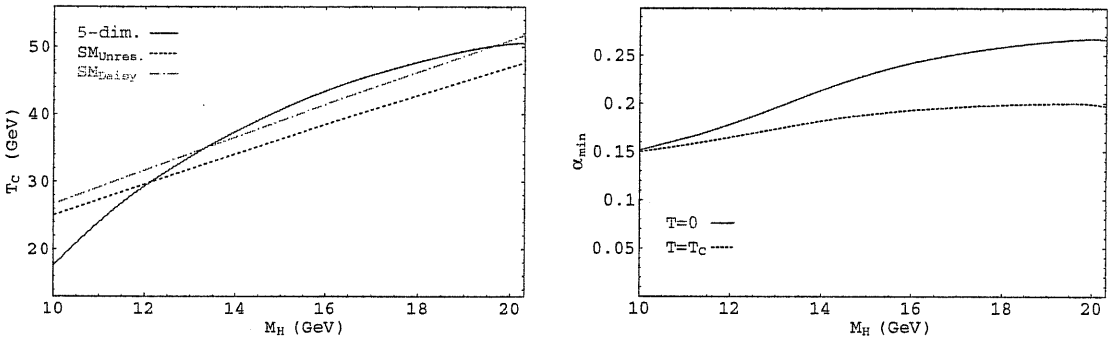

(a) (b)

Figure 5.6: (a) Critical temperature and (b) position of the minimum at $T = 0$ and at $T = T_C$, as function of the Higgs mass (inclusion of boundary fermions).

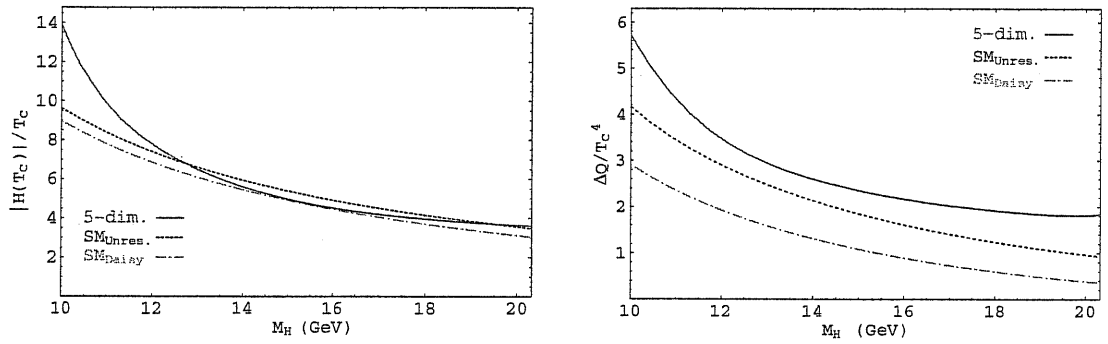

(a) (b)

Figure 5.7: (a) Phase transition strength and (b) latent heat as function of the Higgs mass (inclusion of boundary fermions).

[88, 89].[8] For such low values of the Higgs mass, $10 \div 20$ GeV, the SM effective potential is well described by its one-loop approximation.

Even when boundary fermions are inserted, the behaviour of $\alpha_{min}(T_C)$ and $|H(T_C)|/T_C$ reported in figs. 5.6 (b) and 5.7 (a) is very similar to that found in the previous case with only bulk fermions. This is explained by recalling, as already mentioned, that the potential has a small dependence on the bulk–to–boundary couplings ε_i. All the analytical considerations performed at the end of the previous subsection are then approximately

[8]To obtain the SM results the Landau gauge has been used, which turns out to be a good gauge choice. Indeed, results obtained in this gauge are very similar to the ones obtained in gauge-invariant approaches to the electroweak phase transition, such as the gauge-invariant effective potential [91] and lattice computations [93]. Moreover the cut-off renormalization scheme has been fixed choosing the counterterms so that the position of the zero temperature minimum of the effective potential and the Higgs mass do not change with respect to their tree-level values [86].

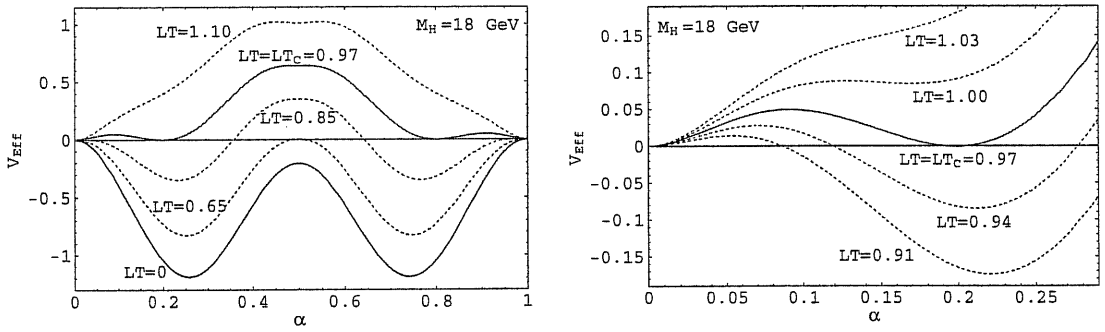

(a) (b)

Figure 5.8: (a) Effective potential (for $m_H = 18\,\text{GeV}$) at various temperatures. (b) Detail near the phase transition (inclusion of boundary fermions).

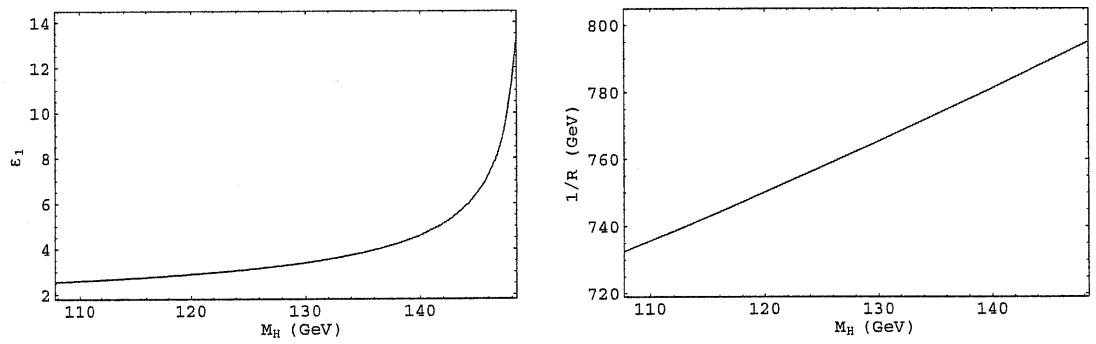

(a) (b)

Figure 5.9: (a) Value of the ε_1 coupling and (b) compactification radius, as function of the Higgs mass (high rank bulk fermions).

valid also in this case.

Theory with High-Rank Bulk Fermions

As we saw, one of the main problems of models based on gauge–Higgs unification is the predicted too low value of the Higgs mass. A possibility to solve this problem is given by the introduction of additional bulk fermions, which do not couple to the localized matter fields, in high rank representations of $SU(3)_w$ (see section 3.7.1). We consider in the following the electroweak phase transition that one obtains in a $5D$ model where, in addition to the fields introduced before, one considers a massive bulk fermion in the completely symmetric rank 8 representation of $SU(3)_w$ and singlet of $SU(3)_s$. The mass of this fermion has been fixed to $\lambda_{HR} = 2.15$. The bulk–to–boundary couplings ε_i have been fixed requiring that $m_t = 45$ GeV, with $\varepsilon_2 = 0.5\,\varepsilon_1$. The effective potential is studied

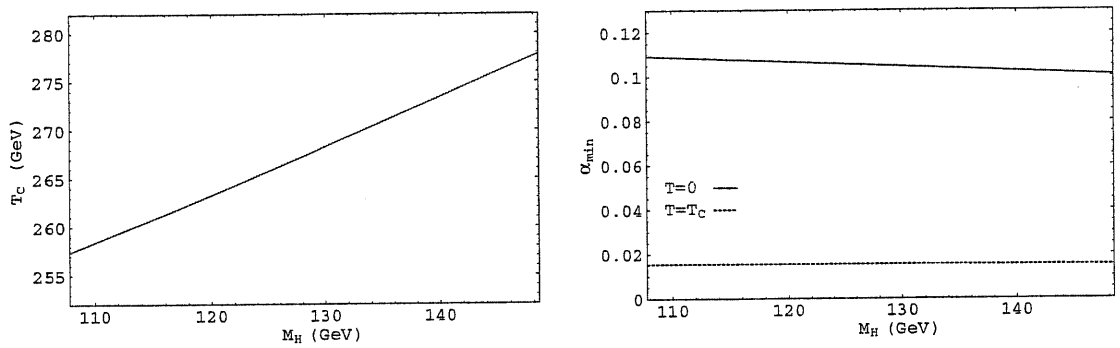

(a) (b)

Figure 5.10: (a) Critical temperature and (b) position of the minimum at $T = 0$ and at $T = T_C$, as function of the Higgs mass (high rank bulk fermions).

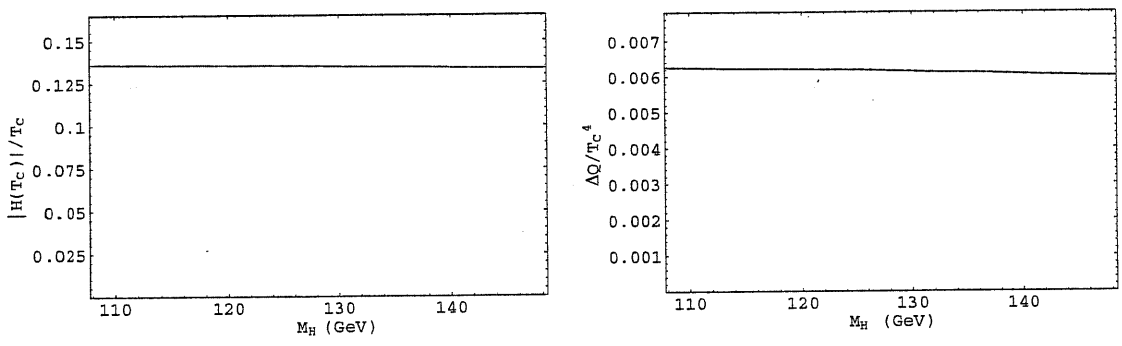

(a) (b)

Figure 5.11: (a) Phase transition strength and (b) latent heat as function of the Higgs mass (high rank bulk fermions).

for $1.6 \leq \lambda \leq 2.4$. For $\lambda > 1.79$ (which corresponds to $m_H > 125\,\mathrm{GeV}$), α_{min} is the global minimum of the potential, which turns to a local minimum for smaller values of λ. The results are summarized in figures 5.9–5.12. The Higgs mass can now reach realistic values (although the top mass is still too low). As is clear from figure 5.11 (a), a very weak first order phase transition is found in this model with $T_C \sim 1/L$.

This behaviour can be understood by means of our general analysis of section 5.1.3. The fermionic potential is dominated by the high rank fermion whose mass is fixed. Since m_H varies only with λ, the small dependence on m_H in figures 5.10 (b) and 5.11 is easily understood. The decreasing of the strength of the phase transition with the rank is clear by noting that

$$\alpha_{min}(T_C) \sim \frac{\sum_i n_i q_i^2}{\sum_i n_i q_i^4}\,, \tag{5.2.2}$$

where i runs over all the fermion components with charge q_i and multiplicity n_i, arising

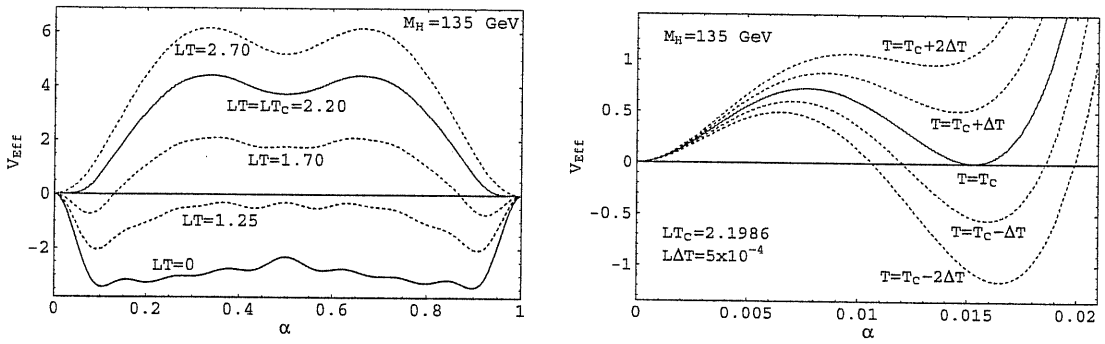

Figure 5.12: (a) Effective potential (for $m_H = 135\,\text{GeV}$) at various temperatures. (b) Detail near the phase transition. The effective potential is multiplied by 10^4 with respect to the (a) diagram (high rank bulk fermions).

from the decomposition of the rank r bulk fermion.

Fermions in too high-rank representations can not be considered, since the value of the UV cut-off Λ_w rapidly decreases as r increases, restricting the range of validity of the effective theory. No comparison with the SM is given, since for such values of the Higgs mass, perturbation theory breaks down close to the critical temperature.

Theory with Localized Gauge Kinetic Terms

As discussed in section 3.7.2, an interesting possibility that is allowed by symmetries is the introduction of localized gauge kinetic terms. These have a significant effect on the phenomenology of the model. In particular, they represent another option, in alternative to the introduction of fermions in high rank representations, to get realistic values for the Higgs mass. Interestingly enough, their presence also allow to get acceptable values for the top mass. As a drawback, they break the custodial symmetry, leading to too large deviations for the SM observables and to a small cut-off.

We introduce localized gauge kinetic terms at only one fixed point of $S^1/\mathbf{Z}_2$, since this is the most phenomenological convenient option. In the notation of section 3.7.2, we take $c_1 \equiv c = 6$ and $c_2 = 0$. The gauge contribution to the Higgs effective potential, in presence of localized kinetic terms, is reported in eq. (G.2.5). The bulk–to–boundary couplings ε_i are chosen so that the top quark mass is 110 GeV, with $\varepsilon_2 = \varepsilon_1$. The effective potential is studied for $0.8 \leq \lambda \leq 1.9$. Interestingly enough, despite the high value of the Higgs mass obtained in this case, $110 \div 170$ GeV (see figures 5.13 and 5.14), the phase transition is still of first order and is also moderately strong, with $|H(T_C)|/T_C \sim 0.7$ (see figure 5.15 (a)). Since this is of order one, it might be strong enough to avoid that sphalerons in the broken phase wash out the previously generated baryon asymmetry (see footnote 6). The

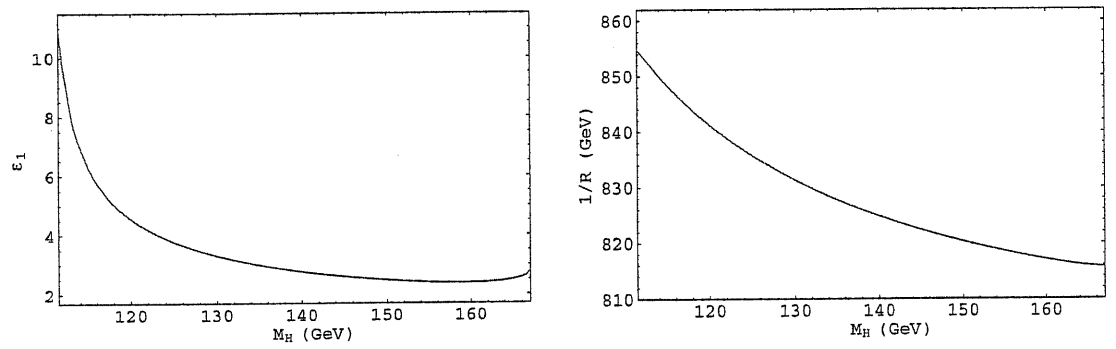

(a) (b)

Figure 5.13: (a) Value of the ε_1 coupling and (b) compactification radius as function of the Higgs mass (localized gauge kinetic terms).

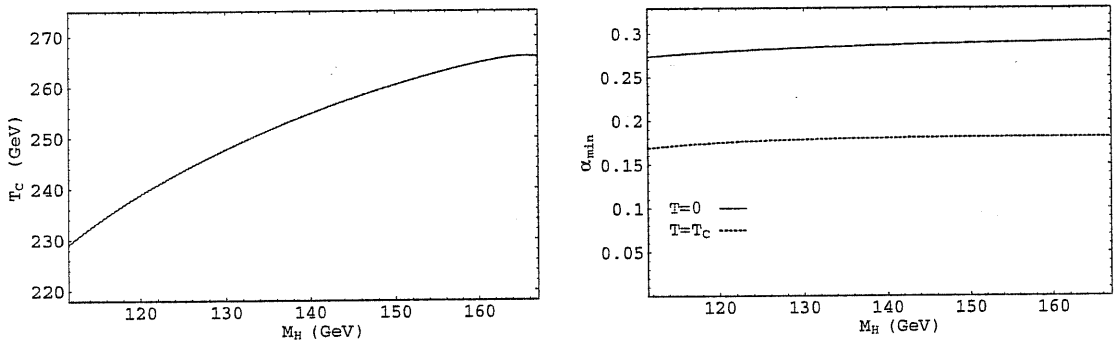

(a) (b)

Figure 5.14: (a) Critical temperature and (b) position of the minimum at $T = 0$ and at $T = T_C$, as function of the Higgs mass (localized gauge kinetic terms).

critical temperature in this model is $\sim 2/L$ (see figures 5.13 (b) and 5.14 (a)).

The behaviour of the phase transition for large values of c is analytically harder to be studied than the previous cases, since the localized gauge field contribution (G.2.5) plays a crucial role. By expanding the total gauge field contribution, it can be shown that the first two terms of the potential in an α expansion, namely the quadratic and cubic term in eq. (5.1.17), scale like $a(x) \sim 1/c$ and $b(x) \sim c^{-3/2}$. Due to the technical complexity, it is not possible to find the exact asymptotic behaviour for large c of the quartic coupling, which, however, seems to be negative as also suggested by the numerical analysis. Neglecting the quartic coupling arising from the bosonic potential, one can show that the critical temperature depends only logarithmically on c and $\alpha_{min}(T_C) \sim 1/\sqrt{c}$. Since $g_5 \sim g_4\sqrt{Lc}$, we get $H(T_C)/T_C \sim 1/c$. The numerical analysis confirms the decrease of the phase transition strength with c, but it shows a behaviour of the type $|H(T_C)|/T_C \sim$

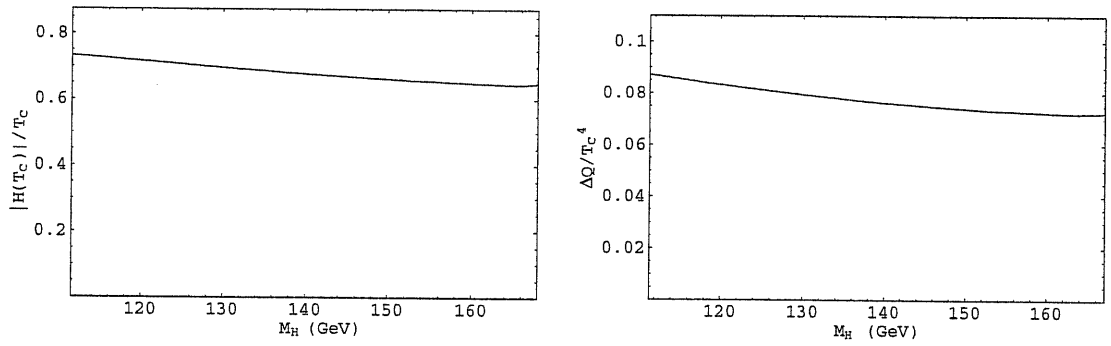

(a) (b)

Figure 5.15: (a) Phase transition strength and (b) latent heat as function of the Higgs mass (localized gauge kinetic terms).

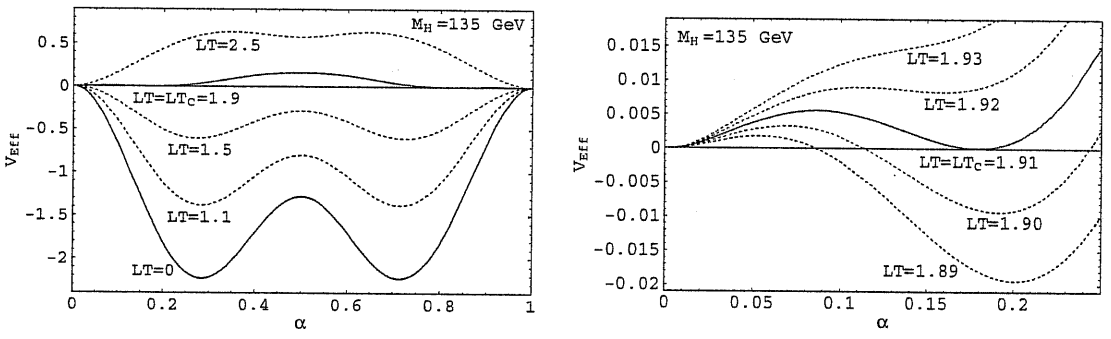

(a) (b)

Figure 5.16: (a) Effective potential (for $m_H = 135\,\text{GeV}$) at various temperatures. (b) Detail near the phase transition (localized gauge kinetic terms).

$1/c^{1/2\div 1}$, which indicates that the bosonic quartic coupling cannot be totally neglected and result in a slightly stronger first-order phase transition.

5.2.2 The EWPT in a Realistic Model

Having analyzed in detail the finite-temperature behaviour of generic GHU theories and in particular the properties of the EWPT, we want now to briefly discuss what happens in the realistic scenario presented in chapter 4.

The main properties of the finite-temperature effective potential can be straightforwardly generalized to the set-up of chapter 4 in which the $SO(4,1)/SO(3,1)$ Lorentz symmetry is broken and a $\mathbf{Z}_2$ mirror symmetry is introduced. The explicit expression of the bulk contribution to the potential can be derived from eq. (5.1.1), where one has to

replace the usual Lorentz-preserving mass tower with the modified one

$$M_n^2 = M^2 + k^2 \frac{(n + \eta/2 + q\alpha)^2}{R^2} \tag{5.2.3}$$

where $\eta = 0, 1/2$ respectively for periodic and antiperiodic fields with charge q with respect to the Higgs. As already noticed, the effect of the Lorentz-breaking parameter k is equivalent to an effective rescaling of the compactification radius $R \to R/k$. On the other hand, the determination of the boundary contribution is more involved due to the fact that fields with different Lorentz-breaking parameters are coupled to the same boundary fields. However, the finite-temperature expressions for the boundary contributions can be derived by a generalization of eqs. (4.2.8) and (4.2.9) (compare appendix G).

The properties of finiteness and gauge invariance of the finite-temperature potential are valid also in the scenario we are considering here. Moreover, the high temperature behaviour of the bosonic and fermionic contributions is unchanged with respect to the Lorentz-preserving case. This means that the gauge contribution, which scales as T at high temperature, eventually becomes more relevant than the fermionic one, which is exponentially suppressed. When this happens the symmetry-preserving phase $\alpha = 0$ becomes a minimum of the potential and an EWPT takes place.

As discussed in chapter 4, a high degree of cancellation in the quadratic term of the effective potential is needed to get acceptable values of α_{min}. This implies that the simplification and approximations, used in section 5.1.3 to derive the properties of the phase transition, are no longer valid in the present set-up. Nevertheless one can derive some properties of the EWPT by a careful analysis of the explicit form of the finite-temperature potential, as we will do in the following.

First of all, we will approximate the zero-temperature effective potential by the SM-like polynomial expression

$$V_0(\alpha) = \frac{4\pi}{g_5^2 R} m_H^2 \left(-\frac{\alpha^2}{2} + \frac{\alpha^4}{4\,\alpha_{min}^2} \right) . \tag{5.2.4}$$

This approximation seems reasonable for small values of α_{min}, however, as we will see, the knowledge of the exact form of the zero temperature potential is not necessary for the following analysis.[9]

The finite-temperature part of the effective potential is finite and can be expressed as a sum of the contributions of each $4D$ KK state as shown in appendix G (compare eq. (G.1.1)). We can obtain the whole finite-temperature potential by considering the complete spectrum of the model and not only the one related to the bulk fields. From eq. (G.1.1) it can be easily seen that the finite-temperature contribution of a state with

[9] In eq. (5.2.4) we did not include possible non-analytic terms as, for instance, $|\alpha|^3$, which, however, are not very relevant as shown by the numerical results.

mass $M \gtrsim T$ is suppressed by a factor $e^{-M/T}$. A more quantitative analysis shows that the KK states which effectively contribute are only those with $M \lesssim \pi T$.

Due to the large gap between the Higgs mass and the compactification scale, or equivalently the small value of α_{min}, needed to obtain a realistic model, it turns out that the critical temperature in this models is always of order $T_C \lesssim 0.5/L$. Given that the compactification scale is of order $1/R \sim 4.5 - 5$ TeV (see fig. 4.4), we can estimate the critical temperature to be always $T_C \lesssim 400$ GeV. As discussed in section 4.2, the lightest non-SM states in the model are charged fermions with a mass $M \sim 1.5 - 2$ TeV. States with such a mass can not give a relevant contribution to the finite temperature part of the potential, so that we can reasonably assume that the finite-temperature corrections are entirely due to the SM states.

Given the approximation in eq. (5.2.4) the whole effective potential in the model is analogous to the SM one, thus we expect a SM-like EWPT.[10] This suggests that a very weak phase transition takes place in the model for phenomenologically acceptable Higgs masses.

To get a quantitative estimate of the critical temperature, we can expand the leading finite-temperature contributions to the quadratic term of the potential as (see *e.g.* [83])

$$V_2(T,\alpha) = \frac{2m_t^2(\alpha) + 2m_W^2(\alpha) + m_Z^2(\alpha)}{8} T^2 \,. \tag{5.2.5}$$

The phase transition takes place approximately at the temperature at which the Higgs mass term vanishes, so that by a rough estimate we find $T_C \sim m_H \sim 0.2/L$. Notice that this estimate of the critical temperature justifies the initial assumption $T_C \lesssim 0.5/L$. From a more careful study of the potential one can also show that the strength of the phase transition (which we defined as $|H(T_C)|/T_C$) decreases as $1/m_H^2$.

The results of a complete numerical analysis performed in the model of [26], confirm the above predictions and give $T_C \sim (0.1 - 0.6)/L$. The phase transition strength is obtained in the range $0.01 \lesssim |H(T_C)|/T_C \lesssim 0.1$, which clearly seems too weak to open the possibility of achieving a successful baryogenesis at the EWPT.

Finally, let us comment on the possibility of studying perturbatively the EWPT when the Higgs mass has a large value. As we said before, in the SM for reasonable Higgs masses ($m_H \gtrsim m_W$) perturbativity breaks down. Lattice computations show that, instead of a weak first order phase transition as predicted perturbatively, a smooth crossover appears in the theory. Given the great similarity of the EWPT in the GHU model we considered here and in the SM, one could ask whether a similar breakdown of perturbativity happens in the $5D$ case or not. As we will discuss in the next section, models with GHU seem to be

[10] It must be noticed that, in order to obtain a finite-temperature contribution analogous to the SM one, we have to assume that the masses of the states which correspond to the SM particles have a dependence on the Higgs VEV as in the SM. This is reasonably true for small values of α_{min} as can be shown using eq. (4.2.10).

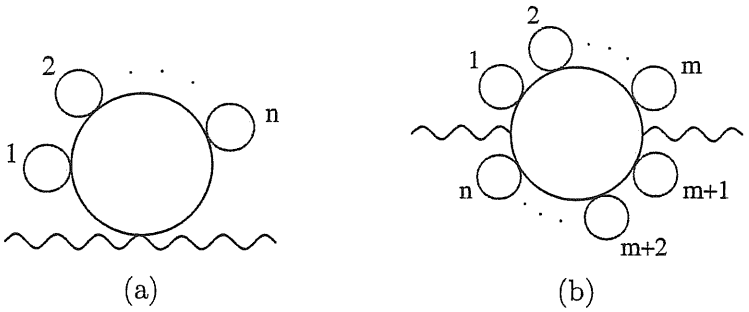

Figure 5.17: Examples of higher-loop daisy diagrams contributing to the mass of the Wilson line phase. Solid and wavy lines represent respectively the charged scalar and the Wilson line phase. For simplicity, we have omitted the arrows in the charged scalar propagators.

less sensitive to higher order corrections than usual $4D$ models and this property suggests that in the model we have considered the perturbative approach can be reliable also for realistic Higgs masses.

5.3 Estimate of Higher-Loop Corrections

The analysis performed in this chapter about the EWPT is based on the computation of a one-loop effective potential. Aim of this section is to estimate the leading higher-loop contributions and determine the range of validity of the one-loop analysis.

It is known that the most important higher-loop contributions to the effective potential in $4D$ theories generally arise from certain IR divergent diagrams, known as "daisy" or "ring" diagrams [81] (see figure 5.17). As shown in [94], the latter are all easily resummed by adding and subtracting to the Lagrangian the one-loop (thermal) mass correction for any field present in the Lagrangian. One then defines a new propagator by adding the thermal mass to the tree-level one, and consider the other (opposite) term as a one-loop mass insertion. Such procedure has been performed both at one [88] and two-loop level [89] in the SM. Interestingly enough, the two-loop improved SM effective potential turns out to give results very similar to that computed by numerical results based on lattice simulations even for values of m_H close to (but less than) m_W, in which case perturbation theory is expected to be a bad approximation.

In the following, we will give an estimate of the contribution of daisy diagrams for models where the order parameter is a Wilson line phase, as in theories with gauge–Higgs unification. For simplicity, we focus on a particularly simple model, scalar QED in 5

dimensions, compactified on a circle S^1 of length $L = 2\pi R$.[11] The Lagrangian is

$$\mathscr{L} = (D_M \Phi)^\dagger D^M \Phi - \frac{\lambda_5}{4}(\Phi^\dagger \Phi)^2 - \frac{1}{4} F_{MN} F^{MN}\,, \tag{5.3.1}$$

where Φ is a complex scalar field with periodic boundary conditions: $\Phi(2\pi R) = \Phi(0)$. Our aim is to study the effective potential for the Wilson line phase $\alpha = A_5 g_5 R$, in the approximation in which the dimensionless 4D gauge coupling $g_4 \ll \lambda$, with $\lambda = \lambda_5/L$. At one-loop order, the effective potential $V(T,\alpha)$ is given by one of the relations reported in the appendix G, eqs. (G.1.3), (G.1.5) or (G.1.6), with $d = 3$, $M = 0$, $\widetilde{\eta} = 0$ and a factor of 2 taking into account the two scalar degrees of freedom. At higher order, the leading contributions arise from the daisy diagrams drawn in figure 5.17. Since $g_4 \ll \lambda$, we can consistently neglect the daisy diagrams involving one-loop mass corrections induced by the gauge field and consider only the one arising from the quartic coupling λ (see figure 5.18).

Let us denote by I_n the $(n+1)$-loop daisy diagrams obtained by summing all possible n one-loop mass insertions at zero external $5D$ momentum and define an effective parameter $\gamma(n) = I_n/I_{n-1}$; if there exists some n for which $\gamma(n) \sim 1$ or higher, perturbation theory breaks down and all daisy diagrams must be resummed. It is not difficult to compute $\gamma(n)$ for $n \gg 1$. In this limit, one has to compute only the diagrams (b) in figure 5.17, since they have a combinatorial factor proportional to n, whereas the diagrams (a) have a constant combinatorial factor. Moreover, the n one-loop mass insertions, namely the "small" bubbles in red in figure 5.17, decouple from the computation and one has only to compute the finite "big" bubble, the one in black in figure 5.17 (b). We get

$$\gamma(n) \simeq -\left[\frac{LM_{1-loop}(T,\alpha)}{2\pi}\right]^2 \frac{\sum_{m,k}\left[(k+\alpha)^2 + (LT)^2 m^2\right]^{\frac{-2n-1}{2}}}{\sum_{m,k}\left[(k+\alpha)^2 + (LT)^2 m^2\right]^{\frac{-2n+1}{2}}}\,. \tag{5.3.2}$$

In eq. (5.3.2), $M^2_{1-loop}(T,\alpha)$ is the one-loop finite thermal mass correction for the field Φ which, for $\lambda \gg g$, is given only by the diagram in figure 5.18 and reads

$$M^2_{1-loop}(T,\alpha) = \frac{(LT)T^2\lambda}{4\pi^2} \sum_{\widetilde{k}=1}^{\infty} \sum_{\widetilde{m}=-\infty}^{\infty} \frac{\cos(2\pi\alpha\widetilde{k})}{\left[\widetilde{m}^2 + (LT)^2\widetilde{k}^2\right]^{3/2}}\,. \tag{5.3.3}$$

The mass correction (5.3.3) is defined in a regularization in which only the finite terms arising from the compactification are left, neglecting the UV divergence taken to be equal to that obtained in non-compact $5D$ space. This is technically achieved by dropping the

[11] We take S^1 and not $S^1/\mathbf{Z}_2$ as compact space because in the former case we can study an Abelian gauge field model, whereas in the latter case the $\mathbf{Z}_2$ orbifold parity forbids the presence of Abelian Wilson line phases and would thus oblige us to consider non-Abelian gauge fields.

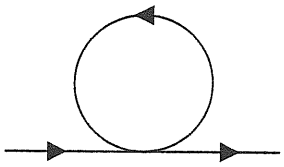

Figure 5.18: The one-loop mass correction M^2_{1-loop} to the charged scalar Φ, induced by the $\lambda(\Phi^\dagger\Phi)^2$ coupling.

Poisson resummed $\widetilde{k} = 0$ term in eq. (5.3.3). We immediately recognize from eq. (5.3.2) that for $\alpha \simeq 0$, the leading contribution to I_n is given by the KK and Matsubara zero modes $k = m = 0$, which give rise to $|\gamma(n)| \sim 1/\alpha^2$. The very low values of the Wilson line phase α are the most affected by daisy diagrams, as is obvious by the fact that IR divergences in the diagrams I_n appear precisely in the limit $\alpha \to 0$. A more transparent estimate of the relevance of resumming daisy diagrams can be performed in the two extreme limits when $LT \ll 1$ and $LT \gg 1$. In these two limits, and for sufficiently high n, $\gamma(n) \simeq \gamma$ is independent of n. For $LT \ll 1$, we can approximate the double sum in eq. (5.3.2) by taking $k = 0$ and substituting the sum over the Matsubara modes with an integral. Viceversa, in eq. (5.3.3), we can take $\widetilde{m} = 0$, retain only the sum over the modes $\widetilde{k}$ and fix $\alpha = 0$.[12] In this way, we get, for $LT \ll 1$,

$$\gamma \simeq -\frac{\lambda\zeta(3)}{4\pi^2 L^2}\frac{1}{(\frac{\alpha}{R})^2} = -\frac{M^2_{1-loop}(0,0)}{M^2_{tree}}, \tag{5.3.4}$$

where $M^2_{tree} = (\alpha/R)^2$ is the tree-level mass of the lowest KK mode for the field Φ. Daisy diagrams start to be relevant when the thermal mass is of the same order (or higher) than the tree-level one.

For very high temperatures, $LT \gg 1$, the double sums in eq. (5.3.2) are well approximated by the leading term $k = m = 0$, whereas in the mass correction (5.3.3) we can approximate the sum over $\widetilde{m}$ with an integral (setting again $\alpha = 0$) and sum over all $\widetilde{k}$. One gets, for $LT \gg 1$,

$$\gamma \simeq -\frac{\lambda LT}{48\pi^2}\frac{1}{\alpha^2}. \tag{5.3.5}$$

As eq. (5.3.4), eq. (5.3.5) can be written as the ratio of the thermal mass at high temperatures over the tree-level mass M^2_{tree}. In fact, as a rough estimate, obtained by taking $k = m = 0$ in the two double sums in eq. (5.3.2), one sees that at any temperature $\gamma \sim -M^2_{1-loop}/M^2_{tree}$.

[12] Notice that for sufficiently high values of α, $\alpha \gtrsim 0.2$, $M^2_{1-loop}(\alpha, T)$ becomes negative and a non-vanishing VEV for the field Φ is induced, which complicates the above analysis. For this reason, we analyze here only the region of low values of α, which are anyway the ones most affected by the daisy diagrams.

Once established the necessity of considering higher-loop daisy diagrams for sufficiently low values of the Wilson line phase α, let us resum all these diagrams by following the procedure outlined in ref. [94]. Since $\gamma < 0$, one can expect some cancellation between daisy diagrams of different order, resulting in a decrease of the effect of the daisy resummation procedure. This is indeed what happens, as we will see. As briefly discussed before, along the lines of ref. [94], the resulting one-loop improved effective potential $V_{imp}(T,\alpha)$ is obtained by one of the relations reported in appendix G, eqs. (G.1.3), (G.1.5) or (G.1.6), but by taking $M = M_{1-loop}(T,0)$ instead of $M = 0$. From eq.(G.1.6), for instance, one gets

$$V_{imp}(T,\alpha) = -\frac{4LT^5}{(2\pi)^{5/2}} \sum_{\widetilde{k}=1}^{\infty} \sum_{\widetilde{m}=-\infty}^{\infty} \frac{\cos(2\pi\widetilde{k}\alpha)}{\left[\widetilde{m}^2 + (LT\widetilde{k})^2\right]^{\frac{5}{2}}} B_{5/2}\left(\frac{M_{1-loop}(T,0)}{T}\sqrt{\widetilde{m}^2 + (LT\widetilde{k})^2}\right). \tag{5.3.6}$$

A good estimate of the higher-order daisy contributions at any temperature is performed by comparing the Wilson line thermal mass obtained from $V_{imp}(T,\alpha)$ with that derived from $V(T,\alpha)$. We denote them respectively $M^2_{imp}(T,\alpha)$ and $M^2(T,\alpha)$ (not to be confused with $M^2_{1-loop}(T,\alpha)$ in eq. (5.3.3), which is the thermal mass of the field Φ). We plot in figure 5.19 (a) $M^2_{imp}(T,\alpha)$ and $M^2(T,\alpha)$ as function of α for $\lambda \sim 1$ and for $LT \sim 1$. As can be seen, the two behaviours are very similar, with deviations which are at most of about 10 % for $\alpha = 0$. As expected, the maximal deviation is found for values of $\alpha \simeq 0$. We find that at low temperatures ($LT \sim 1/10$), the maximal deviations (at $\alpha = 0$) are of order of a few %, whereas at high temperatures ($LT \sim 10$) they are of order 30 %. Notice that, although this model does not have a phase transition in the Wilson line parameter, $LT \sim 1$ is in the range of the critical temperature where the phase transition occurs in such kind of models, as we have explicitly seen in the previous sections. From our analysis we thus find that the leading higher-loop daisy diagrams give small corrections to the effective potential. This can be taken as an evidence of the fact that perturbation theory in our $5D$ models is still valid at $T \sim T_C$. On the contrary, for very high temperatures ($LT \gg 10$), the one-loop improved potential starts to significantly differ from the naïve one-loop potential. This is particularly evident from the equivalent expression of the potential given in eq. (G.1.3). At very high temperatures, the naïve one-loop potential is entirely dominated by the Matsubara zero mode $m = 0$, proportional to T, whereas the one-loop improved potential, due to the non-vanishing argument in the function B_2 appearing in eq. (G.1.3), is exponentially suppressed in $LM \simeq \sqrt{LT}$. The discrepancy that one finds between the two potentials starts however to be very large for temperatures which are well above the cut-off scale Λ. As discussed in footnote 4, it is meaningless to consider such range of temperatures in an effective field theory approach.

It is useful to compare the contribution of daisy diagrams for the $5D$ $U(1)$ model above with that of the $4D$ model arising by trivial dimensional reduction, where all the massive KK modes are neglected. By denoting with a and ϕ the properly normalized zero mode

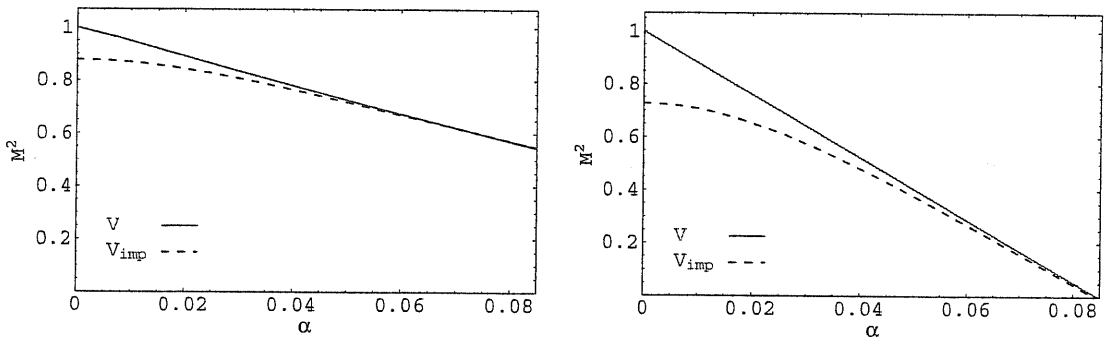

Figure 5.19: (a) Thermal masses in $5D$, from the one-loop naïve potential (red solid line) and the one-loop improved one (blue dashed line). (b) Thermal masses in the reduced $4D$ model, from the one-loop naïve potential (red solid line) and the one-loop improved one (blue dashed line). In both cases $LT \sim 1$, $\lambda \sim 1$ and the normalization is such that $M^2(T, \alpha = 0) = 1$.

components of A_5 and Φ, one gets the following $4D$ Lagrangian:

$$\mathcal{L} = (D_\mu \phi)^\dagger D^\mu \phi + \frac{1}{2}(\partial_\mu a)(\partial^\mu a) - g^2 a^2 \phi^\dagger \phi - \frac{\lambda}{4}(\phi^\dagger \phi)^2 - \frac{1}{4} F_{\mu\nu} F^{\mu\nu} . \tag{5.3.7}$$

The trivial dimensional reduction spoils the 5D Wilson line nature of α, breaking the shift symmetry $\alpha \to \alpha + 1$. Let us study the effective potential $V(\alpha)$ for the VEV of the field a ($\langle a \rangle = \alpha/(gR)$). The contribution of Φ to $V(\alpha)$ is the standard one for a massive scalar field at finite temperature [81]. One has, neglecting terms independent of α,

$$V(T, \alpha) = V(0, \alpha) + \frac{T^4}{\pi^2} \int_0^\infty dx\, x^2 \log \left[1 - e^{-\sqrt{x^2 + (\alpha/RT)^2}} \right] . \tag{5.3.8}$$

In eq. (5.3.8), $V(0, \alpha)$ is the zero temperature effective potential, which is UV divergent. In the $\overline{\text{MS}}$ regularization scheme, it reads

$$V(0, \alpha) = \frac{\alpha^4 \pi^2}{2L^4} \left[\log \left(\frac{\alpha^2}{R^2 \mu^2} \right) - \frac{3}{2} \right] , \tag{5.3.9}$$

where μ is the renormalization scale.

The one-loop improved potential is obtained by substituting in eq. (5.3.8) the tree-level mass with the one-loop improved one, computed in the $4D$ reduced model. For $g \ll \lambda$, this simply amounts to shifting $(\alpha/R)^2 \to (\alpha/R)^2 + \lambda T^2/12$. We plot the thermal masses obtained by the one-loop naïve and improved potentials in figure 5.19 (b) for $LT \sim 1$, $\lambda \sim 1$ and setting $\mu = 1/R$, which is the scale above which our effective theory breaks down. The comparison between figures 5.19 (a) and (b) clearly indicates that the $5D$ model is less sensitive to higher-loop effects than the 4D reduced theory, although both models are not much sensitive to the daisy resummation procedure for $\alpha \gtrsim 0.05$.

Let us now comment on the daisy diagram contributions to the Higgs effective potential in $5D$ gauge–Higgs unification models where no fundamental scalars are present. Fermion loops do not give rise to IR divergences since the Matsubara modes are half integers and there is always an effective non-vanishing thermal mass. Moreover, chiral symmetry implies that fermion mass corrections are always proportional to their tree-level mass and thus they vanish in the IR limit of vanishing mass. There is then no need of resumming daisy diagrams for fermions. Gauge invariance forbids the appearance of any thermal mass correction to the transverse polarization of gauge bosons which are also unaffected by the daisy resummation procedure. The Higgs field itself, H, does not have tree-level self-interactions and hence does not give any higher-loop contribution to its potential in the daisy approximation. Finally, we are left with the longitudinal components A_0 of the gauge fields, that acquire a non-vanishing thermal mass correction (Debye mass); the corresponding contributions to the Higgs potential have to be daisy-resummed. We expect that the latter will be of the same order of magnitude as the one we have estimated in our simple $5D$ model defined by the Lagrangian (5.3.1).

As it happens in the SM, we might expect that the resummation of daisy diagrams in our $5D$ model leads to a change in the cubic term of the approximate Wilson line potential (5.1.17). However, since transverse gauge bosons are not affected by daisy diagrams, this shift would only lead to a slight change of the potential, which will still predict a first-order phase transition.

As final remark, note that the absence of a tree-level potential in Wilson line based models permits to evade Weinberg's rough argument for the necessity of the breakdown of perturbation theory around the phase transition [95]: since the tree-level potential appearing in generic quantum field theories is temperature independent, perturbative corrections (which are instead temperature-dependent) cannot give rise to a drastic change in the potential (as needed for a phase transition), unless perturbation theory breaks down.[13]

[13]The possibility that perturbation theory does not necessarily break down in our $5D$ model is also suggested by the value of the critical temperature $T_C \sim 1/L$, which is independent on any coupling constant. This has to be contrasted, for instance, with the SM case, in which roughly $T_C \sim \sqrt{-\mu^2/\lambda}$, where μ^2 is the Higgs mass term.

Conclusions

The main subject of this thesis has been a study of extra dimensional theories defined on a compact $5D$ space from both a theoretical and a phenomenological point of view. A first, more technical, aspect of our discussion has been the presentation of two different approaches by which one can describe and analyze models with extra dimensions, namely the standard KK decomposition and the recently proposed holographic approach. The latter is an alternative way of deriving an effective description of a $5D$ theory compactified on a generic warped interval and presents many advantages from a computational point of view. At the same time, it proves also very useful to study some rather theoretical aspects of extra dimensional theories. In particular we showed how, within the holographic perspective, one can easily study the effects of the introduction of a CS term into a $5D$ gauge action. More precisely, we proved that the CS term determines the appearance of an anomaly in the $4D$ low energy effective action.

Leaving aside the several applications of the holographic approach as a mere computational tool, it is worth mentioning a particularly interesting case, namely the GHU scenario in the RS set-up, in which the holographic description can offer an insight on the properties of an extra dimensional theory. This kind of $5D$ models, thanks to a (modified) form of the AdS/CFT correspondence, can be equivalently described by a $4D$ dual theory in which the fields of a weakly coupled sector act as sources coupled to the operators coming from a strongly coupled (nearly conformal) sector. In particular the Higgs field, which arises form the gauge field components in the $5D$ picture, is reinterpreted as a Goldstone boson related to a spontaneous breaking of a global symmetry in the strong sector of the $4D$ dual theory. Applying the holographic approach to the $5D$ GHU model, one naturally recovers all these features, and the holographic effective action is actually a description of the $4D$ dual model in which the holographic fields exactly correspond to the $4D$ sources. Moreover, as we discussed in detail in chapter 2, the holographic description naturally includes a Goldstone field, related to the gauge symmetry breaking at the IR brane, which corresponds to the Higgs.

In the second part of this thesis, we carried on the study of extra dimensional theories form a phenomenological point of view. We showed how one can solve the main problems of GHU models compactified on a flat $S^1/\mathbf{Z}_2$ orbifold by the introduction of two simple

ingredients. The first one is a breaking of the $SO(4,1)/SO(3,1)$ Lorentz symmetry along the extra dimension, which allows to obtain larger fermion Yukawa couplings, thus curing the problem of the smallness of the top and Higgs masses. The second ingredient is a $\mathbf{Z}_2$ symmetry, the mirror symmetry, which acts on a subset of the bulk degrees of freedom, giving rise to couples of periodic and antiperiodic fields. This symmetry proves essential to generate a sizable gap between the EW and the compactification scale. As a by-product the mirror symmetry also implies the existence of a stable KK particle which has been shown to be a viable DM candidate.

By an accurate analysis of the constraints deriving from the EW precision measurements, we showed that the model is compatible with the experimental results if a moderate amount of fine-tuning (of the order of a few %) is allowed. Such fine-tuning is certainly acceptable, but it is nevertheless still too high to claim that the model represents a complete solution to the Little Hierarchy Problem. However, it should be emphasized that the required fine-tuning is of the same order of that found in the MSSM. From a combined fit one can also derive a lower bound on the compactification scale $1/R \gtrsim 4$ TeV with allowed Higgs masses up to 600 GeV. However, such high values of the Higgs mass are never reached in the set-up studied in chapter 4, where one actually finds $100 \text{ GeV} \leq m_H \leq 200$ GeV.

Finally, we discussed the properties of GHU models at finite temperature. We showed that the one-loop effective potential is gauge invariant, contrary to ordinary potentials in non-Abelian gauge theories in $4D$, including the SM. We also pointed out that the non-local nature of the potential, which determines its finiteness at zero temperature, is responsible for its mild dependence on quantum corrections at finite temperature. From a more phenomenological point of view, we showed that a phase transition, typically of first order, occurs in GHU models at a temperature of order $1/(2\pi R)$. Moreover, we studied in detail the properties of the EWPT in the realistic model of chapter 4. We found that the transition is predicted to be of first order although very weak, so that baryogenesis at the EWPT seems not possible in this scenario.

In the view of the success of the GHU model we presented, it would be clearly worth studying some aspects of this model which have not been explored thus far. An interesting issue would be the introduction of a realistic flavour structure. We discussed a simple implementation of flavour in section 3.3.2, however a far more detailed study is necessary to build a completely realistic scenario. Another non-secondary aspect would be the study of possible experimental signatures, in particular in collider Physics, which could discriminate our scenario form the several other possibilities.

Acknowledgements

First of all I would like to thank Prof. Marco Serone for his continuous support and his invaluable guidance during my studies and my research in the last four years. I am also very grateful to Andrea Wulzer for his help and for the countless interesting discussions about Physics (and various other subjects) I had with him.

I want also to remember all my friends at SISSA, with whom I spent a large part of my time in Trieste, and in particular Giuseppe Milanesi, Alessio Provenza, Marco Regis, Alberto Salvio and Roberto Valandro.

A special thank to my parents and my sister for their support and encouragement during my university years in Pisa and my PhD studies in Trieste.

Appendix A

The Holographic Gauge-Fixing

In this appendix we discuss a more formal derivation of the gauge-fixing procedure used to obtain an holographic description of a gauge theory in chapter 2. In particular, the procedure described in the following is necessary when one considers a gauge theory with a CS term which breaks the G invariance of the theory at the IR boundary (see section 2.6).

Let us start from the holographic partition function (2.2.3), we want to gauge-fix its local $\mathcal{G}_B$ invariance. Looking at eq. (2.2.10) we see that it can not be used to fix the gauge as the g elements one integrates over do not reduce to H at the IR. It is then convenient to rewrite the integral on the group isolating the integral on the IR variables, and again split the latter in integrals over H and G/H.[1] Be F any functional on the local group, we have

$$\begin{aligned}\int \mathcal{D}g(x,z)_{\widehat{g}=\mathbb{1}} F[g] &= \int \mathcal{D}\widetilde{g}(x) \int \mathcal{D}g(x,z)_{\widehat{g}=\mathbb{1},\, g_{IR}=\widetilde{g}} F[g] \\ &= \int_{G/H} \mathcal{D}\widetilde{\gamma}(x) \int_H \mathcal{D}\widetilde{h}(x) \int \mathcal{D}g(x,z)_{\widehat{g}=\mathbb{1},\, g_{IR}=\widetilde{\gamma}\circ\widetilde{h}} F[g]\,, \end{aligned} \tag{A.0.1}$$

where $\widetilde{\gamma}$ is an element the right G/H coset, $\widetilde{h} \in H$ and the left Haar measure is understood in all group integrals. We can now remove the G/H component of g_{IR} by performing a change of variable in the g integral with a $5D$ transformation $\widetilde{\Lambda}$ such that $\widetilde{\Lambda}(z_{\text{UV}}) = \mathbb{1}$ and $\widetilde{\Lambda}(z_{\text{IR}}) = \widetilde{\gamma}$.[2] After the change of variable, $g_{IR} = \widetilde{h}$ belongs to H so that when putting together the $\mathcal{D}\widetilde{h}(x)$ and $\mathcal{D}g(x,z)$ integrals we obtain an integral over the bulk gauge group

[1] If G is a compact Lie group and H a closed subgroup, the group integral can be split as [96]

$$\int_G dg\, f[g] = \int_{G/H} d\gamma \Big\{ \int_H dh\, f[\gamma \circ h] \Big\}.$$

where the appropriate left invariant Haar measures are understood in all integrals.

[2] We are assuming that $\pi_4(G/H)$ is trivial (see footnote 5 in chapter 2) so that the existence of $\widetilde{\Lambda}$ is guaranteed.

$\mathcal{G}_B$, *i.e.* with the correct restriction at the IR. Then, we have

$$\int \mathcal{D}g(x,z)_{\widehat{g}=\mathbb{1}} F[g] = \int_{G/H} \mathcal{D}\widetilde{\gamma}(x) \int_{\mathcal{G}_B} \mathcal{D}g(x,z)_{\widehat{g}=\mathbb{1}} F[\widetilde{\Lambda} \circ g] \,. \tag{A.0.2}$$

Note that $\widetilde{\gamma}(x)$ can be identified with the Goldstone boson Σ we defined in sect. 2.2.1, so that we will change name to it from now on.[3]

Let us now multiply the partition function (2.2.3) by "1" written as in eq. (2.2.10) and use eq. (A.0.2) to rewrite the group integral. Changing variables in the gauge field integral we get

$$Z[B_\mu] = \int_{\mathcal{G}_B} \mathcal{D}g \int \mathcal{D}\Sigma \int \mathcal{D}A_\mu(x,z)_{\widehat{A}_\mu = B_\mu} \exp\left[iS\left[\left(A^{(\widetilde{\Lambda}^{-1})}\right)^{(g^{-1})}\right]\right], \tag{A.0.3}$$

where we used the delta function to perform the A_z integral, so that in the above equation A indicates a $5D$ vector with zero fifth component. Moreover, we neglected the determinant of eq. (2.2.10) and did not specify the IR boundary condition of the $\mathcal{D}A_\mu$ integral. After the $\widetilde{\Lambda}$ transformation those are given by eq. (2.2.8). Our action, including the CS term, is by definition invariant under the elements of $\mathcal{G}_B$ since they reduce to H at the IR. The $\mathcal{G}_B$ integral then factorizes out in eq. (A.0.3), we drop it and finally obtain the gauge-fixed partition function. Ordinary IR boundary conditions (2.2.2) are restored by changing variable in the $\mathcal{D}A_\mu$ integral with a $5D$ gauge transformation of parameter $\Sigma(x)$. The result is reported in eq. (2.6.8).

In the case of AdS/QCD a slight change in the above derivation is needed in order to match the standard parametrization of the Goldstone boson fields. The analogue of eq. (A.0.1) reads now

$$\begin{aligned}
&\int \mathcal{D}g_{\mathrm{R}}(x,z)\mathcal{D}g_{\mathrm{L}}(x,z)F[g_{\mathrm{L}},g_{\mathrm{R}}] \\
&= \int \mathcal{D}\widetilde{g}_{\mathrm{R}}(x)\mathcal{D}\widetilde{g}_{\mathrm{L}}(x) \int \mathcal{D}g_{\mathrm{R}}(x,z)_{g_{\mathrm{R}}(z_{\mathrm{IR}})=\widetilde{g}_{\mathrm{R}}} \mathcal{D}g_{\mathrm{L}}(x,z)_{g_{\mathrm{L}}(z_{\mathrm{IR}})=\widetilde{g}_{\mathrm{L}}} F[g_{\mathrm{L}},g_{\mathrm{R}}] \\
&= \int \mathcal{D}\widetilde{g}_{\mathrm{R}}(x)\mathcal{D}\widetilde{\gamma}(x) \int \mathcal{D}g_{\mathrm{R}}(x,z)_{g_{\mathrm{R}}(z_{\mathrm{IR}})=\widetilde{g}_{\mathrm{R}}} \mathcal{D}g_{\mathrm{L}}(x,z)_{g_{\mathrm{L}}(z_{\mathrm{IR}})=\widetilde{\gamma}\circ\widetilde{g}_{\mathrm{R}}} F[g_{\mathrm{L}},g_{\mathrm{R}}] \,,
\end{aligned} \tag{A.0.4}$$

where we performed a change of variable $\widetilde{g}_{\mathrm{L}}(x) \to \widetilde{\gamma} \circ \widetilde{g}_{\mathrm{R}}(x)$ with $\widetilde{\gamma} \in \Gamma$ and omitted for shortness the UV restriction $\widehat{g}_{\mathrm{L,R}} = \mathbb{1}$. Changing variables in the g_{L} integral by a $5D$ transformation $\widetilde{\Lambda}$ such that $\widetilde{\Lambda}(z_{\mathrm{IR}}) = \widetilde{\gamma}$ and $\widetilde{\Lambda}(z_{\mathrm{UV}}) = \mathbb{1}$ we get

$$\begin{aligned}
&\int \mathcal{D}g_{\mathrm{R}}(x,z)_{\widehat{g}_{\mathrm{R}}=\mathbb{1}} \mathcal{D}g_{\mathrm{L}}(x,z)_{\widehat{g}_{\mathrm{L}}=\mathbb{1}} F[g_{\mathrm{L}},g_{\mathrm{R}}] \\
&= \int \mathcal{D}\widetilde{\gamma}(x) \int \mathcal{D}\widetilde{g}_{\mathrm{R}}(x) \int \mathcal{D}g_{\mathrm{R}}(x,z)_{g_{\mathrm{R}}(z_{\mathrm{IR}})=\widetilde{g}_{\mathrm{R}}} \mathcal{D}g_{\mathrm{L}}(x,z)_{g_{\mathrm{L}}(z_{\mathrm{IR}})=\widetilde{g}_{\mathrm{R}}} F[\widetilde{\Lambda} \circ g_{\mathrm{L}},\, g_{\mathrm{R}}] \,.
\end{aligned} \tag{A.0.5}$$

[3] To ensure G-invariance, the measure $\mathcal{D}\Sigma$ for the Goldstone bosons must be the left invariant Haar measure of G/H, and this is exactly what we will find. The explicit form of $\mathcal{D}\Sigma$ is in general non-trivial, and could be relevant for particular applications. A brief discussion of this subject and references to the original literature can be found in [97].

Putting the $\widetilde{g}_{\mathrm{R}}$ and $g_{\mathrm{R,L}}$ integrals together we obtain an integral over the $\mathcal{G}_B$ bulk gauge group. The matrix $\widetilde{\gamma} \in \Gamma$ can be identified with the Goldstone boson matrix U^{-1} of $\chi\mathbf{PT}$. We can now follow the procedure used in the general case and we get the same as eq. (2.6.8) in which Λ is now given by eq. (2.6.21).

Appendix B

Holography with Boundary Terms

In this appendix we will briefly discuss how to derive the holographic effective action in the presence of localized terms at the IR and UV branes. Such terms appear in many interesting situations. In the presence of bulk scalars in AdS_5, for instance, localized masses are needed in order to have a zero mode. Furthermore, boundary terms for fermions or gauge fields as well as fields localized on the UV boundary are often present in realistic models both in flat [15, 27] and in warped space [19, 20, 21].

The inclusion of localized IR terms in the holographic procedure is simply accomplished by modifying the IR boundary conditions.[1] The latter are indeed modified by the boundary terms and are derived requiring the variation of the action at the IR boundary to vanish. Once the bulk equations of motion are solved with these new IR conditions, the tree-level effective action can be computed as in section 2.3 by plugging the solutions back into the $5D$ action.

The treatment of UV localized terms is even more straightforward. These terms are functions of the field values at the UV boundary, thus they are functions of the holographic fields and can be directly inserted into the effective action. This is clearly true for gauge and scalar fields, indeed in such cases one always chooses the boundary values of the non-vanishing fields at the UV boundary as holographic degrees of freedom and a localized term can be simply translated into a term of the effective action

$$S_{loc}^{UV} = \int d^4x \int dz\ \delta(z - z_{\rm UV}) \mathscr{L}(A_\mu, \Phi) \to S_h = \int d^4x\ \mathscr{L}(B_\mu, \phi)\,, \qquad \text{(B.0.1)}$$

where B_μ and ϕ are the sources corresponding respectively to the gauge field A_μ and to the scalars Φ.

A slightly different approach must be used when localized UV terms for the fermions are present. In this case left- and right-handed components are related by the bulk equa-

[1] Notice that the inclusion of IR boundary terms may induce a breaking of G/H at that boundary directly into the action and not only through the boundary conditions. In such case the correct gauge-fixing procedure is the one described in appendix A.

tions of motion and only one of the two can be chosen as holographic degree of freedom. Usually one chooses holographic fields of only one chirality, say left, independently of the actual UV boundary conditions of the fields. In this case, as explained in section 2.3.3, one introduces some Lagrange multipliers in the effective action in order to set to zero the components with Dirichlet UV boundary conditions.

In the presence of localized terms for a component which is non-vanishing at the UV boundary two possibilities can arise. As a first case, if that component has been chosen as a holographic degree of freedom, the localized terms can be directly included in the effective action as we did for the bosonic fields

$$S_{loc}^{UV} = \int d^4x \int dz\ \delta(z - z_{\rm UV}) \mathscr{L}(\psi_L) \to S_h = \int d^4x\ \mathscr{L}(\chi_L)\,, \tag{B.0.2}$$

where χ_L is the source related to ψ_L. Otherwise, if the boundary term is a function of a component which is not present among the holographic fields, one can include it into the effective action using the corresponding Lagrange multiplier (see [37] for a more detailed discussion)

$$S_{loc}^{UV} = \int d^4x \int dz\ \delta(z - z_{\rm UV}) \mathscr{L}(\psi_R) \to S_h = \int d^4x\ \mathscr{L}(\lambda_R)\,, \tag{B.0.3}$$

where λ_R is the Lagrange multiplier associated to ψ_R.

Another situation which can be easily handled within the holographic procedure is when localized fields at the UV boundary are coupled with bulk fields. The action for the localized fields can be directly introduced into the effective action once their couplings with the bulk fields are rewritten in terms of the sources (or, if necessary, in terms of the Lagrange multipliers).

B.1 Effective Action for Scalars with Localized Mass Terms

To clarify the treatment of boundary terms within the holographic procedure, let us derive the effective action for a bulk scalar field Φ, in a certain representation of the bulk group G, with localized mass terms. The bulk action is given by

$$S_5 = \frac{1}{g_5^2} \int d^4x \int_{z_{\rm UV}}^{z_{\rm IR}} dz\ \sqrt{g} \left[\frac{1}{2} D_M \Phi^\dagger D^M \Phi - \frac{1}{2} m_\phi^2 \Phi^\dagger \Phi \right]. \tag{B.1.1}$$

For the components which are non-vanishing at the boundaries we also add localized mass terms

$$S_{loc} = \frac{1}{2g_5^2} \int d^4x \int_{z_{\rm UV}}^{z_{\rm IR}} dz\, a^4(z) \left\{ \delta(z - z_{\rm IR}) \sum_a b_{\rm IR}^a \Phi^{a\dagger} \Phi^a - \delta(z - z_{\rm UV}) \sum_{a'} b_{\rm UV}^{a'} \Phi^{a'\dagger} \Phi^{a'} \right\}, \tag{B.1.2}$$

where the sum indices a (a') run over the components which are non-vanishing at the IR (UV) boundary.

The holographic procedure, in analogy with the case of gauge and fermion fields (compare eq. (2.3.21)), determines a relation between the UV value of the bulk fields and the sources

$$\widehat{\Phi}^A(x) = (\phi^{(\Sigma_s^{-1})})^A(x)\,, \tag{B.1.3}$$

where ϕ represents the dynamical sources on the UV boundary, and Σ_s is the Goldstone boson matrix in the appropriate G representation. To compute the quadratic effective action we must solve the linearized bulk EOM's (see eq. (C.3.3)) and express the solutions as functions of the values of the fields at the UV boundary

$$\Phi^A(p,z) = \widehat{\Phi}^A(p) f_s^A(p^2,z)\,, \tag{B.1.4}$$

with $f_s^A(p^2, z_{\rm UV}) = 1$. The IR boundary conditions induced by the boundary terms are

$$\begin{cases} [\partial_z \Phi^a(p,z) - a(z) b^a_{\rm IR} \Phi^a(p,z)]|_{z=z_{\rm IR}} = 0\,, \\ \Phi^{\widehat{a}}(p, z_{\rm IR}) = 0\,. \end{cases} \tag{B.1.5}$$

Substituting the solutions into the action and using eq. (B.1.3) we find the tree-level holographic action

$$S_h = \frac{1}{2g_5^2}\int d^4x \sum_A \left(\phi^\dagger \Sigma_s\right)^A \Pi_s^A(-\partial^2) \left(\Sigma_s^\dagger \phi\right)^A - \frac{1}{2g_5^2}\int d^4x \sum_a b^a_{\rm UV} \phi^{a\dagger}\phi^a\,, \tag{B.1.6}$$

where $\Pi_s^A(p^2) = \partial_z f_s^A(p^2,z)|_{z=z_{\rm UV}}$.

The computation of the contribution to the one-loop effective potential coming from scalar fields is similar to the one described for gauge bosons and fermions in section 2.4, thus we will briefly report the results. The quadratic effective action for a scalar field, in the presence of a background $\overline{\Sigma}$ for the Goldstone bosons, can be written as

$$S_h = \frac{1}{g_5^2}\int d^4x \sum_{a,b} \phi^{a\,\dagger} \Pi_s^{a,b}(\overline{\Sigma})\, \phi^b\,, \tag{B.1.7}$$

where the sum is over the dynamical fields. The scalar contribution to the one-loop effective potential is

$$V_s(\overline{\Sigma}) = \int \frac{d^4p_E}{(2\pi)^4} \log\left[\mathrm{Det}\left(\Pi_s(\overline{\Sigma})\right)\right]\,, \tag{B.1.8}$$

where the momentum has been rotated into the Euclidean space.

Appendix C

Bulk Wave Functions

In this appendix we report the form of the solutions of the bulk EOM's, which are needed to compute the holographic action and the effective potential. We derive the wave functions for gauge fields, fermions and scalars in the AdS_5 and flat space cases. For gauge fields and fermions we consider an action without localized terms. In the case of scalars, as customary, we include also the boundary mass terms which are needed to obtain $4D$ zero modes in the AdS_5 case.

C.1 Gauge Fields

We consider a gauge theory with gauge group G broken to a subgroup H at the IR boundary. We will denote by t^a the unbroken generators, namely those in H, and by $t^{\widehat{a}}$ the broken generators, namely those in G/H. The $5D$ action in the gauge $A_z = 0$ is given by

$$S_B = \frac{1}{g_5^2}\int d^4x \int_{z_{\rm UV}}^{z_{\rm IR}} dz\ a(z)\ {\rm Tr}\left[-\frac{1}{2}F_{\mu\nu}F^{\mu\nu} + \partial_z A_\mu \partial_z A^\mu\right]. \tag{C.1.1}$$

The bulk EOM's are

$$\partial_\mu \partial^\mu A^A_{t,\nu} - \frac{1}{a(z)}\partial_z(a(z)\partial_z)A^A_{t,\nu} = 0\,, \qquad -\frac{1}{a(z)}\partial_z(a(z)\partial_z)A^A_{l,\nu} = 0\,, \tag{C.1.2}$$

where $A^\mu_{t,l}$ are, respectively, the transverse and longitudinal components. The IR boundary conditions are

$$\begin{cases} \partial_z A^a_{t,l\,\nu}\Big|_{z=z_{\rm IR}} = 0\,, \\ A^{\widehat{a}}_{t,l\,\nu}\Big|_{z=z_{\rm IR}} = 0\,. \end{cases} \tag{C.1.3}$$

In the following we will denote generically by A^+ and A^- any field corresponding respectively to the unbroken subgroup H or to the broken generators in G/H.

Using the definitions in eq. (2.3.13) and in eq. (2.3.15) in the AdS_5 case ($a(z) = L/z$) we find

$$p^2 F^{\pm}(p,z) + z\partial_z \left(\frac{1}{z}\partial_z\right) F^{\pm}(p,z) = 0\,, \tag{C.1.4}$$

with the IR boundary conditions

$$\begin{cases} \partial_z F^{+}(p,z)|_{z=z_{\rm IR}} = 0\,, \\ F^{-}(p,z)|_{z=z_{\rm IR}} = 0\,. \end{cases} \tag{C.1.5}$$

At the UV boundary we must impose

$$F^{\pm}(p,z_{\rm UV}) = 1\,. \tag{C.1.6}$$

The general solution of eq. (C.1.4) is

$$F^{\pm}(p,z) = b\, z(J_1(pz) + c\, Y_1(pz))\,. \tag{C.1.7}$$

Imposing the boundary conditions we get

$$F^{\pm}(p,z) = \frac{h_{\pm}(p,z)}{h_{\pm}(p,z_{\rm UV})}\,, \tag{C.1.8}$$

with

$$\begin{cases} h_{+}(p,z) = z\left(Y_0(pz_{\rm IR})J_1(pz) - J_0(pz_{\rm IR})Y_1(pz)\right)\,, \\ h_{-}(p,z) = z\left(Y_1(pz_{\rm IR})J_1(pz) - J_1(pz_{\rm IR})Y_1(pz)\right)\,. \end{cases} \tag{C.1.9}$$

The derivatives of $h_{\pm}$ with respect to z are

$$\begin{cases} h'_{+}(p,z) = pz\left(Y_0(pz_{\rm IR})J_0(pz) - J_0(pz_{\rm IR})Y_0(pz)\right)\,, \\ h'_{-}(p,z) = pz\left(Y_1(pz_{\rm IR})J_0(pz) - J_1(pz_{\rm IR})Y_0(pz)\right)\,, \end{cases} \tag{C.1.10}$$

so that

$$\Pi_t^{\pm} = \frac{h'_{\pm}(p,z_{\rm UV})}{h_{\pm}(p,z_{\rm UV})}\,, \tag{C.1.11}$$

A simple relation links Π_t^A to Π_t^0 and Π_t^1:

$$\Pi_t^{\pm} = \Pi_t^0 \pm \Pi_t^1\,. \tag{C.1.12}$$

For a theory compactified on a flat space ($a(z) = 1$, $z_{\rm UV} = 0$ and $z_{\rm IR} = \pi R$), the definitions in eqs. (C.1.8), (C.1.11) and (C.1.12) remain valid and $h_{\pm}$ are given by

$$\begin{cases} h_{+}(p,z) = \cos(p(\pi R - z))\,, \\ h_{-}(p,z) = \sin(p(\pi R - z))\,. \end{cases} \tag{C.1.13}$$

C.2 Fermions

We consider a bulk fermion Ψ whose action is given in eq. (1.3.3). The bulk equations of motion are (see eq. (1.3.5))

$$\left[\partial_z + 2\frac{\partial_z a(z)}{a(z)} \pm a(z)M\right]\psi_{L,R} = \pm \not{p}\,\psi_{R,L}\,. \tag{C.2.1}$$

The bulk equation can be solved rewriting $\psi_{R,L}$ as

$$\psi_{R,L}(p,z) = d_{R,L}(p,z)\widehat{\psi}_{R,L}(p) \equiv \frac{h_{R,L}(p,z)}{h_{R,L}(p,z_{\rm UV})}\widehat{\psi}_{R,L}(p)\,, \tag{C.2.2}$$

where $\widehat{\psi}_{R,L}$ are the values of the fields on the UV boundary and $d_{R,L}$ satisfy the condition $d_{R,L}(p,z_{\rm UV}) = 1$. The equations of motion relate $\widehat{\psi}_R$ and $\widehat{\psi}_L$:

$$\not{p}\,\widehat{\psi}_R(p) = p\,\frac{h_R(p,z_{\rm UV})}{h_L(p,z_{\rm UV})}\widehat{\psi}_L(p) = p\,f_R(p,z_{\rm UV})\widehat{\psi}_L(p)\,, \tag{C.2.3}$$

so that only one of the two fields can be chosen as holographic degree of freedom.

In the AdS_5 case, the bulk equations of motion become

$$[z\partial_z - (2 \mp ML)]\,h_{L,R}(p,z) = \pm z\,p\,h_{R,L}(p,z)\,. \tag{C.2.4}$$

Denoting by $d^{\pm}$ the solutions in the cases in which $\psi_{R,L}$ has Dirichlet boundary conditions at the IR one finds

$$\begin{cases} h_L^{\pm}(p,z) = z^{5/2}\left[Y_{c\mp 1/2}(pz_{\rm IR})J_{c+1/2}(pz) - J_{c\mp 1/2}(pz_{\rm IR})Y_{c+1/2}(pz)\right]\,, \\ h_R^{\pm}(p,z) = z^{5/2}\left[Y_{c\mp 1/2}(pz_{\rm IR})J_{c-1/2}(pz) - J_{c\mp 1/2}(pz_{\rm IR})Y_{c-1/2}(pz)\right]\,, \end{cases} \tag{C.2.5}$$

where $c \equiv ML$.

In the flat space case one finds

$$\begin{cases} h_L^{-}(p,z) = \sin(\omega(\pi R - z))\,, \\ h_R^{-}(p,z) = \dfrac{1}{p}\left[-\omega\cos(\omega(\pi R - z)) + M\sin(\omega(\pi R - z))\right]\,, \end{cases} \tag{C.2.6}$$

and

$$\begin{cases} h_L^{+}(p,z) = \dfrac{1}{p}\left[\omega\cos(\omega(\pi R - z)) + M\sin(\omega(\pi R - z))\right]\,, \\ h_R^{+}(p,z) = \sin(\omega(\pi R - z))\,, \end{cases} \tag{C.2.7}$$

where $\omega^2 = p^2 - M^2$.

C.3 Scalars

We consider a bulk scalar field Φ with bulk action given in eq. (B.1.1). For a field which is non-vanishing at both boundaries we also add localized mass terms of the form

$$S_{loc} = \frac{1}{2g_5^2}\int d^4x \int_{z_{\rm UV}}^{z_{\rm IR}} dz\; a^4(z)\left\{-b\left[\delta(z-z_{\rm UV})-\delta(z-z_{\rm IR})\right]\Phi^\dagger\Phi\right\}, \tag{C.3.1}$$

where $b=(2\pm\alpha)/L$ and $\alpha=\sqrt{4+m_\phi^2L^2}$. This particular choice of the coefficients is the one which allows a $4D$ scalar zero mode for an AdS metric. Of course when the scalar field satisfies Dirichlet conditions at a boundary the corresponding mass term in eq. (C.3.1) is not included.

In this appendix we are interested in computing the solutions of the bulk EOM's with fixed UV values for the fields, thus we only need to consider the IR localized terms. In order to solve the linearized equations of motion we write the fields as

$$\Phi(p,z)=\widehat{\Phi}(p)f(z)\,. \tag{C.3.2}$$

Imposing the variation of the action in eq. (B.1.1) to vanish, we find

$$p^2f(z)+\frac{1}{a^3(z)}\partial_z(a^3(z)\partial_z f(z))-a^2(z)m_\phi^2 f(z)=0\,, \tag{C.3.3}$$

while the IR boundary conditions are

$$\begin{cases}(a^{-1}(z)\partial_z-b)f^+(z)|_{z=z_{\rm IR}}=0\,,\\ f^-(z)|_{z=z_{\rm IR}}=0\,,\end{cases} \tag{C.3.4}$$

where $f^\pm$ represent the solutions which are respectively non-vanishing at the IR boundary or satisfy Dirichlet conditions.

In the AdS_5 case the solutions of the equations of motions are

$$f^\pm(p,z)=\frac{h^\pm(p,z)}{h^\pm(p,z_{\rm UV})}\,, \tag{C.3.5}$$

where

$$\begin{cases}h^+(p,z)=z^2\left[Y_{\alpha\pm1}(pz_{\rm IR})J_\alpha(pz)-J_{\alpha\pm1}(pz_{\rm IR})Y_\alpha(pz)\right]\,,\\ h^-(p,z)=z^2\left[Y_\alpha(pz_{\rm IR})J_\alpha(pz)-J_\alpha(pz_{\rm IR})Y_\alpha(pz)\right]\,,\end{cases} \tag{C.3.6}$$

with the $\pm$ signs corresponding to the cases $b=(2\pm\alpha)/L$.

In the flat space case with arbitrary b, the solutions of the equations of motion can be written as in eq. (C.3.5) with

$$\begin{cases}h^+(p,z)=\cos(\omega(\pi R-z))-\dfrac{b}{\omega}\sin(\omega(\pi R-z))\,,\\ h^-(p,z)=\sin(\omega(\pi R-z))\,,\end{cases} \tag{C.3.7}$$

where $\omega^2=p^2-m_\phi^2$.

Appendix D

Mode Decomposition

In this Appendix we report the decomposition of fields in various representations of the gauge group $SU(3)$ in the presence of the orbifold projection matrix Z given in eq. (3.2.1). The various components are classified in terms of representations of the unbroken gauge subgroup $SU(2) \times U(1)$.

If we denote by $\Psi_{\mathcal{R}}$ a field multiplet transforming in the representation $\mathcal{R}$, we have (compare eq. (1.4.12))

$$\Psi_{\mathcal{R}}(-y) = \eta_{\Psi} \mathcal{R}(Z) \gamma_5 \Psi_{\mathcal{R}}(y) \,, \tag{D.0.1}$$

where $\mathcal{R}$ denotes the embedding of the projection in the $\mathcal{R}$ representation, and $\eta_{\Psi} = \pm 1$. Left-handed and right-handed components have opposite orbifold parities, so that only one chirality has a zero mode. In the decomposition of the multiplets we will also include a $+$ or $-$ sign for each component which gives the relative parities of the fields, *i.e.* the parity of the fields under the operation $\Psi_{\mathcal{R}} \to \mathcal{R}(Z)\Psi_{\mathcal{R}}$.

Fundamental

For the fundamental representation we have simply $\mathcal{R}(Z) = Z$. A field $\Psi_{\mathbf{3}}$ in the **3** representation decomposes as

$$\Psi_{\mathbf{3}} = \begin{pmatrix} \psi_1^- \\ \psi_2^- \\ \chi^+ \end{pmatrix} , \tag{D.0.2}$$

where we denoted by ψ_1 and ψ_2 the up and down components of the $SU(2) \times U(1)$ doublet $\mathbf{2}_{1/6}$, and by χ the singlet $\mathbf{1}_{-1/3}$. The basis in which the coupling of the triplet to the VEV of A_y is diagonal is given by

$$\Psi^{(1)} = \psi_1 \,, \qquad \Psi^{(2)} = \psi_2 + \chi \,. \tag{D.0.3}$$

The $\Psi^{(1)}$ field does not couple with the VEV of A_y, so that it gives a KK tower with masses n/R (with $n \in \mathbb{N}_0$). The $\Psi^{(2)}$ field couples with the Higgs with charge $q^{(2)} = 1$, so

that its KK tower is $(n+\alpha)/R$ (with $n \in \mathbb{Z}$).

For a field in the antifundamental representation we have

$$\Psi_{\overline{\mathbf{3}}} = \begin{pmatrix} \psi_2^- \\ -\psi_1^- \\ \chi^+ \end{pmatrix}, \tag{D.0.4}$$

where we denoted by ψ_1 and ψ_2 the up and down components of the $SU(2)\times U(1)$ doublet $\mathbf{2}_{-1/6}$, and by χ the singlet $\mathbf{1}_{1/3}$. The diagonal basis and the mass spectrum is analogous to the one for the fundamental representation.

Symmetric

For the symmetric representation we have $\mathcal{R}(Z) = Z \otimes Z^T$. The expansion of the $\Psi_{\mathbf{6}}$ field in the symmetric representation is given by

$$\Psi_{\mathbf{6}} = \frac{1}{\sqrt{2}} \begin{pmatrix} \sqrt{2}\phi_1^+ & \phi_3^+ & \psi_1^- \\ \phi_3^+ & \sqrt{2}\phi_2^+ & \psi_2^- \\ \psi_1^- & \psi_2^- & \sqrt{2}\chi^+ \end{pmatrix}, \tag{D.0.5}$$

where, as before, $\psi_{1,2}$ denote the components of the $SU(2)\times U(1)$ doublet $\mathbf{2}_{-1/6}$, χ is the singlet $\mathbf{1}_{-2/3}$ and the triplet $\mathbf{3}_{1/3}$ is given by $\phi_{1,2,3}$. The diagonal basis is defined by

$$\begin{aligned} \Psi^{(1)} &= \psi_1 - \phi_3\,, \qquad \Psi^{(2)} = \psi_2 + \frac{\chi - \phi_2}{\sqrt{2}}\,, \\ \Psi^{(3)} &= \phi_1\,, \qquad \Psi^{(4)} = \frac{\chi + \phi_2}{\sqrt{2}}\,. \end{aligned} \tag{D.0.6}$$

The states which couple with the Higgs are $\Psi^{(1)}$ with charge $q^{(1)} = 1$ and $\Psi^{(2)}$ with charge $q^{(2)} = 2$; their mass levels are thus given by $(n + q^{(i)}\alpha)/R$ (with $n \in \mathbb{Z}$). The $\Psi^{(3)}$ and $\Psi^{(4)}$ fields do not couple with the VEV of A_y, and their mass levels are simply n/R (with $n \in \mathbb{N}_0$).

A field in the antisymmetric representation decomposes as

$$\Psi_{\overline{\mathbf{6}}} = \frac{1}{\sqrt{2}} \begin{pmatrix} \sqrt{2}\phi_1^+ & \phi_3^+ & \psi_2^- \\ \phi_3^+ & \sqrt{2}\phi_2^+ & -\psi_1^- \\ \psi_2^- & -\psi_1^- & \sqrt{2}\chi^+ \end{pmatrix}, \tag{D.0.7}$$

where $\psi_{1,2}$ denote the components of the $SU(2)\times U(1)$ doublet $\mathbf{2}_{1/6}$, χ is the singlet $\mathbf{1}_{2/3}$ and the triplet $\overline{\mathbf{3}}_{-1/3}$ is given by $\phi_{1,2,3}$. The diagonal basis and the KK masses are similar to the ones previously given for the symmetric representation.

Adjoint

For the adjoint representation we have $\mathcal{R}(Z) = Z \otimes Z^\dagger$. This representation decomposes as $\mathbf{8} = \mathbf{3}_0 \oplus \mathbf{2}_{1/2} \oplus \mathbf{2}_{-1/2} \oplus \mathbf{1}_0$ and $\Psi_\mathbf{8}$ can be written explicitly as

$$\Psi_\mathbf{8} = \frac{1}{\sqrt{2}} \begin{pmatrix} \left(Z + \frac{1}{\sqrt{3}}\chi\right)^+ & Y^+ & \psi_1^- \\ \left(Y^\dagger\right)^+ & \left(-Z + \frac{1}{\sqrt{3}}\chi\right)^+ & \psi_2^- \\ \left(\psi_1^\dagger\right)^- & \left(\psi_2^\dagger\right)^- & -\frac{2}{\sqrt{3}}\chi^+ \end{pmatrix}, \tag{D.0.8}$$

where, as before, $\psi_{1,2}$ are the components of the $SU(2)\times U(1)$ complex doublet $\mathbf{2}_{1/2}\oplus\mathbf{2}_{-1/2}$, the singlet $\mathbf{1}_0$ is χ, and Z, Y and $Y^\dagger$ constitute the triplet $\mathbf{3}_0$. The diagonal basis is

$$\begin{aligned} \Psi^{(1)} &= Y - \psi_1\,, & \Psi^{(2)} &= \mathrm{Re}\,\psi_2 + \frac{Z - \sqrt{3}\chi}{2}\,, \\ \Psi^{(3)} &= \frac{\sqrt{3}Z + \chi}{2}\,, & \Psi^{(4)} &= \mathrm{Im}\,\psi_2\,, \end{aligned} \tag{D.0.9}$$

the charges of this fields with respect to the Higgs are $q^{(1)} = 1$, $q^{(2)} = 2$ and $q^{(3)} = q^{(4)} = 0$. In this case we have two KK towers with masses $(n+\alpha)/R$ (with $n \in \mathbb{Z}$) which correspond to the complex $\Psi^{(1)}$ field, one tower with masses $(n + 2\alpha)/R$ (with $n \in \mathbb{Z}$) given by $\Psi^{(2)}$, and, finally, two towers with masses n/R (with $n \in \mathbb{N}_0$) corresponding to $\Psi^{(3)}$ and $\Psi^{(4)}$.

Appendix E

Computation of the $\widehat{Z}\overline{b}_L b_L$ Vertex Corrections

In section (4.4.1) we used the holographic approach to determine the corrections to the $\widehat{Z}\overline{b}_L b_L$ vertex. In this appendix we want to show explicitly how to perform such computation considering a simplified set-up, which however presents the same features of the general case. As a by-product, the explicit computation will give us the possibility to better understand how to use the holographic approach to compute interactions (see section 2.3.1). Moreover, by comparing the mass spectra derived here with the ones obtained by a KK computation in appendix F, one can get another check of the equivalence of the holographic and the KK approach.

Let A_M be a $U(1)$ bulk gauge field, ψ and χ a couple of bulk charged fermions and q_R a chiral $4D$ fermion localized at $y = 0$, which mixes with ψ_L. The gauge field components A_μ and A_5 satisfy respectively Neumann and Dirichlet boundary conditions at $y = \pi R$, whereas for the fermions we have $\psi_R(\pi R) = \chi_L(\pi R) = 0$. The action is given by

$$\begin{aligned} S = \int_0^{\pi R} dy\, d^4x \Big\{ -\frac{1}{4} F_{MN}F^{MN} + \Big[\frac{1}{2}(\overline{\psi} i \not{D}_5 \psi + \overline{\chi} i \not{D}_5 \chi) - M\overline{\chi}\psi + h.c.\Big]\Big\} \\ + \int d^4x \frac{1}{2}\Big[\overline{q}_R i \not{D}_4 q_R + e\,\overline{q}_R \psi_L(0) + e\,\overline{\psi}_L(0) q_R + \overline{\psi}(0)\psi(0) + \overline{\chi}(0)\chi(0)\Big], \end{aligned} \tag{E.0.1}$$

where we added the localized mass terms which are required by the choice of using the left-handed components of the bulk fields as holographic degrees of freedom.

The solutions of the equations of motion for the bulk fermions are given by

$$\begin{cases} \psi_L = \dfrac{\cos(\omega(y-\pi R))}{\cos(\omega\pi R)}\widehat{\psi}_L\,, \\ \chi_L = -\dfrac{\sin(\omega(y-\pi R))}{\sin(\omega\pi R)}\widehat{\psi}_L\,, \end{cases} \qquad \begin{cases} \psi_R = -\dfrac{\not{p}}{p^2}\left(\dfrac{\omega\,\widehat{\psi}_L}{\cos(\omega\pi R)} + \dfrac{M\,\widehat{\chi}_L}{\sin(\omega\pi R)}\right)\sin(\omega(y-\pi R))\,, \\ \chi_R = -\dfrac{\not{p}}{p^2}\left(\dfrac{\omega\,\widehat{\chi}_L}{\sin(\omega\pi R)} - \dfrac{M\,\widehat{\psi}_L}{\cos(\omega\pi R)}\right)\cos(\omega(y-\pi R))\,, \end{cases} \tag{E.0.2}$$

where $\omega = \sqrt{p^2 - M^2}$. For the transverse components of the gauge field one easily finds

$$A_\mu(p,y) = \frac{\cos\left[p(\pi R - y)\right]}{\cos\left[p\,\pi R\right]} \widehat{A}^t_\mu(p)\,, \tag{E.0.3}$$

where $p = \sqrt{p^\mu p_\mu}$.

Substituting the solutions into the action in eq (E.0.1) we find at the quadratic level

$$\mathscr{L} = -\frac{1}{2}\Pi(p)\widehat{A}^t_\mu \widehat{A}^{t\,\mu} + \overline{\widehat{\psi}}_L \frac{\not{p}}{p^2}\omega\tan(\omega\pi R)\widehat{\psi}_L + \frac{1}{2}\left(\overline{q}_R \not{p}_4\, q_R + e\,\overline{q}_R\widehat{\psi}_L + e\,\overline{\widehat{\psi}}_L q_R\right)\,, \tag{E.0.4}$$

where we already set to zero the non-dynamical source $\widehat{\chi}_L$. The quadratic Lagrangian for the gauge field and the boundary field q_R is obtained integrating out the $\widehat{\psi}_L$ holographic field. Using the solution of the equations of motion

$$\widehat{\psi}_L = -\frac{e\not{p}}{2\omega}\cot(\omega\pi R) q_R \tag{E.0.5}$$

we get

$$\mathscr{L}_{holo} = -\frac{1}{2}\Pi(p)\widehat{A}^t_\mu \widehat{A}^{t\,\mu} + \frac{1}{2} Z_q \overline{q}_R \not{p}_4\, q_R\,, \tag{E.0.6}$$

where we defined

$$\Pi(p) = p\tan(p\pi R)\,, \quad Z_q = 1 - \frac{e^2}{2}\,\frac{\cot\omega\pi R}{\omega}\,. \tag{E.0.7}$$

The holographic procedure can also be used to study interaction terms. Again, one has simply to substitute into the action (E.0.1) the solutions (E.0.2) and (E.0.3). Then one has to put to zero the non-dynamical source $\widehat{\chi}_L$ and integrate out the holographic field $\widehat{\psi}_L$ using eq. (E.0.5). It is useful to see how this works by computing the distortion to the $U(1)$ gauge coupling g of q_R to $\widehat{A}_\mu$ due to the massive modes. This interaction is encoded in the following Lagrangian term:

$$\begin{aligned}\mathscr{L}^{(3)} = g\int_0^{\pi R} dy \Big[\overline{\psi}(p+q,y)\not{A}(q,y)\psi(p,y) + \overline{\chi}(p+q,y)\not{A}(q,y)\chi(p,y)\Big] \\ + \frac{g}{2}\,\overline{q}_R(p+q)\not{\widehat{A}}(q) q_R(p)\,.\end{aligned} \tag{E.0.8}$$

In order to simplify our computation, let us consider the kinematic configuration in which the fermion is on-shell, $p^2 = (p+q)^2 = 0$, and $q^2 = \mu^2 \ll M^2$. By direct substitution and after a bit of algebra, one gets the following cubic interaction, up to terms of order μ^2/M^2:

$$\mathcal{L}^{(3)} = \frac{g}{2}\Big[Z_q + \frac{e^2\,\mu^2\,\pi R}{8M^2} F(\pi R M)\Big]\overline{q}_R(p+q)\not{\widehat{A}}^t(q) q_R(p)\,, \tag{E.0.9}$$

where Z_q is computed at zero momentum and we have defined

$$F(x) \equiv 1 - \frac{1}{x}\coth x + \coth^2 x\,. \tag{E.0.10}$$

As expected, the form of the interaction vertex at $\mu^2 = 0$ has precisely the same structure as the quadratic term in (E.0.6), as required by gauge invariance, which forbids any correction to g. At quadratic order in the gauge boson momentum, however, we get a correction

$$\delta g = \frac{g\, e^2\, \pi R}{8 Z_q} \frac{\mu^2}{M^2} F(\pi R M) \,. \tag{E.0.11}$$

Notice that eq. (E.0.11) coincides exactly with eq. (4.4.1), when fixing $\mu^2 = m_Z^2$ and taking into account the SM coupling of the b_L. This is a further proof that no corrections arise in our model from the mixing of b_L with fields with different isospin quantum numbers, the only effect being given by the partial delocalization of the field, resulting in couplings with the "massive" gauge fields $A_\mu(y)$, with $y \neq 0$.

Appendix F

Fermion Localization

In this appendix we examine the wave functions of the KK modes of the fermions arising from the mixing of the bulk fields with the fields localized at $y = 0$. The purpose of this analysis is to illustrate how much the SM fermions are localized in the model described in chapter 4. As we will see, in fact, the top quark is not localized at all, whereas the bottom is only partially localized (see figs. F.1 and F.2). In order to simplify the discussion, we focus on the wave functions of right-handed singlets before EWSB. Left-handed localized fields are more involved since they couple to two different bulk fields, as shown in eq. (4.1.5).

The relevant quadratic Lagrangian describing the coupling of a localized right-handed fermion with the bulk fields is easily extracted from the full Lagrangian (4.1.2). It reads

$$\begin{aligned}\mathcal{L} = &\overline{\psi}(i\not{\partial}_4 + k\partial_5\gamma_5)\psi + \overline{\widetilde{\psi}}(i\not{\partial}_4 + k\partial_5\gamma_5)\widetilde{\psi} - M(\overline{\psi}\widetilde{\psi} + \overline{\widetilde{\psi}}\psi) \\ &+\delta(y)[\overline{q}_R i\not{\partial}_4 q_R + e\overline{q}_R\psi_L + e\overline{\psi}_L q_R],\end{aligned} \tag{F.0.1}$$

where ψ and $\widetilde{\psi}$ are the singlet components of the periodic bulk fermions Ψ^t_+ and Ψ^b_+, respectively for $q_R = t_R$ and $q_R = b_R$. For simplicity of notation, we denote the bulk–to–boundary mixing parameter simply as e in both cases. Due to the latter and the bulk mass M, the equations of motion for ψ, $\widetilde{\psi}$ and q_R are all coupled with each other. The $4D$ KK mass eigenstates $\chi^{(n)}_{L,R}(x)$ of eq. (F.0.1) will then appear spread between the fields ψ, $\widetilde{\psi}$ and q_R. In other words, we expand the various fields as follows:

$$\begin{cases} q = \sum_n g_n \chi^{(n)}_R\,, \\ \psi_{L,R} = \sum_n f^{(n)}_{L,R}(y)\,\chi^{(n)}_{L,R}\,, \\ \widetilde{\psi}_{L,R} = \sum_n \widetilde{f}^{(n)}_{L,R}(y)\,\chi^{(n)}_{L,R}\,, \end{cases} \tag{F.0.2}$$

where $f^{(n)}_{L,R}(y)$ and $\widetilde{f}^{(n)}_{L,R}(y)$ are the wave functions along the fifth dimension and g_n are constants. The χ fields satisfy the 4-dimensional Dirac equation

$$i\not{\partial}_4\chi^{(n)} = m_n\chi^{(n)}\,, \tag{F.0.3}$$

where $\chi^{(n)} = \chi_L^{(n)} + \chi_R^{(n)}$, and m_n is the mass of the n^{th} state (it is useful to recall that in our conventions $\gamma_5 \chi_{R,L} = \pm \chi_{R,L}$). By solving the equations of motion, one finds two distinct towers of eigenstates: an "unperturbed" tower with only massive fields and a "perturbed" one containing a right-handed massless field. We will also see how the mass spectra found here with the usual KK approach match with the one deduced from eq. (E.0.7) using the holographic approach.

The unperturbed tower

This tower has no component along the localized fields and is entirely build up with bulk fields. The wave functions are analytic over the whole covering space and the left-handed ones vanish at $y = 0$. The mass levels are given by

$$m_n = \sqrt{M^2 + \left(\frac{kn}{R}\right)^2}\,, \tag{F.0.4}$$

but with $n \geq 1$, without the $n = 0$ mode. The corresponding wave functions are

$$\begin{cases} g_n = 0\,, \\ f_L^{(n)} = 0\,, \\ \widetilde{f}_L^{(n)} = \dfrac{1}{\sqrt{\pi R}} \sin\left(\dfrac{n}{R} y\right)\,, \end{cases} \qquad \begin{cases} f_R^{(n)} = \dfrac{M}{m_n \sqrt{\pi R}} \sin\left(\dfrac{n}{R} y\right)\,, \\ \widetilde{f}_R^{(n)} = \dfrac{nk/R}{m_n \sqrt{\pi R}} \cos\left(\dfrac{n}{R} y\right)\,. \end{cases} \tag{F.0.5}$$

Although e does not explicitly appear in eqs. (F.0.4) and (F.0.5), its presence constrains the left-handed fields to vanish at $y = 0$ and thus it indirectly enters in the above expressions. When e vanishes, indeed, one recovers the usual mode $n = 0$.

The perturbed tower

This tower is distorted by the coupling with the localized fields. Its massive levels are given by the solutions of the transcendental equation

$$\tan\left(\pi R \frac{\omega_n}{k}\right) = \frac{\varepsilon^2}{\pi R k \omega_n}\,, \tag{F.0.6}$$

where $\omega_n \equiv \sqrt{(m_n^2 - M^2)}$ and $\varepsilon = \sqrt{\pi R/2}\, e$. Notice that the masses defined by eq. (F.0.6) exactly coincide, for $k = 1$, with the zeroes of Z_q in eq. (E.0.7). The mass equation has a tower of solutions with $m_n > M$, whose wave functions are[1]

$$\begin{cases} f_L^{(n)} = -\dfrac{\varepsilon m_n g_n}{\sqrt{2\pi R k \omega_n}} \dfrac{\cos\left((y - \pi R)\omega_n/k\right)}{\sin(\pi R \omega_n/k)}\,, \\ \widetilde{f}_L^{(n)} = 0\,, \end{cases} \qquad \begin{cases} f_R^{(n)} = \dfrac{\varepsilon g_n}{\sqrt{2\pi R k}} \dfrac{\sin\left((y - \pi R)\omega_n/k\right)}{\sin(\pi R \omega_n/k)}\,, \\ \widetilde{f}_R^{(n)} = -\dfrac{\varepsilon M g_n}{\sqrt{2\pi R k \omega_n}} \dfrac{\cos\left((y - \pi R)\omega_n/k\right)}{\sin(\pi R \omega_n/k)}\,, \end{cases} \tag{F.0.7}$$

[1] In eq. (F.0.7) and in eq. (F.0.9) we report the wave functions for $0 \leq y \leq \pi R$, the continuation for generic y can be obtained using the properties of the fields under parity and under translation.

The constants g_n in eq. (F.0.2) are determined by imposing the canonical normalization of the $4D$ fields. One gets

$$g_n = \left[1 + \frac{\varepsilon^2}{2\pi R k^2 \omega_n^2}\left(\frac{\pi R m_n^2}{\sin^2(\pi R\omega_n/k)} + k\frac{M^2-\omega_n^2}{\omega_n}\cot(\pi R\omega_n/k)\right)\right]^{-1/2}. \qquad \text{(F.0.8)}$$

Notice that some care has to be used in taking the limit $\varepsilon \to 0$ in the above expressions, since one encounters apparently ill-defined expressions in eqs. (F.0.7) and (F.0.8).

The zero mode

The zero mode is of particular interest, being identified with a SM field. Its wave function is

$$\begin{cases} f_L^{(0)} = 0\,, \\ \widetilde{f}_L^{(0)} = 0\,, \end{cases} \qquad \begin{cases} f_R^{(0)} = \dfrac{\varepsilon g_0}{\sqrt{2\pi R k}}\dfrac{\sinh\left((y-\pi R)M/k\right)}{\sinh(\pi RM/k)}\,, \\ \widetilde{f}_R^{(0)} = \dfrac{\varepsilon g_0}{\sqrt{2\pi R k}}\dfrac{\cosh\left((y-\pi R)M/k\right)}{\sinh(\pi RM/k)}\,, \end{cases} \qquad \text{(F.0.9)}$$

where again g_0 is determined by the normalization conditions and equals

$$g_0 = \left[1 + \frac{\varepsilon^2}{\pi RMk}\coth(\pi RM/k)\right]^{-1/2}. \qquad \text{(F.0.10)}$$

The constant g_0 indicates how much of the zero mode field is composed of the localized field. When $\varepsilon \ll 1$ and $g_0 \sim 1$, as expected, the wave function of the massless state is mostly given by the localized field, the bulk components (F.0.9) being proportional to ε and thus small. On the contrary, for large mixing $\varepsilon \gg 1$, one has $g_0 \ll 1$ and the localized field is completely "dissolved" into the bulk degrees of freedom. In the latter case, then, the localization of the ψ_R and $\widetilde{\psi}_R$ components of the zero mode is essentially determined by the adimensional quantity $\pi RM/k$. The bulk wave functions at $y = \pi R$ are suppressed by a factor $\exp(-\pi RM/k)$ with respect to their value at $y = 0$ so that, independently of ε, for large values of $\pi RM/k$ the chiral field is still localized at $y = 0$.

Summarizing, the zero mode is localized at $y = 0$ for small mixing with the bulk fields and arbitrary bulk masses, or for large bulk masses and arbitrary mixing. The requirement of having the correct top mass after EWSB implies a large mixing and a small bulk mass, giving rise to a delocalized top wave function. In fig. F.1 we illustrate the wave function profiles of the right-handed top and bottom quark components for typical acceptable values of input parameters, before EWSB.

The computation of the mass spectrum and fermion wave functions for the antiperiodic fermions Ψ_- and $\widetilde{\Psi}_-$ is straightforward, since they do not couple with the localized fields.

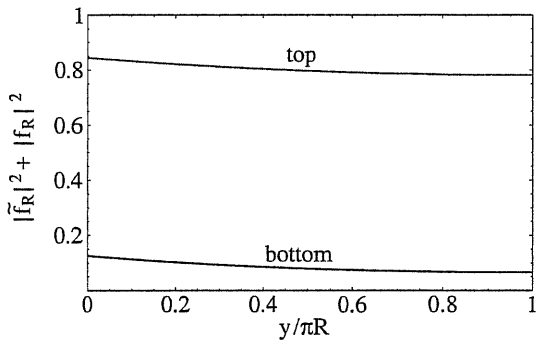

Figure F.1: Top (red) and bottom (blue) quark wave function profiles (right handed components). The areas below the lines represent the amount of the delocalized part of the fields.

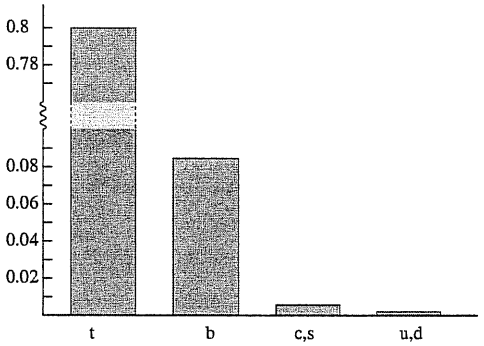

Figure F.2: Delocalized part of the quark wave functions. The fraction of bulk wave function is shown for the various quarks.

Their wave functions can be written as

$$\begin{cases} f_L^{(n)} = \dfrac{1}{\sqrt{2\pi R}} \cos\left(\dfrac{n+1/2}{R} y\right), \\ \tilde{f}_L^{(n)} = \dfrac{\pm 1}{\sqrt{2\pi R}} \sin\left(\dfrac{n+1/2}{R} y\right), \end{cases} \quad \begin{cases} f_R^{(n)} = \dfrac{\pm M - (n+1/2)k/R}{m_n \sqrt{2\pi R}} \sin\left(\dfrac{n+1/2}{R} y\right), \\ \tilde{f}_R^{(n)} = \dfrac{M \pm (n+1/2)k/R}{m_n \sqrt{2\pi R}} \cos\left(\dfrac{n+1/2}{R} y\right), \end{cases} \tag{F.0.11}$$

where $n \geq 0$ and $\pm$ stands for the two towers of mass eigenstates, both with masses given by

$$m_n = \sqrt{M^2 + \left(\frac{k(n+1/2)}{R}\right)^2}. \tag{F.0.12}$$

After EWSB, all above relations are clearly modified by $O(\alpha)$ effects. In particular, a small fraction of the SM fields is now spread also among the bulk fermion components whose mixing were forbidden by $SU(2)_L \times U(1)_Y$ symmetry. We do not write the modification to the mass formula (F.0.6) for the deformed tower, the form of which can be deduced from the zeroes of the integrand of eqs. (4.2.8) and (4.2.9) (with the $4D$ momentum rotated back to the Minkowskian).

Appendix G

Explicit Form of the Finite-Temperature Potential

In this appendix we report the explicit form of the finite temperature potential for a Wilson line phase. For simplicity, we consider the Lorentz preserving case and we include only periodic fields. The bulk contributions are computed for a couple of fields $\Psi, \widetilde{\Psi}$ with opposite orbifold parities and with a bulk mass M. The boundary contribution is computed for the set-up considered in section 5.2.1, namely a couple of bulk fields in the $(\mathbf{3}, \overline{\mathbf{6}})$ representation of the $SU(3)_s \times SU(3)_w$ gauge group coupled with the a localized $SU(2)$ doublet Q_L and a singlet t_R. The matter Lagrangian, for an arbitrary localization of the boundary fields, is given by

$$\begin{aligned}\mathscr{L}_{mat} = & \overline{\Psi} i \not{D}_5 \Psi + \overline{\widetilde{\Psi}} i \not{D}_5 \widetilde{\Psi} - M \left(\overline{\Psi} \widetilde{\Psi} + \overline{\widetilde{\Psi}} \Psi \right) \\ & + \delta(y - y_0) \left[\overline{Q}_L i \not{D}_4 Q_L + \left(e_1 \, \overline{Q}_L \psi + \text{h.c.} \right) \right] \\ & + \delta(y - y_1) \left[\overline{t}_R i \not{D}_4 t_R + \left(e_2 \, \overline{t}_R \chi + \text{h.c.} \right) \right] , \end{aligned} \tag{G.0.1}$$

where $y_{0,1} = 0, \pi R$. We also report the finite-temperature correction to the gauge contribution to the potential in the presence of localized kinetic terms (see section 3.7.2).

The generalization of these results to the Lorentz breaking case and to antiperiodic bulk is straightforward. The bulk contribution can be obtained from eq. (5.1.1) where one has to substitute the appropriately modified mass tower. Also the manipulations of the bulk contribution used in the following can be easily adapted. The boundary contributions can be obtained by generalizing eqs. (4.2.8) and (4.2.9) at finite temperature.

G.1 Bulk Fields Contribution

There are various ways of computing eq. (5.1.1) for bulk fields. For generality, we will report in the following the result that one obtains in d non-compact dimensions. A possible

computation is to disentangle the $T = 0$ and $T \neq 0$ terms in eq. (5.1.1) and compute the T-dependent term as usually done in 4D for each KK state. In this case, one simply gets (see *e.g.* [81, 89])

$$V(T, q\alpha) = V(T = 0, q\alpha) + (-1)^{2\widetilde{\eta}}\, T \sum_{k=-\infty}^{+\infty} \int \frac{d^d p}{(2\pi)^d} \log\left[1 - (-1)^{2\widetilde{\eta}} e^{-\frac{\sqrt{p^2+M_k^2}}{T}}\right], \quad \text{(G.1.1)}$$

where p^2 denotes the d dimensional non-compact momentum square, and $\widetilde{\eta} = 0$ for bosons and $\widetilde{\eta} = 1/2$ for fermions.

Other useful and more explicit forms of the potential are obtained by using the relation $\mathrm{tr}\,\log A = -\int_0^\infty dt/t\,\mathrm{tr}\,e^{-tA}$ in eq. (5.1.1), valid up to irrelevant constants. Subsequently, one can use the Poisson resummation formula

$$\sum_{n=-\infty}^{+\infty} e^{-\pi t(n+a)^2} = \frac{1}{\sqrt{t}} \sum_{\widetilde{n}=-\infty}^{+\infty} e^{-\frac{\pi \widetilde{n}^2}{t}} e^{2i\pi \widetilde{n} a}\,. \quad \text{(G.1.2)}$$

The above formula can be applied in eq. (5.1.1) to the KK modes k, to the Matsubara ones m, or to both, resulting in different but equivalent ways of computing the effective potential. In the three cases, one gets, respectively:

$$V(T, q\alpha) = \frac{2T(-1)^{2\widetilde{\eta}-1}}{(2\pi)^{\frac{d+1}{2}} L^d} \sum_{\widetilde{k}=1}^{\infty} \sum_{m=-\infty}^{\infty} \frac{\cos(2\pi \widetilde{k} q\alpha)}{\widetilde{k}^{d+1}} B_{\frac{d+1}{2}}\left[L\widetilde{k}\sqrt{M^2 + [2\pi(m+\widetilde{\eta})T]^2}\right], \quad \text{(G.1.3)}$$

where

$$B_{\frac{d+1}{2}}(x) \equiv x^{\frac{d+1}{2}} K_{\frac{d+1}{2}}(x) \quad \text{(G.1.4)}$$

and K_n are the modified Bessel functions. By Poisson resumming over m, we get

$$\begin{aligned} V(T, q\alpha) = {} & (-1)^{2\widetilde{\eta}-1} \frac{L}{\pi(2\pi)^{\frac{d}{2}}} \sum_{\widetilde{k}=1}^{\infty} \frac{\cos(2\pi \widetilde{k} q\alpha)}{(L\widetilde{k})^{d+2}} B_{\frac{d+2}{2}}(LM\widetilde{k}) \quad \text{(G.1.5)} \\ & + 2(-1)^{2\widetilde{\eta}-1} \sum_{k=-\infty}^{\infty} \sum_{\widetilde{m}=1}^{\infty} (-1)^{2\widetilde{m}\widetilde{\eta}} \left(\frac{T}{\widetilde{m}\sqrt{2\pi}}\right)^{d+1} B_{\frac{d+1}{2}}\left(\frac{M_k \widetilde{m}}{T}\right), \end{aligned}$$

where a Poisson resummation over k has been performed in the first term ($\widetilde{m} = 0$). Finally, by Poisson resumming in both indices, one finds

$$\begin{aligned} V(T, q\alpha) = {} & (-1)^{2\widetilde{\eta}-1} \frac{LT^{d+2}}{\pi(2\pi)^{\frac{d}{2}}} \sum_{\widetilde{k}=1}^{\infty} \sum_{\widetilde{m}=-\infty}^{\infty} (-1)^{2\widetilde{\eta}\widetilde{m}} \left[\widetilde{m}^2 + (LT\widetilde{k})^2\right]^{-\frac{d+2}{2}} \cdot \\ & \cdot B_{\frac{d+2}{2}}\left[\frac{M}{T}\sqrt{\widetilde{m}^2 + (LT\widetilde{k})^2}\right] \cos(2\pi \widetilde{k} q\alpha)\,. \quad \text{(G.1.6)} \end{aligned}$$

In eqs. (G.1.3), (G.1.5) and (G.1.6) an irrelevant α-independent term has always been omitted. All these relations also hold for vanishing bulk mass term, $M = 0$, by noticing that $\lim_{x\to 0} B_\alpha(x) = 2^{\alpha-1}\Gamma(\alpha)$, where α is any positive integer or half-integer number.

G.2 Boundary–Bulk Fields Contribution

The contribution to the Higgs effective potential of bulk and boundary fields is substantially more involved than that of purely bulk fields. One has essentially to compute $V(T, q\alpha)$ directly from eq. (5.1.1), where M_k^2 are the mass eigenvalues of the bulk-boundary system. It turns out that the full contribution can be written as a sum of a purely bulk contribution and a remaining boundary term. The bulk contribution is that given by the bulk fermions Ψ and $\widetilde{\Psi}$ with $e_1 = e_2 = 0$, whereas the boundary contribution is a simple generalization of the one found at $T = 0$:

$$\begin{aligned} V_u(T,\alpha) = -\frac{8T}{\pi^2 L^3} \sum_{m=-\infty}^{+\infty} \int_0^\infty dx\, x^2 \ln \Bigg[\prod_{i=1}^{2} \Bigg[1 + \delta_{i2} \frac{{\varepsilon_2}^2}{2\widetilde{x}_\lambda} f_0(\widetilde{x}_\lambda, 0) \\ + \frac{{\varepsilon_i}^2}{2^{\delta_{i2}} \widetilde{x}_\lambda} f_0(\widetilde{x}_\lambda, 2\alpha) \Bigg] + \prod_{i=1}^{2} \left[\frac{{\varepsilon_i}^2}{2^{\delta_{i2}} \widetilde{x}} f_{1,3}(\widetilde{x}_\lambda, 2\alpha) \right] \Bigg], \\ V_d(T,\alpha) = -\frac{8T}{\pi^2 L^3} \sum_{m=-\infty}^{+\infty} \int_0^\infty dx\, x^2 \ln \left[\prod_{i=1}^{2} \left[1 + \delta_{i1} \frac{{\varepsilon_1}^2}{2\widetilde{x}_\lambda} f_0(\widetilde{x}_\lambda, \alpha) \right] \right], \end{aligned} \tag{G.2.1}$$

where the two cases in which the boundary fields are localized at the same or at different fixed points correspond respectively to the choice f_1 or f_3 in the last term in the expression of $V_u(T, \alpha)$. In eq. (G.2.1) we also used the definition

$$\widetilde{x}^2 \equiv x_0^2 + x^2 \quad \text{and} \quad \widetilde{x}_\lambda^2 \equiv (x_0^2 + x^2 + \lambda^2), \tag{G.2.2}$$

and $x_0 = (m + 1/2)\pi LT$ is the properly rescaled Matsubara frequency for a fermion. The functions $f_{0,1}$ are defined in eqs. (3.3.8) and (3.3.9), while $f_{2,3}$ are given by

$$f_2(\widetilde{x}_\lambda, \alpha) = \mathrm{Re}\left[\sinh^{-1}(\widetilde{x}_\lambda + i\pi\alpha)\right] = \frac{2\cos(\pi\alpha)\sinh(\widetilde{x}_\lambda)}{\cosh(2\widetilde{x}_\lambda) - \cos(2\pi\alpha)}, \tag{G.2.3}$$

$$f_3(\widetilde{x}_\lambda, \alpha) = \mathrm{Im}\left[\sinh^{-1}(\widetilde{x}_\lambda + i\pi\alpha)\right] = -\frac{2\sin(\pi\alpha)\cosh(\widetilde{x}_\lambda)}{\cosh(2\widetilde{x}_\lambda) - \cos(2\pi\alpha)}. \tag{G.2.4}$$

In presence of localized gauge kinetic terms, the gauge field contribution is given by the sum of the purely bulk term and an additional boundary term. The latter, for a field which couples diagonally with the Higgs field with charge q, can be written as

$$V_g^{c_i}(T, q\alpha) = \frac{6T}{\pi^2 L^3} \sum_{m=-\infty}^{+\infty} \int_0^\infty dx\, x^2 \ln \left[\prod_{i=1}^{2} \left[1 + c_i \widetilde{x} f_0(\widetilde{x}, q\alpha) \right] - \prod_{i=1}^{2} \left[c_i \widetilde{x} f_2(\widetilde{x}, q\alpha) \right] \right], \tag{G.2.5}$$

with $\widetilde{x}$ defined as in eq. (G.2.2), but with $x_0 = m\pi LT$.

Bibliography

[1] R. Barbieri and A. Strumia, *What is the limit on the Higgs mass?*, *Phys. Lett.* **B462** (1999) 144–149, [hep-ph/9905281].

[2] R. Barbieri, *Electroweak symmetry breaking as of 2003, on the way to the large hadron collider*, hep-ph/0312253.

[3] S. Weinberg, *Implications of dynamical symmetry breaking: An addendum*, *Phys. Rev.* **D19** (1979) 1277–1280;
L. Susskind, *Dynamics of spontaneous symmetry breaking in the Weinberg-Salam theory*, *Phys. Rev.* **D20** (1979) 2619–2625.

[4] D. B. Kaplan and H. Georgi, *SU(2) x U(1) breaking by vacuum misalignment*, *Phys. Lett.* **B136** (1984) 183;
D. B. Kaplan, H. Georgi, and S. Dimopoulos, *Composite Higgs scalars*, *Phys. Lett.* **B136** (1984) 187;
H. Georgi, D. B. Kaplan, and P. Galison, *Calculation of the composite Higgs mass*, *Phys. Lett.* **B143** (1984) 152;
H. Georgi and D. B. Kaplan, *Composite Higgs and custodial SU(2)*, *Phys. Lett.* **B145** (1984) 216;
M. J. Dugan, H. Georgi, and D. B. Kaplan, *Anatomy of a composite Higgs model*, *Nucl. Phys.* **B254** (1985) 299.

[5] C. Csaki, C. Grojean, H. Murayama, L. Pilo, and J. Terning, *Gauge theories on an interval: Unitarity without a Higgs*, *Phys. Rev.* **D69** (2004) 055006, [hep-ph/0305237].

[6] C. Csaki, C. Grojean, L. Pilo, and J. Terning, *Towards a realistic model of Higgsless electroweak symmetry breaking*, *Phys. Rev. Lett.* **92** (2004) 101802, [hep-ph/0308038].

[7] N. Arkani-Hamed, A. G. Cohen, and H. Georgi, *Electroweak symmetry breaking from dimensional deconstruction*, *Phys. Lett.* **B513** (2001) 232–240, [hep-ph/0105239].

[8] N. Arkani-Hamed *et. al.*, *The minimal moose for a little Higgs*, *JHEP* **08** (2002) 021, [hep-ph/0206020];
N. Arkani-Hamed, A. G. Cohen, E. Katz, and A. E. Nelson, *The littlest Higgs*, *JHEP* **07** (2002) 034, [hep-ph/0206021].

[9] N. Arkani-Hamed, S. Dimopoulos, and G. R. Dvali, *The hierarchy problem and new dimensions at a millimeter*, *Phys. Lett.* **B429** (1998) 263–272, [hep-ph/9803315];

I. Antoniadis, N. Arkani-Hamed, S. Dimopoulos, and G. R. Dvali, *New dimensions at a millimeter to a fermi and superstrings at a TeV*, *Phys. Lett.* **B436** (1998) 257–263, [hep-ph/9804398].

[10] I. Antoniadis, *A possible new dimension at a few TeV*, *Phys. Lett.* **B246** (1990) 377–384;
I. Antoniadis, C. Munoz, and M. Quiros, *Dynamical supersymmetry breaking with a large internal dimension*, *Nucl. Phys.* **B397** (1993) 515–538, [hep-ph/9211309];
A. Delgado, A. Pomarol, and M. Quiros, *Supersymmetry and electroweak breaking from extra dimensions at the TeV-scale*, *Phys. Rev.* **D60** (1999) 095008, [hep-ph/9812489];
I. Antoniadis, S. Dimopoulos, A. Pomarol, and M. Quiros, *Soft masses in theories with supersymmetry breaking by TeV-compactification*, *Nucl. Phys.* **B544** (1999) 503–519, [hep-ph/9810410].

[11] N. S. Manton, *A new six-dimensional approach to the Weinberg-Salam model*, *Nucl. Phys.* **B158** (1979) 141;
D. B. Fairlie, *Higgs' fields and the determination of the Weinberg angle*, *Phys. Lett.* **B82** (1979) 97; *Two consistent calculations of the Weinberg angle*, *J. Phys.* **G5** (1979) L55;
P. Forgacs and N. S. Manton, *Space-time symmetries in gauge theories*, *Commun. Math. Phys.* **72** (1980) 15;
S. Randjbar-Daemi, A. Salam, and J. A. Strathdee, *Spontaneous compactification in six-dimensional Einstein-Maxwell theory*, *Nucl. Phys.* **B214** (1983) 491–512;
N. V. Krasnikov, *Ultraviolet fixed point behavior of the five-dimensional Yang-Mills theory, the gauge hierarchy problem and a possible new dimension at the TeV scale*, *Phys. Lett.* **B273** (1991) 246–249.

[12] H. Hatanaka, T. Inami, and C. S. Lim, *The gauge hierarchy problem and higher dimensional gauge theories*, *Mod. Phys. Lett.* **A13** (1998) 2601–2612, [hep-th/9805067].

[13] G. R. Dvali, S. Randjbar-Daemi, and R. Tabbash, *The origin of spontaneous symmetry breaking in theories with large extra dimensions*, *Phys. Rev.* **D65** (2002) 064021, [hep-ph/0102307];
I. Antoniadis, K. Benakli, and M. Quiros, *Finite Higgs mass without supersymmetry*, *New J. Phys.* **3** (2001) 20, [hep-th/0108005];
M. Kubo, C. S. Lim, and H. Yamashita, *The Hosotani mechanism in bulk gauge theories with an orbifold extra space S(1)/Z(2)*, *Mod. Phys. Lett.* **A17** (2002) 2249–2264, [hep-ph/0111327];
C. A. Scrucca, M. Serone, L. Silvestrini, and A. Wulzer, *Gauge-Higgs unification in orbifold models*, *JHEP* **02** (2004) 049, [hep-th/0312267];
C. Biggio and M. Quiros, *Higgs-gauge unification without tadpoles*, *Nucl. Phys.* **B703** (2004) 199–216, [hep-ph/0407348].

[14] C. Csaki, C. Grojean, and H. Murayama, *Standard model Higgs from higher dimensional gauge fields*, *Phys. Rev.* **D67** (2003) 085012, [hep-ph/0210133].

[15] C. A. Scrucca, M. Serone, and L. Silvestrini, *Electroweak symmetry breaking and fermion masses from extra dimensions*, *Nucl. Phys.* **B669** (2003) 128–158, [hep-ph/0304220].

[16] L. J. Hall, Y. Nomura, and D. R. Smith, *Gauge-Higgs unification in higher dimensions*, *Nucl. Phys.* **B639** (2002) 307–330, [hep-ph/0107331];

N. Haba, M. Harada, Y. Hosotani, and Y. Kawamura, *Dynamical rearrangement of gauge symmetry on the orbifold S(1)/Z(2)*, *Nucl. Phys.* **B657** (2003) 169–213, [hep-ph/0212035], erratum *ibid.* **B669** (2003) 381;
N. Haba and Y. Shimizu, *Gauge-Higgs unification in the 5 dimensional E(6), E(7), and E(8) guts on orbifold*, *Phys. Rev.* **D67** (2003) 095001, [hep-ph/0212166];
K.-w. Choi *et. al.*, *Electroweak symmetry breaking in supersymmetric gauge-Higgs unification models*, *JHEP* **02** (2004) 037, [hep-ph/0312178];
I. Gogoladze, Y. Mimura, and S. Nandi, *Gauge Higgs unification on the left-right model*, *Phys. Lett.* **B560** (2003) 204–213, [hep-ph/0301014]; *Unification of gauge, Higgs and matter in extra dimensions*, *Phys. Lett.* **B562** (2003) 307–315, [hep-ph/0302176]; *Model building with gauge-Yukawa unification*, *Phys. Rev.* **D69** (2004) 075006, [hep-ph/0311127].

[17] G. Burdman and Y. Nomura, *Unification of Higgs and gauge fields in five dimensions*, *Nucl. Phys.* **B656** (2003) 3–22, [hep-ph/0210257].

[18] R. Contino, Y. Nomura, and A. Pomarol, *Higgs as a holographic pseudo-Goldstone boson*, *Nucl. Phys.* **B671** (2003) 148–174, [hep-ph/0306259].

[19] K. Agashe, R. Contino, and A. Pomarol, *The minimal composite Higgs model*, *Nucl. Phys.* **B719** (2005) 165–187, [hep-ph/0412089].

[20] K. Agashe and R. Contino, *The minimal composite Higgs model and electroweak precision tests*, *Nucl. Phys.* **B742** (2006) 59–85, [hep-ph/0510164].

[21] R. Contino, L. Da Rold, and A. Pomarol, *Light custodians in natural composite Higgs models*, *Phys. Rev.* **D75** (2007) 055014, [hep-ph/0612048].

[22] L. Randall and R. Sundrum, *A large mass hierarchy from a small extra dimension*, *Phys. Rev. Lett.* **83** (1999) 3370–3373, [hep-ph/9905221]; *An alternative to compactification*, *Phys. Rev. Lett.* **83** (1999) 4690–4693, [hep-th/9906064].

[23] N. Arkani-Hamed, M. Porrati, and L. Randall, *Holography and phenomenology*, *JHEP* **08** (2001) 017, [hep-th/0012148];
R. Rattazzi and A. Zaffaroni, *Comments on the holographic picture of the Randall-Sundrum model*, *JHEP* **04** (2001) 021, [hep-th/0012248].

[24] J. M. Maldacena, *The large n limit of superconformal field theories and supergravity*, *Adv. Theor. Math. Phys.* **2** (1998) 231–252, [hep-th/9711200];
S. S. Gubser, I. R. Klebanov, and A. M. Polyakov, *Gauge theory correlators from non-critical string theory*, *Phys. Lett.* **B428** (1998) 105–114, [hep-th/9802109].

[25] E. Witten, *Anti-de sitter space and holography*, *Adv. Theor. Math. Phys.* **2** (1998) 253–291, [hep-th/9802150].

[26] G. Panico, M. Serone, and A. Wulzer, *A model of electroweak symmetry breaking from a fifth dimension*, *Nucl. Phys.* **B739** (2006) 186–207, [hep-ph/0510373].

[27] G. Panico, M. Serone, and A. Wulzer, *Electroweak symmetry breaking and precision tests with a fifth dimension*, *Nucl. Phys.* **B762** (2007) 189–211, [hep-ph/0605292].

[28] Y. Hosotani, *Dynamical mass generation by compact extra dimensions*, *Phys. Lett.* **B126** (1983) 309; *Dynamical gauge symmetry breaking as the Casimir effect*, *Phys. Lett.* **B129** (1983) 193; *Dynamics of nonintegrable phases and gauge symmetry breaking*, *Ann. Phys.* **190** (1989) 233.

[29] G. Cacciapaglia, C. Csaki, and S. C. Park, *Fully radiative electroweak symmetry breaking*, *JHEP* **03** (2006) 099, [hep-ph/0510366].

[30] M. Regis, M. Serone, and P. Ullio, *A dark matter candidate from an extra (non-universal) dimension*, *JHEP* **03** (2007) 084, [hep-ph/0612286].

[31] T. Appelquist, H.-C. Cheng, and B. A. Dobrescu, *Bounds on universal extra dimensions*, *Phys. Rev.* **D64** (2001) 035002, [hep-ph/0012100].

[32] G. Servant and T. M. P. Tait, *Is the lightest Kaluza-Klein particle a viable dark matter candidate?*, *Nucl. Phys.* **B650** (2003) 391–419, [hep-ph/0206071].

[33] R. Barbieri, A. Pomarol, and R. Rattazzi, *Weakly coupled Higgsless theories and precision electroweak tests*, *Phys. Lett.* **B591** (2004) 141–149, [hep-ph/0310285].

[34] C. Csaki, C. Grojean, J. Hubisz, Y. Shirman, and J. Terning, *Fermions on an interval: Quark and lepton masses without a Higgs*, *Phys. Rev.* **D70** (2004) 015012, [hep-ph/0310355].

[35] J. Hirn and V. Sanz, *Interpolating between low and high energy QCD via a 5d Yang-Mills model*, *JHEP* **12** (2005) 030, [hep-ph/0507049].

[36] M. A. Luty, M. Porrati, and R. Rattazzi, *Strong interactions and stability in the DGP model*, *JHEP* **09** (2003) 029, [hep-th/0303116].

[37] R. Contino and A. Pomarol, *Holography for fermions*, *JHEP* **11** (2004) 058, [hep-th/0406257].

[38] G. Panico and A. Wulzer, *Effective action and holography in 5d gauge theories*, *JHEP* **05** (2007) 060, [hep-th/0703287].

[39] G. Nordstrom, *On the possibility of unifying the electromagnetic and the gravitational fields*, *Phys. Z.* **15** (1914) 504–506, [physics/0702221];
T. Kaluza, *On the problem of unity in physics*, *Sitzungsber. Preuss. Akad. Wiss. Berlin (Math. Phys.)* **1921** (1921) 966–972;
O. Klein, *The atomicity of electricity as a quantum theory law*, *Nature* **118** (1926) 516.

[40] T. Gherghetta, *Warped models and holography*, hep-ph/0601213.

[41] J. Scherk and J. H. Schwarz, *Spontaneous breaking of supersymmetry through dimensional reduction*, *Phys. Lett.* **B82** (1979) 60; *How to get masses from extra dimensions*, *Nucl. Phys.* **B153** (1979) 61–88.

[42] Y. Grossman and M. Neubert, *Neutrino masses and mixings in non-factorizable geometry*, *Phys. Lett.* **B474** (2000) 361–371, [hep-ph/9912408];
T. Gherghetta and A. Pomarol, *Bulk fields and supersymmetry in a slice of AdS*, *Nucl. Phys.* **B586** (2000) 141–162, [hep-ph/0003129].

[43] M. Perez-Victoria, *Randall-Sundrum models and the regularized AdS/CFT correspondence*, *JHEP* **05** (2001) 064, [hep-th/0105048].

[44] R. Barbieri, A. Pomarol, R. Rattazzi, and A. Strumia, *Electroweak symmetry breaking after LEP1 and LEP2*, *Nucl. Phys.* **B703** (2004) 127–146, [hep-ph/0405040].

[45] K.-y. Oda and A. Weiler, *Wilson lines in warped space: Dynamical symmetry breaking and restoration*, *Phys. Lett.* **B606** (2005) 408–416, [hep-ph/0410061];
A. Falkowski, *About the holographic pseudo-Goldstone boson*, *Phys. Rev.* **D75** (2007) 025017, [hep-ph/0610336].

[46] J. Erlich, E. Katz, D. T. Son, and M. A. Stephanov, *QCD and a holographic model of hadrons*, *Phys. Rev. Lett.* **95** (2005) 261602, [hep-ph/0501128].

[47] L. Da Rold and A. Pomarol, *Chiral symmetry breaking from five dimensional spaces*, *Nucl. Phys.* **B721** (2005) 79–97, [hep-ph/0501218]; *The scalar and pseudoscalar sector in a five-dimensional approach to chiral symmetry breaking*, *JHEP* **01** (2006) 157, [hep-ph/0510268].

[48] J. Gasser and H. Leutwyler, *Chiral perturbation theory: Expansions in the mass of the strange quark*, *Nucl. Phys.* **B250** (1985) 465.

[49] C. T. Hill, *Exact equivalence of the $d = 4$ gauged Wess-Zumino-Witten term and the $d = 5$ Yang-Mills Chern-Simons term*, *Phys. Rev.* **D73** (2006) 126009, [hep-th/0603060].

[50] J. Wess and B. Zumino, *Consequences of anomalous Ward identities*, *Phys. Lett.* **B37** (1971) 95.

[51] E. Witten, *Global aspects of current algebra*, *Nucl. Phys.* **B223** (1983) 422–432.

[52] C.-S. Chu, P.-M. Ho, and B. Zumino, *Non-abelian anomalies and effective actions for a homogeneous space g/h*, *Nucl. Phys.* **B475** (1996) 484–504, [hep-th/9602093].

[53] C. A. Scrucca, M. Serone, L. Silvestrini, and F. Zwirner, *Anomalies in orbifold field theories*, *Phys. Lett.* **B525** (2002) 169–174, [hep-th/0110073];
R. Barbieri, R. Contino, P. Creminelli, R. Rattazzi, and C. A. Scrucca, *Anomalies, Fayet-Iliopoulos terms and the consistency of orbifold field theories*, *Phys. Rev.* **D66** (2002) 024025, [hep-th/0203039].

[54] N. Arkani-Hamed, A. G. Cohen, and H. Georgi, *Anomalies on orbifolds*, *Phys. Lett.* **B516** (2001) 395–402, [hep-th/0103135].

[55] E. D'Hoker and S. Weinberg, *General effective actions*, *Phys. Rev.* **D50** (1994) 6050–6053, [hep-ph/9409402].

[56] W. A. Bardeen, *Anomalous Ward identities in spinor field theories*, *Phys. Rev.* **184** (1969) 1848–1857.

[57] O. Kaymakcalan, S. Rajeev, and J. Schechter, *Nonabelian anomaly and vector meson decays*, *Phys. Rev.* **D30** (1984) 594.

[58] A. Masiero, C. A. Scrucca, M. Serone, and L. Silvestrini, *Non-local symmetry breaking in Kaluza-Klein theories*, *Phys. Rev. Lett.* **87** (2001) 251601, [hep-ph/0107201].

[59] M. B. Green and J. H. Schwarz, *Anomaly cancellation in supersymmetric d=10 gauge theory and superstring theory*, *Phys. Lett.* **B149** (1984) 117–122;
E. Witten, *Some properties of O(32) superstrings*, *Phys. Lett.* **B149** (1984) 351–356;
M. Dine, N. Seiberg, and E. Witten, *Fayet-Iliopoulos terms in string theory*, *Nucl. Phys.* **B289** (1987) 589.

[60] G. von Gersdorff, N. Irges, and M. Quiros, *Bulk and brane radiative effects in gauge theories on orbifolds*, *Nucl. Phys.* **B635** (2002) 127–157, [hep-th/0204223]; *Finite mass corrections in orbifold gauge theories*, hep-ph/0206029.

[61] A. Delgado, A. Pomarol, and M. Quiros, *Electroweak and flavor physics in extensions of the standard model with large extra dimensions*, *JHEP* **01** (2000) 030, [hep-ph/9911252].

[62] M. Carena, T. M. P. Tait, and C. E. M. Wagner, *Branes and orbifolds are opaque*, *Acta Phys. Polon.* **B33** (2002) 2355, [hep-ph/0207056].

[63] G. R. Dvali, G. Gabadadze, and M. A. Shifman, *(Quasi)localized gauge field on a brane: Dissipating cosmic radiation to extra dimensions?*, *Phys. Lett.* **B497** (2001) 271–280, [hep-th/0010071].

[64] F. del Aguila, M. Perez-Victoria, and J. Santiago, *Bulk fields with general brane kinetic terms*, *JHEP* **02** (2003) 051, [hep-th/0302023].

[65] F. del Aguila, M. Perez-Victoria, and J. Santiago, *Effective description of brane terms in extra dimensions*, *JHEP* **10** (2006) 056, [hep-ph/0601222].

[66] A. Lewandowski and R. Sundrum, *RS1, higher derivatives and stability*, *Phys. Rev.* **D65** (2002) 044003, [hep-th/0108025].

[67] N. Maru and T. Yamashita, *Two-loop calculation of Higgs mass in gauge-Higgs unification: 5d massless QED compactified on s**1*, *Nucl. Phys.* **B754** (2006) 127–145, [hep-ph/0603237].

[68] Z. Han and W. Skiba, *Effective theory analysis of precision electroweak data*, *Phys. Rev.* **D71** (2005) 075009, [hep-ph/0412166];
C. Grojean, W. Skiba, and J. Terning, *Disguising the oblique parameters*, *Phys. Rev.* **D73** (2006) 075008, [hep-ph/0602154].

[69] G. Cacciapaglia, C. Csaki, G. Marandella, and A. Strumia, *The minimal set of electroweak precision parameters*, *Phys. Rev.* **D74** (2006) 033011, [hep-ph/0604111].

[70] M. E. Peskin and T. Takeuchi, *Estimation of oblique electroweak corrections*, *Phys. Rev.* **D46** (1992) 381–409.

[71] G. Altarelli, R. Barbieri, and F. Caravaglios, *Nonstandard analysis of electroweak precision data*, *Nucl. Phys.* **B405** (1993) 3–23.

[72] K. Agashe, A. Delgado, M. J. May, and R. Sundrum, *RS1, custodial isospin and precision tests*, *JHEP* **08** (2003) 050, [hep-ph/0308036];
G. Burdman and Y. Nomura, *Holographic theories of electroweak symmetry breaking without a Higgs boson*, *Phys. Rev.* **D69** (2004) 115013, [hep-ph/0312247];
G. Cacciapaglia, C. Csaki, C. Grojean, and J. Terning, *Curing the ills of Higgsless models: The S parameter and unitarity*, *Phys. Rev.* **D71** (2005) 035015, [hep-ph/0409126].

[73] G. Altarelli and M. W. Grunewald, *Precision electroweak tests of the Standard Model*, *Phys. Rept.* **403-404** (2004) 189–201, [hep-ph/0404165].

[74] R. Barbieri and G. F. Giudice, *Upper bounds on supersymmetric particle masses*, *Nucl. Phys.* **B306** (1988) 63.

[75] G. W. Anderson and D. J. Castano, *Measures of fine tuning*, *Phys. Lett.* **B347** (1995) 300–308, [hep-ph/9409419].

[76] E. Bergshoeff, M. de Roo, M. B. Green, G. Papadopoulos, and P. K. Townsend, *Duality of type II 7-branes and 8-branes*, *Nucl. Phys.* **B470** (1996) 113–135, [hep-th/9601150].

[77] G. Cacciapaglia, C. Csaki, C. Grojean, M. Reece, and J. Terning, *Top and bottom: A brane of their own*, *Phys. Rev.* **D72** (2005) 095018, [hep-ph/0505001];
R. Foadi and C. Schmidt, *An effective Higgsless theory: Satisfying electroweak constraints and a heavy top quark*, *Phys. Rev.* **D73** (2006) 075011, [hep-ph/0509071].

[78] G. Panico and M. Serone, *The electroweak phase transition on orbifolds with gauge-Higgs unification*, *JHEP* **05** (2005) 024, [hep-ph/0502255].

[79] V. A. Kuzmin, V. A. Rubakov, and M. E. Shaposhnikov, *On the anomalous electroweak baryon number nonconservation in the early universe*, *Phys. Lett.* **B155** (1985) 36;
A. G. Cohen, D. B. Kaplan, and A. E. Nelson, *Progress in electroweak baryogenesis*, *Ann. Rev. Nucl. Part. Sci.* **43** (1993) 27–70, [hep-ph/9302210].

[80] K. R. Dienes, E. Dudas, T. Gherghetta, and A. Riotto, *Cosmological phase transitions and radius stabilization in higher dimensions*, *Nucl. Phys.* **B543** (1999) 387–422, [hep-ph/9809406].

[81] L. Dolan and R. Jackiw, *Symmetry behavior at finite temperature*, *Phys. Rev.* **D9** (1974) 3320–3341.

[82] J. R. Espinosa, M. Losada, and A. Riotto, *Symmetry nonrestoration at high temperature in little Higgs models*, *Phys. Rev.* **D72** (2005) 043520, [hep-ph/0409070].

[83] M. Quiros, *Finite temperature field theory and phase transitions*, hep-ph/9901312.

[84] C.-L. Ho and Y. Hosotani, *Symmetry breaking by Wilson lines and finite temperature effects*, *Nucl. Phys.* **B345** (1990) 445–460.

[85] K. Shiraishi, *Finite temperature and density effect on symmetry breaking by wilson loops*, *Z. Phys.* **C35** (1987) 37.

[86] G. W. Anderson and L. J. Hall, *The electroweak phase transition and baryogenesis*, *Phys. Rev.* **D45** (1992) 2685–2698.

[87] D. A. Kirzhnits and A. D. Linde, *Macroscopic consequences of the Weinberg model*, *Phys. Lett.* **B42** (1972) 471–474.

[88] M. E. Carrington, *The effective potential at finite temperature in the Standard Model*, *Phys. Rev.* **D45** (1992) 2933–2944.

[89] P. Arnold and O. Espinosa, *The effective potential and first order phase transitions: Beyond leading-order*, *Phys. Rev.* **D47** (1993) 3546–3579, [hep-ph/9212235], erratum *ibid.* **D50** (1994) 6662.

[90] M. Laine, *The two loop effective potential of the 3-d SU(2) Higgs model in a general covariant gauge*, *Phys. Lett.* **B335** (1994) 173–178, [hep-ph/9406268].

[91] W. Buchmuller, Z. Fodor, and A. Hebecker, *Gauge invariant treatment of the electroweak phase transition*, *Phys. Lett.* **B331** (1994) 131–136, [hep-ph/9403391]; *Thermodynamics of the electroweak phase transition*, *Nucl. Phys.* **B447** (1995) 317–339, [hep-ph/9502321]; A. Hebecker, *The electroweak phase transition*, hep-ph/9506418.

[92] K. Kajantie, M. Laine, K. Rummukainen, and M. E. Shaposhnikov, *Is there a hot electroweak phase transition at $m_h \gtrsim m_w$?*, *Phys. Rev. Lett.* **77** (1996) 2887–2890, [hep-ph/9605288].

[93] K. Kajantie, M. Laine, K. Rummukainen, and M. E. Shaposhnikov, *The electroweak phase transition: A non-perturbative analysis*, *Nucl. Phys.* **B466** (1996) 189–258, [hep-lat/9510020];
F. Csikor, Z. Fodor, J. Hein, A. Jaster, and I. Montvay, *Numerical tests of the electroweak phase transition and thermodynamics of the electroweak plasma*, *Nucl. Phys.* **B474** (1996) 421–445, [hep-lat/9601016].

[94] R. R. Parwani, *Resummation in a hot scalar field theory*, *Phys. Rev.* **D45** (1992) 4695–4705, [hep-ph/9204216], erratum *ibid.* **D48** (1993) 5965.

[95] S. Weinberg, *Gauge and global symmetries at high temperature*, *Phys. Rev.* **D9** (1974) 3357–3378.

[96] A. Weil, *L'intégration dans les groupes topologiques et ses applications.* Paris Hermann, p. 42-45 (1979).

[97] H. Leutwyler, *On the foundations of chiral perturbation theory*, *Ann. Phys.* **235** (1994) 165–203, [hep-ph/9311274].